An-Najah National University

Faculty of Graduate Studies

Seismic Assessment of Historical Buildings in Palestine
Nativity Church as a Case-Study

By

Ali Abdellatif Ali Abu Safiyeh

Supervisors

Dr. Munther Ibrahim

This Thesis is submitted in a Partial Fulfillment of the Requirements for the Degree of Master of Structural Engineering, Faculty of Graduate Studies, An-Najah National University, Nablus, Palestine.

2019

Seismic Assessment of Historical Buildings in Palestine
Nativity Church as a Case Study

By

Ali Abdellatif Ali Abu Safiyeh

This Thesis Was Defended Successfully on 22/7/2019 and Approved by:

Defense Committee Members	**Signature**
- **Dr. Munther Ibrahim/Supervisor**	.....
- **Dr. Belal Almassri/External Examinar**	09/09/2019 .....
- **Dr. Mohammad Samaaneh/Internal Examinar**	.....

Dedication

This Thesis is dedicated to my Dear Parents First of all,

To my Beloved Wife Fidaa,

To my Sisters and Brothers,

To my Daughter Amal, and Son Abdellatif,

To my Great Family and my Loyal Friends.

May Allah (SWT) Grant You Endless Happiness and Peace.

Acknowledgement

First of all, praise is to Allah for helping completing this thesis.

After that many thanks and sincere gratitude to my supervisor: Dr. Munther Diab for his assistance, guidance, and recommendations.

Special thankfulness to;

My Parents, my beloved wife, brothers, sisters, friends.

I would like to thank everyone who has contributed to accomplishing this thesis.

لإقرار

أنا الموقع أدناه، مقدم الرسالة التي تحمل العنوان:

Seismic Assessment of Historical Buildings in Palestine

Nativity Church as a Case-Study

أقرّ بأنّ ما اشتملت عليه هذه الرّسالة إنما هي نتاج جهدي الخاصّ، باستثناء ما تمت الإشارة إليه حيثما ورد، وأن هذه الرسالة كاملة، أو أي جزء منها لم يقدم من قبل لنيل أي درجة علمية أو بحث علمي أو بحثي لدى أي مؤسسة تعليمية أو بحثية أخرى.

Declaration

The work provided in this thesis, unless otherwise referenced, is the researcher's own work, and has not been submitted elsewhere for any other degree or qualification.

Student's name: **اسم الطالب:**

Signature: **التوقيع:**

Date: **التاريخ:**

Table of content

Dedication		III
Acknowledgment		IV
Declaration		V
Table of Contents		VI
List of Tables		XI
List of Figures		X
Abstract		XIV

CHAPTER ONE : INTRODUCTION

1.1	General	2
1.2	Thesis Need	3
1.3	Thesis Objectives	4
1.4	Problem Statement	5
1.5	Organization of Thesis	7
	1.5.1 Chapter 1	7
	1.5.2 Chapter 2	7
	1.5.3 Chapter 3	7
	1.5.4 Chapter 4	7
	1.5.5 Chapter 5	8
	1.5.6 Chapter 6	8
	1.5.7 Chapter 7	8

CHAPTER TWO : LITERATURE REVIEW

2.1	Masonry Structure	10
	2.11. General Characteristics	11
	2.1.2 Failure Behavior	12
	2.1.3 Possible Failure Mechanisms	13
2.2	Analysis of Seismic Behavior	17
	2.2.1 Analysis Methods	18
	2.2.1.1 Pushover Analysis	19
	2.2.1.2 Time History Analysis	21
2.3	Seismic Hazard	23
2.4	Seismic Risk	26
2.5	Seismicity of Palestine	26
	2.5.1 General	26

	2.5.2 Fault of Dead Sea	28
	2.5.3 Seismicity of the Site	29
2.6	Recent Studies	30
	2.6.1 Over The World	26
	2.6.2 Relevant Studies for Palestine	46
2.7	Progressive Collapse of Masonry	49
	2.7.1 Introduction	49
	2.7.2 Researches of Progressive Collapse	49
	2.7.3 Relevant Codes and Standards	54
	2.7.3.1 IBC 2012	54
	2.7.3.2 ASCE 7-10	55
	2.7.3.3 MSJC-13	56
	2.7.3.4 GSA 2013	56
	2.7.3.5 UFC 04-023-03	57
	2.7.3.6 ASCE 41-13	57
	2.7.3.7 EUROCODE	58

CHAPTER THREE : MODELING of CASE STUDY

3.1	Introduction	62
3.2	Case Study: The Church of Nativity	62
3.3	Finite Element Method	63
	3.3.1 Software's used in the Study	65
	3.3.2 Mechanical Properties for Models	68
	3.3.3 Verifications of Models	69
	3.3.3.1 Modal Shapes	69
	3.3.3.2 Modal Analysis	73

CHAPTER FOUR NON-LINEAR STATIC ANALYSIS

4.1	Introduction	77
4.2	Constitutive Model	77
4.3	Cracks Propagation	81
	4.3.1 Cracks Pattern in X – Direction	81
	4.3.2 Cracks Pattern in Y – Direction	85

CHAPTER FIVE : NON-LINEAR DYNAMIC ANALYSIS

5.1	Introduction	91
5.2	Used earthquakes	91
5.3	Relative Displacement	95

5.3.1 X – Direction 96
5.3.2 Y – Direction 109

CHAPTER SIX : PROGRESSIVE COLLAPSE

6.1 Introduction 124
6.2 Analysis Procedures 124
6.3 Failure Criterion 127
6.4 Principle Stresses 129
6.4.1 X - Direction 129
6.4.2 Y - Direction 131
6.5 Critical Region Identification 134
7.5.1 Evaluation Results : X-Direction 135
7.5.2 Evaluation Results: Y-Direction 137

CHAPTER SEVEN : DISCUSSION AND CONCLUSION

7.1 Discussion of Results 140
7.1.1 Discussion of Pushover analysis Results 141
7.1.2 Discussion of Time History Analysis Results 143
7.1.3 Discussion of Progressive Collapse Results 148
7.2 Conclusion 149
7.3 Recommendations and Future Studies 152

References 154
Appendices 160
الملخص ب

List of tables

Table (3.1)	Properties OF Nativity Church	69
Table (3.2)	corresponding modal periods for the first 8 modes	74
Table (7.1)	Max Crack Width In X Vs. Y Directions	143
Table (7.2)	Effect of Relative Displacement Analysis	144
Table (7.3)	Effect of Progressive Collapse Analysis	149

List of Figures

Figure (1.1)	**Some of Historical Religious Buildings for Muslims in Palestine.**	**2**
Figure (1.2)	**Some of Historical Religious Buildings for Christians in Palestine.**	**3**
Figure (2.1)	**Modeling Strategies of Masonry Structures.**	**11**
Figure (2.2)	**Yield Criterion and a Typical Stress-Strain Model for Brick Unit.**	**13**
Figure (2.3)	**In-Plane Failure Mechanisms.**	**14**
Figure (2.4)	**Out of Plane Failure Mechanisms.**	**15**
Figure (2.5)	**Force-Displacement Curve Corresponding to Out of Plane Failure.**	**16**
Figure (2.6)	**Earth Disturbances Recorded by Seismograph.**	**18**
Figure (2.7)	**Load Displacement Curve.**	**20**
Figure (2.8)	**Mass and Stiffness Proportional Damping - Rayleigh Damping**	**22**
Figure (2.9)	**Seismic Hazard Map for Palestine.**	**24**
Figure (2.10)	**Hazard Response Spectra for 2% & 10 %, POE in 50 Years.**	**25**
Figure (2.11)	**Dead Sea Fault.**	**27**
Figure (2.12)	**Fault Line Between the African and Arabian Plates.**	**29**
Figure (2.13)	**General View of St. James Church and the Numerical model.**	**31**
Figure (2.14)	**Virtual Collapse Mechanisms.**	**32**
Figure (2.15)	**Camponeschi Palace - L'Aquila, Italy.**	**33**
Figure (2.16)	**Photograph of Madre Santa Maria del Borgo church, Italy.**	**34**
Figure (2.17)	**Armenian Church in Famagusta.**	**36**
Figure (2.18)	**Sonic Test Applied to the Armenian Church.**	**36**
Figure (2.19)	**Views of the Temple of San Antonio.**	**37**
Figure (2.20)	**Plan and Cross-Section of the Church of the Poblet Monastery.**	**38**
Figure (2.21)	**Principal Tensile and Shear Stresses for Jama.**	**40**
Figure (2.22)	**Elti Hatun Mosque with its Outside and Inside View**	**41**
Figure (2.23)	**General and 3D view of Cathedral of the Blessed Sacrament**	**41**
Figure (2.24)	**General and 3D view of Kaisariani Monastery in Athens.**	**43**
Figure (2.25)	**General and 3D view of Civic Museum.**	**44**
Figure (2.26)	**3D model of Fresco.**	**45**
Figure (2.27)	**Location and 3D of St. Salvatore church.**	**46**

Figure (2.28)	**3D Finite Element Model for the Nativity church.**	**47**
Figure (2.29)	**Aerial View of the South Wall.**	**48**
Figure (2.30)	**Masonry Barrel Vault with Possible Loads Paths in the Arches.**	**51**
Figure (2.31)	**Picture for the Bund 18 Building, and its Plan View of First Floor**	**52**
Figure (2.32)	**The 3D Model with Collapse Due to Removal of Some Columns**	**53**
Figure (3.1)	**Perspective Picture for Church of the Nativity**	**63**
Figure (3.2)	**Different Approaches for Modeling of Masonry Walls**	**66**
Figure (3.3)	**Eight Node Solid Element in SAP2000**	**66**
Figure (3.4)	**3D Numerical Model Built in DIANA FEA Software**	**67**
Figure (3.5)	**3D Solids Used in Modeling According to DIANA Manual**	**70**
Figure (3.6)	**Periods and Modal Shapes Concerning the 3D model – SAP2000**	**72**
Figure (3.7)	**Periods and Modal Shapes Concerning the 3D model – DIANA FEA**	**75**
Figure (3.8)	**Comparison Between Frequencies of Two Models**	**75**
Figure (4.1)	**Material Models Used for the Behavior of Masonry.**	**78**
Figure (4.2)	**Force Control Versus Displacement Control.**	**79**
Figure (4.3)	**Load Increment Methods Characteristics and Arc-Length Control.**	**80**
Figure (4.4)	**Crack Widths Generated by Gravity Loads Analysis in X – Direction.**	**82**
Figure (4.5)	**Crack Widths Generated by Pushover Analysis in X – Direction.**	**84**
Figure (4.6)	**Crack Widths Generated by Gravity Loads Analysis in Y – Direction.**	**86**
Figure (4.7)	**Crack Widths Generated by Pushover Analysis In Y – Direction.**	**88**
Figure (5.1):	**Elastic and Design Spectra Concerning the Site Seismicity.**	**92**
Figure (5.2)	**Accelerograms Used for Dynamic Analysis.**	**93**
Figure (5.3)	**Rayleigh Damping Model.**	**94**
Figure (5.4)	**Locations of Reference Nodes for Dynamic Analysis.**	**95**
Figure (5.5)	**Points of Masonry Block where the Displacements Measured.**	**96**
Figure (5.6)	**Relative Displacement for Node (1) - X direction**	**97**
Figure (5.7)	**Relative Displacement for Node (2) - X direction**	**97**
Figure (5.8)	**Relative Displacement for Node (3) - X direction**	**98**
Figure (5.9)	**Relative Displacement for Node (4) - X direction**	**99**
Figure (5.10)	**Relative Displacement for Node (6) - X direction**	**99**

Figure (5.11)	**Relative Displacement for Node (7) - X direction**	**100**
Figure (5.12)	**Clear Separation in the Longitudinal Wall.**	**100**
Figure (5.13)	**Relative Displacement for Node (8) - X direction**	**101**
Figure (5.14)	**Relative Displacement for Node (9) - X direction**	**102**
Figure (5.15)	**Ties of Masonry Buildings**	**102**
Figure (5.16)	**Relative Displacement for Node (10) - X direction**	**103**
Figure (5.17)	**Relative Displacement for Node (11) - X direction**	**103**
Figure (5.18)	**Relative Displacement for Node (12) - X direction**	**104**
Figure (5.19)	**Relative Displacement for Node (13) - X direction**	**104**
Figure (5.20)	**Relative Displacement for Node (14) - X direction**	**105**
Figure (5.21)	**Relative Displacement for Node (15) - X direction**	**105**
Figure (5.22)	**Relative Displacement for Node (16) - X direction**	**106**
Figure (5.23)	**Relative Displacement for Node (17) - X direction**	**106**
Figure (5.24)	**Relative Displacement for Node (18) - X direction**	**107**
Figure (5.25)	**Relative Displacement for Node (19) - X direction**	**107**
Figure (5.26)	**Relative Displacement for Node (20) - X direction**	**108**
Figure (5.27)	**Maximum Relative Displacement for all Nodes - X direction**	**108**
Figure (5.28)	**Relative Displacement for Node (1) - Y direction**	**109**
Figure (5.29)	**Relative Displacement for Node (2) - Y direction**	**110**
Figure (5.30)	**Relative Displacement for Node (3) - Y direction**	**110**
Figure (5.31)	**Relative Displacement for Node (4) - Y direction**	**111**
Figure (5.32)	**Relative Displacement for Node (5) - Y direction**	**111**
Figure (5.33)	**Relative Displacement for Node (6) - Y direction**	**112**
Figure (5.34)	**Relative Displacement for Node (7) - Y direction**	**112**
Figure (5.35)	**Relative Displacement for Node (8) - Y direction**	**113**
Figure (5.36)	**Relative Displacement for Node (9) - Y direction**	**114**
Figure (5.37)	**Relative Displacement for Node (10) - Y direction**	**115**
Figure (5.38)	**Relative Displacement for Node (11) - Y direction**	**115**
Figure (5.39)	**Relative Displacement for Node (12) - Y direction**	**116**
Figure (5.40)	**Relative Displacement for Node (13) - Y direction**	**117**
Figure (5.41)	**Relative Displacement for Node (14) - Y direction**	**117**
Figure (5.42)	**Relative Displacement for Node (15) - Y direction**	**118**
Figure (5.43)	**Relative Displacement for Node (16) - Y direction**	**118**
Figure (5.44)	**Relative Displacement for Node (17) - Y direction**	**119**

Figure (5.45)	**Relative Displacement for Node (18) - Y direction**	**120**
Figure (5.46)	**Relative Displacement for Node (19) - Y direction**	**120**
Figure (5.47)	**Relative Displacement for Node (20) - Y direction**	**121**
Figure (5.48)	**Maximum Relative Displacement for all Nodes - Y direction**	**122**
Figure (6.1)	**Accelerogram of El Centro Earthquake.**	**126**
Figure (6.2)	**Modified Von-Mises failure Criterion for Masonry Structures**	**127**
Figure (6.3)	**Locations of the Reference Nodes for Progressive Analysis**	**128**
Figure (6.4)	**Connections Between Transverse Walls and Façade**	**129**
Figure (6.5)	**Principle Stresses for X – Direction**	**130**
Figure (6.6)	**The Church's Plan, Showing locations of South and North Walls.**	**131**
Figure (6.7)	**South Masonry Wall Location with Geometric Section Height.**	**132**
Figure (6.8)	**Principle Stresses for Y – Direction**	**133**
Figure (6.9)	**Von Misses Function for Church Components, X – Direction.**	**135**
Figure (6.10)	**Lateral Walls Failure After 7.53 sec**	**136**
Figure (6.11)	**Lateral Walls Failure after as a Second Stage.**	**136**
Figure (6.12)	**Von Misses Function for Church Components, Y – Direction.**	**137**
Figure (6.13)	**External and Internal lateral Walls Failure**	**138**
Figure (7.1)	**Maximum Crack Propagation in Each Direction With Respect to Load Step**	**141**
Figure (7.2)	**Maximum Crack Propagation, X- Direction.**	**144**
Figure (7.3)	**Inadequate Connection Between Wythes**	**145**
Figure (7.3)	**Maximum Crack Propagation, Y- Direction.**	**146**

Seismic Assessment of Historical Buildings in Palestine
Nativity Church as a Case-Study

By
Ali Abdellatif Ali Abu Safiyeh
Supervisors
Dr. Munther Ibrahim

Abstract

This thesis addresses the study of the seismic assessment of historical structures in Palestine, by focusing on general condition and structural stability of The Church of Nativity in Bethlehem, which is the most valuable structure over the world, because it is earliest Christian structures, and the birth place of Jesus.

The work of this thesis can be divided into the following main phases: a focus on the one case study with its properties, review of the state of art, preparation and calibration of a 3D finite element models, and the structural analysis to assess the seismic behavior of the Church. The assessment was done by using the static pushover and dynamic time history methods and the results of these analyses are studied in terms of the generated cracks propagation in each direction, effects of relative displacement of masonry blocks and progressive collapse analysis for the structures elements.

In particular, the results of the pushover analysis carried out, conclude that the transversal direction is the most vulnerable and the damage concentrates at the main lateral (longitudinal) walls, mainly at the south and north alignment walls, also at the vaults and at the connections of

the vaults to the apses. On the other hand, the dynamic analysis presented similar conclusions in terms of structural performance. Furthermore, it allowed conclude that for the considered earthquake, the relative displacement of adjacent masonry blocks (RDAMB) indicates the locations of failure, and the prediction of reasons. Furthermore, the progressive collapse technique is able to predict the critical regions, and effect of rock falls in masonry walls of the structure.

Chapter One

Introduction

Chapter One

Introduction

1. Introduction

1.1 General

Buildings may be classified as historical for two main reasons summarized as; long time has passed upon its construction, and they are irreplaceable with associated acts of historical importance. It is well known from past and recent earthquakes that traditional masonry buildings, do not respond well to strong dynamic demands, so due to these causes (damage and loss of cultural heritage) more and more attention given for need of safety evaluation of old buildings in the seismic zones. Figure (1.1) show some historical structures in Palestine which are considered very special religious landmarks for Muslims, for example, the Dome of Rock, with Al-Aqsa Mosque in Jerusalem, also Cave of the Patriarchs in Hebron.

The Dome of Rock with Al-Aqsa Mosque

Cave of the Patriarchs

Figure (1.1); Some of Historical Religious Buildings for Muslims in Palestine

Also for Christians, Church of Holy Sepulcher in Jerusalem, and Church of Nativity in Bethlehem are considered very holy structures in Palestine, figure (1.2).

Church of Holy Sepulcher

Church of Nativity

Figure (1.2); Some of Historical Religious Buildings for Christians in Palestine

1.2 Thesis Need

Palestine is vulnerable to earthquake events, and until now there is no seismic code for designing buildings for the Palestinian Authority, although engineers design their buildings depending on national and international building codes, which they are not subordinate under certain regulation for Palestinian authority, however in the last years, a strong earthquake event took place in this area, averagely, every hundreds of years i.e. 1837 earthquake that took place in the northern part of Palestine, also the 1927 earthquake resulted in hundreds of victims and a lot of damage.

The need of this thesis was generated due to the architectural complex of historical structures in Palestine, most of the existing historical monumental structures are made of masonry, using stone or brick blocks, these unreinforced blocky masonry structures cannot be considered

continuum, but rather an assemblage of compact stone or brick elements linked by means of mortar joints, so the mortar replacement, stabilization, and repair interventions are often insufficient to prevent cultural losses caused by poor structural performance of these buildings during earthquakes.

In this case, the upgrading of a historical buildings require deliberation of such building, which is based on the following aspects

1- The life safety judgment,

2- Prevention of damage to building elements and components,

3- Cultural significance.

1.3 Thesis Objectives

The main objective of this thesis is the assessment of the seismic performance of an existing unreinforced masonry building subjected to seismic loading, the area under consideration is Bethlehem, locating in Palestine, and has the historical building; The Church of Nativity, which is the case study of this thesis.

In additional to the main objective, this thesis aims to predict the materials' properties and expected damage in these materials, for the used building of the case study.

This work intends also to contribute for the discussion of using static and dynamic analysis to evaluate the seismic performance, thus, in order to satisfy these objectives, the following tasks were carried out:

1. Review of the methods used to examine masonry structures.
2. Review of the state of art of seismic analysis methods commonly used for the assessment of the response of structures.
3. Preparation and calibration of two models based on the finite element method.
4. Comparing the 3D finite element models of the Case Study "The Church of Nativity" considering the main geometrical features of the building.
5. To perform a non-linear finite element analysis of the church for gravity and lateral loading, employing two different methods: non-linear static pushover analysis and non-linear time-history analysis.
6. To perform progressive collapse of the church based on non-linear time-history analysis to evaluate the performance against collapse.
7. To assess the current safety of the church.

1.4 Problem Statement

Regrettably, most of restoration projects for historical buildings in Palestine have been done with concentration on architectural features of

historical buildings, not on the response of such buildings to the earthquakes excitations. For example, between years 2015-2017, the restoration of Nativity Church has been done, and concentrated on rehabilitation works for scaffolding and temporary roof, wall mosaics, external stone surfaces, paintings of columns, repairing floor mosaics, modification of lighting system, adding new fire alarm etc... With now adequate structural and seismic rehabilitation for the church, knowing that this church inscribed on the world heritage list in 2012, also it is classified on the list of world heritage in danger due to the lack of repair of the roof structure.

So the main scope of the present work consists of the characterization of the seismic performance of historical buildings in Palestine as general, and will study in details the case study of The Church of Nativity by a non-linear static and dynamic analysis, to generate a pattern for cracks propagation in masonry and their relative displacement in elements, in order to predict the failure mechanisms of this type of buildings.

Also, buildings like that may be prone to rock falls caused by lateral forces, this direct the analyst to assess the building against progressive collapse, which is an approach based on progressive analysis and used recently to check the sudden and unexpected loads that leading to the collapse of the entire building or substantial part.

1.5 Organization of Thesis

This thesis is organized into seven chapters, including the present introduction. Also the appendices and references are stated in the last. The following subsections summarize each chapter with its content:

1.5.1 Chapter 1

It is an introduction to the research; define the research's need, objectives, problem statement, and the scope of the work.

1.5.2 Chapter 2

Address the historical development of seismic analysis of masonry structures, discussing the present limitations and inherent uncertainties of the various approaches, with mention of similar researches done over the world, and in the Palestine.

1.5.3 Chapter 3

Show brief about the used case study, with how the finite element continuum macro-models are prepared to study the response of the structure, also this chapter discuss the model analyses and compare them between different methods used.

1.5.4 Chapter 4

Focus on the non-linear static analysis for the structure, and show the results of pushover analysis.

1.5.5 Chapter 5

Present the non-linear dynamic analysis for the same structure used, and show the results of time history analysis, based on using three different accelerograms each of them for a different earthquake.

1.5.6 Chapter 6

Make the progressive analysis, use the data of El Centro earthquake, in order to define the critical regions and load paths.

1.5.7 Chapter 7

This final chapter, discusses the results of approaches used, and includes the conclusions, and future research topics to extend the current work.

CHAPTER TWO

LITERATURE REVIEW

2. Literature Review

2.1 Masonry Structures

Masonry structures have been separated widely all over the world. They are a much types of constructions which can be built rapidly, cheaply and often without particular technical competence. Thus, historical materials such as stone's masonry are characterized by very complex mechanical and strength phenomena, which still challenging the modeling abilities. In particular, masonry is characterized by its high rigidity, low shear and tensile strength, low capacity of bearing reverse loading, and low ductility. These are the main reasons for the frequent collapse of masonry buildings during earthquakes excitations, as a result, masonry properties can vary depending on the type of stone units and mortar used, in additions; other factors influencing the behavior of masonry are the dimensions of the units, the mortar width and the arrangement of units, (Mosalam, Glascoe, & Bernier, 2009).

Masonry can be classified into three main categories depending on the construction method used, the first one is the confined masonry, which consists of horizontal and vertical RC members, the second, reinforced masonry where steel bars are usually used for the reinforcement, and the third, is unreinforced masonry which refers to stand alone masonry units.

2.1.1 General Characteristics

Masonry is a composite material showing an anisotropic behavior; it is characterized by distinct directional properties due to the existence of mortar joints, which act as planes of weakness. The numerical representation of masonry structures can vary based on the level of accuracy needed; the following modeling strategies, figure (2.1), can be used:

A. **Detailed Micro Modeling**: continuum elements represent units and mortar in the joints, whereas their interface is represented by discontinuous elements, as figure (2.1a&b) show.

B. **Simplified Micro Modeling**: expanded units are represented by continuum elements, while their interface is lumped in discontinuous elements, as figure (2.1c) show.

C. **Macro Modeling**: units, mortar and interface are smeared out in the continuum, as figure (2.1d) show.

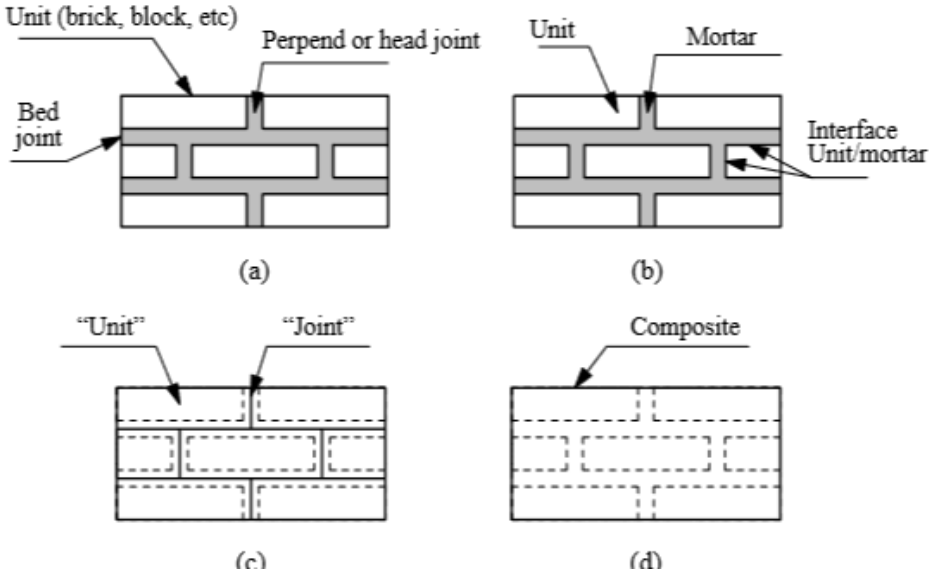

Figure (2.1): Modeling Strategies of Masonry Structures. [Lourenço , 2013]

The mechanical properties of masonry depend on many parameters, such as the material properties of units and mortar, the arrangement of bed and head joints, anisotropy of units, dimensions of units, joint width, quality of workmanship, degree of curing, age of construction and environment.

2.1.2 Failure Behavior

Masonry usually characterized by a quasi-brittle behavior, which refers to the way the force is transferred through the material. In details, after the peak load is reached the force gradually decreases to zero, which is called softening procedure, which is defined as the gradual decrease of resistance under a continuous increase in force caused deformation upon a material's structure. It is a notable feature of quasi-brittle materials like concrete, ceramics, clay brick, mortar, and rock, which fail due to a process of progressive internal crack growth. The phenomenon of softening has been well identified in parallel in tensile and shear failures of masonry, (Lawrence Livermore National Laboratory, 2009). Otherwise, in compression, softening behavior depends on the boundary conditions in the experiments and sizes of the specimen, figure (2.2) below, present the stress-strain relationship of unreinforced brick masonry and the yield criterion.

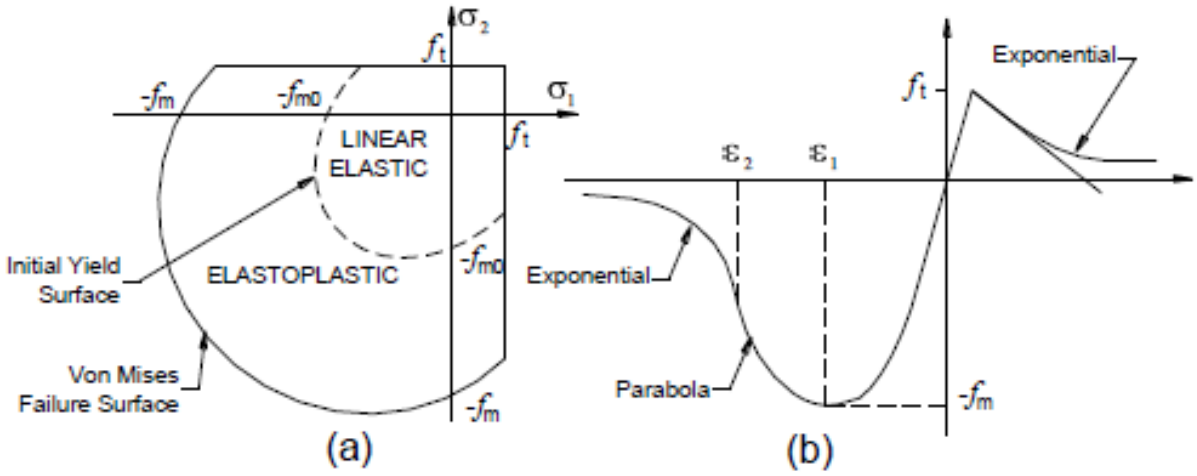

Figure (2.2): Yield Criterion and a Typical Stress-strain Model for Brick Unit.

[Lawrence Livermore National Laboratory, 2009].

2.1.3 Possible Failure Mechanisms

Unreinforced masonry structures should be examined considering its horizontal and vertical effects, because the types of failure may be occurring in plane and out of plane mechanisms. Observed failure in unreinforced masonry structures from past earthquakes expose that the two types of failure are independent, so they should be examined in parallel. The general modes of failure related to unreinforced masonry structures buildings include;

A. In-plane failure.

B. Out-of plane failure.

C. Lack of anchorage or anchors failure.

D. Diaphragm related failures.

When the in plane behavior is examined, the actual behavior of masonry walls looks like the shear walls behavior, Anthoine and Magonette, and Kikuchi et al. (2015) have been thoroughly examined, and generate the following two types of failure:

a. **Flexural Failure:** The compression and tension failures are combined, because the exceedance of tensile bond strength which results in a crack in the interface of mortar and brick, is followed by loss of the resisting section in compressive crushing, and these also known as toe crushing.
b. **Diagonal Failure:** The Cracks which developed through the unit mortar interface and the units itself as a case of biaxial tension compression state. Unfortunately there are low aspect ratios and lower axial load characterize this failure.

Also, Elgawady, Badoux, & Lestuzzi, 2006; Magenes & Penna, 2009, can show the types of failure but separated in three main forms, figure (2.3), summarized as flexural failure, shear failure, and sliding failure. These are also defined as global response mechanisms.

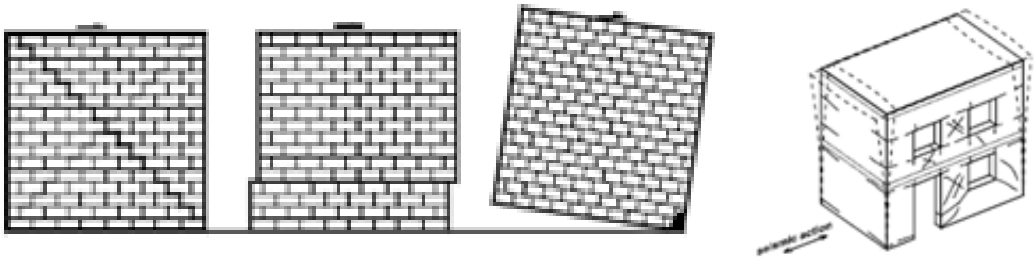

Shear Sliding Flexural Global response

Figure (2.3): In-plane Failure Mechanisms. [Elgawady, Badoux, & Lestuzzi, 2006; Magenes & Penna, 2009]

On the other hand, the out of plane failure mechanisms are important for the overall structural behavior of the masonry structures. Some types of failures are associated to the spandrels of walls, which are not well restrained by structural elements, which might generate rocking falling when earthquake loads are present, (Calvi, Pinho, Magenes, Bommer, Restrepo-Vélez, & Crowley, 2006). Possible out of plane collapse mechanisms are presented in figure (2.4).

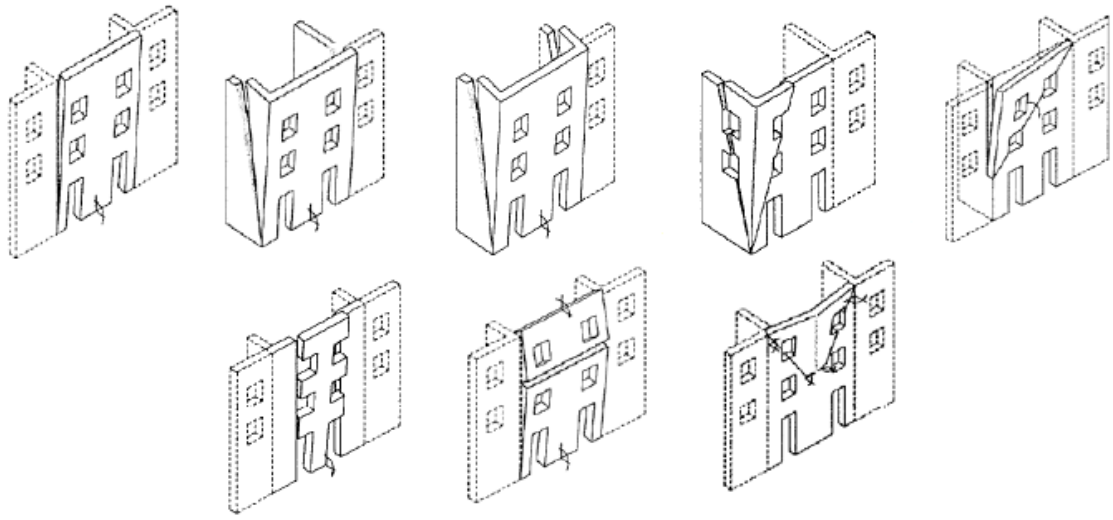

Figure (2.4): Out of Plane Failure Mechanisms. [Calvi, Pinho, Magenes, Bommer, Restrepo-Vélez, & Crowley, 2006]

Figure (2.5) can show the main line connecting the point of force corresponding to rocking mechanism (λW) and the point of displacement where instability happened under static loads (Δ), assumes that the system is cracked before the movements of parts considering to wall panels participating to rocking behave as rigid bodies. Also the dashed line, however, is a more accurate representation of the real behavior, it assumes, the wall can be initially avert cracks, and the point around which the

rocking is activated has finite dimensions. A more detailed description of the phenomena is given in Doherty et al. (2002).

When the failure is associated to the connections of diaphragms to the masonry walls, three of the failure modes are identified; (1) parapet failure, (2) wall diaphragm shear failure, and (3) wall diaphragm tension tie failure.

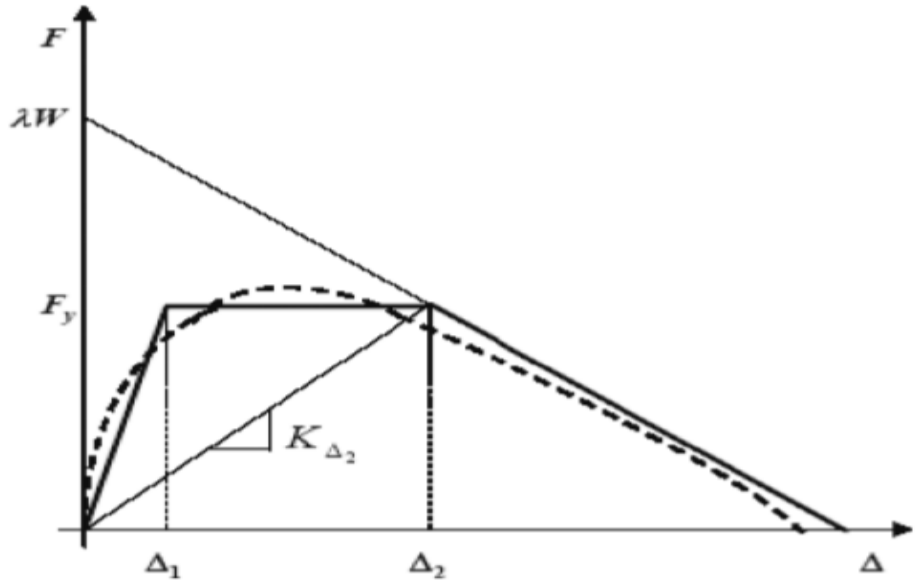

Figure (2.5): Force-Displacement Curve Corresponding to Out of Plane Failure [Doherty et al. 2002].

Also for the roof and floor diaphragms, they can be considered as: (1) Flexible, (2) Semi rigid and (3) Rigid. Diaphragms are considered flexible when the maximum lateral displacement along its length is greater than twice the average inter story drift of the vertical lateral load resisting elements, (Doherty et al. 2002). Otherwise the diaphragms range from semi

rigid to rigid. According to FEMA 356, unreinforced masonry buildings with timber floors can be considered flexible; the connections between masonry walls are defined as weak points and are expected to separate during cyclic loading.

2.2 Analysis of Seismic Behavior

An earthquake is defined as ground shaking caused by the sudden release of energy in the Earth's crust, caused by tectonic movements. The main cause is that when tectonic plates collide, one ride over the other, and this create relative motion between the plates leads to increasing the stresses.

The tectonic movements originate from different sources, for instance, volcanic activities, releasing of locations of the crust, folding and faulting, or even by human made explosions (USGS, 2005). Thus, while earthquakes are defined as natural disturbances, Richter has provided a list of major earth disturbances recorded by seismographs as shown in figure (2.6).

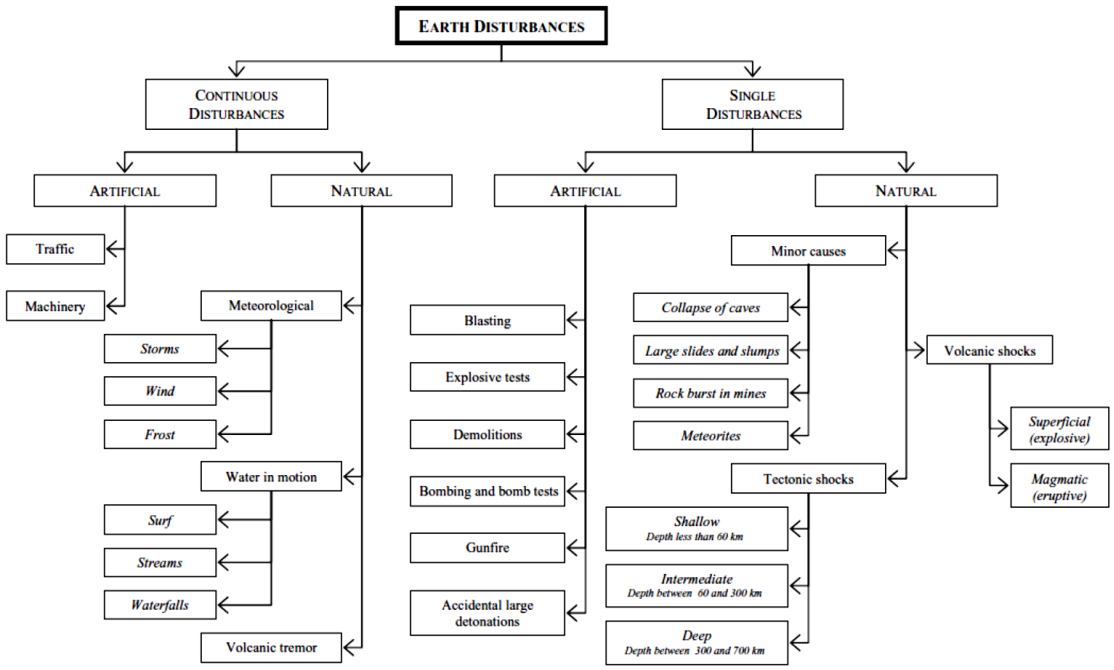

Figure (2.6): Earth Disturbances Recorded by Seismograph, [Dowrick, 2009]

2.2.1 Analysis Methods

The impact of the excitations to the structure can be caught by different methods;

A. **Lateral force analysis:** which is static analysis where the seismic action is applied as a concentrated force to the center of mass for each floor,

B. **Response spectrum analysis:** this method cicatrized by linear dynamic analysis where the seismic action is given as a spectrum,

C. **Nonlinear pushover analysis:** the load is applied statically but in nonlinear influence, and the material nonlinearity is taken into account,

D. **Nonlinear time history analysis:** the load is applied as an accelerogram and the nonlinearity of the material is also considered.

The following sections, show in details the two methods of analysis used in this work. This thesis set up on static and dynamic analysis both.

2.2.1.1 Pushover Analysis

It is a simple method, used to predict the nonlinear behavior of the structure, under seismic loads. The pushover analysis process employs the lateral forces with increasing loads used to push the structure until the ultimate displacement is reached. This method provides useful data about the peak response in terms of floor's displacement, story's drift, and other deformations quantities. (Chopra, 2012), also it can help demonstrate how progressive failures in structure can really occur, and differentiate the mode of final failure.

Capacity curve is a characteristic curve to be defined by a pushover analysis, where the displacements are plotted versus the base shear, i.e. capacity curve where the difference between experimental and numerical results is emphasized is illustrated in the following figure (2.7). However, pushover analysis can also estimate the strength capacity of a structure beyond its elastic limit up to its ultimate strength in the post elastic range. In the process, the method also predicts potential weak areas in the structure, by keeping track of the sequence of damages of each and every member in the structure by use of what are called hinges.

Different ways for the application of the load can be performed, for defining different types of pushover analysis. A monotonic pushover analysis considers a monotonic lateral load pattern which pushes the structure until the lateral capacity is reached; therefore the capacity of the structure is dependent mainly on the loading pattern.

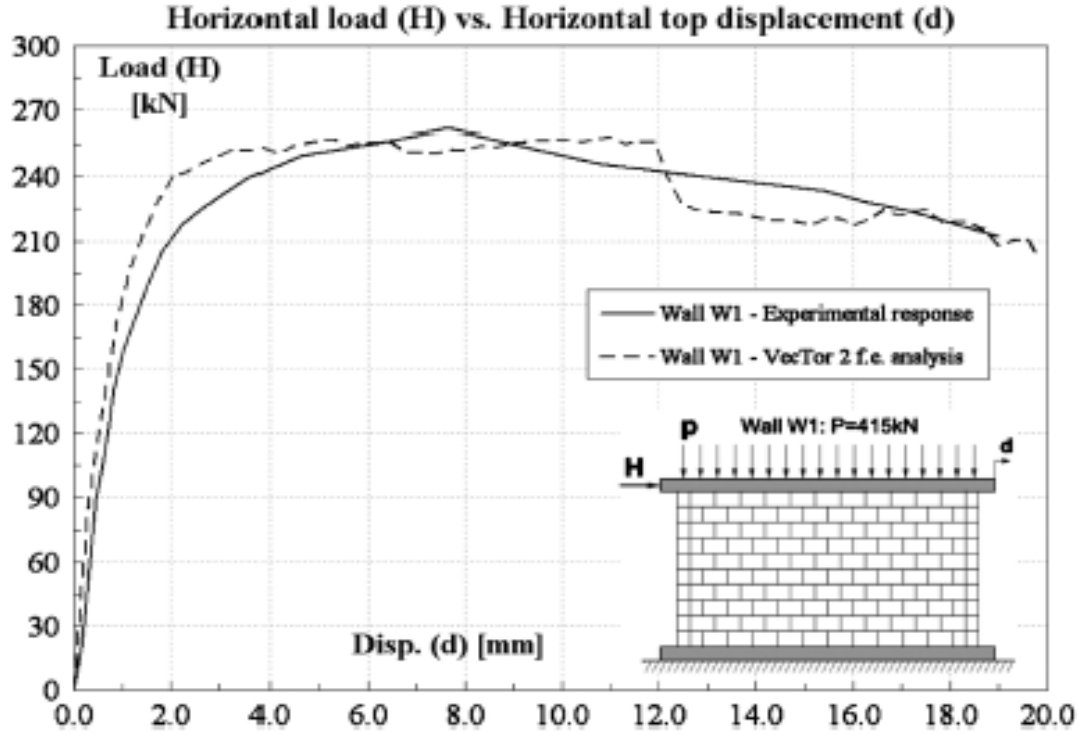

Figure (2.7): Load Displacement Curve. [Facconi, Plizzari, & Vecchio, 2013]

In Euro code the pushover analysis is defined as a nonlinear static analysis with constant gravity loads and monotonically increasing horizontal loads, for masonry buildings capacity is defined in terms of roof displacement (EN 1998-1, 2004). The ultimate displacement capacity is taken at the point of roof displacement where total lateral resistance has

dropped below 80% of peak resistance, (EN 1998-3 , 2005) due to failure of lateral load resisting elements and progressive damage.

2.2.1.2 Time History Analysis

The Nonlinear dynamic analysis utilizes the combination of ground motion records with a detailed structural model, which is the most advanced method so far, therefore it is capable of giving results with relatively low uncertainty. Theoretically time histories have complete information about the seismic event in a certain location and record three traces which are two in horizontal, and one in vertical, (Chen & Lui, 2005).

The nonlinear properties of the structure are considered as part of a time domain analysis and this approach is the most rigorous, required by some building codes for buildings of unusual configuration or of special importance. However, the calculated response can be very sensitively to the characteristics of the individual ground motion used as seismic input; therefore, several analyses are required using different ground motion records to achieve a reliable estimation of the nearly realistic distribution of structural response. Correia, Almeida, and Pinho, 2013, can show the damping models available to represent, categorized as:

a. Mass-proportional.

b. Initial stiffness-proportional.

c. Tangent proportional.

d. Rayleigh damping.

Rayleigh damping, figure (2.8), is the most type of damping, used in time history analysis, which can be expressed by the following equation as shown by (Chopra, 2012):

$$c = a_0.m + a_1.k \qquad (2.1)$$

Where;

- *c*; damping matrix,
- *m*; mass matrix,
- *k*; stiffness matrix,
- a_0; mass proportional coefficients;
- a_1; stiffness proportional coefficients;

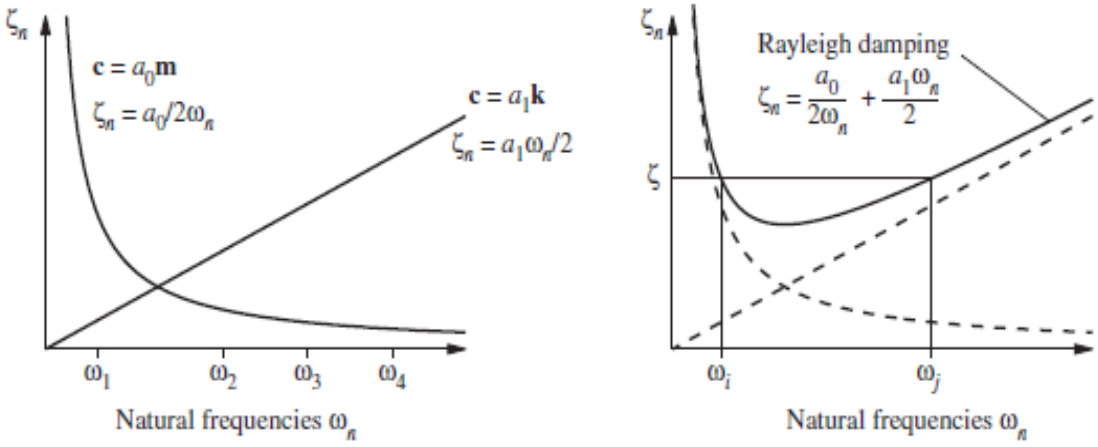

Figure (2.8): Mass and Stiffness Proportional Damping - Rayleigh Damping.

[Chopra, 2012]

2.3 Seismic Hazard

The seismic hazard, defined as the probability that an earthquake will occur in a given geographic area, within a given range of time, and ground motion intensity exceeding a given threshold. It is used as the first step in a process used to assess risk. In details, the process of quantitatively estimating the ground motion at region of interest based on the characteristics of seismic sources.

The seismic hazard is either analyzed in a probabilistic or deterministic way. In the deterministic analysis, a particular earthquake scenario is assumed, while the probabilistic explicitly considers uncertainties, while the probabilistic analysis the earthquake source needs to be identified. The source is identified using all possible sources such as fault maps giving geological, tectonic and historic information as well as instrumental records of seismicity of the past.

The outputs of the hazard's analysis is either a curve showing the exceedance probabilities for various ground motions, or a graphical map shows the estimated magnitude distribution of ground motion that has a specific exceedance probability over a specified time period at a region. The output maps developed for Palestine is shown in figure (2.9).

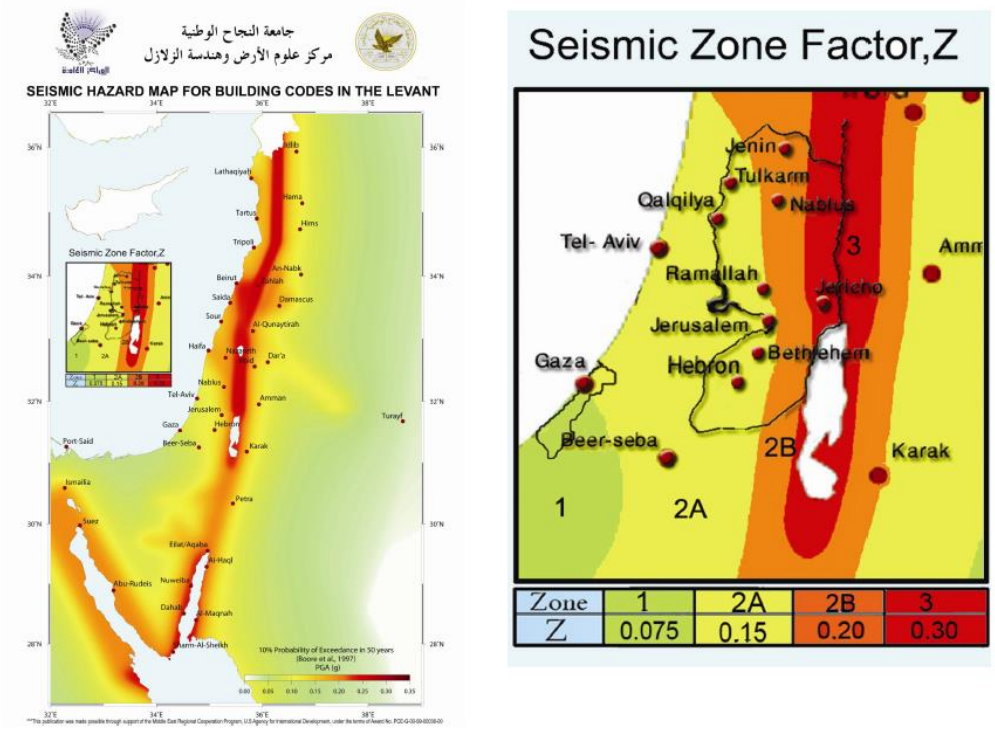

Figure (2.9): Seismic Hazard Map for Palestine,

[ESSEC, USAID-MERC (M18-057)]

For seismic risk analysis, Poisson model can be used, which is the standard model considered the best model for large earthquake occurrence, in which the tectonic stress is released when a fault breaks, however, according to the Poisson model, the probability of at least one earthquake equal to or greater than a specific magnitude (M) occurring within t years is,

$$P = 1 - e^{\frac{-t}{\tau}} \qquad (2.2)$$

Where τ is the average recurrence interval. For 2% and 10% probability of exceedance in 50 years that are commonly considered in

earthquake engineering, gives τ of 2500 and 475 years, respectively, figure (2.10)

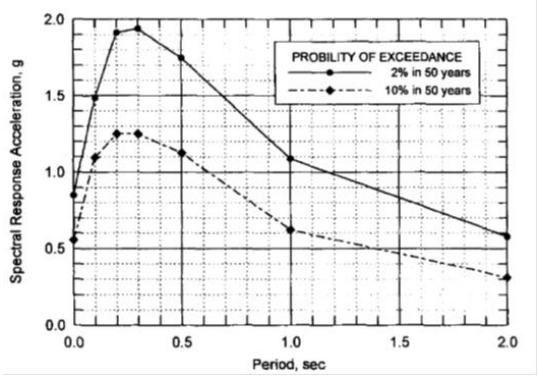

A. San Francisco

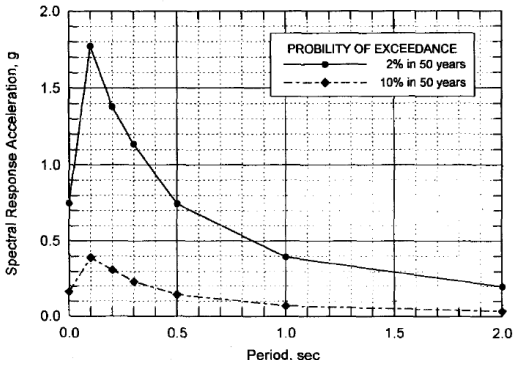

B. South Carolina

Figure (2.10): Hazard Response Spectra for 2% & 10 %, POE in 50 years.

In IBC, the maximum considered earthquake spectral response accelerations for short periods, S_{MS}, and at 1 second period, S_{M1} adjusted for site class effect is determined from the following equations:

$$S_{MS} = F_a S_S \qquad (2.3)$$

$$S_{M1} = F_v S_1 \qquad (2.4)$$

Where F_a and F_v are site coefficients and S_S and S_1 are mapped parameters that indicate the 5% damped spectral acceleration of the Maximum Considered Earthquake, in short and long periods (0.2 s and 1.0 s), respectively. The design spectral acceleration parameters in IBC are S_{DS} and S_{D1} rather than seismic zone factor used in UBC and can be found by:

$$S_{DS} = (2/3)S_{ms} \qquad (2.5)$$

$$S_{D1} = (2/3)S_{M1} \qquad (2.6)$$

2.4 Seismic Risk

Many seismologists have said that “the earthquakes don't kill people, their structures do”, this is because most deaths from earthquakes are caused by main damage of structures or other human construction falling down during an earthquake. So before any assessments start, a good practice to study two fundamentally different concept of the hazards and risk. In general terms, Risk, in its simple manner, is the probability of harm if someone or something that is vulnerable to expose the hazard, the hazard can be defined as a phenomenon that has potential to cause harm. Phenomena are both natural and man-made. For example, earthquakes, hurricanes, fires, and floods are natural hazards; whereas car crashes, and terror attacks are man-made hazards.

Seismic risk = (Seismic hazard) × (Vulnerability) × (Value)

Where Vulnerability is the amount of damage induced by a given degree of hazard, and expressed as a fraction of the Value of the damaged item under consideration.

2.5 Seismicity of Palestine

2.5.1 General

The area of Palestine is affected mainly by seismic activities along the Syrian - African fault, which is included; the Jordan Valley, Dead Sea, Gulf of Aqqaba and Near Sharm-El Sheikh in Sinai. Also Palestine may be affected by earthquakes in the Mediterranean, or in Turkey. Almost the

earthquakes which have occurred in the Mediterranean area during this century have not left any significant effects.

In recent years, there were much seismic studies have improved, due to the installation of more sophisticated equipment's, i.e. accelerometers and seismographs; the measurement of accelerations indicates that the geological structure of Palestine generates faster attenuation than assumed earlier.

However, other evidence, concerning the activity of secondary faults, besides the one in the Jordan Valley that may indicate a higher activity than previously thought. Palestine is located between the Arabian and African plates (Klinger, Avouac, Dorbath, Abou Karaki, and Tisnerat, 2000), as the figure (2.11) present.

Figure (2.11): Dead Sea Fault, [Klinger, Avouac ,Dorbath, Abou Karaki, and Tisnerat , 2000]

2.5.2 Fault of Dead Sea

The Dead Sea fault defined as separating the Sinai sub-plate and Arabian plate. It is about 1.200 km long, and connects the Taurus Zagros compressional front in the north, to the extensional zone of the Red Sea in the south (Yankelevsky, 2008).

Over the past million years tectonic movements have shaped the Dead Sea Fault system. It is one of the most seismically active regions in the Middle East. The region has a remarkable historical and geological record of seismicity, and several historical earthquakes have caused extensive damage in the area. Places such as Jericho, the oldest city in the world one of the largest cities in the region in Roman time, were greatly affected by seismic activity.

The recent studies of crustal structure, shown the crust directly under the fault valley is somewhat different from that on the sides, so as a result, these differences in crustal structure may have controlled the evolution of physiography in the region (Ben-Avraham, Lazar, Schattner, Marco 2001). Moreover, the physiography of the Dead Sea fault is also affected by the vertical motion, which caused settlements of the floor of the rift and uplift of its shoulders. The Dead Sea fault characteristics can be arranged into into four main segments; S1: Ghab Valley segment, S2: Missyf Graben segment, S3: Lebanon Bend segment, and S4: Jordan & Araba Valley segment.

2.5.3 Seismicity of The Site

Bethlehem is located between two areas of low to medium seismicity, one to the east and one to the west side. It is situated close to the fault line separating the African and Arabian tectonic plates, figure (2.12), and has been affected by several minor and major earthquakes with epicenters in the surrounding areas, such as the 1927 Palestine earthquake, also called Jericho Earthquake. Many Palestinian cities were heavily damaged, thousands of people were left homeless and at least 500 were estimated to be killed. (Touqan, and Salawdeh, (2016)),

District of Bethlehem, where the Church of Nativity is located, is similar in seismicity to the eastern parts of the states, so 10% probability of exceedance in 50 years used in this dissertation with no limitations, therefore, IBC 2015 can be used without using previous equitation's (2.5 and 2.6) with no need for concerning the factor of safety 1.5 (factor times the design earthquake features).

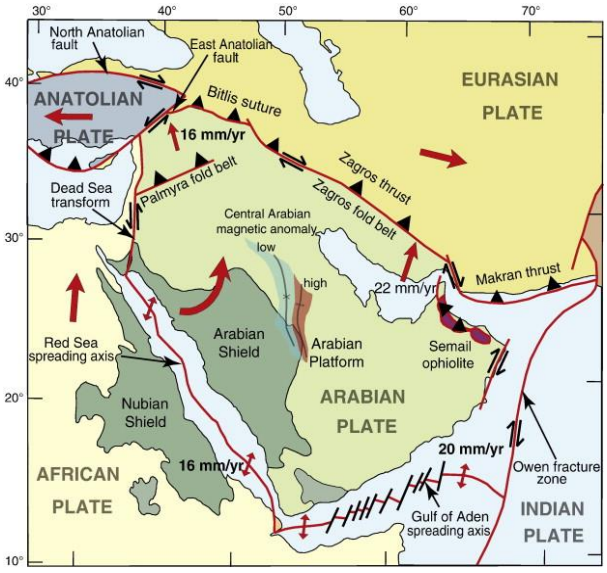

Figure (2.12): Fault Line Between the African and Arabian plates.

2.6 Recent Studies

2.6.1 Over The World

The purpose of investigating the seismic behavior concerning the monuments, such as masonry structures is divided for two paths, the first is to identify the mechanisms to be used for the protection of monuments for the purpose to help it avoiding structural collapse and destructions during earthquakes excitations, and the second is to select the most effective and suitable rehabilitation aspects.

Most of historical and monumental structures consist of masonry material, as mentioned before, which is considered to be the historically oldest structural material, and they may be located in geographically regions subjected to a higher risk of earthquakes, i.e. around the Mediterranean Sea, also the investigation of an old masonry structure is often combined with several difficulties, such as, the difficulty to find the original designs and architectural plans. Over the time, changes may have occurred to the structure, these might be structural modifications due to changes of use or renovations. Another reason may be any new technical installations such as a heating system that fixed during the life of the structure, epically these modifications often concern the structural system, and if modifications took place, they should be notified in the building chronology.

Over the years, and especially in last twenty years, researchers have studied the seismic assessment and performance of historical buildings, including their details, difficulties, mechanisms, regions, and rehabilitation process. One of the important studies was done by, Araújo, Lourenço, Oliveira and Leite, in 2012, for the St James Church, which was studied and assessed by means of pushover analysis (Before and After the New Zealand Earthquake), and presents a numerical study in details for the seismic assessment of the St James Church in Christchurch- South Island, The structural behavior of the Church has been evaluated using the finite element modeling technique, by using it; the nonlinear behavior of the structure has been taken into account by proper constitutive assumptions, figure (2.13).

Figure (2.13): General View of St. James Church and the Numerical Model.

[Araújo, B. Lourenço, Oliveira, Leite, 2012]

After the nonlinear pushover analyses are carried out on both principal directions, the Church can no longer be considered safe. The analysis results of the model show moderate agreement with the visual inspection performed in the site, which further validates the model used,

and finally, the limit analysis using macro block analysis was also carried out to validate the main local collapse mechanisms of the Church.

Paulo Lourenço, with cooperation with another team consisted of João Roque, and Daniel Oliveira, in the same year (2012), investigates the seismic safety of Monastery Church in Geronimo – Portugal. The work was done with a full data about the seismic behavior of the Church of Monastery of Geronimo, which is discussed with a numerical simulation, figure (2.14). Using artificial seismic acceleration time histories in agreement with three seismic hazard scenarios for 475, 975 and 5000 years return periods, allowing assessing its seismic safety. The detailed analysis for vertical loading and seismic loading results is indicating that the safety level of the structure is adequate for vertical and horizontal loadings. Also, the monitoring system installed allows the structural health of the church to be monitored, particularly in case of future earthquakes, providing excellent feedback for future analysis of damage.

Figure (2.14): Virtual Collapse Mechanisms. [P. Lourenço, J. Roque, D. Oliveira, 2012]

In similar manner, F. Bucchi, S. Arangio and F. Bontempi, in 2013, work on the seismic assessment of an historical masonry structures, using the nonlinear static analysis. They give the attention for the nonlinear static analysis of equivalent frames models, and under the propose of giving a measure of the response of the structure with simple implement.

In particular, its application with SAP2000 is presented; this approach is applied to a façade of an historical building that was damaged by the 2009 L'Aquila earthquake central Italy. The considered building is the Camponeschi Palace which is shown in figure (2.15), located in L'Aquila city center. The damage mechanisms obtained are compared with the observed damage and with those obtained from other approaches.

Figure (2.15): Camponeschi Palace - L'Aquila, Italy. [F. Bucchi, S. Arangio and F. Bontempi , 2013]

In the same topic, G. Castellazzi, C. Gentilini, and L. Nobile, in 2013, study the seismic vulnerability of the Basilica of church which is located in Italy, by means of limit analysis and nonlinear finite element analysis, figure (2.16). The attention here is posed similarly to the failure mechanisms of the façade of the church and its interaction with the lateral

walls. For more details, the limit analysis and the nonlinear finite element analysis provide an estimate of the load collapse multiplier of the failure mechanisms.

Investigations based on results obtained from limit analysis and nonlinear finite element analysis have been conducted on some macro elements with special attention to those that interact with the façade, and the results obtained from both approaches are in agreement and can support the selection of possible rehabilitation process and scenarios in order to decrease the vulnerability under seismic loads.

Figure (2.16): Photograph of Madre Santa Maria del Borgo Church, Italy. [G. Castellazzi, C. Gentilini, and L. Nobile , 2013]

P.G. Asteris , M.P. Chronopoulos , C.Z. Chrysostomou , H. Varum , V. Plevris , N. Kyriakides , and V. Silva, in 2014, presents a methodology for earthquake resistant assessment of the masonry structures. The entire process is established using case studies of historical masonry structures

located in the area of Europe; In particular, the reliability of the proposed method is checked using analysis of existing masonry buildings in three different countries, i.e. Cyprus, Greece and Portugal, for different seismicity levels that influencing the risk impacting the masonry structures. They conclude according to the analysis of results for the strengthened structures. The methodology followed, has been proved helpful to the analysis of existing masonry historical buildings.

Andrés Braga, and Paulo B. Lourenço, published their thesis under a title of Study the Armenian Church in Famagusta. The detailed study of the medieval Armenian Church in Famagusta was done in three main research steps. The first step concerning the historical analysis and restoration works of the edifice. This work phase included the characterization of the current condition of the structure based on an in-situ visual inspection, figure (2.17). The second step corresponded to the application of nondestructive tests (namely dynamic analysis, using ambient vibration techniques, and sonic tests) to the Armenian Church members as figure (2.18) shows. The results of these investigation techniques allowed identifying important dynamic properties of the structure, such as frequencies and modes of vibration, and the dynamic modulus of elasticity of the church masonry. And the final research step regarded the construction of a tridimensional finite element model of the Armenian Church.

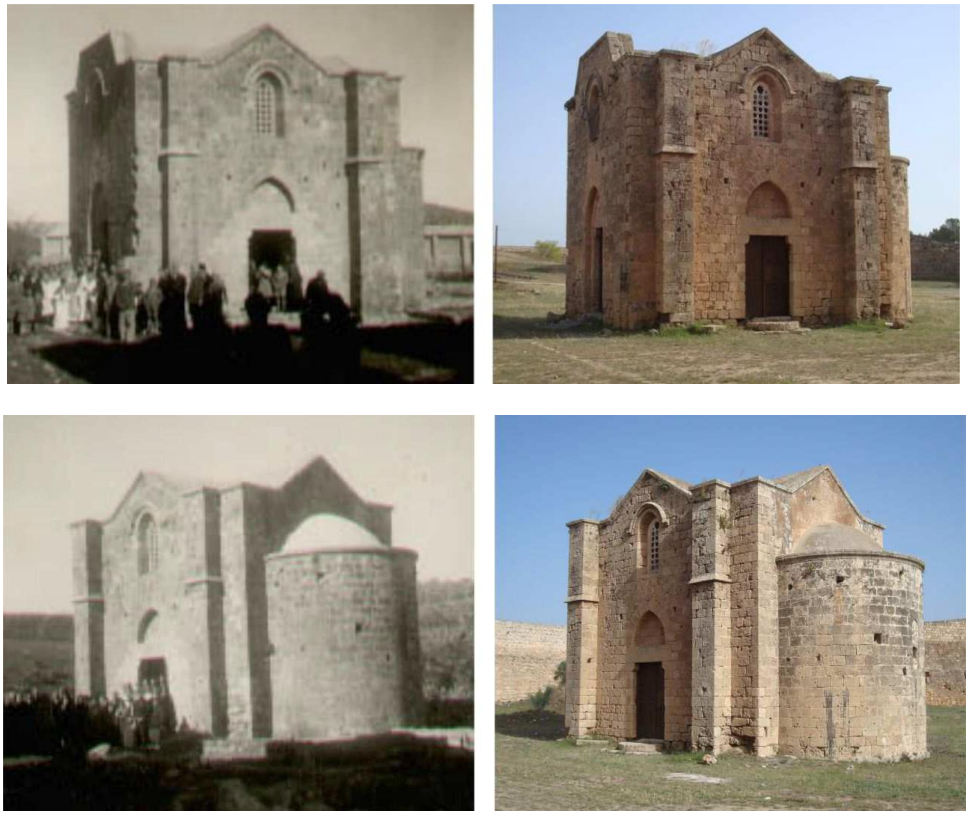

Figure (2.17): Armenian Church in Famagusta [Paulo B. Lourenço, Andrés Braga, 2013]

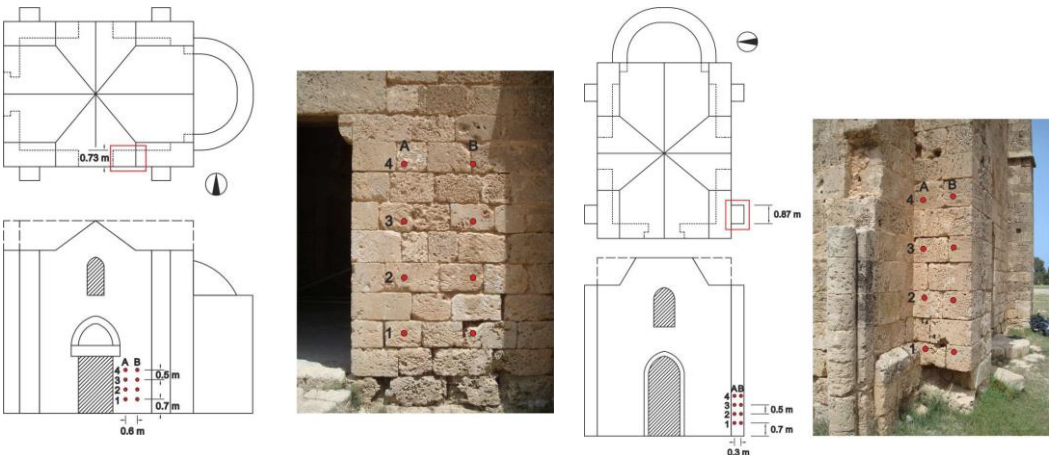

Figure (2.18): Sonic Test Applied to the Armenian Church [Paulo B. Lourenço, Andrés Braga, 2013]

After the aforementioned work, the results indicate that the building presents a considerable safety level in terms of seismic performance, as well as a good overall vertical loading; these characteristics can be attributed to the regularity of the masonry structure and to the high stiffness and almost moderate height of the masonry walls.

Another adapted methodology was followed by H. Animas, M. Navarro, J. Pacheco Martínez, J. L. García, T. Cordero, C. J. Esparza, and J. A. Ortiz-Lozano, in the year of 2014, with purpose of perform an structural analysis of the temple of San Antonio in Aguascalientes, México, figure (2.19) According to this work, three-dimensional analytical macro models are evaluated using the finite element method, the analysis was performed taking into account the linear and non-linear behavior of the masonry.

Figure (2.19): Views of The Temple of San Antonio, [H. Animas, M. Navarro, J. Pacheco Martínez, J. L. García, T. Cordero, C. J. Esparza, and J. A. Ortiz-Lozano, , 2014]

The safety level of the structure was evaluated, and the higher probability zones to be damaged were located, also the seismic vulnerability calculated using a pushover approach. The dynamic response of the structure was determine for different values of the material properties, after that a comparative assessment between all of the results was performed, in order to determine how the change of the properties can affect the results of the modal analysis.

Turning to Spain, the assessment of the structural damage and stability of the church of the Royal Monastery of Santa Maria de Poblet, was done by Savvas Saloustros, Luca Pelà, Pere Roca, and Jorge Portal, in the year of 2015, figure (2.20). This case study is one of the UNESCO World Heritage sites.

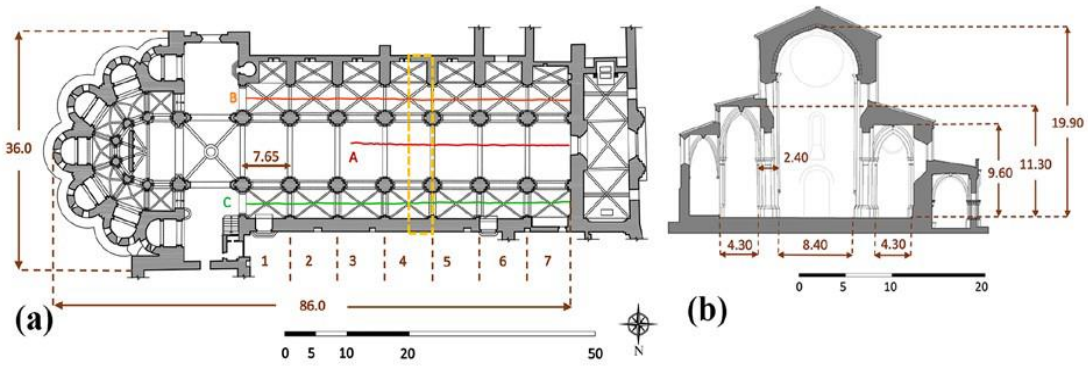

Figure (2.20): Plan and Cross-Section of The Church of the Poblet Monastery,

[Savvas Saloustros, Luca Pelà, Pere Roca, and Jorge Portal, 2015]

The analysis presents damage affecting the lateral aisles and main nave, including existence of the cracking in the vaults and deformation in the clerestory walls. Based on the historical survey and site visiting, a

sophisticated finite element model was used for the structural analysis. The 3D model was developed on the basis of the results of the terrestrial laser scanning survey, in order to take into consideration the current deformed state of the structure. The continuum damage model allowed a realistic representation of the masonry behavior under tension and compression, and simulation of past reported or possible actions i.e. structural alterations and settlements and earthquakes, provided valuable information on the causes of the present deformation and damage of the church.

Also in India, M. Shariqa, S. Haseebb and M. Arifc, 2016, investigate the analysis of existing masonry heritage building subjected to earthquake loading. The work was done on an existing masonry heritage building situated in Aligarh city based on the time history method using El-Centro earthquake data which has been employed for seismic performance of the chosen building. The maximum principal tensile stress and maximum shear stress has been observed and compared with permissible stresses as figure (2.21) presents. It has been found that these stresses exceed the permissible limit at few locations such as dome-wall junction, wall-roof junctions and the minarets. It has also been found that these locations are the most critical portion of the building under earthquake forces.

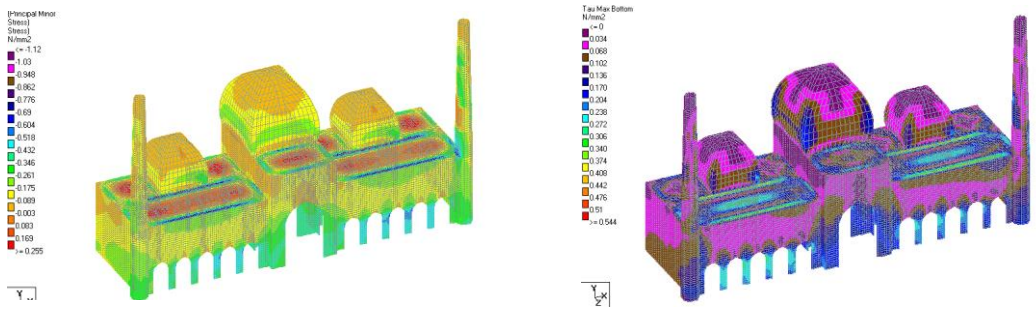

Figure (2.21): Principal Tensile and Shear Stresses for Jama Masjid [M. Shariqa, S. Haseebb and M. Arifc, 2016]

For the Turkey historical moments, again P. B. Lourenço with L. Mangia, B. Ghisaasi, E. Sayın, O. Onat, show the pushover analysis of a historical masonry structure Elti Hatun Mosque, figure (2.22), which is located in Tunceli, Turkey. It is located in the seismic zone 2 according to seismic zone map of Turkey. The modeling and analyzing with Diana finite element software based on real dimensions measured by site visiting, and by adapting macro modeling strategy to model masonry elements.

The results show that the structure is two times weaker in the transversal direction than longitudinal direction, for the main reason referred to existence of the main gate of the structure which works as a rigid support system in the longitudinal direction. On the other hand, the vertical pushover analysis also was done in the same manner, to investigate the safety factor of the mosque under its self-weight, the results is acceptable in all directions. However, the presented results are only a prediction of the behavior due to several uncertainties about the material properties.

Fig.(2.22): Elti Hatun Mosque with its Outside and Inside View. [P. B. Lourenço with L. Mangia, B. Ghisaasi, E. Sayın, O. Onat, 2016]

K. Ip, J. Lester and A. Brown, in 2016, investigate the Cathedral of the Blessed Sacrament, Christchurch – New Zealand, and focusing on the seismic nonlinear analysis of these damaged historic buildings, because as they said, there is no existence for any established guidelines and the only methods of prediction of the structural behavior of historic buildings is empirical. Their used approach is to combine the advantages of the continuum method i.e. Finite elements, with the discrete method, by using constitutive models and contact surface algorithms, which are available in the numerical simulation software LS-DYNA, figure (2.23)

Figure (2.23) : General and 3D View of Cathedral of the Blessed Sacrament. [K. Ip, J. Lester and A. Brown, 2016]

In details, the discrete element and finite element can simulate the complex nonlinear dynamic behavior, and the macro and micro damage modeling in the initial analysis can provide a reasonable estimation of stiffness and strength degradation for the existing cathedral. Also, a good correlation with observed damage on site, can be obvious by the crack patterns, such the estimated stiffness reduction gives a physical measure of the level of damage. The crack, stiffness and strength degradation can be carried over to the pushover analysis or the nonlinear time history analysis as an initial stage situation.

The results of pushover analysis show the existing cathedral as a brittle structure with no ductility, with assumption of damping 5% and the structure is elastic for base shear demand (i.e. $\mu=1$) without considering the strength reduction factor (i.e. $\phi=1$), the ultimate residual base shear capacity could be up to 53%.By the way, the actual capacity is limited by the local instability of structural components; this performance was further confirmed by dynamic analysis, which verified the dynamic response and identifies the local instability considering the structure. The results show also, there is no global collapse occurred, but the arch and portico mega columns completely lost stability under the strong ground shaking.

Panagiotis G. Asteris , Maria G. Douvika, Maria Apostolopoulou, and Antonia Moropoulou, 2017, present a new stochastic computational framework for earthquake-resistant design of masonry structural systems. The proposed framework is based on the probabilistic behavior of crucial

parameters, such as seismic characteristics, material strength, and utilizes fragility analysis based on different failure criteria. The application of the entire methodology is illustrated in the case of a historical and monumental masonry structure, namely the assessment of the seismic vulnerability of the Kaisariani Monastery in Athens, Greece, figure (2.24).

Figure (2.24): General and 3D view of Kaisariani Monastery in Athens, [Asteris , Douvika, Apostolopoulou, and Moropoulou, 2017]

Based on the 3d analysis, the new stochastic computational framework for earthquake-resistant design of masonry structural systems has been established, namely, the fragility analysis has been applied based on the probabilistic behavior of crucial parameters involved in the modeling of the structure, such as the values of materials' strength and the peak ground acceleration. According to the analysis, it has been shown that the proposed approach offers a ranking method that supports civil authorities in optimizing decisions for choosing, among a plethora of structures, which ones present the highest levels of vulnerability and are in need of immediate strengthening. It also plays an important role for the

engineers, in choosing the optimal repairing scenario among a number of competing scenarios.

Giulio Castori , Antonio Borri , Alessandro De Maria , Marco Corradi , and Romina Sisti, 2017, presents the results of analysis carried out on a the monumental masonry building, known as the Civic Museum of the small city of Sansepolcro in Tuscany – Italy, figure (2.25). The building characterized as one of the most important and renowned civic structures, and by presence of one of the masterpieces of late 15th-Century Renaissance art. A full three-dimensional non-linear static analysis based on the limit analysis theorems are used for understand the macro scale structural behavior.

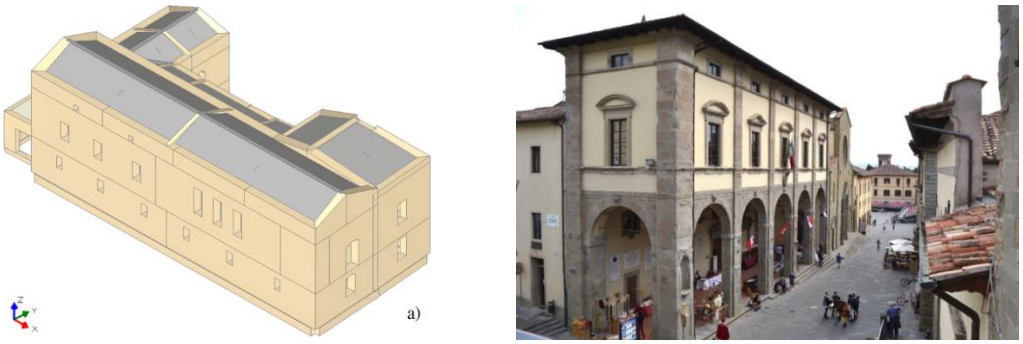

Figure (2.25): General and 3D View of Civic Museum, [Castori , Borri , Maria , Corradi , and Sisti, 2017]

Afterwards, the results of the finite element method analyses performed on a detailed 3D model of the wall panel containing the fresco, which are used for investigating the causes of the cracks patterns. The

results 3D pushover analysis show, on the one hand, the results of the limit analysis and, on the other one, the calibration of the use of a refined 3D finite element model for catching the response of the wall containing the fresco. The results highlight some problems related to the ability of the construction to withstand and offer a good performance levels for both the conservation of the fresco and safety of people who use the Museum. The simplified scheme of limit analysis and the results obtained from the non-linear static analysis presents that the structural behavior in the transversal direction is poor and inadequate, due to the out of plane mechanism, figure (2.26). Also, the application of 3D pushover analysis confirmed some structural deficiencies also in the in plane behavior of the wall panel supporting the fresco, however the observed damage is mainly associated for the presence of shear failure mechanisms.

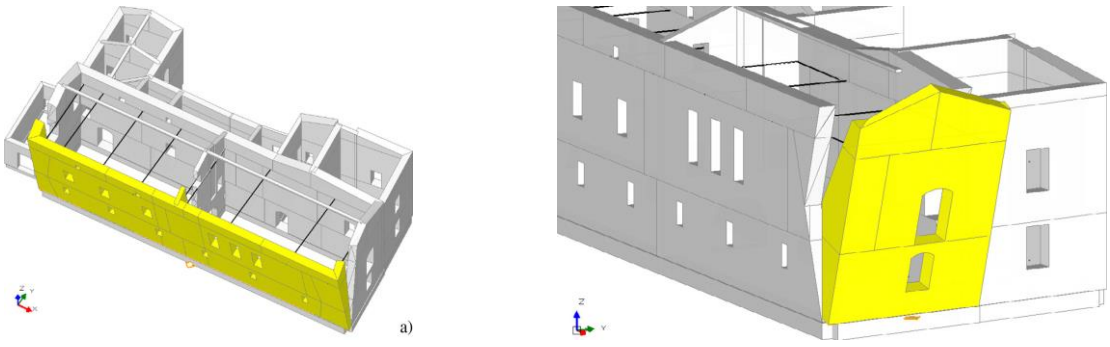

Figure (2.26): 3D Model of Fresco. [Castori , Borri , Maria , Corradi , and Sisti, 2017]

Stay in Italy, in 2018, Gessica Papa, and Benedetta Silva, propose an approach for the assessment of seismic vulnerability from the perspective of prevention and conservation. A comparison of the state of damage has been carried out based on using the case study, St. Salvatore church, figure

(2.27), which underwent two important seismic events in the Central Italy area, the 1997 and the 2016 earthquakes.

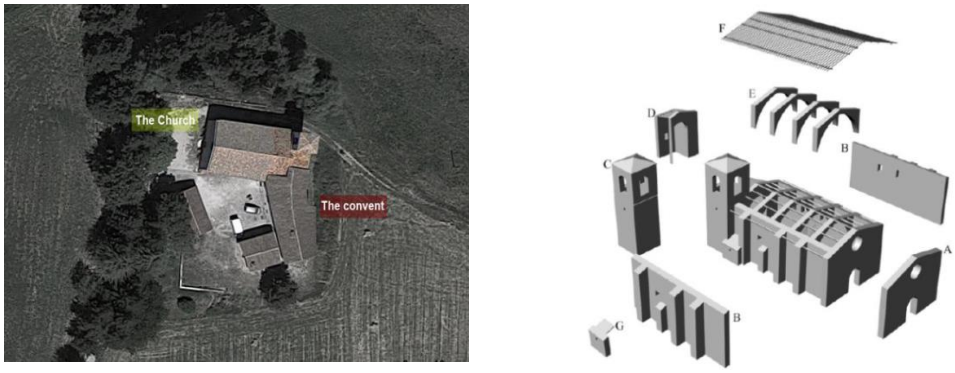

Figure (2.27): Location and 3D of St. Salvatore Church. [Papa, and Silva, 2018]

The multidisciplinary procedure for the assessment of seismic damage demonstrates the advantages in terms of a more exhaustive vision of the damage. This methodology could be applied to other churches in similar manner in Italy and to other similar situations.

2.6.2 Relevant Studies for Palestine

Gabriele Milani, Marco Valente, and Claudio Alessandri, in 2016, present some results of investigations of advanced numerical model carried out on the church of Nativity in Bethlehem. They studied the seismic response of the church and identify possible causes of failure. In details, three dimensional finite element models of the church are developed with the damage plasticity of the material figure (2.28). Nonlinear bidirectional dynamic analysis is first performed on the model in the actual configuration and resulting in observe the damage in the semi-domes, vault system, and near the interlocking of the walls. In second step, the narthex is separated from the church and analyzed under seismic excitation only in the longitudinal direction.

The narthex is considerably affected by presence of vaults which act as connecting element between the façade of the Church and the façade of the narthex. The vault system is subjected to severe damage due to significant stresses. The second critical element of the narthex is the western façade, which tends to show a local overturning mechanism due to the gradual accumulation of damage near the base of the vault system. Also, the façade of the narthex can reach displacements under seismic actions with a_g=0.25g. The results seem to indicate that the rotation of the narthex façade, with a consequent maximum out-of-plane displacement of 40 cm approximately, is probably due to a seismic event of great intensity or to several seismic events occurred in sequence over time. Certainly, results closer to the measured data can be obtained by introducing proper unilateral contact conditions at the interface between vaults and façade walls or between longitudinal walls and façade walls.

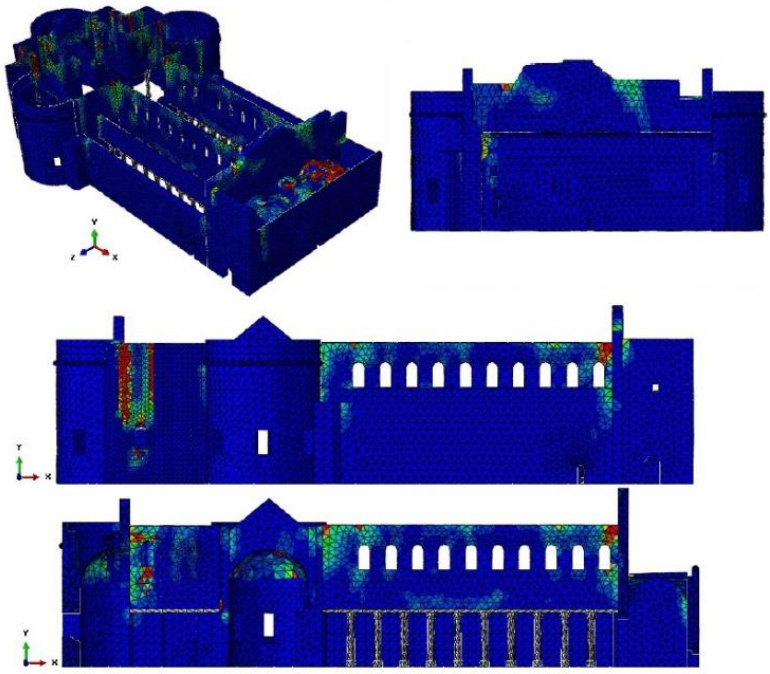

Figure (2.28) : 3D Finite Element Model for The Nativity Church. [Milani, Valente, Alessandri, 2016]

In another side, Claudio Alessandri, with cooperation with Jessica Turrionim in 2017, propose an innovative technique for reinforcing the wall of the Church of the Nativity against earthquakes. Local seismicity data and the parameters of an equivalent Italian site provided the input data for a design earthquake, and 3D modal analysis of the entire Church revealed that the structure is characterized by clear local modes of vibration. As per the most recent studies on masonry structures, local assessment based on limit analysis procedures was performed. This showed that in the event of an earthquake, a Crusade era wall addition is at risk of collapse via simple overturning around its own base, due to the lack of firm connections with the orthogonal walls of the façade and the transept. Hence, a novel double system of horizontal steel tension structures was designed to consolidate the wall, conforming to the main restoration Charter requirements, i.e. lightness, non-invasiveness and reversibility, and being hidden from the sight of visitors. In the absence of reliable local regulations, all analyses, computations and checks on the proposed intervention were carried out with reference to the Italian technical regulations.

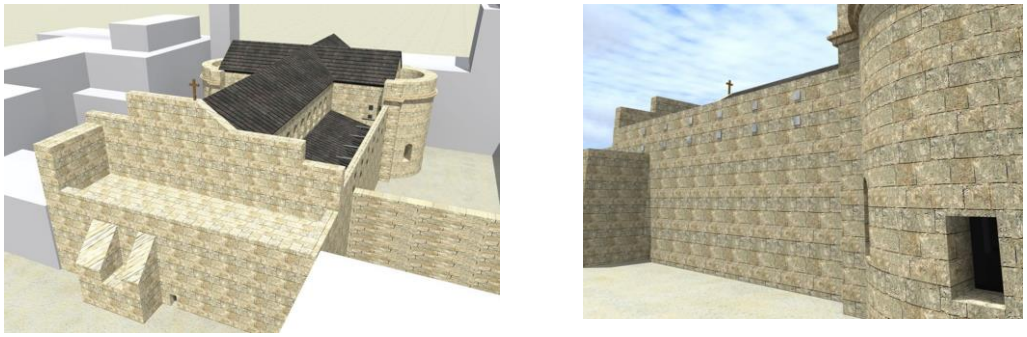

Figure (2.29): Aerial View of the South Wall. [Claudio Alessandri, Jessica Turrionim, 2017]

2.7 Progressive Collapse of Masonry

2.7.1 Introduction

ASCE, which is known as the American Society of Civil Engineers, makes a definition for the progressive collapse, summarizes as the process, by which the failure can spread among the parts of the structure, and by the end, total or partial collapse of a structure occurred.

Seismic excitation, and the need for heightened security of life safety, has created an increased concern for structural design and analysis against progressive collapse for new and existing buildings. Many of the existing structures that are in need of strengthening for those considerations are the masonry structures and monuments. In particular, due to the load bearing wall system and material characteristics of masonry, a loss of load bearing members can lead to multi locational failures, without much warning or time for evacuation of the building. Furthermore, progressive collapse assessment and rehabilitation of the masonry structures can be difficult due to the heterogeneous and anisotropic characteristics of the material, also the brittle nature considering the material, and lack of redundancy in the structural system.

2.7.2 Researches of Progressive Collapse

McGuire and Leyendesker, in 1974, studied five different existing unreinforced masonry buildings and their response to the explosions loads, also if the building would be critical to the progressive collapse. The results

summarized as, two of the buildings are considered to be critical to the progressive collapse, one building has no conclusive results, and the final two buildings are found not critical. Surly at that time, no adequate information for masonry structures, and this led to make the analysis and assumptions different than what they may be today, as an example, the cracking or tensile stress limits of masonry was ambiguous at that time. But today, the Masonry Standard Joint Committee (MSJC) code 2013 provides information and guidelines for dealing with masonry. In details some of the assumptions and outcomes generated from McGuire and Leyendecker in 1974 will be different if done today.

Alternative path examples vary due to the different situations possible with masonry buildings. Providing alternative load paths in masonry structures is dependent upon the connection between load bearing elements and the floor system. The arch behavior, and large openings, with other unique capabilities of masonry are important aspects to consider when looking into progressive. Joint and ties continuity help to resist progressive collapse, and add some integrity to the building. After strenuous efforts, the researcher concluded that there are slight researches in the topic of progressive collapse in masonry structures. Due to this inadequate researching work of directly relevant literature, and to attempt finding information related to progressive collapse analysis of masonry structures, the following approaching topics will be showed:

F. Palmisano, A. Vitone, & C. Vitone, 2005, published their research of the title, “Load path method in the interpretation of masonry vault behavior”, which deals with the performance of application of load path method, figure (2.30). This method offers an interpretation of masonry vaults behavior which is immediately exhibits the correlation between geometry, and distribution of loads, it can be very useful to understand the link between structure and form to diagnose the pathologies of the masonry structures.

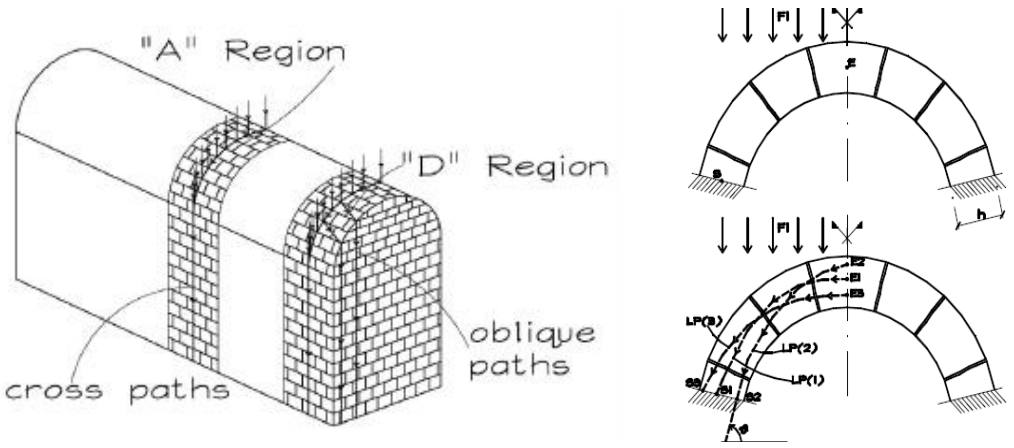

Figure (2.30): Masonry Barrel Vault With Possible Loads Paths in the Arch’s. [F. Palmisano, A. Vitone, & C. Vitone, 2005]

In similar manner, LIN Feng, WANG Ying, GU Xianglin and ZHAO Xinyuan, in 2010, evaluate historical building structures against progressive collapse. They state, for historical buildings, two aspects make them different from the modern buildings, its properties are usually deteriorated to some extent, and the structural constructions may not meet the requirements of current codes. Therefore, a method for evaluations the

performance of the historical buildings to resist progressive collapse is shown here started from evaluate the building layout to protect the inhabitants from the possible collapses, investigate the geometrical information considering the structural constructions and the material properties, and finally analyze the structure with means of alternative path method and tie force method, to establish the resistance capacity for progressive collapse. The proposed method is illustrated by means of a case study of a steel frame historic building in Shanghai, China, namely the Bund 18 building, shown in figure (2.31).

Figure (2.31): The Bund 18 Building, and its Plan View of First Floor.

[LIN Feng, WANG Ying, GU Xianglin and ZHAO Xinyuan, 2010]

The case study (Bund 18 building) was built in 1923, having a total floor area of 10,450 m^2, with height reaches 53.10 m. the current situation of the Historic Building in Shanghai is excellent. In the original design the building was mainly used for as offices, but its function now transformed into a commercial building.

The evaluation of building layout shows that the roads around the building are straightforward with no obstructions, also, the distance between building and the roadside is about 5m, which is less than requirements 25m in the relative criterion (DoD 2003). In addition, there is no explosion proof wall around the sides of the building according to the retrofitting plan, and no any protective measures taken for the structural elements. For the investigation of geometrical information and material properties, an in situ inspection technique used to determine it. And finally, the analysis of the structure with means of alternative path method and tie force method, gives the results proved that the constructions of the building meet the requirements of DoD (2005), for all types of tie forces. Also for alternative path method, a computational model, using finite element method and based on computer program SAP2000, shown in figure (2.33), used for removal of some columns, and analyze the building with the nonlinear static analysis, to evaluate the performance of this structure to resist progressive collapse, which is relatively concluded well.

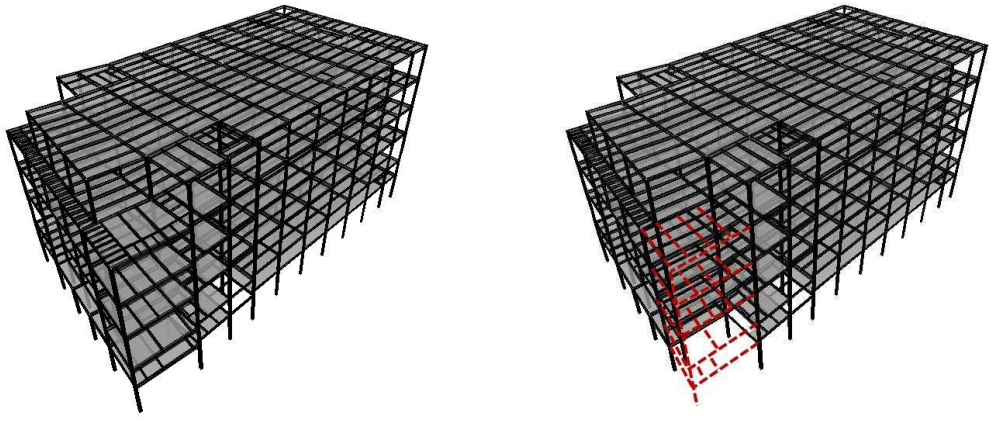

Figure (2.32): The 3D Model With Collapse Due to Removal of Some Columns.

[LIN Feng, WANG Ying, GU Xianglin and ZHAO Xinyuan, 2010]

On the other hand, Xu, Zhen, Lu, Xinzhrng, Guan, Hong, Lu, Xiao, Ren, and Aizhu, in 2013, Published a paper of “Progressive Collapse Simulation and Critical Region Identification of a Stone Arch Bridge” In Journal of Performance of Constructed Facilities. The need for this paper was generated due to occurring of progressive collapses of arch bridges in recent years, which is resulting in many damages and significant losses.

2.7.3 Relevant Codes and Standards

In this part, the reader will see the codes and standards which are studied to resist progressive collapse, and to determine deficiencies that may exist in the analysis for existing masonry buildings. The researcher focuses on current codes and standards starting from American standards to Europe codes, in order to find differences that may exist.

2.7.3.1 IBC 2012

The International building code (IBC) 2012, establish the foundation for minimum requirements considering buildings and public safety. In particular, for high rise buildings, or high risk regions, IBC, lays out, the requirements to ensure the structural integrity, also for load bearing structures, the vertical ties are required in all walls, in addition to transversal, longitudinal ties at each floor. IBC goes on, to provide design methods and equations in order to meet these design requirements.

2.7.3.2 ASCE 7-10

The American Society of Civil Engineers (ASCE) 2010, in similar manner, provides minimum design requirements for buildings through the United States. ASCE provides a minimum requirement for structural integrity for all buildings, in particular, the section 1.4 of ASCE 7-10 states that “all structures must have a continuous load path for the structure and a lateral force resisting system capable of resisting the appropriate notional loads for each level derived from the structure’s weight”.

The commentary of section 1.4 indicates that these requirements are intended for “normal service and minor unanticipated events”.

ASCE 7-10 also, provides load combinations for design, in two general approaches, known as direct and indirect, and provides guidelines for the provision of general structural integrity, as shown below: Indirect Design: defined in ASCE 7-10 as “implicit consideration of resistance to progressive collapse, during the design process through the provision of minimum levels of strength, continuity, and ductility”. The indirect design method will be difficult to use for existing masonry buildings, due to the addition of ties. Direct Design: defined in ASCE 7-10 as “explicit consideration of the resistance to progressive collapse during the design process”. Two procedures, known as alternate path method and specific local resistance method, are presented to accomplish this consideration. These procedures allows local failure to occur, but seeks to provide alternate load paths so that the damage is absorbed and major collapse is

averted" while the local resistance method "seeks to provide sufficient strength to resist failure from accidents or misuse" (ASCE, 2009).

Guidelines for the Provision of General Structural Integrity: ASCE 7-10 shows several concepts that would achieve the required structural integrity of buildings, i.e. adding load bearing members or partitions, adding reinforcement in slabs, and changing the direction of span of floor slabs.

2.7.3.3 MSJC-13

The Building Code Requirements and Specification for Masonry Structures (Masonry Standards Joint Committee, 2013), states that, the masonry structures are load bearing systems, so it is important to review the guidelines that may be presented within masonry code requirements, with regard to progressive collapse. Also, states that masonry structures may be required to have enhanced structural integrity as part of a comprehensive design against progressive collapse due to accident, misuse, sabotage or other causes" (MSJC, 2013). So, it goes on to reference the commentary section 1.4 of ASCE 7-10, as general design guidance.

2.7.3.4 GSA 2013

The General Service Administration (Alternate Path Analysis and Design Guidelines for Progressive Collapse Resistance) which is known shortly as General Services Administration, (GSA, 2013), publish the latest previsions in October 2013 and replaced the document "GSA Progressive

Collapse Analysis and Design Guidelines for New Federal Office Buildings and Major Modernization Projects" which was published in June 2003. The new provisions have good modifications which can be summarized as elimination of the tie force method and the local resistance method, which presented in Unified Facilities Criteria (UFC) 04-023-03: Design of Buildings to Resist Progressive Collapse for all materials, which leave only the alternative path method for design and analysis.

2.7.3.5 UFC 04-023-03

Design of Buildings to Resist Progressive Collapse, (Department of Defense, 2009), shows the guidelines for progressive collapse were updated in 2009. These guidelines are written by the United States Department of Defense, and state three different design procedures that can be used with masonry, such that, tie force, alternate path , and Enhanced Local Resistance. Occupancy category ensures for applying the tie force and enhanced local resistance procedures, but when tie force requirements cannot be met, the alternate path method must be used. It is noted within the UFC that the alternate path method is "often the most practical choice" for load bearing wall structures (DoD, 2009).

2.7.3.6 ASCE 41-13

American Society of Civil Engineers, 2014, (ASCE 41-13) is referenced by UFC 04-023-03 for analysis procedures with respect to the building material of the structure. All details and material sections in ASCE

41-13 provide analysis guidelines such as modeling criteria, acceptance criteria, and strength calculations. For the strength calculations as an example, it lacks in some areas when compared to the steel and concrete sections of the standard. These areas include information about recommendations for retrofit strategies, and connections in masonry structures. The masonry section of ASCE 41- 13 addresses the condition assessment for existing buildings, and the strength requirements of reinforced masonry, unreinforced masonry, infill panels, and foundation elements.

2.7.3.7 EUROCODE

This national standard for European countries lays out guidelines and requirements for designing buildings to resist progressive collapse. Euro code: Basis of Structural Design (EN 1990) sets out the general requirements for structural design by stating “A structure shall be designed and executed in such a way that it will not be aged by events such as: (1) explosion, (2) impact, and (3) the consequences of human errors, to an extent disproportionate to the original cause” (European Committee for Standardization, 2001). It continues on to state that this shall be avoided or limited by selecting and designing a structural system such that it can survive adequately from the accidental removal of an individual member (aka: progressive collapse) Euro code 1 – “Actions on structures – Part 1-7 (EN 1991-1-7): General Actions – Accidental Actions” (European Committee for Standardization, 2006): This section gives more specific

requirements for progressive collapse actions on structures and the strategies that should be used to prevent progressive collapse depending on the risk category of the structure. Along with taking measures to reduce the probability of an event that would cause progressive collapse, the design strategies mentioned include the use of horizontal and vertical ties, and/or ensuring that upon the removal of an element, the building remains stable and damage does not extend past a certain limit. The limit stated in this national standard is 100 m2 or 15% of the floor area, whichever is smaller. For load-bearing structures, the length of wall to be removed for analysis is 2.25 times the story height for internal masonry walls and for exterior masonry, the length between other vertical lateral supports. In the event of using notional removal of a section of wall for design, these sections are referred to as key elements and should be designed to withstand the recommended load of 34 kN/m2. Similarly to UFC, Eurocode states that for load-bearing wall structures, the notional removal of a section of wall is most likely the most practical approach for design compared to using ties. Eurocode 6 – "Design of Masonry Structures – Part 1-1 (EN 1996-1-1): General Rules for Reinforced and Unreinforced Masonry Structures" (European Committee for Standardization, 2005): This section for masonry design demands that masonry structures are to be designed so there is a "reasonable probability" the structure will not be damaged to an extent that causes progressive collapse due to accidental situations. The section also lists the design methods discussed in EN 1991-1-7 in order to ensure progressive collapse does not occur. Like the masonry standard, other Euro

codes for steel and concrete also reference EN 1991-1-7 for design against progressive collapse. Unlike the UFC 04-023-03 and the GSA provisions referencing ASCE 41, the Euro code does not reference the seismic analysis procedures that exist in the Euro code to be used for analysis of progressive collapse.

CHAPTER THREE

MODELING of CASE STUDY

3. Modeling of Case Study

3.1 Introduction

The seismic assessment for any structure needs to study fundamental dynamic properties. In this thesis, the needed dynamic properties are obtained by using the finite element method. 3D linear and nonlinear analyses are done for the case study which is the church of nativity. The model built using two software's, the first by SAP2000, and the another by DIANA FEA, this work done after the survey of archeological existing building, and making the data acquisition to produce a clear geometrical Image.

3.2 Case Study: The Church of Nativity

This Church is one of the earliest Christian structures, which is the birth place of Jesus. The original Basilica, created in the 4th century by Emperor Constantine, which was completely damaged in the Samaritan Revolt, (Qustandi Shomali (2015)). It was replaced later on the same site, by another Basilica; it was different in its plan and had at that time, modified parts of the original building, figure (3.1) present this basilica.

The location of church is Bethlehem, separated as a 10 km south of Jerusalem, which was built over fertile limestone hills. The district center developed moderately two hills and the extent of the settlement that existed at the end of the 19th century has been delineated as the 'historic center' for management and conservation processes. Appendix (A), show the general drawings of the case study

Figure (3.1): Perspective Picture for Church of the Nativity

The church mainly constructed of masonry walls, which are composite material consisting of an assemblage of stones and mortar joints, each of them has different properties, and due to the low tensile and shear bond strength, mortar joints act as a plane of weakness.

3.3 Finite Element Method

The Finite Element Method FEM is a numerical technique used to perform analysis for any given physical phenomenon, its solution is the most spread one among researchers because it offers accurate representation of complex geometry, permit researchers to work with inclusion of dissimilar material properties, capture of local effects, and also support variety of possibilities for the description of the structures made of masonry. In more details, when creating a Finite Element model it is usual

make some assumptions to simplify the work, such as, boundary conditions and connections between different structural parts which are not modeled with complete certainty. In addition, this method is based upon the material properties (Young's modulus, mass density, etc.). The shape function of the chosen elements determines the distribution of the mass and stiffness properties, so that the terms in the mass and stiffness matrices can be understood physically. However, alternative elements are available with different shape functions and for that reason the Finite Element models are meaningful but non-unique. Consequently, the researcher will need to examine the sensitivity of the created model, and its results to changes in the mesh configuration and/or boundary constraints.

For the case study of church, there are two main approaches to model masonry walls, the first one can be by studying walls as each component like solid elements, mortar, and backfill which is summarized by micro level, and the other one can be by studying it as composite material which is summarized as macro level.

The aforementioned approaches refer to different fields of application; micro 3D models are applicable when the object of the study is specified in local behavior of masonry itself, while macro 3D models are used when there must be a compromise between accuracy and efficiency. When using macro modeling, every component of wall such as unit, mortar and their contact is represented as a homogeneous anisotropic block, and meshes are very simple, since the internal structure of the masonry is not

described, and may not reproduce the masonry pattern which is make this approach is less mathematical and computations demanding, as a result most researchers prefer! On the other side macro models are used when the purpose of research is scrutiny seismic behavior of historical, archaeological, and complex structures (i.e. cathedrals, bridges).

3.3.1 Software's used in the Study

Through the study of SAP2000 and DIANA FEA software's which are used, in the analysis, important highlights can be shown, in the first hand; SAP2000 is a finite element package used mainly by civil engineers, can analyses general structures, i.e. buildings, bridges, dams, and solids etc. but, in the second hand, DIANA FEA is advanced finite element software usually used for advanced works and simulations, also mainly in academic purposes. In details; the physical problems concerning fluids flow, heating, contact analysis, also, static and dynamic analysis can be simulated by DIANA FEA easily.

The solid element used by SAP2000 is an eight node; each solid element has six quadrilateral faces, with a joint located at each of the eight corners as shown in Figure (3.2), in addition, the solid elements of SAP2000 have three translational degrees of freedom at each joint, and the rotational degrees of freedom are not active. The stresses are evaluated by using the standard Gauss integration points of the elements and extrapolated to the joints.

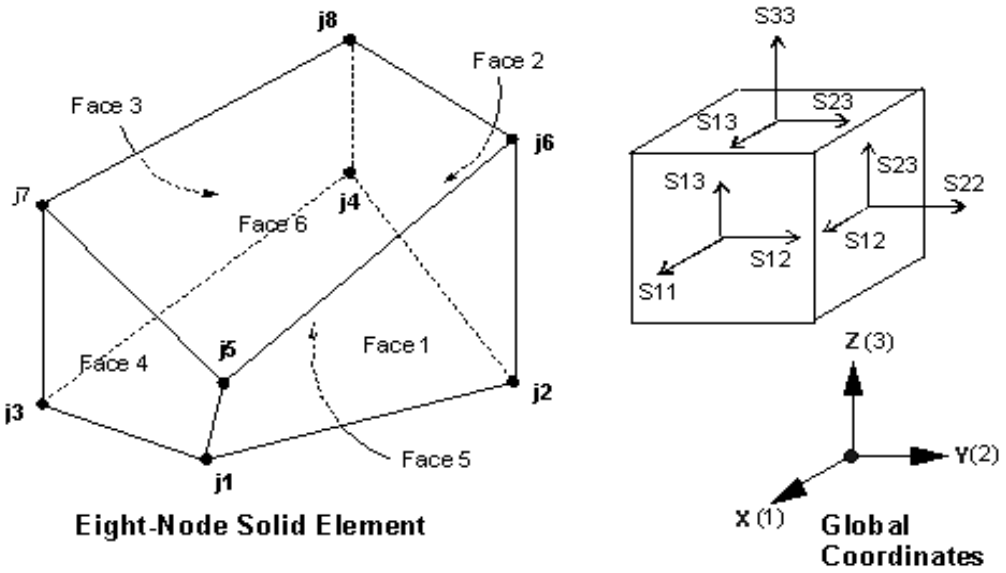

Figure (3.2): Eight Node Solid Element in SAP2000

After investigating the SAP2000, the DIANA FEA takes the place, and gives numerous kinds of solid elements. The type of regular solid elements used for the numerical model, figure (3.3), according to the DIANA FEA manual, are; firstly, HX24L element, which is brick geometric element with eight nodes, figure (3.4a), and establish about 17280 unit in the model.

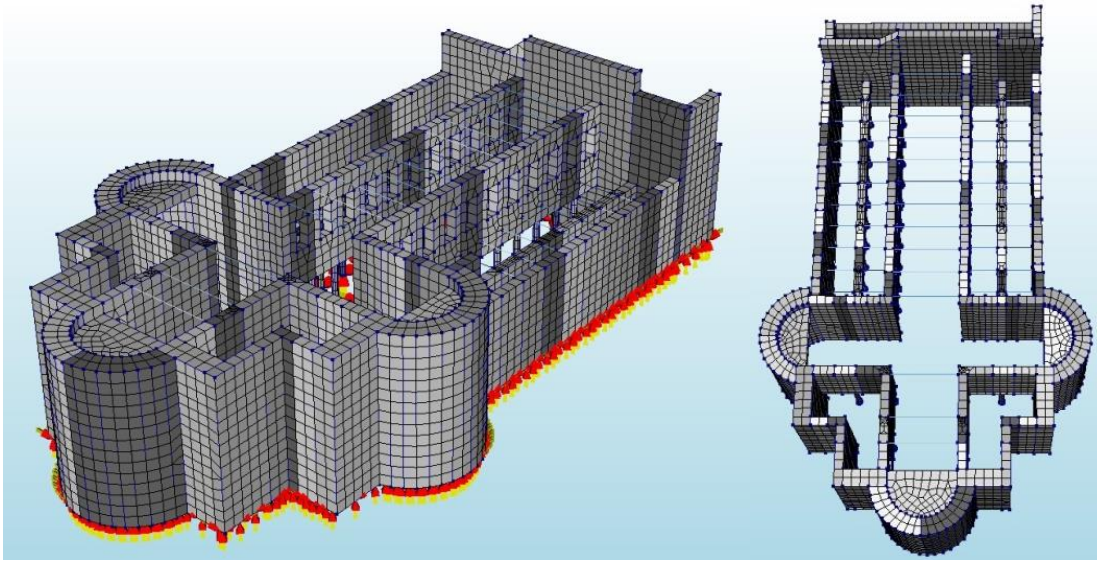

Figure (3.3): 3D Numerical Model Built in DIANA FEA Software.

Secondly, PY15L element which is pyramid geometric element with 5 nodes, 4 sides, and found in 238 location in the model, figure (3.4b), thirdly, there are a 624 units of TE12L element, figure (3.4c), which is characterized as tetrahedron geometric element with 4 nodes and 3 sides, and in the final, the trusses elements in model, are modeled as bars which meet the condition that the dimension D perpendicular to the bar axis are small in relation to the bar's length L, as figure (3.4d), and exist in 47 location as 480 units.

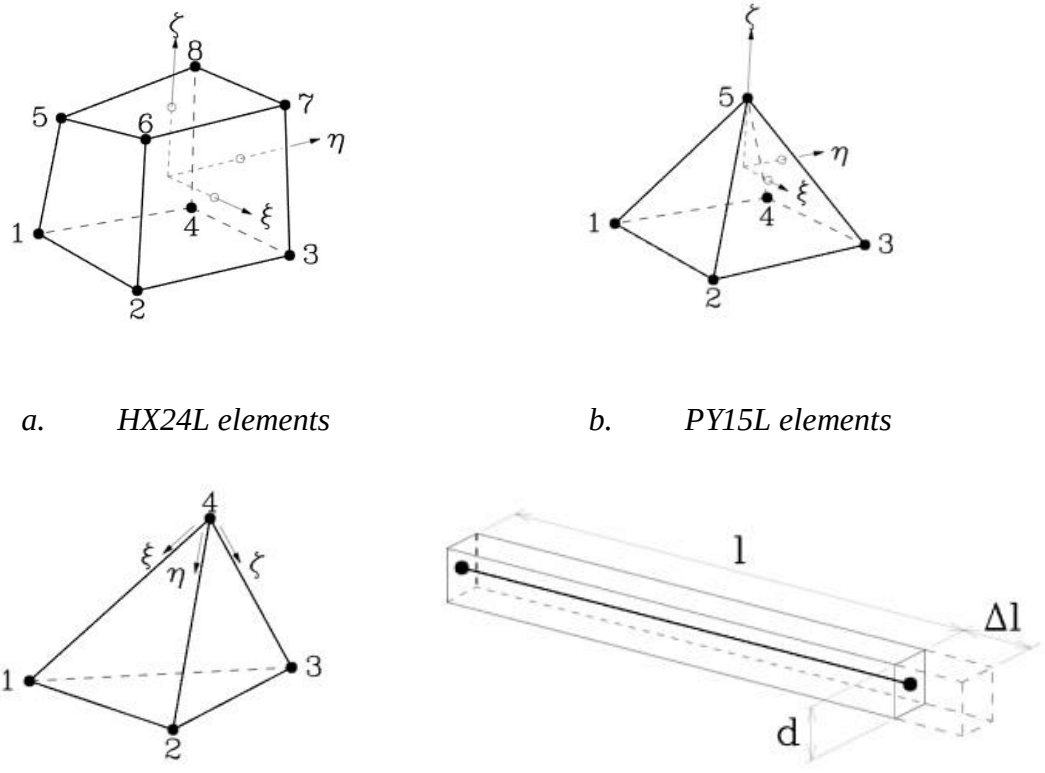

a. HX24L elements *b. PY15L elements*

c. TE12L elements *t. Trusses elements*

Figure (3.4): 3D Solids Used in Modeling According to DIANA Manual

3.3.2 Mechanical Properties for Models

It's important to show that, a finite element model of the Nativity church is created by using both software's SAP2000 and DIANA FEA, with the same material characteristics. In details, the Nativity Church has different materials which are can noticed through a visual inspection.

The use of in situ inspection techniques such as coring, flat jack tests, thermo vision, sonic tomography, etc. is not applicable in some cases for obtaining all the desirable information, sometime these limitations due to saintliness, privacy, and no permissible demolitions in the structure. As a result, and due to lack of laboratory information for materials of the church, the mechanical properties of the material observed will be used based on a number of onsite tests have been carried out by Claudio Alessandri and Jessica Turrioni in 2017, and published in their paper under the title of "The Church of the Nativity in Bethlehem: Analysis of a Local Structural Consolidation". These tests focusing on the structural components of the Church, and generating the material properties of masonry walls like compressive strength (F_m), shear strength (t_d), Young's modulus (E), shear modulus (G), Poisson coefficient υ, and own weight (w). The constitutive model is a macro model with the given elastic material properties summarized in table (3.1) reports the selected values needed for the definition of the model parameters with respect to some principal elements.

Another important two points must be discussed; the first which is the most predominant characteristic of masonry is that it has a very low

tensile strength. So in the analysis work, the tensile strength will be assumed 5% of the compression strength of the macro model elements. In more details, for narthex and the church walls, the tensile strength is 0.233 MPa, for some specific narthex components it is 0.175 MPa, and finally it is 0.05 MPa for the vaults. The second point, considering the shear transfer coefficients which are taken 0.1 for open cracks and 0.9 for closed cracks. This means that 90% of the force is redistributed to the adjacent nodes when the crack opens and 10% of the force are redistributed when a crack closes.

Table (3.1) ; Properties OF Nativity Church

Properties for Perimeter walls of the narthex and the Church itself			
F_m (MPa)	t_d (MPa)	E (MPa)	G (MPa)
4.66	0.089	1429	460.75
Properties for some specific narthex components			
F_m (MPa)	t_d (MPa)	E (MPa)	G (MPa)
3.49	0.067	868.38	147.25
Properties for vaults			
F_m (MPa)	t_d (MPa)	E (MPa)	G (MPa)
1.01	0.02	456.75	147.25

3.3.3 Verifications of Models

3.3.3.1 Modal Shapes

The modal shapes concerning the deformations established using SAP2000 and DIANA FEA, are summarized and compared in this section. The following figures show the deformed shapes for the first 8 modes, for the model built using SAP2000, figure (3.5) show the arrangement start from mode (1) to mode (8). Similarly, for the model built using DIANA

FEA, figure (3.6) arranges them also from mode (1) to mode (8). It is manifest that both models give analogical modal shapes.

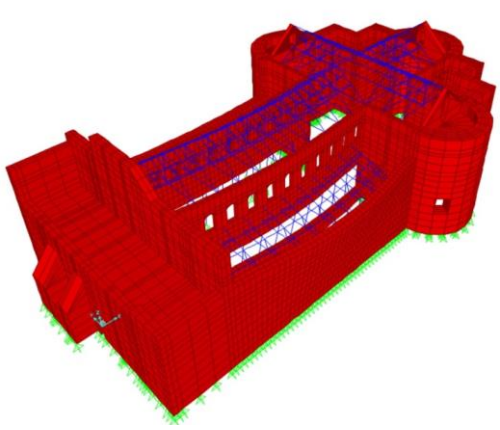

Mode (1): T = 0.53 sec, f = 1.89 Hz

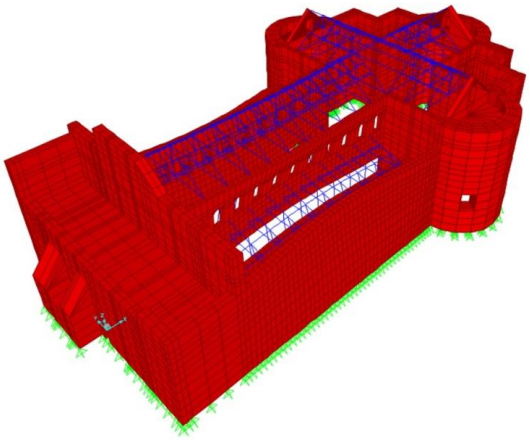

Mode (2): T = 0.45 sec, f = 2.22 Hz

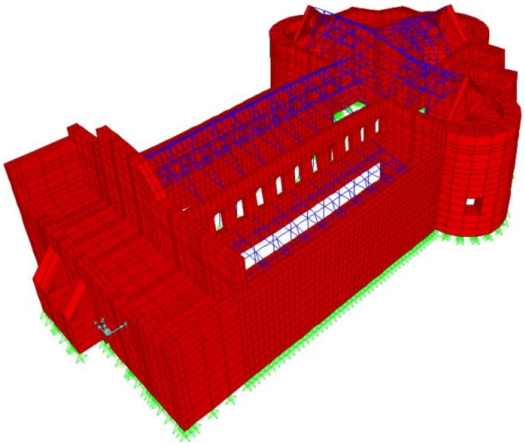

Mode (3): T = 0.35 sec, f = 2.86 Hz

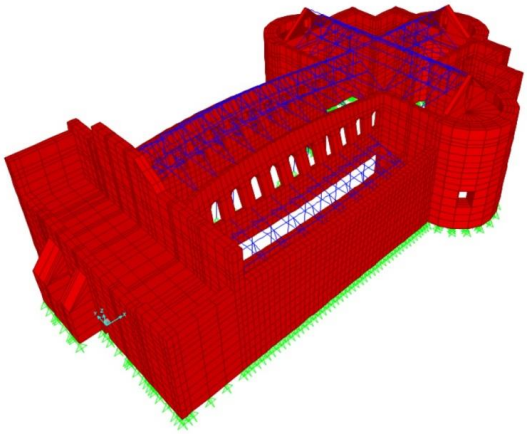

Mode (4): T = 0.29 sec, f = 3.45 Hz

Figure (3.5): Periods and modal shapes concerning the 3D model – SAP2000

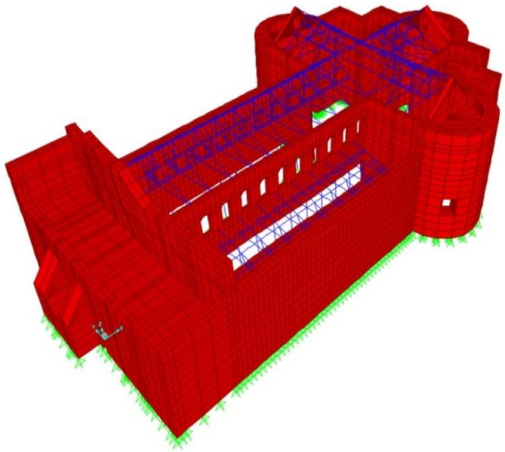

Mode (5): T = 0.25 sec, f = 4.00 Hz

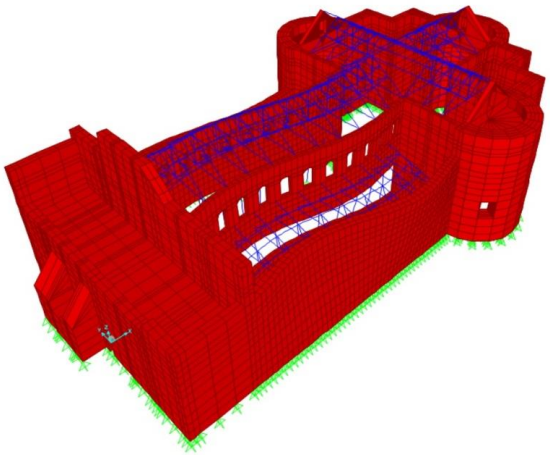

Mode (6): T = 0.24 sec. f = 4.17 Hz

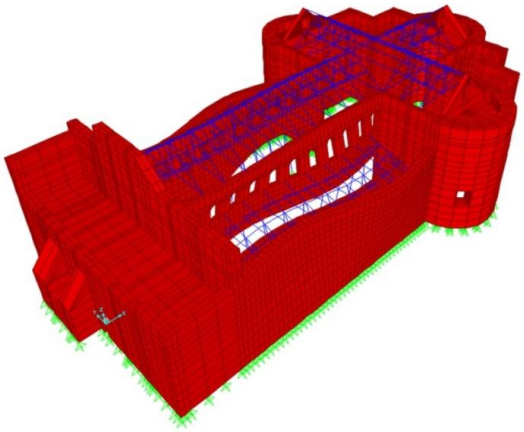

Mode (7): T = 0.20 sec, f = 5.00 Hz

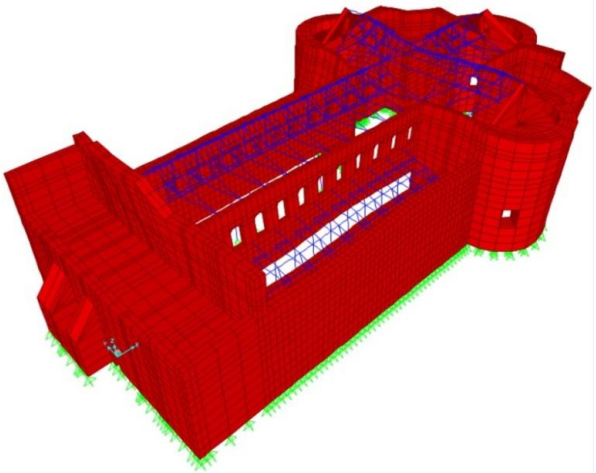

Mode (9): T = 0.18 sec, f = 5.56 Hz

Figure (3.5): Periods and Modal Shapes Concerning the 3D Model – SAP2000 – Cont'd

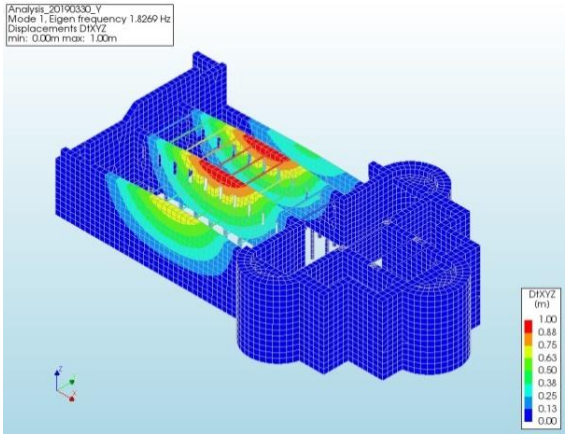

Mode (1): T = 0.55 Sec, f = 1.83 Hz

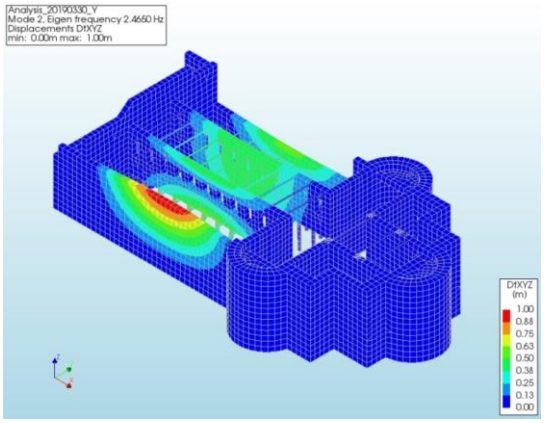

Mode (2): T = 0.41 Sec, f = 2.47 Hz

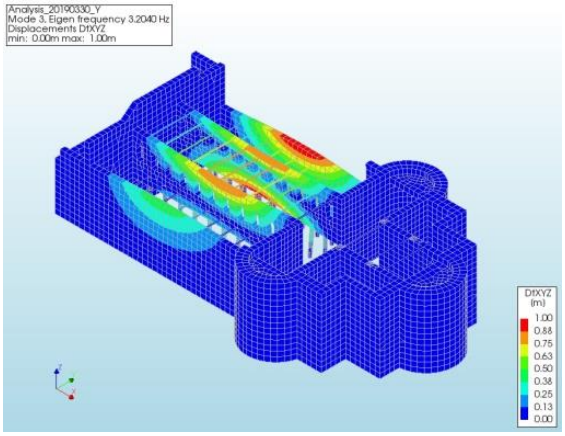

Mode (3): T = 0.31 Sec, f = 3.20 Hz

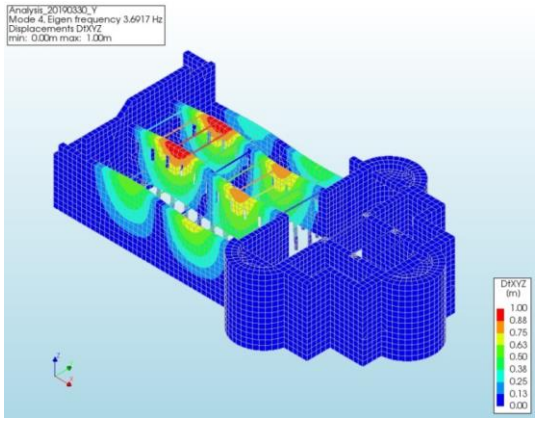

Mode (4): T = 0.27 Sec, f = 3.69 Hz

Figure (3.6): Periods and Modal Shapes Concerning the 3D Model – DIANA FEA

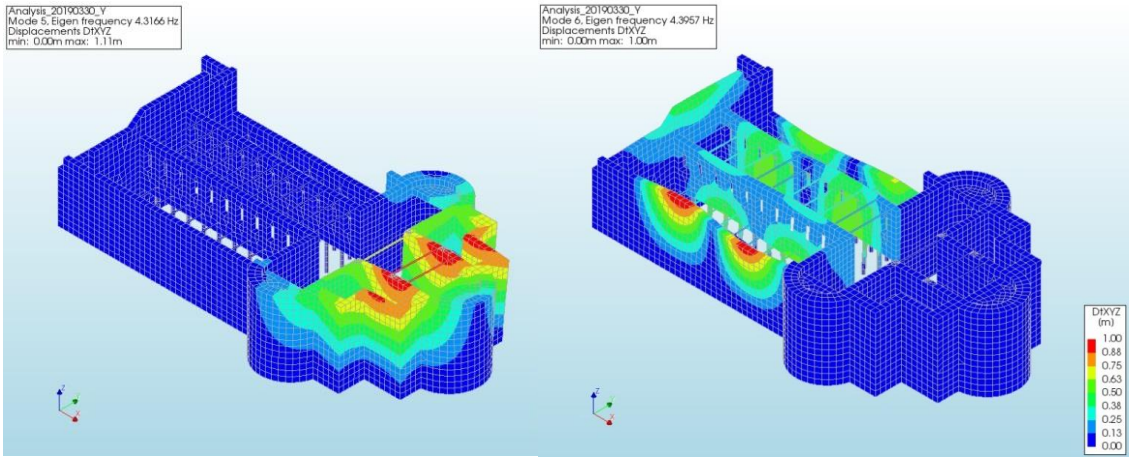

Mode (5): T = 0.23 Sec, f = 4.32 Hz

Mode (6): T = 0.23 Sec, f = 4.40 Hz

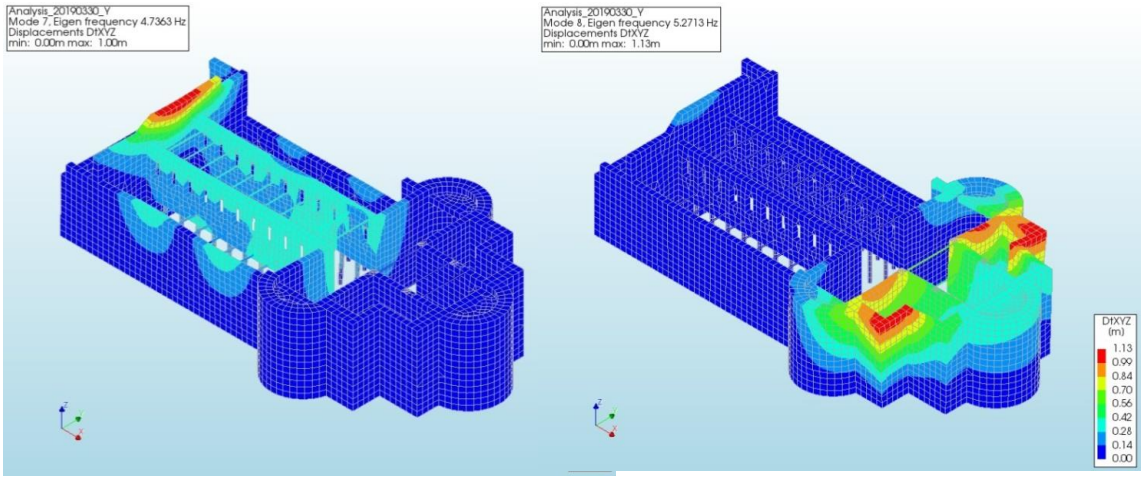

Mode (7): T = 0.21 sec, f = 4.74 Hz

Mode (8): T = 0.19 sec, f = 5.27 Hz

Figure (3.6): Periods and Modal Shapes Concerning the 3D Model – DIANA FEA – Cont'd

3.3.3.2 Modal Analysis

Although, the real structure has infinite number of modes, not the all modes in practice for application, or can be concerned. In this section, investigation of figures (3.5) and Figure (3.5) represents the modal analysis which shows the vulnerability and possibility for out of plane mechanisms, in details the first, forth, and sixth modes show the applicability of interior walls to overturn and move in harmonically motion. In addition, out of plane mechanisms are possible also for the southern and northern walls, whose safety assessment would be necessary with a local analysis, and can be confirmed in the second and third modes. As similar, the five and eight modes of the "as is" model involves the translation motion in the two principal directions of churches shoulders, these shoulders which have the properties of perimeter walls, plays an important role in connections between semi-circular apses, and finally the seventh mode shows the

overturning mechanism of the façade, which undergoes larger displacement.

Table (3.2)			
No.	**Mode**	**SAP2000**	**DIANA FEA**
1	Mode (1)	0.55 Sec	0.53 Sec
2	Mode (2)	0.41 Sec	0.45 Sec
3	Mode (3)	0.31 Sec	0.35 Sec
4	Mode (4)	0.27 Sec	0.29 Sec
5	Mode (5)	0.23 Sec	0.25 Sec
6	Mode (6)	0.23 Sec	0.24 Sec
7	Mode (7)	0.21 Sec	0.20 Sec
8	Mode (8)	0.19 Sec	0.18 Sec

Table (3.2) shows the corresponding modal periods for the first 8 modes, and followed by a comparison between them. One of the expected behaviors of this kind of a masonry structure is low modal periods. The results verify this anticipation as shown. Also, the Figure (3.7) and Figure (3.8) show the modal frequencies and the error corresponding to the modal periods assuming DIANA FEA results as more accurate. It’s obvious that modal periods are very close to each other and the maximum percentage error is 11.23%.

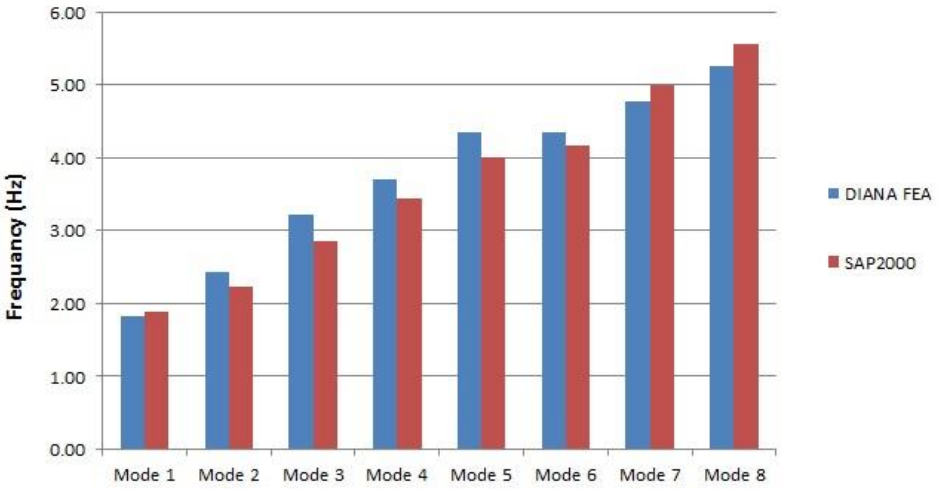

Figure (3.7): Comparison Between Frequencies of Two Models

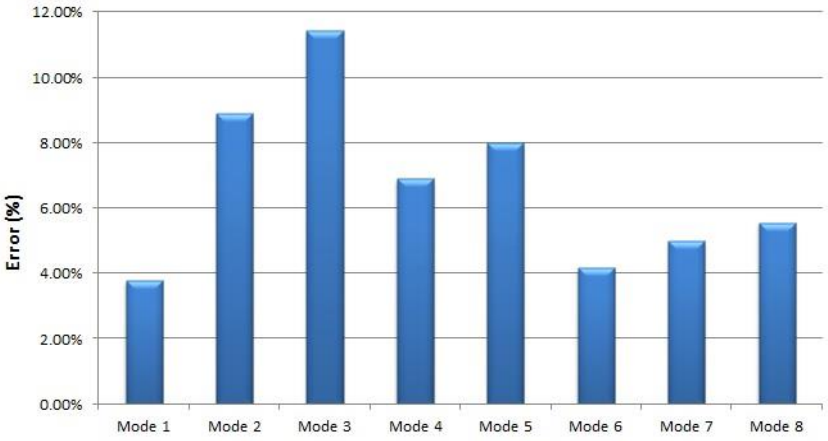

Figure (3.8): Errors Between Frequencies of Two Models

CHAPTER FOUR
NON-LINEAR STATIC ANALYSIS

4. Non – Linear Static Analysis

4.1 Introduction

The non-linear static analysis with horizontal forces, also known as pushover analysis, is carried out with the finite element program DIANA FEA after modeling the structure of The Church of Nativity. The model is close to the real condition and used to simulate the historical masonry components, and it is provide reliable results.

In the first stage, the seismic analysis are performed and concerning the first unidirectional mass proportional load pattern, in both directions, X direction, as a longitudinal direction, and Y direction, which is refer to the transversal direction, and uses an incremental iterative procedure with monotonically increasing horizontal loads, with constant gravity loads.

The purposes that direct the researcher to apply this method start from the goal of estimation the distribution of damage, expected failure mechanisms, and ends with the assessment of structural performance of the existing building, i.e. the static loads applied in horizontal direction and a selected control displacement caused by these loads (EN 1998-1, 2004).

4.2 Constitutive Model

The material model used for the behavior of masonry combines the plasticity model for compression (Drucker-Prager failure criterion), and the smeared cracking model for tension (Rankine failure criterion), figure

(4.1). In details, the Smeared cracking is specified as a combination of shear retention, tension softening and tension cutoff, with constant stress cut off is chosen. The linear tension softening based on the energy of fracture was selected, and used the crack bandwidth, where the cracks are not described one by one but are continuously spread within the element and reduce the stiffness, and finally, constant shear retention is chosen due to the cracking of the material, results of shear stiffness to be usually reduced.

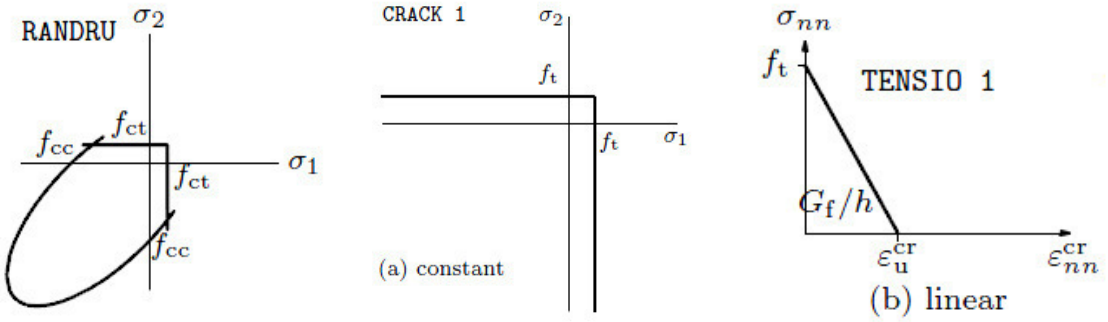

Rankine & Drucker-Prager Tension cut-off Tension softening.

Figure (4.1): Material Models Used for The Behavior of Masonry.

Also, in the modeling procedure, the overestimation of the stiffening effect given by the flexible roof is avoided, so in other words, only the weight of the new roof was estimated, and lower values of the mechanical properties are applied to the connections. These values are used in connections between facade and upper wall of the nave, transept and nave, transept and apses. The buttresses supporting the chapel vaults are assumed totally connected with the wall of the narthex.

Note that all the other linear and non-linear material parameters stated before are used with no modifications, and finally, for the entire aforementioned pushover analyses, uses the regular Newton-Raphson method for the iteration process, an energy convergence control with a tolerance of 10e6, the line search algorithm and arc length control.

In Force control method, and for models experiencing the softening, this method cannot lead to a solution when the load applied is higher than the capacity, on another hand, in a displacement control analysis the displacement of a reference point is incrementally applied. Figure (4.2) show the way of two procedures.

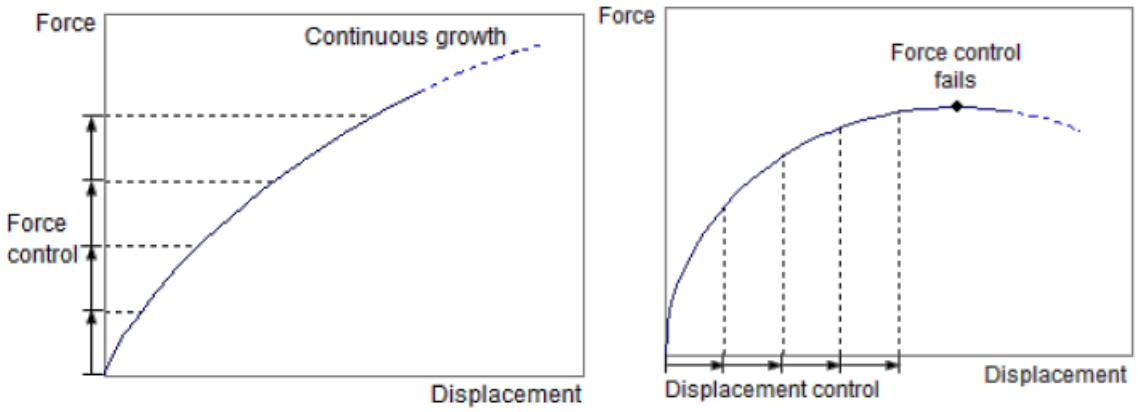

Figure (4.2): Force Control Versus Displacement Control. [Palacio, 2013]

After that, the details of arch length should be present, when the curve of load-displacement is almost horizontal, the prediction of the displacements increment are very large, also when the loads increment is fixed, this mean the result of predictions the displacements will be large. This overcome this behavior, the analyst use an arc-length control, where

the increment is adjusted. This method works is illustrated in the figure (4.3).

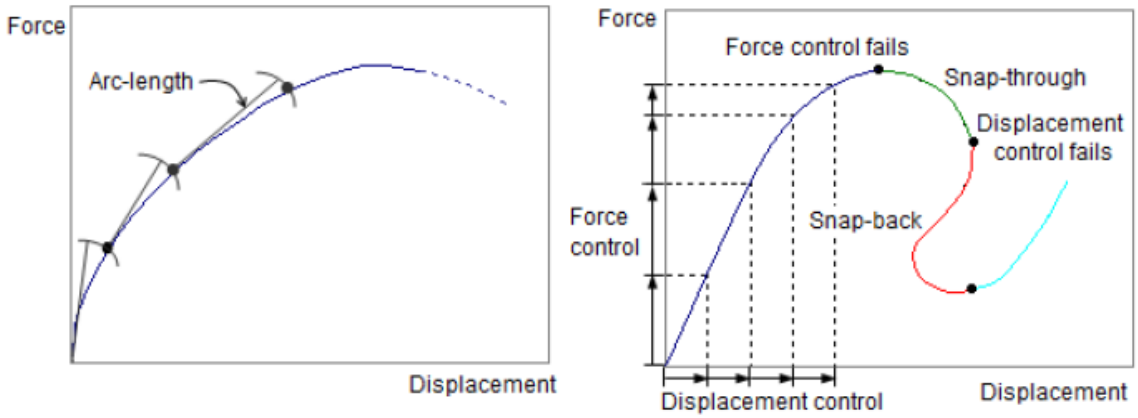

Figure (4.3): Load Increment Methods Characteristics and Arc-Length Control. [Palacio, 2013]

Appendix (C), show the iterative process as defined in DIANA FEA. In all processes the total displacement increment is adapted iteratively by the increment till equilibrium is achieved. The total displacement of iteration is therefore defined as:

$$\Delta_{ui+1} = \Delta_{ui} + \delta_{ui+1} \qquad 4.1$$

Where:

Δ_{ui+1}: Total displacement increment at iteration (i);

Δ_{ui} : Total displacement increment at iteration (i+1);

δ_{ui+1} :Iterative increment.

4.3 Cracks Propagation

The prediction of monuments response against detachment is necessary to reduce the risk of damage for this architectural heritage, but unfortunately, majority of the masonry research's deal with failure due to either in plane or out of plane behaviors. However, failure of masonry walls due to cracks propagation, though frequent, has not been researched much.

Such a method of modeling is effective in determining the propagation of cracks through the masonry structures is pushover analysis, this analysis method very often used to evaluate the seismic performance of masonry structures by making the seismic action simulated by means of static horizontal forces and the material exhibits nonlinear behavior, by which the cracking pattern can be generated, suggests the mechanism to be considered in the limit state analysis and offers an indication on the potential strengthening design (Lourenço and Oliveira 2007). By the way, this chapter shows the results of cracks propagation in the whole church in the both directions X and Y, which helps in understanding the general failure pattern.

4.3.1 Cracks Pattern in X – Direction

The analysis of the Church of Nativity determines the critical elements of the structure by monitoring the cracks propagations in each element, i.e. some church elements often present significant cracks in

gravity loads without any lateral loads excitations, figure (4.4). In details the contours in the figure (4.4) show the values of cracks in some locations with reference to load steps for the self-load of the structure only, it's obvious that the cracks reached the max value of 5.97 mm in the vaults of narthex, and the apses.

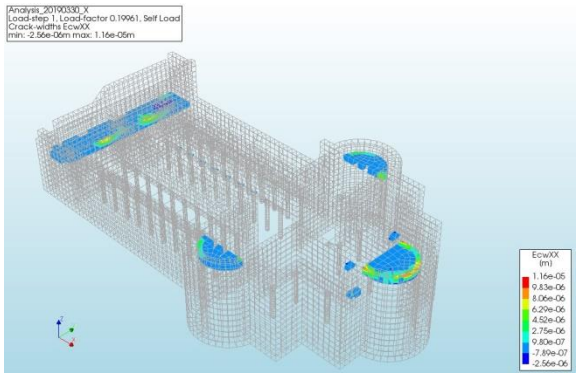

Load Step (1) : Crack width 0.012 mm

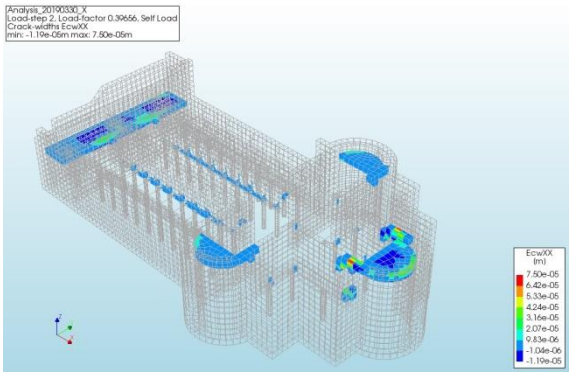

Load Step (2) : Crack width 0.075 mm

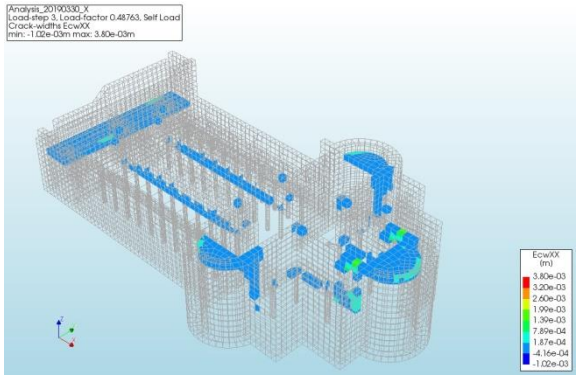

Load Step (3) : Crack width 3.80 mm

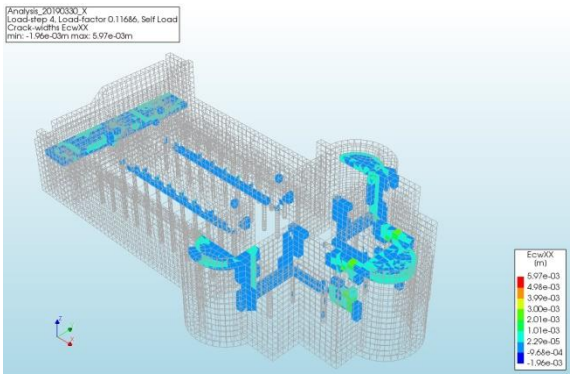

Load Step (4) : Crack width 5.97 mm

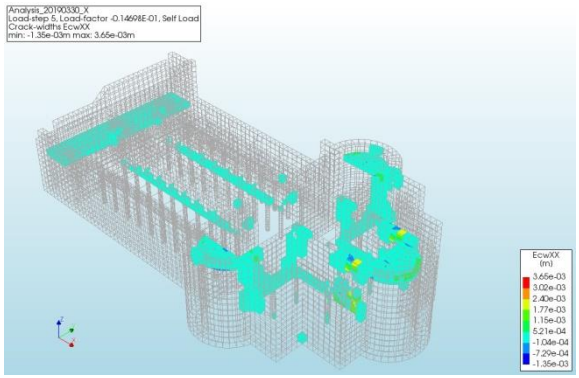

Load Step (5) : Crack width 3.65 mm

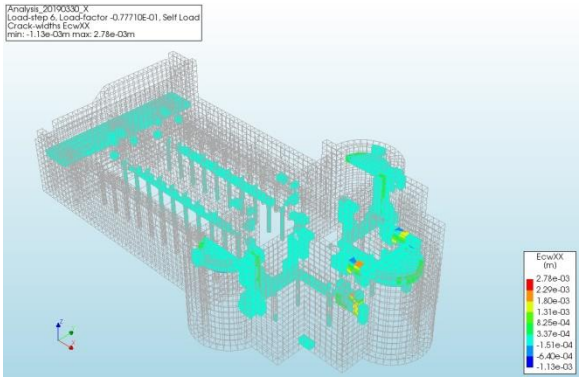

Load Step (6) : Crack width 2.78 mm

Figure (4.4): Crack widths generated by gravity loads analysis in X – direction.

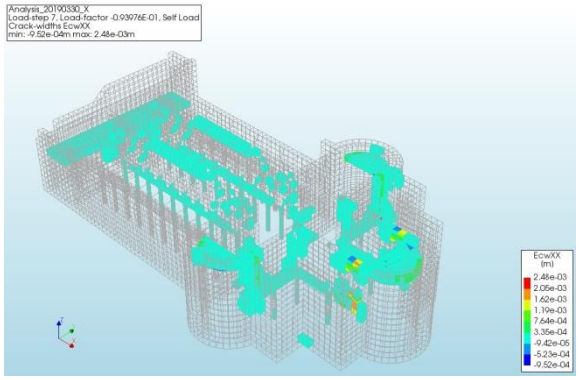

Load Step (7) : Crack width 2.48 mm

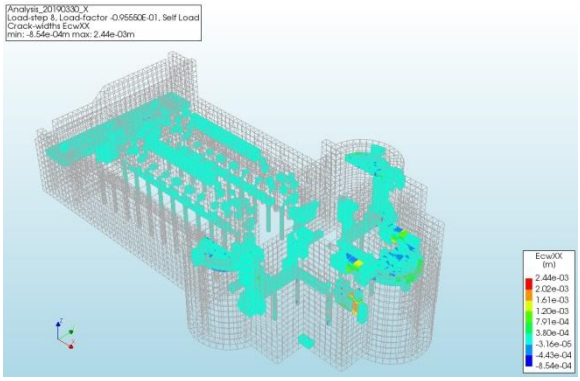

Load Step (8) : Crack width 2.44 mm

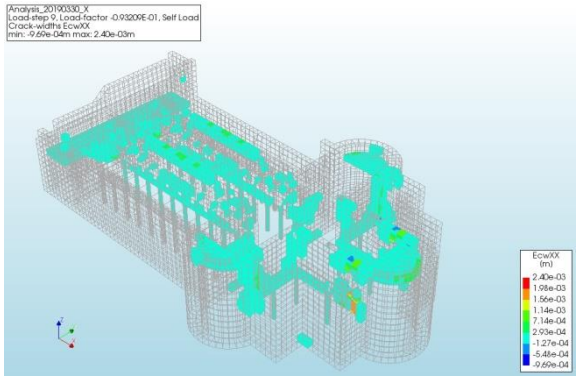

Load Step (9) : Crack width 2.40 mm

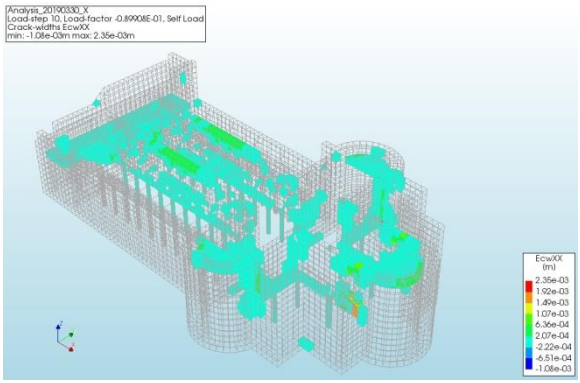

Load Step (10) : Crack width 2.35 mm

Figure (4.4): Crack Widths Generated by Gravity Loads Analysis in X – direction – cont'd

It is clear that church components are coherent under gravity loads, with suffering from superficial deposit of atmospheric particulate, but the gross cracks generated from pushover excitations have to be monitored and require an assessment of the structural soundness of the elements. For that purpose, the model of Church of Nativity which used as a damage monitoring method, to validate the decision about the cracks stability and integrity state of elements, also used for determination of cracks after the application of lateral loads, figure (4.5).

The results show that the masonry building are subjected to partially collapses during nonlinear static monotonic load, due to loss of equilibrium of masonry portions, and enlargement of cracks widths as shown form load

step (11) to load step (20). Expected local mechanisms which are generated form the analysis, are very important issues in the seismic analysis of masonry buildings.

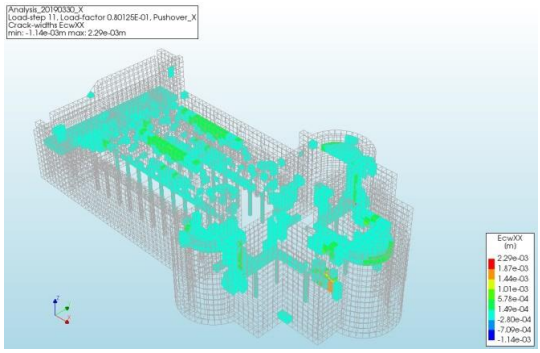

Load Step (11) : Crack width 2.29 mm

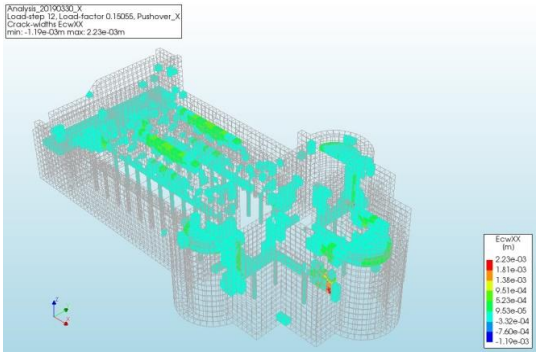

Load Step (12) : Crack width 2.23 mm

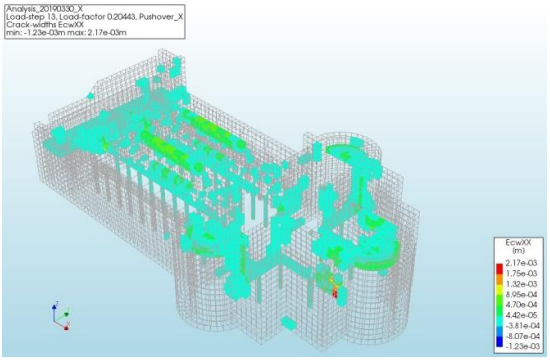

Load Step (13) : Crack width 2.17 mm

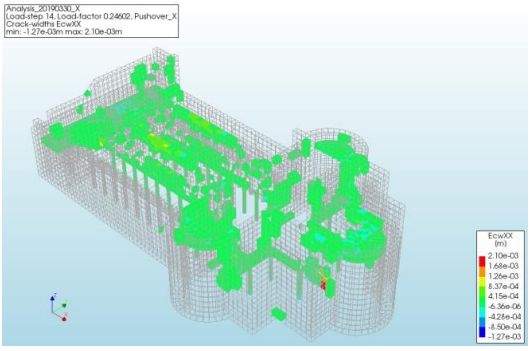

Load Step (14) : Crack width 2.10 mm

Figure (4.5): Crack Widths Generated by Pushover Analysis in X – Direction.

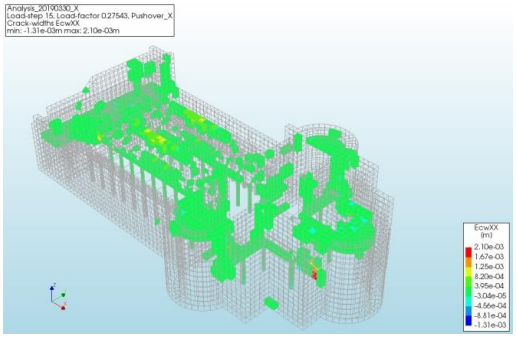

Load Step (15) : Crack width 2.10 mm

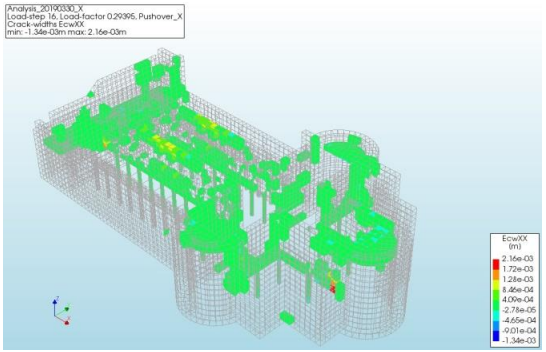

Load Step (16) : Crack width 2.16 mm

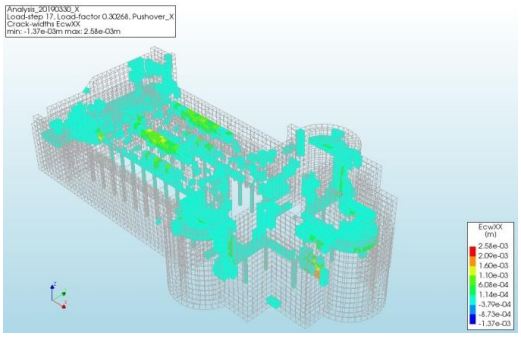

Load Step (17) : Crack width 2.58 mm

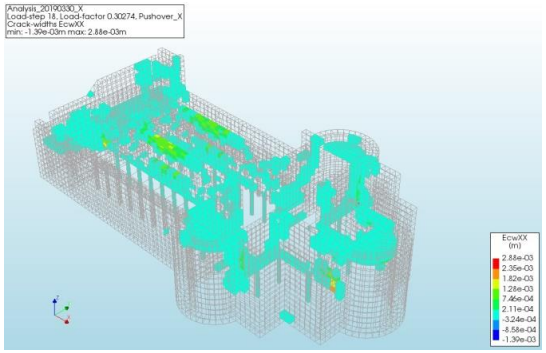

Load Step (18) : Crack width 2.88 mm

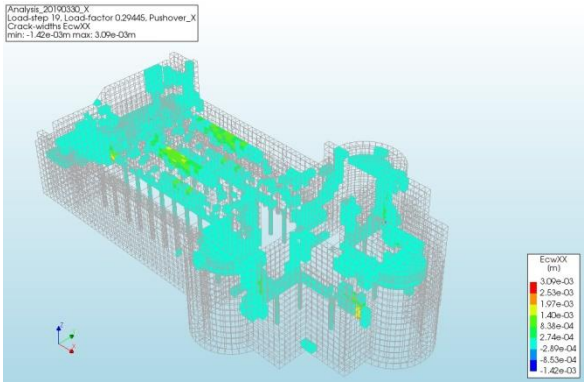

Load Step (19) : Crack width 3.09 mm

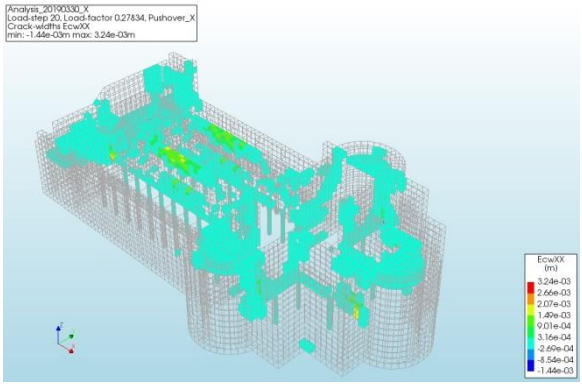

Load Step (20) : Crack width 3.24 mm

Figure (4.5): Crack Widths Generated by Pushover Analysis in X – Direction – Cont'd

4.3.2 Cracks Pattern in Y – Direction

In the other direction Y, the damage propagation generated as a result of gravity loads is symmetrical around the longitudinal east-west axis as shown in figure (4.6). Most cracks are situated above narthex vaults, apses vaults, also propagates in the bottom parts of lateral walls of the nave and shoulders of the church (premier walls).

In general, the structure presents a global damage behavior, in Y direction, without evident damage causing localized failures, the counters of figure (4.6), also show the values of cracks in some locations with reference to the load steps for the self-load, it's obvious that the cracks

reached a maximum value of 4.94 mm in the vaults of narthex, and the apses.

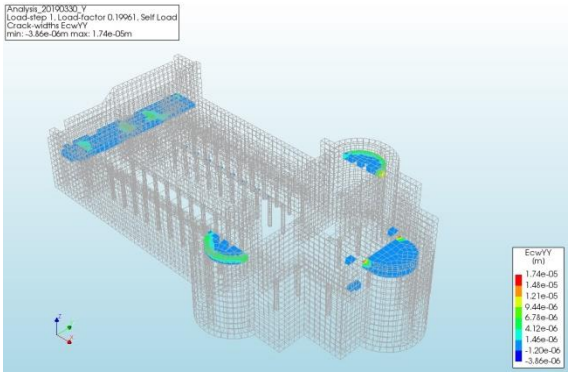

Load Step (1) : Crack width 0.017 mm

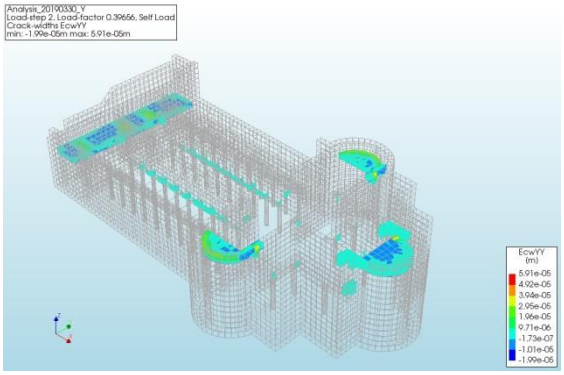

Load Step (2) : Crack width 0.059 mm

Figure (4.6): Crack Widths Generated by Gravity Loads Anaalysis in Y – Direction.

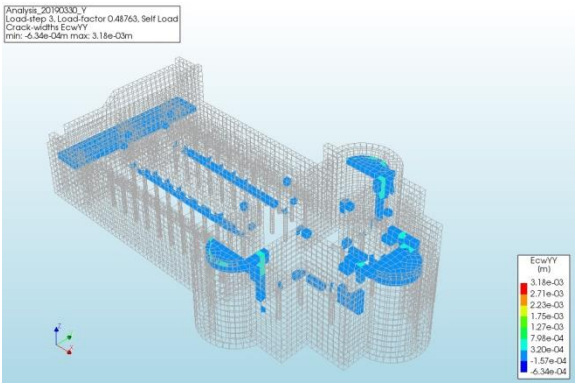

Load Step (3) : Crack width 3.1aaaaa8 mm

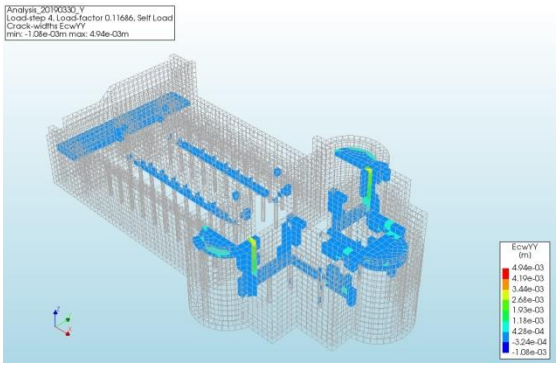

Load Step (4) : Crack width 4.94 mm

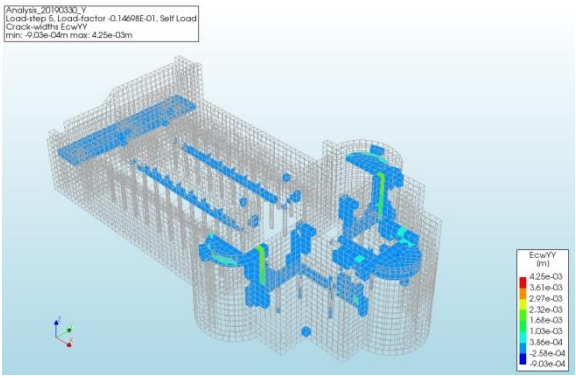

Load Step (5) : Crack width 4.25 mm

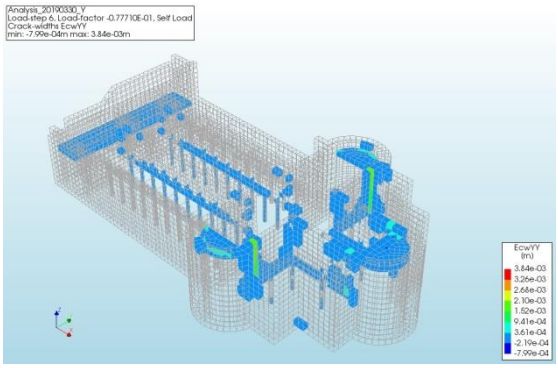

Load Step (6) : Crack width 3.84 mm

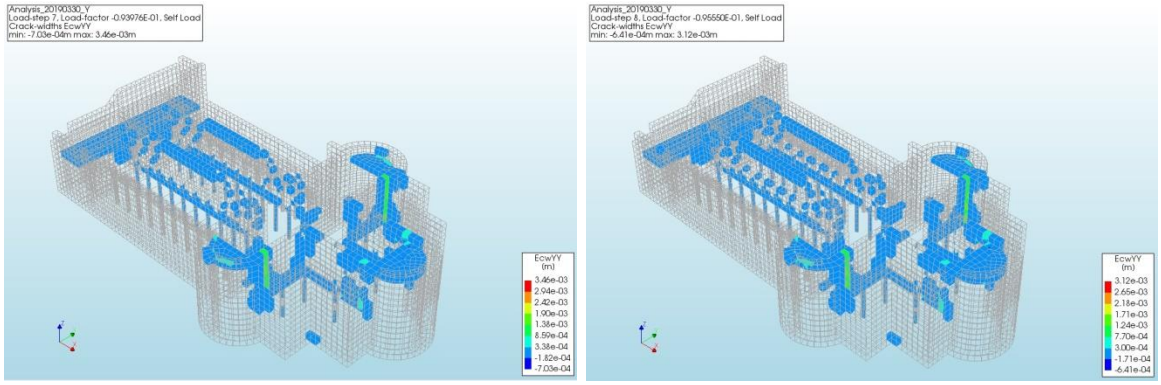

Load Step (7) : Crack width 3.46 mm Load Step (8) : Crack width 3.12 mm

Figure (4.6): Crack Widths Generated by Gravity Loads Analysis in Y – Direction – Cont'd

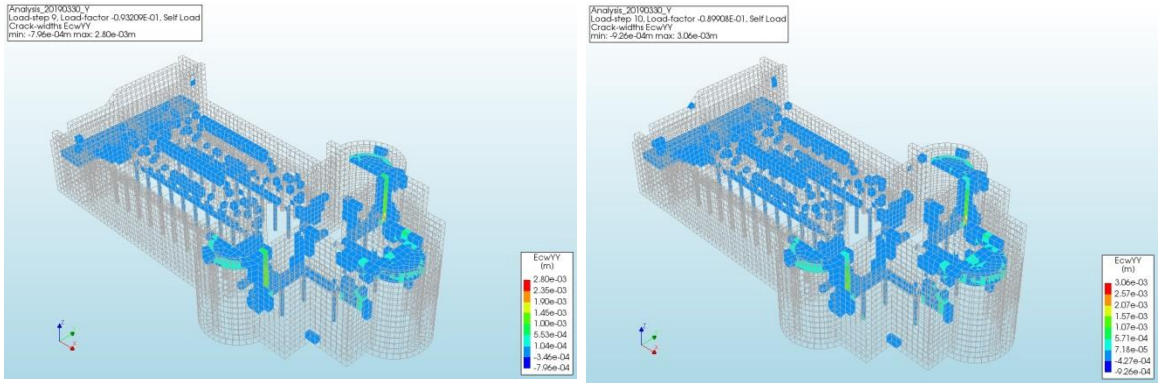

Load Step (9) : Crack width 2.80 mm Load Step (10) : Crack width 3.06 mm

Figure (4.6): Crack Widths Generated by Gravity Loads Analysis in Y – Direction – Cont'd

With pushover analysis tool, also the out of plane behavior can be investigated. It is rather difficult to suggest detailed or realistic out of plane mechanisms, but the excitations of lateral loads, verified by figure (4.7), show the enlargement of widths and locations for the cracks which reach a maximum width of 13.7 mm! (Blue color).

The out of plane movement is the most dangerous of this cases, the vertical cracks on the connection between frontal and lateral facades

indicate the activation of the façade overturning and the formation of hinges.

The main structural causes of this mechanism are the weak connection with the orthogonal walls (90° walls), poor masonry quality, no box behavior, and the absence of links on the top, these results allow the researchers to verify the possibility of collapse caused by the plasticization of the material.

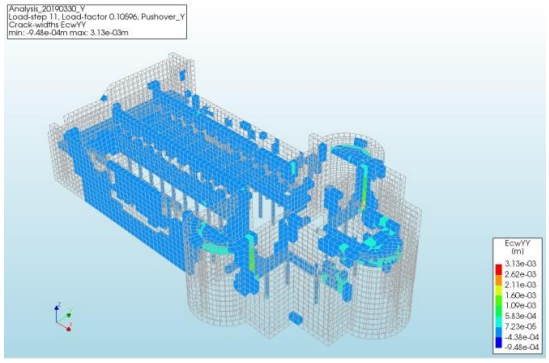

Load Step (11) : Crack width 3.13 mm

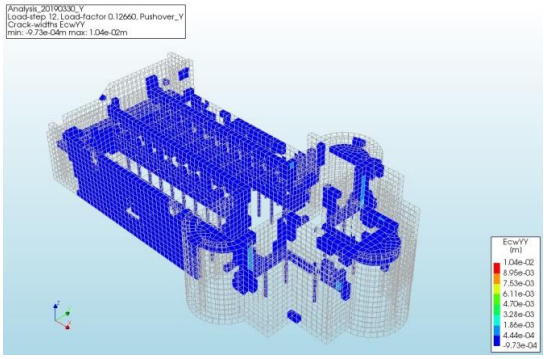

Load Step (12) : Crack width 10.4 mm

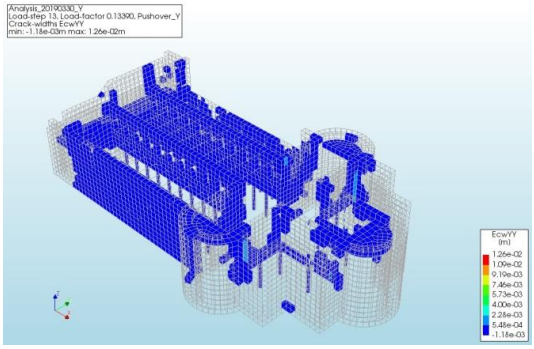

Load Step (13) : Crack width 12.6 mm

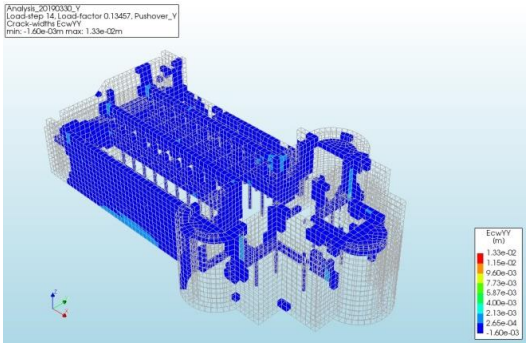

Load Step (14) : Crack width 13.3 mm

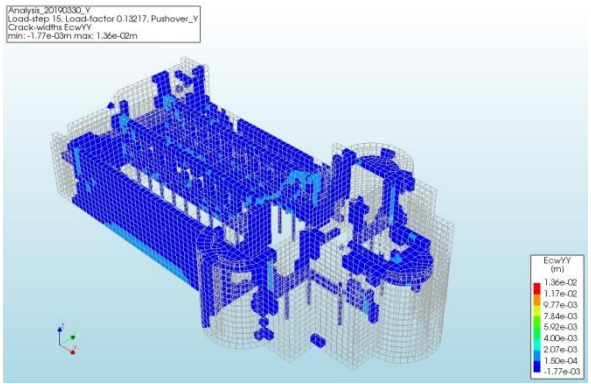

Load Step (15) : Crack width 13.6 cm

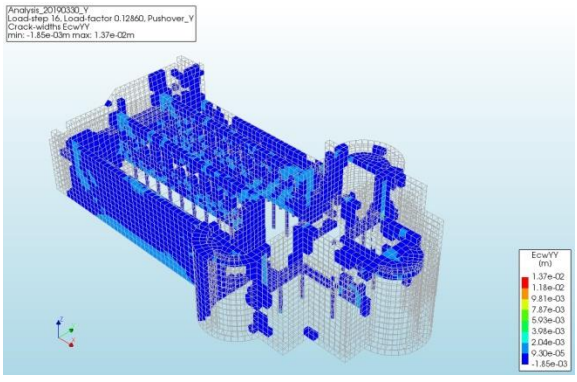

Load Step (16) : Crack width 13.7 mm

Figure (4.7): Crack Widths Generated by Pushover Analysis in Y – Direction.

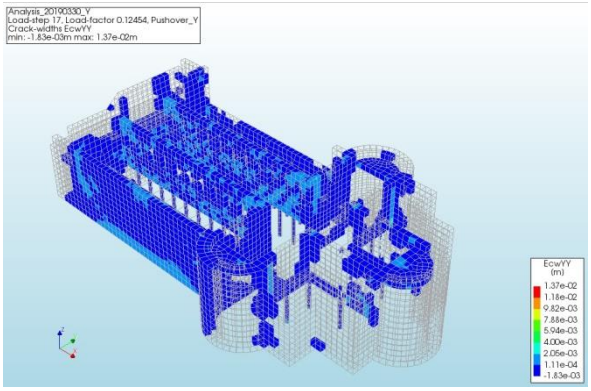

Load Step (17) : Crack width 13.7 mm

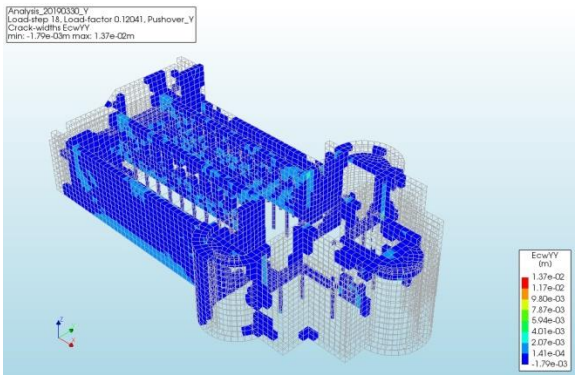

Load Step (18) : Crack width 13.7 mm

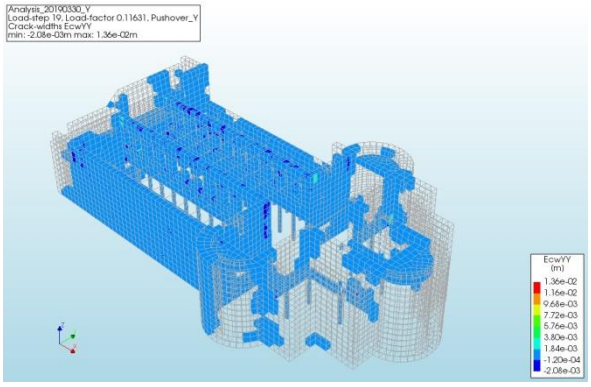

Load Step (19) : Crack width 13.6 mm

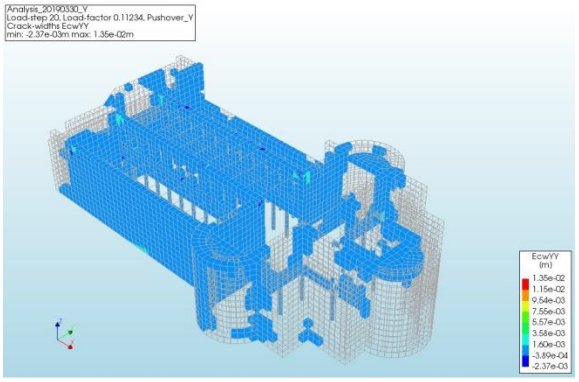

Load Step (20) : Crack width 13.5 mm

Figure (4.7): Crack Widths Generated by Pushover Analysis in Y – Direction.

For the procedure of pushover analysis, the appendix (B) gives more details with figures of steps followed.

CHAPTER FIVE

NON-LINEAR DYNAMIC ANALYSIS

5. Non – Linear Dynamic Analysis

5.1 Introduction

Under dynamic excitations, the application of nonlinear time history analysis Considers the nonlinearity of materials behavior in the time domain, the seismic action is dynamically represented by accelerograms applied at the base of the church, which can be obtained from real earthquakes, or sometimes artificially generated. In details, the accelerogram is a time history of acceleration, which expresses the ground motion due to a certain seismic action in a precise location.

The nonlinear dynamic analysis method provides a more accurate assessment of the structural response to strong ground shaking compared to the pushover analysis, according to Euro code 8 – part (3/2005), it is an alternative procedure, for analyzing the nonlinear behavior of masonry structures subjected to seismic effects.

5.2 Used earthquakes

The main important issues considered for selecting the input ground motions for nonlinear dynamic analysis are; target hazard where the study is done, source of the ground motions, and, the number of ground motions needed.

For the first issue, the laws and available data concerning the site seismicity are insufficient for conducting an accurate seismic analysis of the Church, Claudio Alessandri and Jessica Turrioni endeavored in previous research to identify a comparable site on the basis of the seismic zoning of Palestine and the Italian technical standards for constructions by

referring to the Italian regulations and comprehensive data of seismic activity in Italy. In more details, Alessandri and Turrioni select the Italian site which has the same ground acceleration (a_g=0.15g) and the same altitude (600 m) as Bethlehem, with comparable return period of 475 years. By treating all these data and the geographical coordinates of the Italian equivalent site, they use the computer code SPETTRI NTC, (Claudio Alessandri, Jessica Turrionim, 2017), and generate the response spectrum of the Bethlehem. The horizontal component (S_{d0}), the design spectrum in the vertical component (S_{dv}) and elastic spectrum (S_e), obtained and shown in figure (5.1).

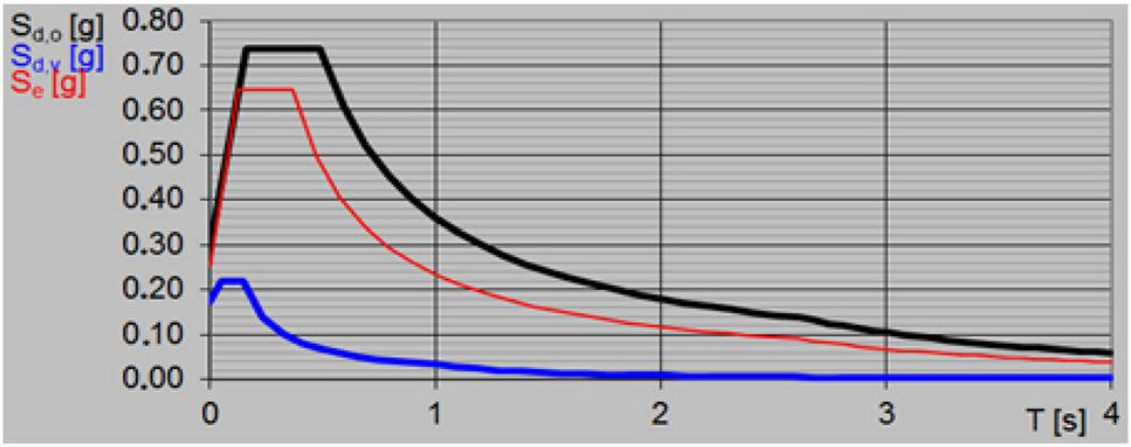

Figure (5.1): Elastic and Design Spectra Concerning The Site Seismicity, [Claudio Alessandri, Jessica Turrionim, 2017].

For the second issue, there are sources of ground motions summarized as, artificial accelerograms, natural records of past earthquakes, and simulated accelerograms (Deierlein et al., 2010). In this chapter, the records of the three different accelerograms of three different real earthquakes are used, figure (5.2), each of them is scaled to the PGA where the case study is located, also these three earthquakes with different

magnitudes are likely to be rather different, and so the maximum results generated from them will be dependable.

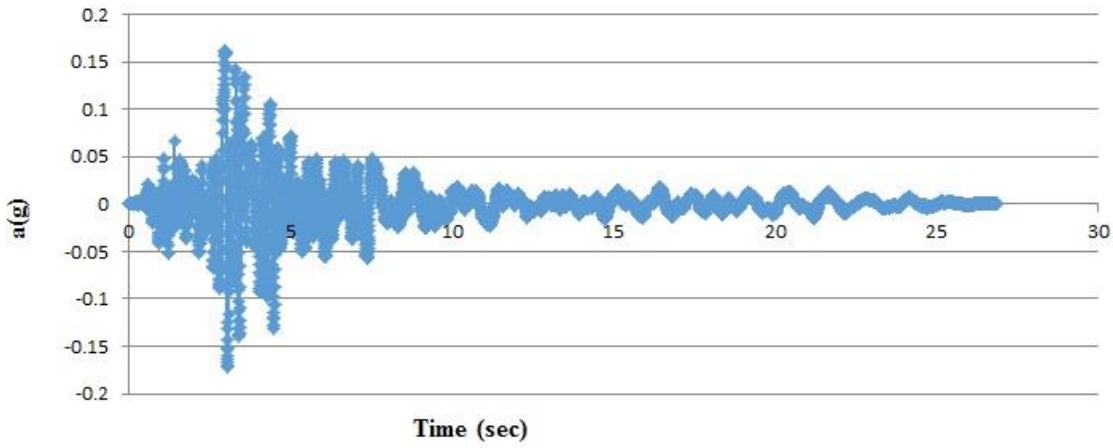

Accelerogram for First Earthquake Used with PGA 0.165g.

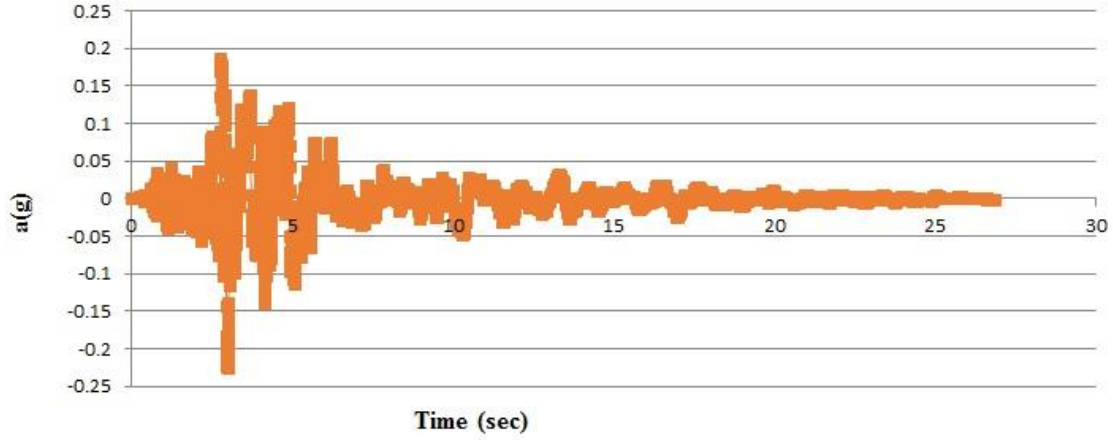

Accelerogram for Second Earthquake Used with PGA 0.195g.

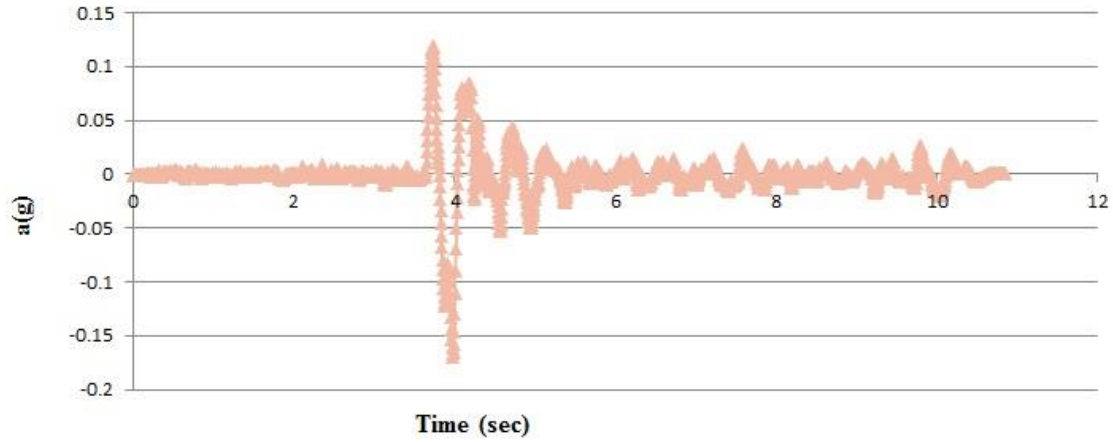

Accelerogram for Third Earthquake Used with PGA 0.120g.

Figure (5.2): Accelerograms Used for Dynamic Analysis, [USGS]

Finally, the number of ground motions needed, section 16.2.4 of ASCE/SEI 7-05 presents how individual member inelastic deformations, member forces, and the drifts of each story are computed for design, and how the Peak response quantities are computed for each analysis, so if seven or more accelerograms are used for analysis, the arithmetic mean of the peak response is used for component and story checking, if fewer than seven analyses are performed, the maximum value of the peak response quantities is used for components and story checking.

There are two criteria to set the time step for the model built in DIANA FEA. The first is, Δ_t which is referred to the time step, must be defined as the Ti divided by 20 (error less than 5%) (Mendes, 2012). Thus, the Δ_t was assumed 0.005 sec for all the dynamic analyses, and the second, is that Δ_t should be significantly lower than the total duration of the analysis. Finally it's important to show the damping ratio which are presented in figure (5.3). For the evaluation of the relative displacements in each direction, the same control points adopted in the pushover are considered, and plotted each displacement at each control point.

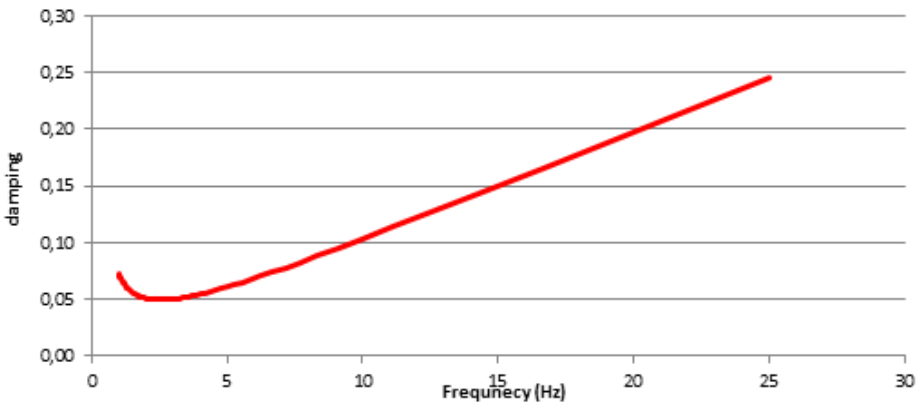

Figure (5.3): Rayleigh Damping Model.

5.3 Relative Displacement

The relative displacement, which is defined as a displacement of the point located on the structure with respect to its origin, or adjacent point defined on the structure, and briefly defined (RDAMB). It can be an effective method for the damage quantification, and of great potential benefit due to the lack of knowledge among researchers. The primary objectives of this section are to estimate the relative displacement of references node selected. Figure (5.4) show the reference nodes that will excited to time history analysis for three different earthquakes as mentioned before and measuring the maximum relative deformations among three earthquakes.

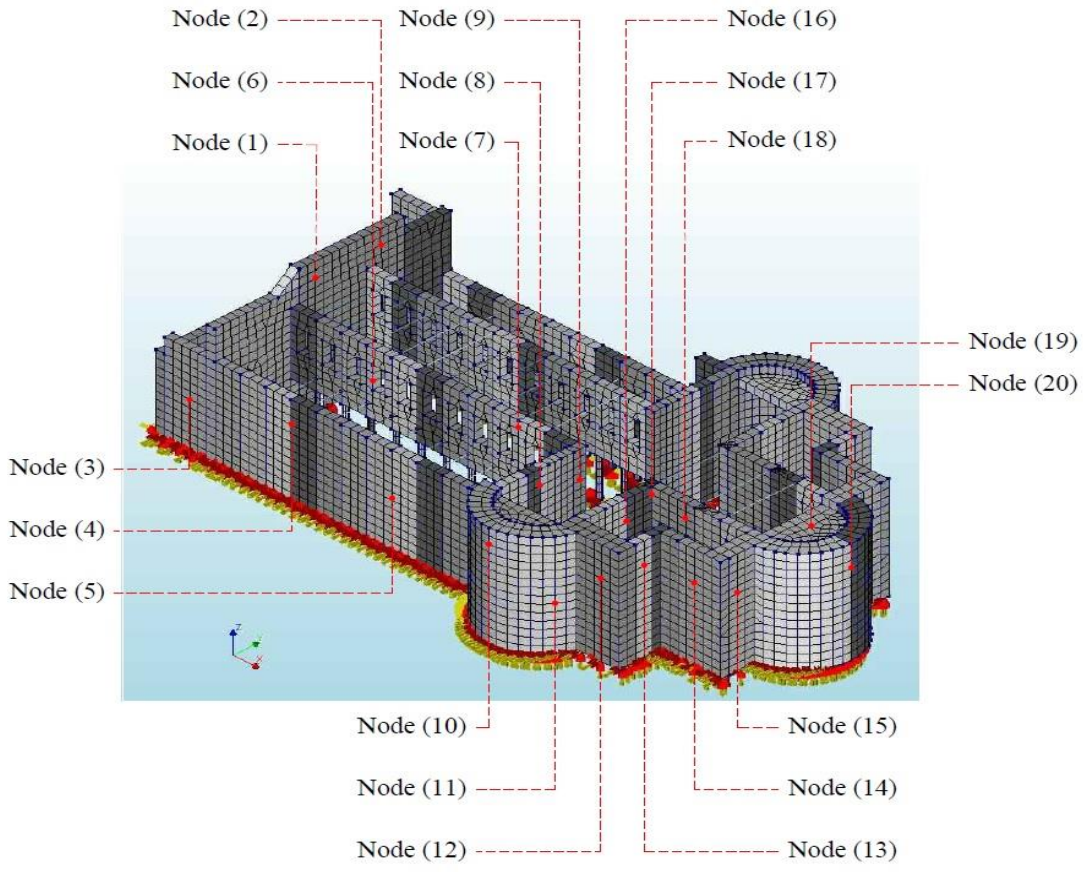

Figure (5.4): Locations of Reference Nodes for Dynamic Analysis.

the relative displacements for selected nodes are calculated over the steps of accelerograms based on difference between of the two corners of stone unit in the masonry walls (point 1 - point 2) as figure (5.5) present. The displacements shown are in the plane direction, and the maximum values being resulted from the three accelerograms are used.

5.3.1 X – Direction

By analyzing the model in X – direction, the relative displacements for selected nodes are calculated over the steps of accelerograms based on difference between of the two corners of stone unit (point 1 - point 2) as the figure (5.5) show.

It's obvious that absolute relative displacement function for node (1) gives a maximum 4.19 mm, figure (5.6), and for node (2) which is located at the same structural element (The narthex) it is 3.47 mm, and this is can be shown on figure (5.7).

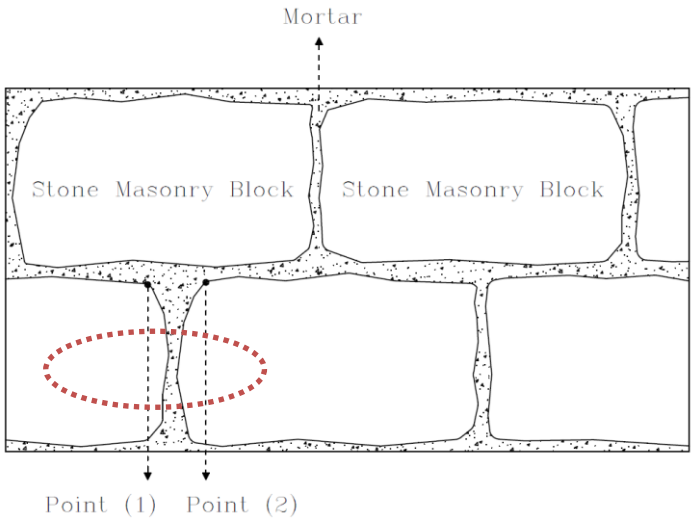

Figure (5.5): Points of Masonry Block Where The Displacements Measured.

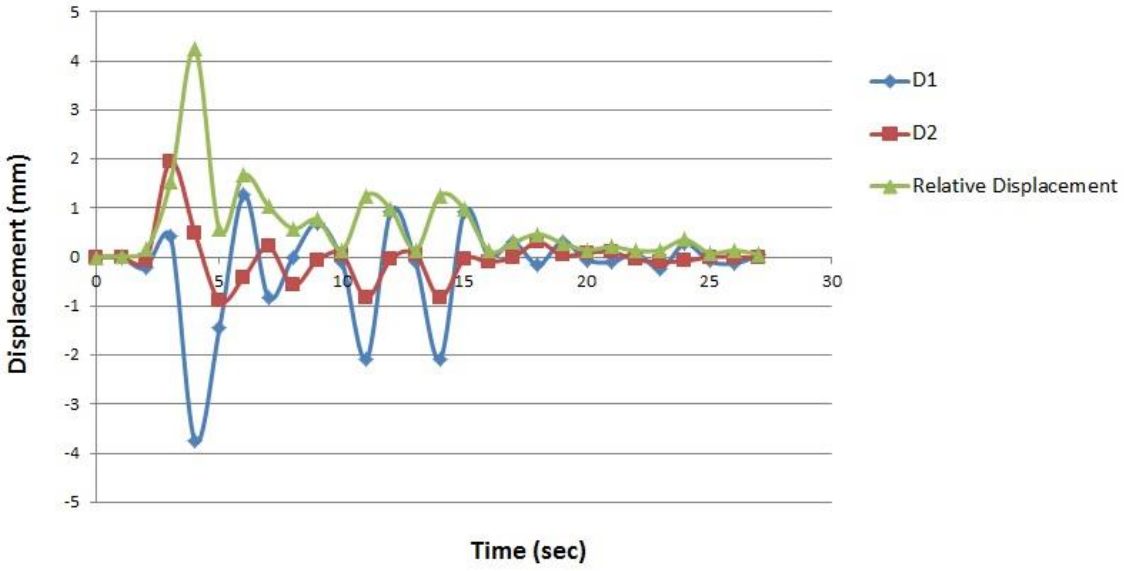

Figure (5.6): Relative Displacement for Node (1) - X direction

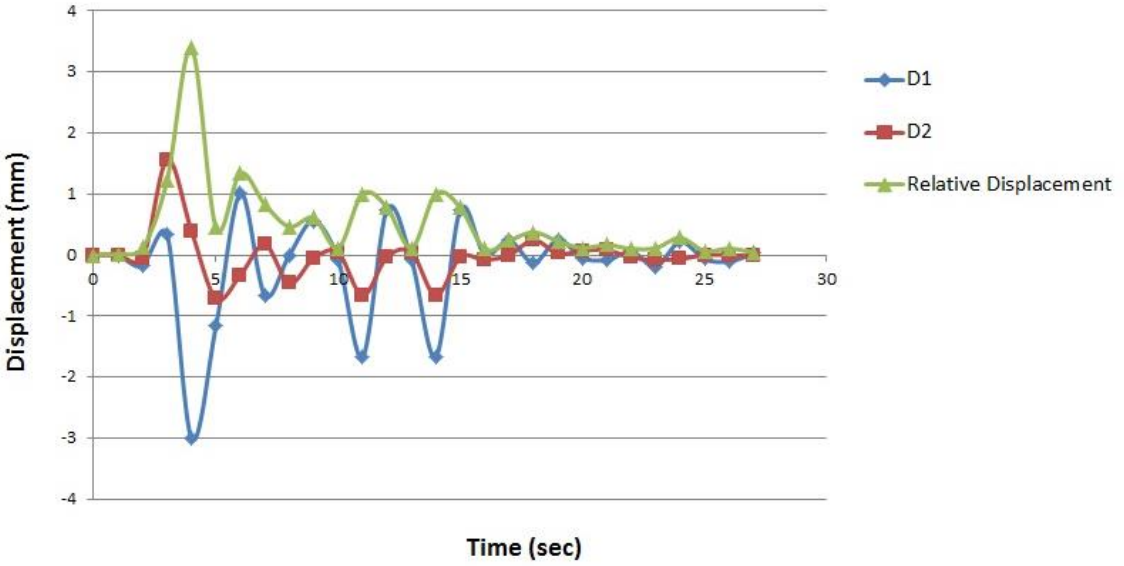

Figure (5.7): Relative Displacement for Node (2) - X direction

By moving to nodes (3), (4), and (5) which are located on the south wall, their functions of relative displacement show 0.072 mm, 0.051 mm, 0.022 mm, respectively, in details figure (5.8), show the details of node (3).

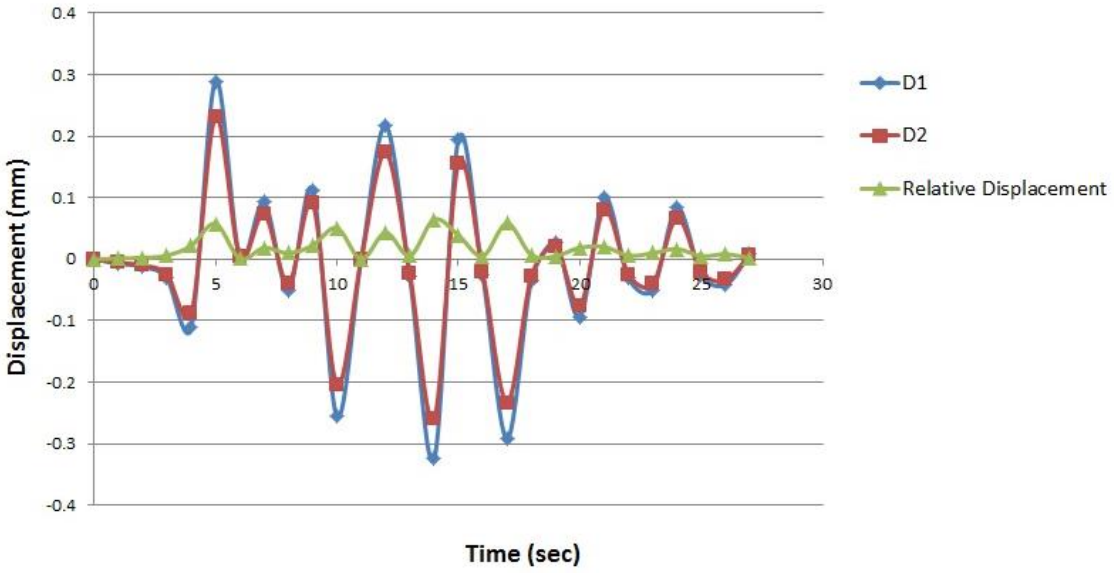

Figure (5.8): Relative Displacement for Node (3) - X direction

The previous figure emphasize that points of the blokes, where node (3) chosen have consensual movement, which mean a relatively very small relative displacement between them.

Also, figure (5.9), the one related to node (4), present a similar movement as node (3), the two points located at the corner of the block are consistent in their movement and give a small (converge to zero) relative displacement.

These relatively very small values explain how much these type of walls are stiff and strong in the plane direction.

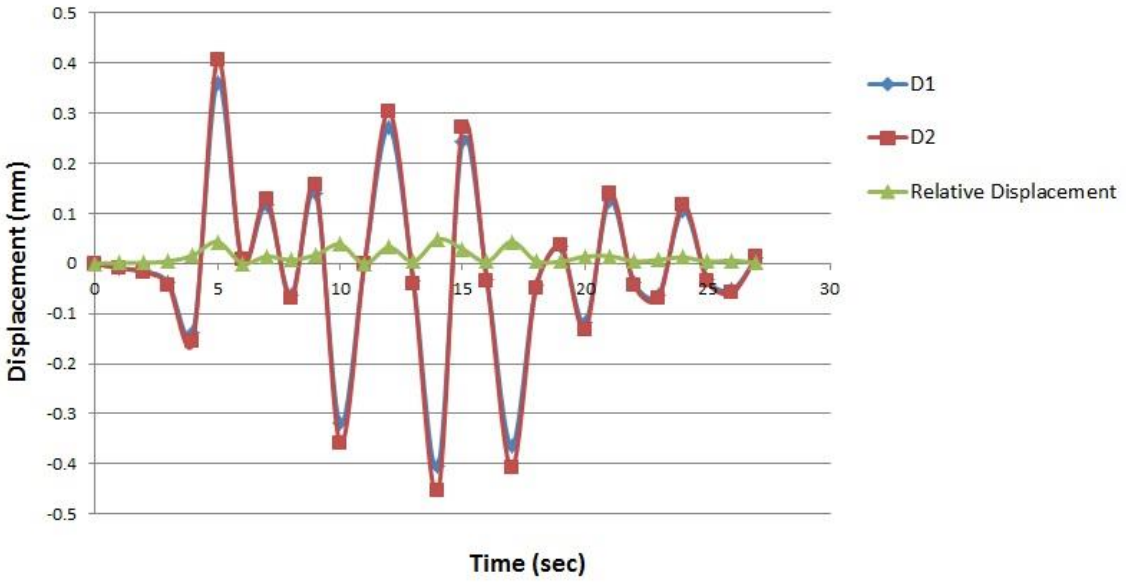

Figure (5.9): Relative Displacement for Node (4) - X direction

On the other hand, nodes (6) and (7) have a situation properly different, the existence of windows, in the interior walls decreases the stiffness of these elements, and also these walls are rest on columns not on continues wall, in sure these columns show less stability for these walls. By the way, figure (5.10) explain the relative displacements which are 3.83 mm for node (6).

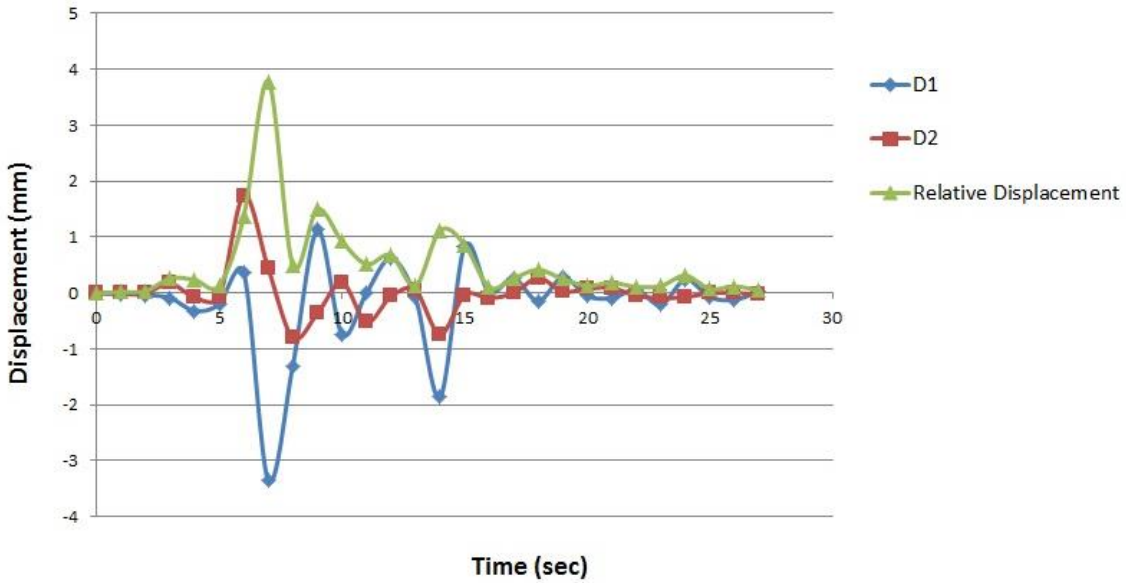

Figure (5.10): Relative Displacement for Node (6) - X direction

As a same way, for node (7), the relative displacement is 3.17mm and can be shown in the figure (5.11).

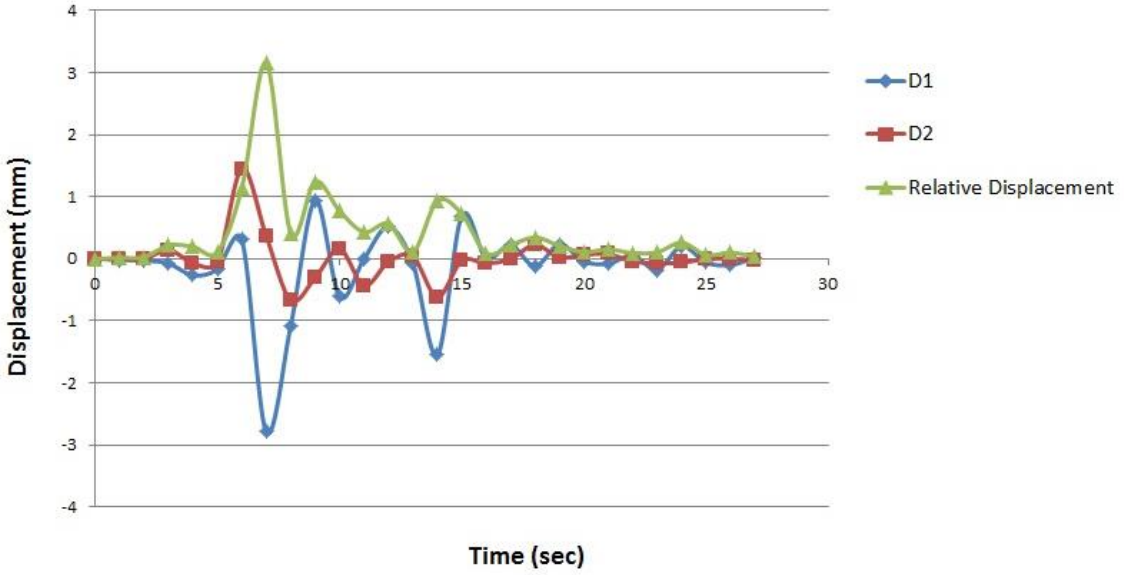

Figure (5.11): Relative Displacement for Node (7) - X direction

The relative displacement for node (7) is less than node (6) (about 82.80 % of node (6)) although they are located on the same wall, this referred to the location of node (7) at the center of element between two adjacent windows, which is surly critical and present clear separation, figure (5.12)

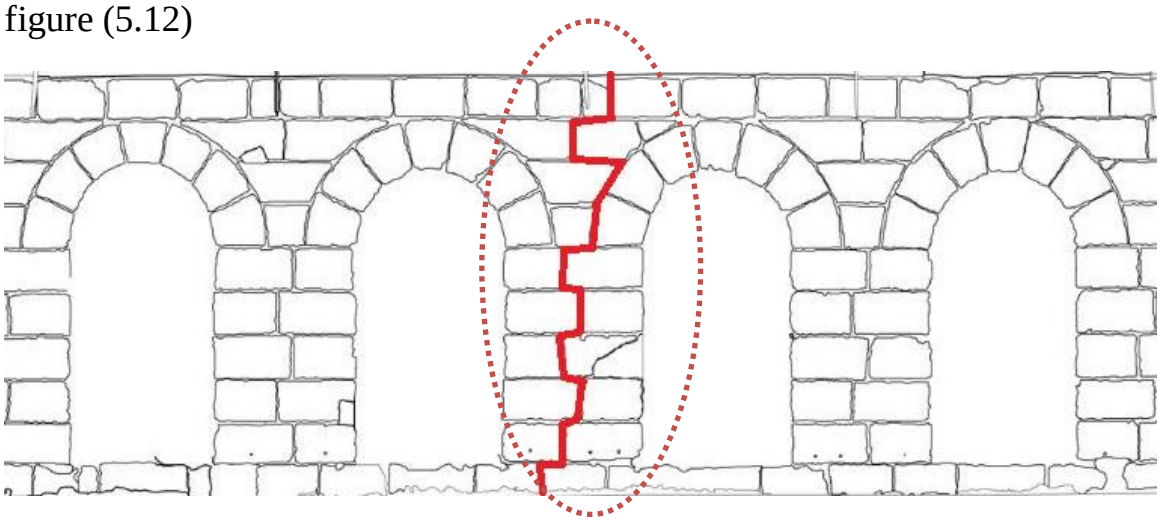

Figure (5.12): Clear Separation in the Longitudinal Wall.

For the nodes located on transvers walls, which are numbered by (8), and (9), their displacements curves represent the relative displacement at two critical locations; the first is located at the center of transverse wall, and the other on the connection between transverse and longitudinal wall.

For the point located at center which is designating as (8), figure (5.13) present the maximum relative displacement as 2.68 mm, it's obvious that it has two jumps in the function, which is mean the two corners separated twice times during the seismic excitations.

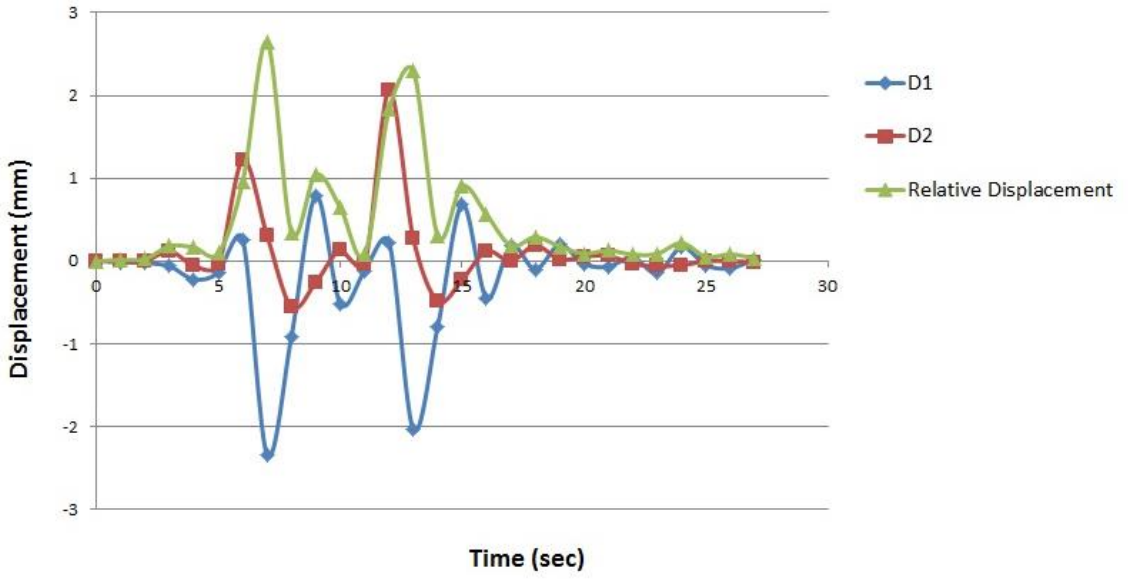

Figure (5.13): Relative Displacement for Node (8) - X direction

For the node (9), figure (5.14) show the relative displacement is 2.94mm, this can generate a scare about the connection between walls in the historical buildings, this explain why there are a lot of ties in masonry buildings, figure (5.15).

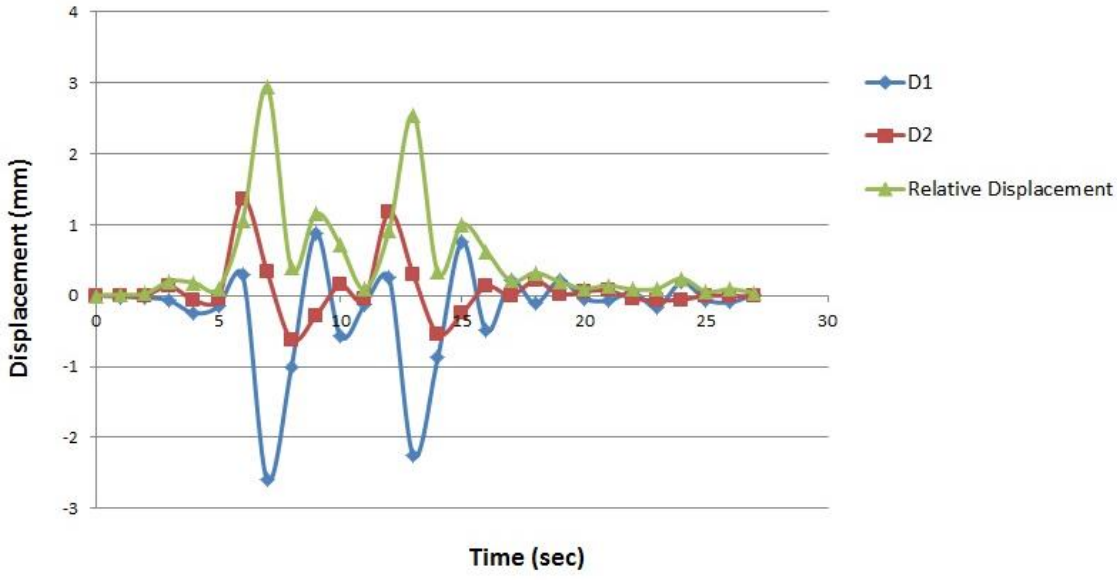

Figure (5.14): Relative Displacement for Node (9) - X direction

Figure (5.15): Ties of Masonry Buildings

After finishing the analysis of points located on nave of the church, the ones located on apses and shoulder walls, are studied. The node (10), located on the vaults of side apse, exposed to maximum relative displacement of 2.97 mm, figure (5.16).

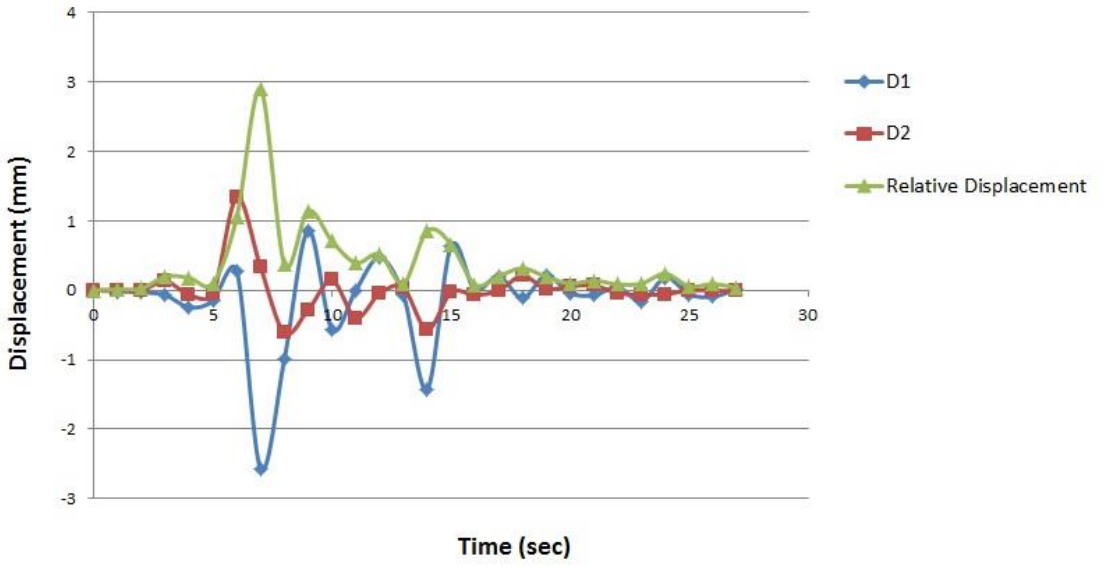

Figure (5.16): Relative Displacement for Node (10) - X direction

But for the point located of the outer side and denoted by Node (11), the maximum relative displacement relatively small, about 0.56 mm, figure (5.17).

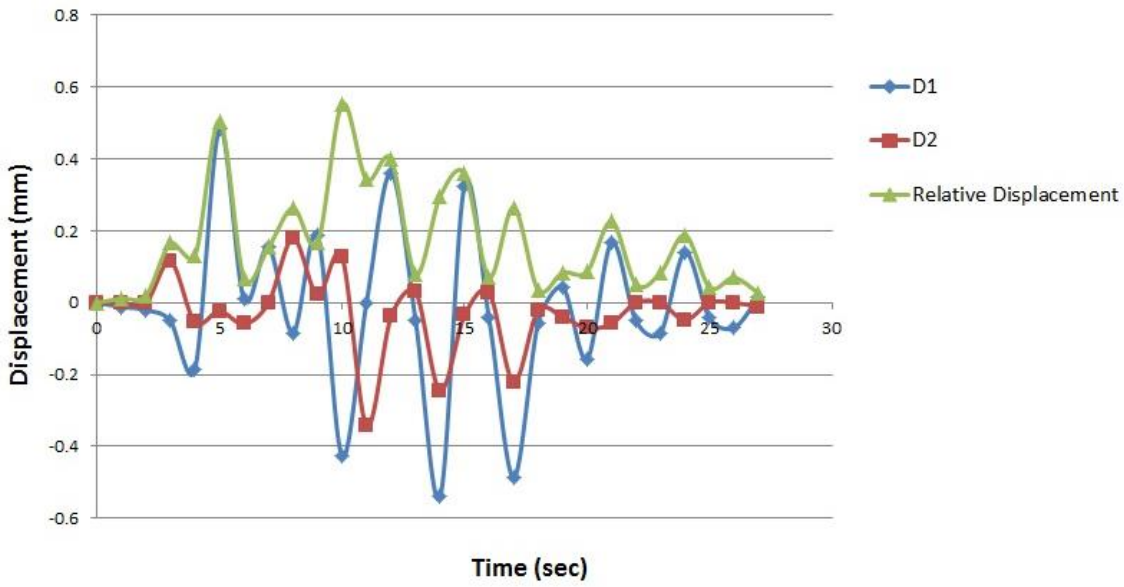

Figure (5.17): Relative Displacement for Node (11) - X direction

Also for points locating on shoulder walls, which are denoted by nodes (12), (13), (14), and (15), their maximum relative displacement

ranges from 0.24 mm, 1.07 mm, 0.30 mm, and 1.30mm, respectively. it's certainly that out of plane direction is less stiffness compromised to in plane direction, so the nodes (12) and (14), have relatively small values 0.24 mm, 0.30 mm, figures (5.18,5.19,5.20, and 5.21)

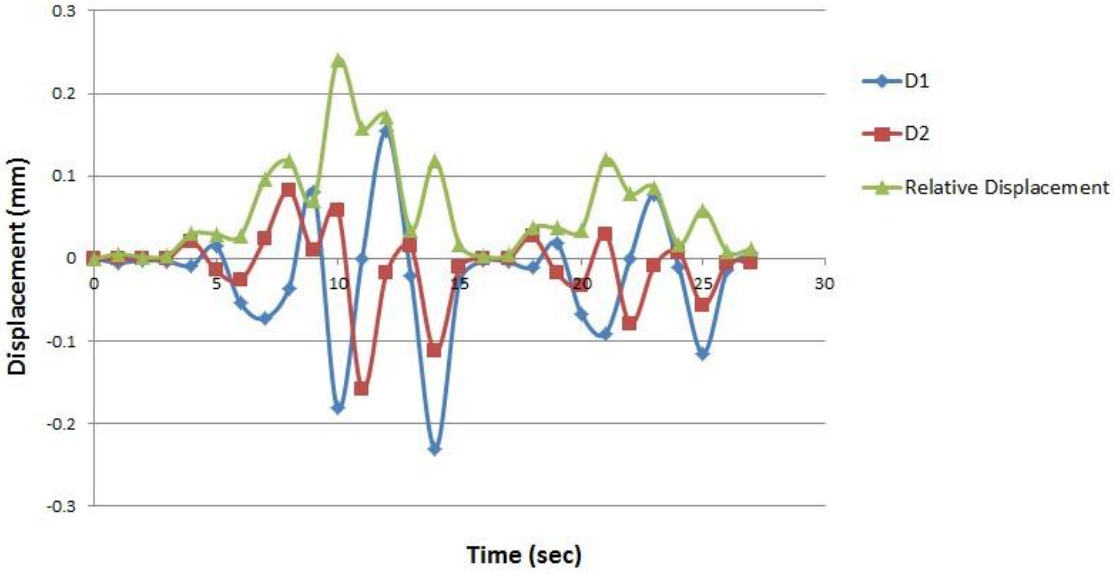

Figure (5.18): Relative Displacement for Node (12) - X direction

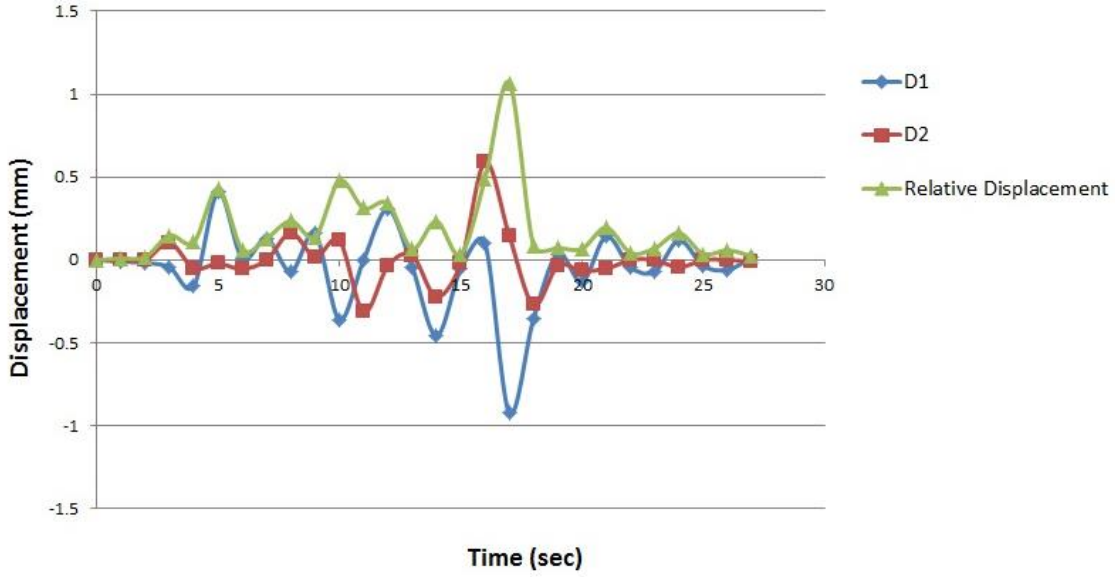

Figure (5.19): Relative Displacement for Node (13) - X direction

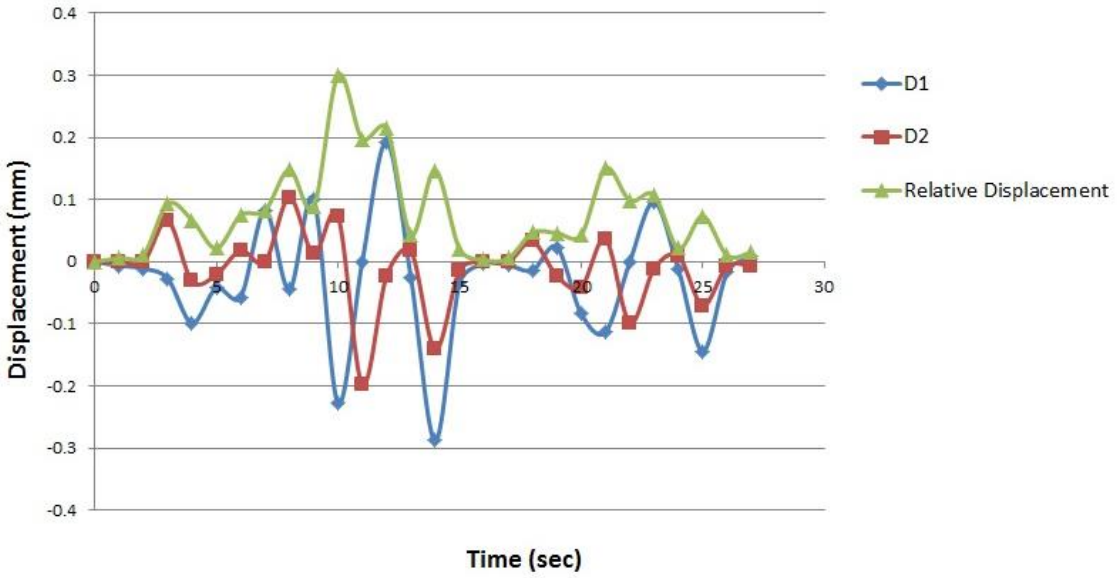

Figure (5.20): Relative Displacement for Node (14) - X direction

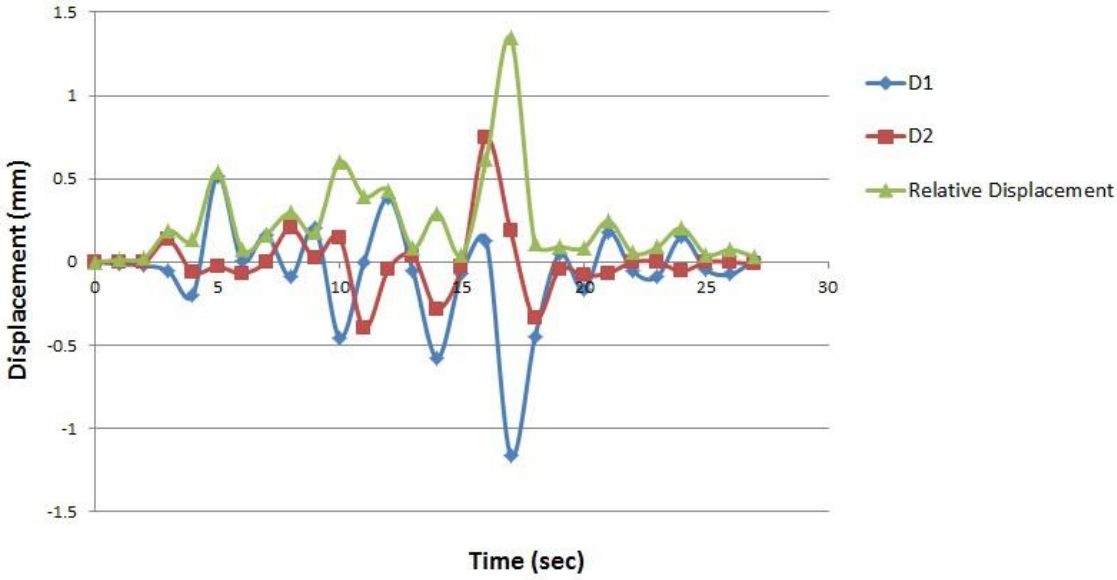

Figure (5.21): Relative Displacement for Node (15) - X direction

In the same pattern, Nodes (16), (17), and (18), have maximum relative displacement of 1.37 mm, 2.52 mm, and 1.73mm respectively. For the node (16), its located in the interior walls of the church, in spite of this wall is relatively short, but it still as the previous interior walls located on columns, which means less stability and rigidity, figure (5.22).

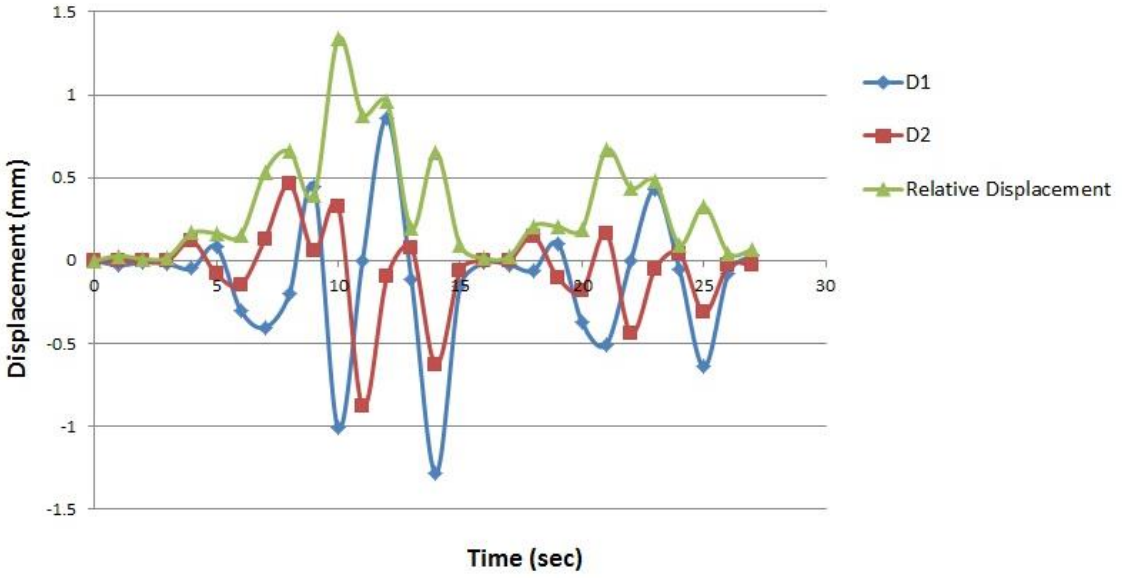

Figure (5.22): Relative Displacement for Node (16) - X direction

It is clear that node (17), situated on the connection between walls, this give an indication that the connection exposed to discontinuity during horizontal movement, and needs to be reinforced by ties, or any proposed pattern, as mentioned before, figure (5.23).

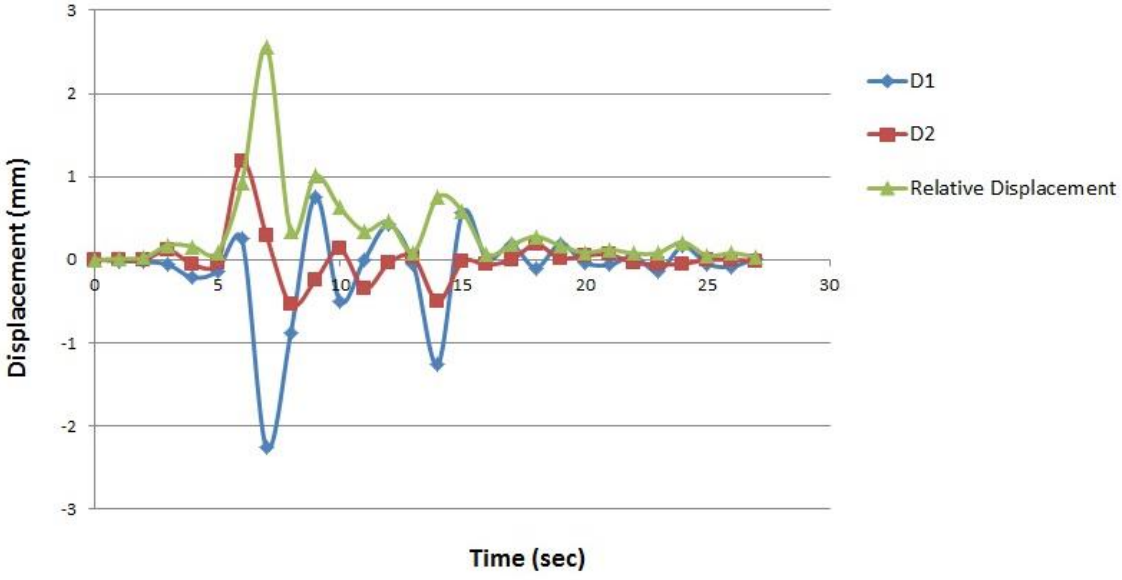

Figure (5.23): Relative Displacement for Node (17) - X direction

For the node (18), it's located in the interior walls as node (16), so this confirms why its behavior is absolutely the same, figure (5.24).

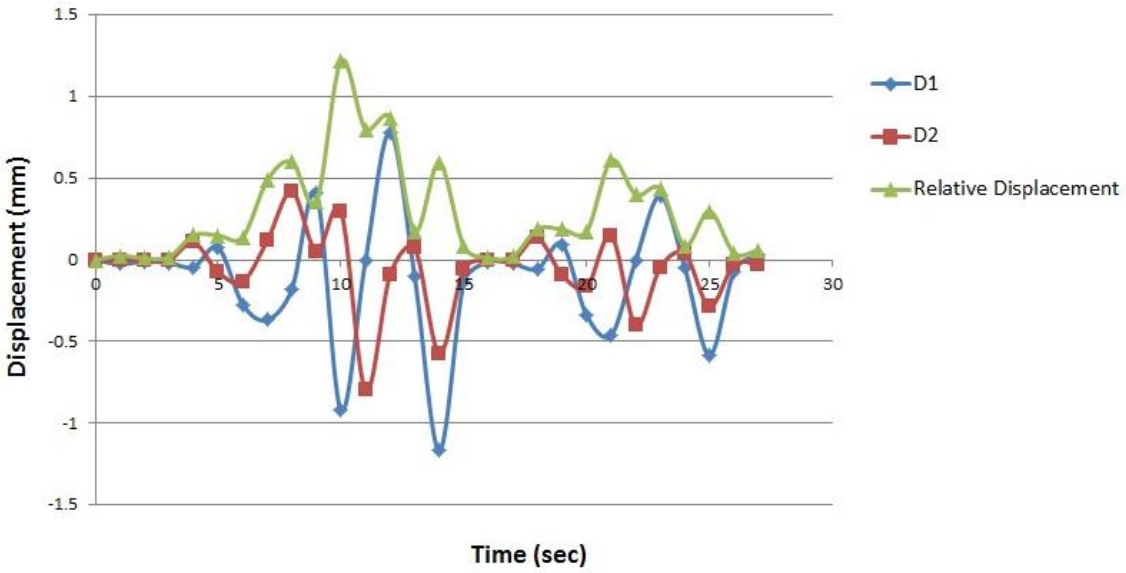

Figure (5.24): Relative Displacement for Node (18) - X direction

The node (19), located on the vaults of central apse, exposed to maximum relative displacement of 2.21 mm, its surly in X – direction, this curved wall will prone to visible cracks, figure (5.25).

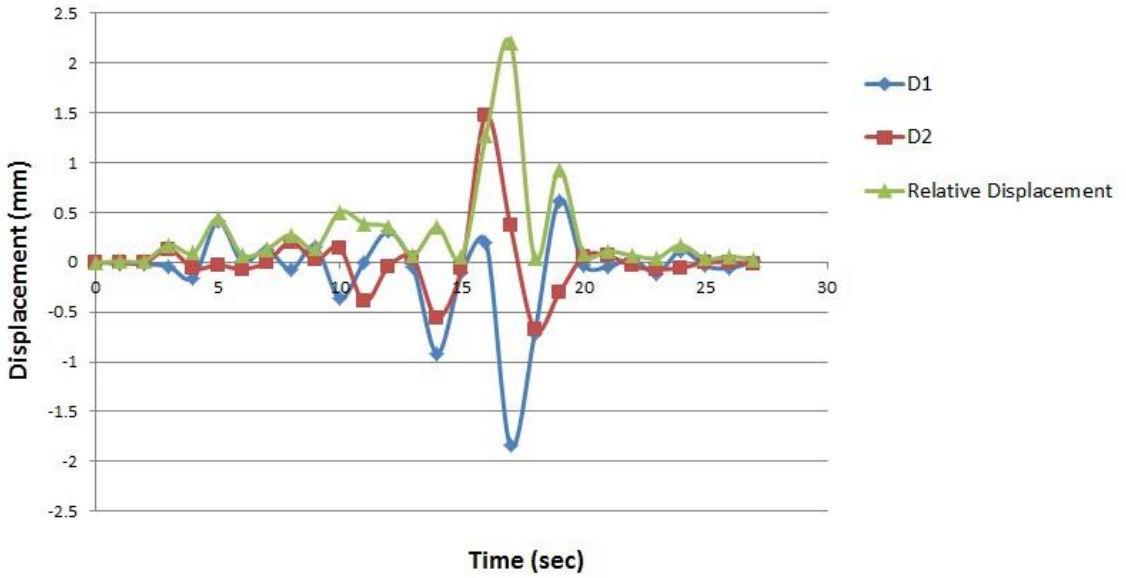

Figure (5.25): Relative Displacement for Node (19) - X direction

Finally, for the point located of the outer side and designated by (20), the maximum relative displacement reaches 1.77 mm, figure (5.26).

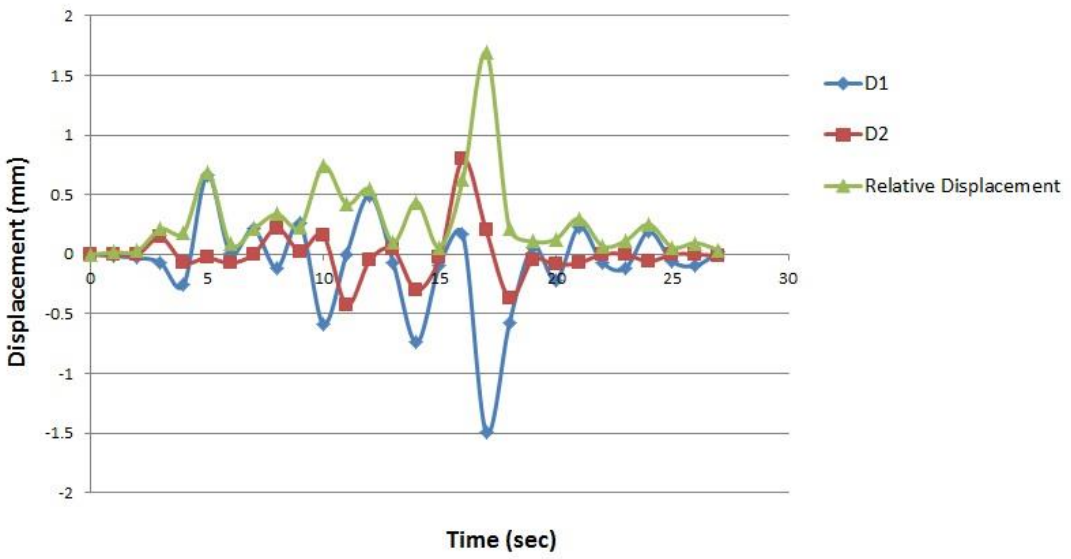

Figure (5.26): Relative Displacement for Node (20) - X direction

Appendix (C), present all the numerical results for the calculations of relative displacement, while the following figure (5.27) summarizes the maximum results for the nodes shown before.

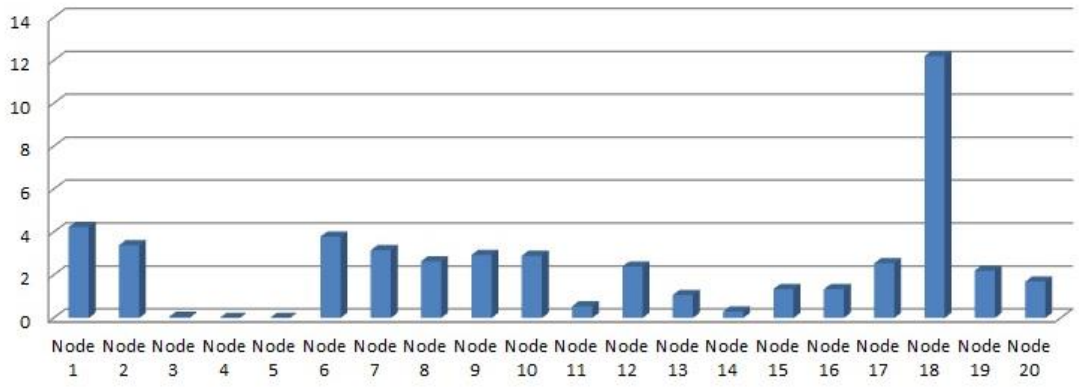

Figure (5.27): Maximum Relative Displacement for all Nodes - X direction

5.3.2 Y – Direction

Similarly, as done for the model in X – direction, the work for Y-direction also affording curves of relative displacement for the nodes selected before in figure (5.4). By beginning with node (1), the function of absolute relative displacement gives 3.07 mm in its maximum point, figure (5.28), its visible that this value reached after mostly the excitations of earthquakes are done, which mean the narthex is very stiff, but after relatively long duration of seismic actions, it may prone to stones falling.

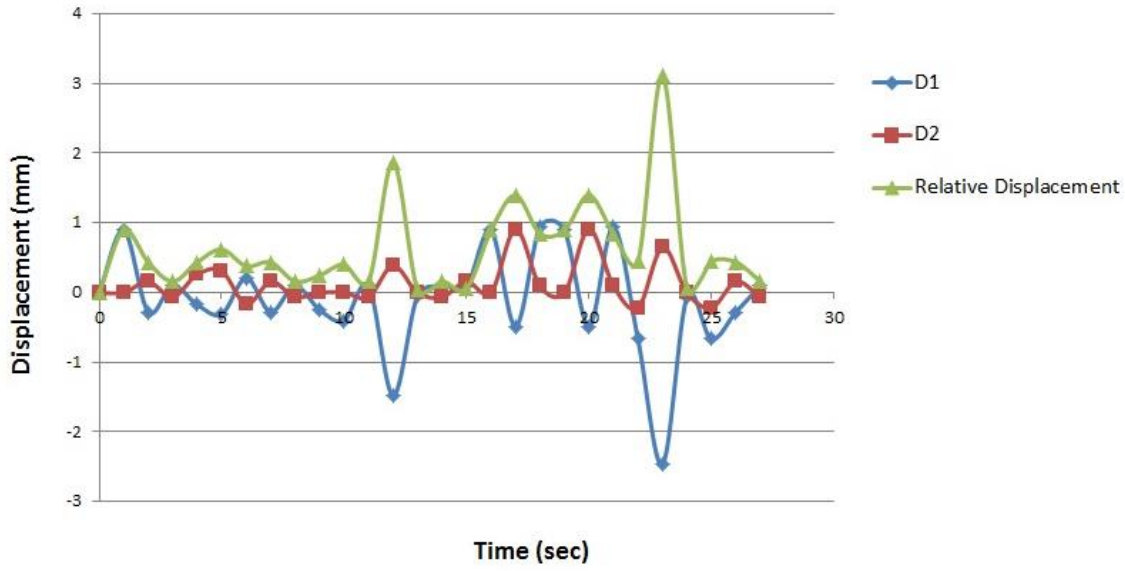

Figure (5.28): Relative Displacement for Node (1) - Y direction

also for node (2) which is located at the same alignment on the narthex, it has a 2.61 mm deformation, and this is can be shown on figure (5.29), the two values of nodes of narthex have disparity of 18%, and this is acceptable.

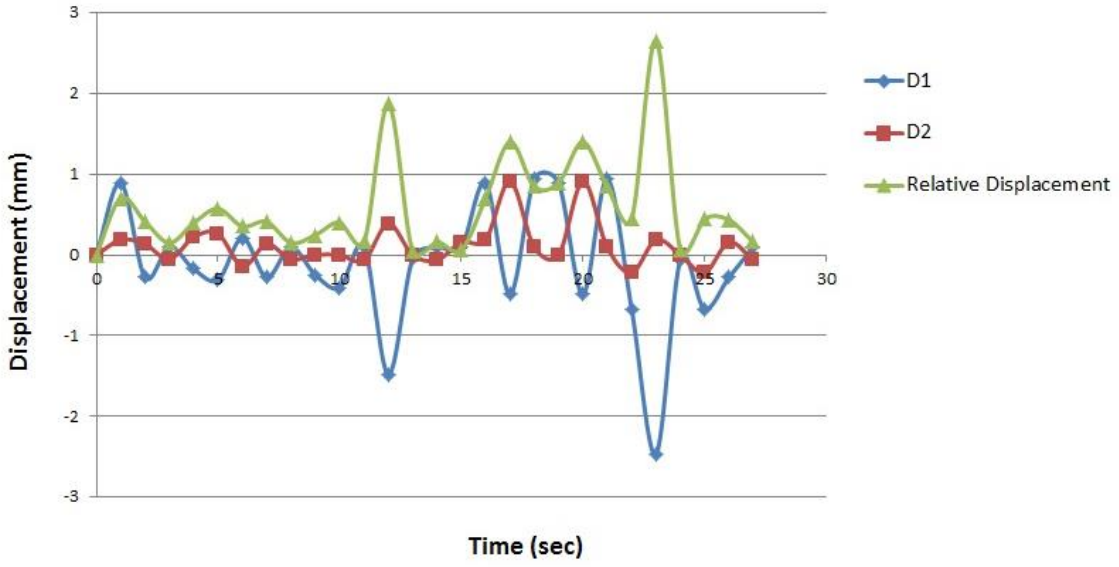

Figure (5.29): Relative Displacement for Node (2) - Y direction

Similarly by showing the results of nodes (3), (4), and (5) which are located on the south wall, their relative displacements are 9.02 mm, 12.64 mm, 10.10 mm, respectively, figures (5.30, 5.31, and 5.32). These results are predictable, due to low tensile strength, and out of plane orientation of these unreinforced masonry walls.

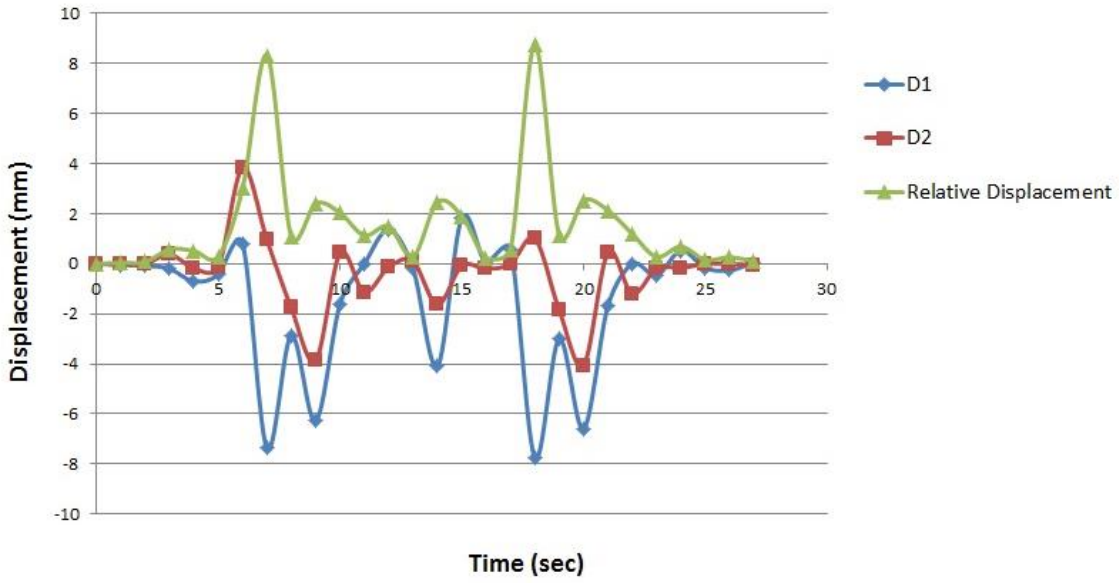

Figure (5.30): Relative Displacement for Node (3) - Y direction

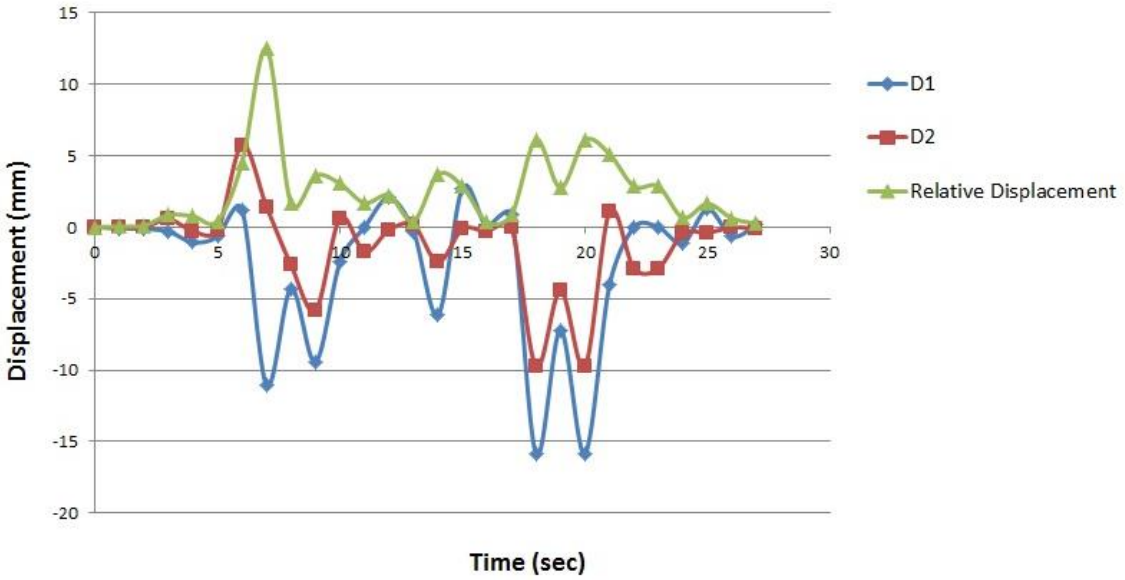

Figure (5.31): Relative Displacement for Node (4) - Y direction

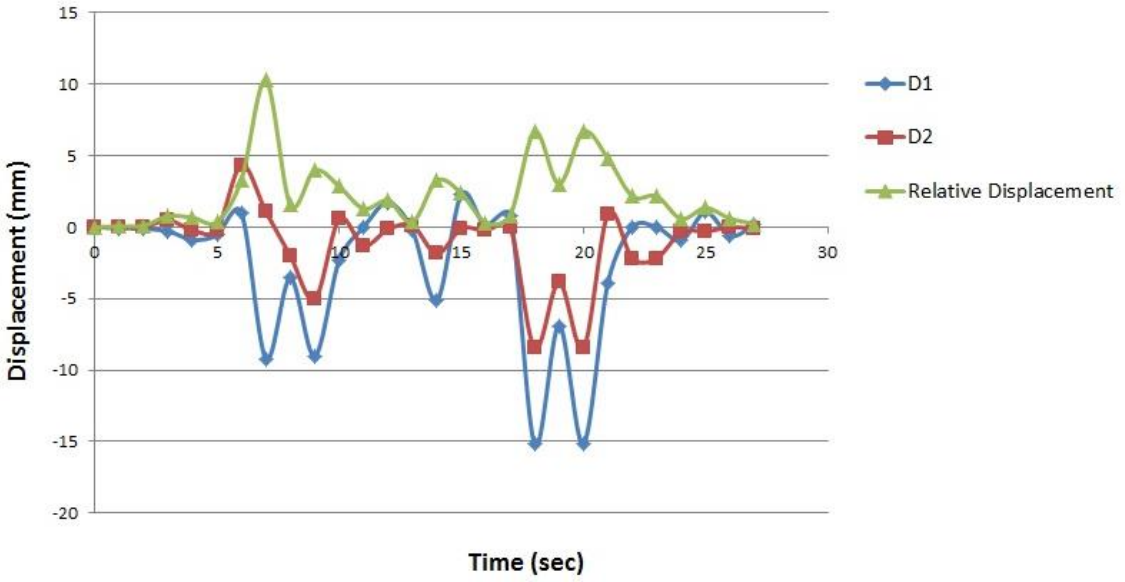

Figure (5.32): Relative Displacement for Node (5) - Y direction

For the inspector of these functions of the last three nodes, the behavior are very similar, the curves prove that after roughly 25% of the duration the wall resist first stones detachment, and still resist the excitations until the clear second detachment after 75% of the duration.

Turning to nodes (6) and (7), the behavior is integrated, and the existence of windows in the interior walls also encouraging the out of plane failure, so the absolute relative displacement for the two nodes chosen, are worrying, they summarized as 12.51 mm and 13.04 mm, respectively, figures (5.33 and 5.34).

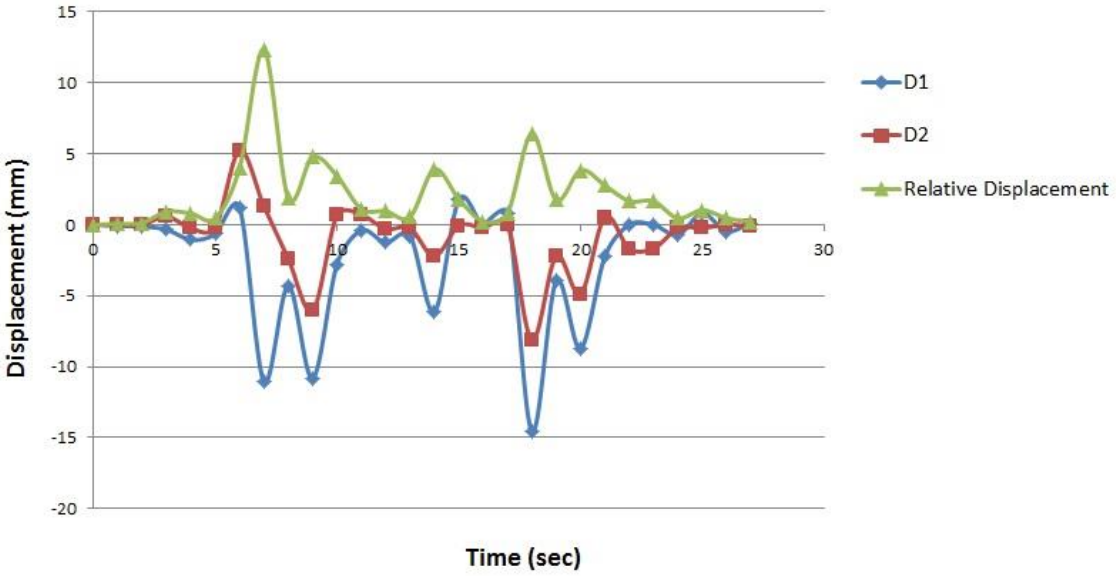

Figure (5.33): Relative Displacement for Node (6) - Y direction

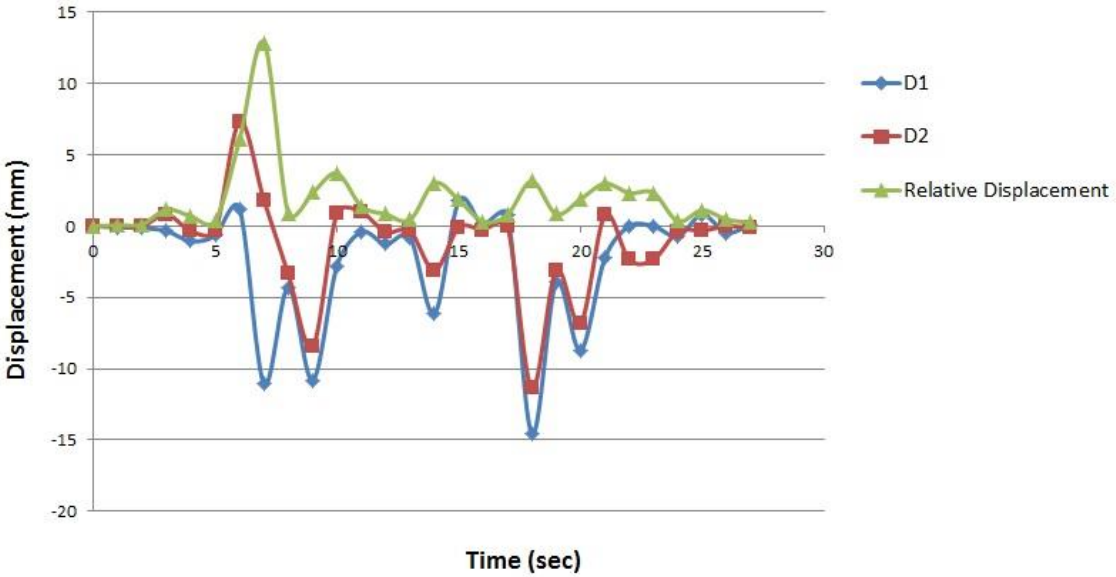

Figure (5.34): Relative Displacement for Node (7) - Y direction

By remembering these nodes with its relative displacement in X – direction, it was 3.83 mm, and 3.17 mm for nodes (6) and Node (7) respectively. Looking carefully for these points, the Y-direction has a relative displacement about 265% of X – direction, this dreadful percentage indicate the next researchers should study the out of plane behavior in scrutiny way.

In a similar context, the nodes located on transvers walls, which are denoted by (8), and (9) have displacements curves shown in figures (5.35 and 5.36)

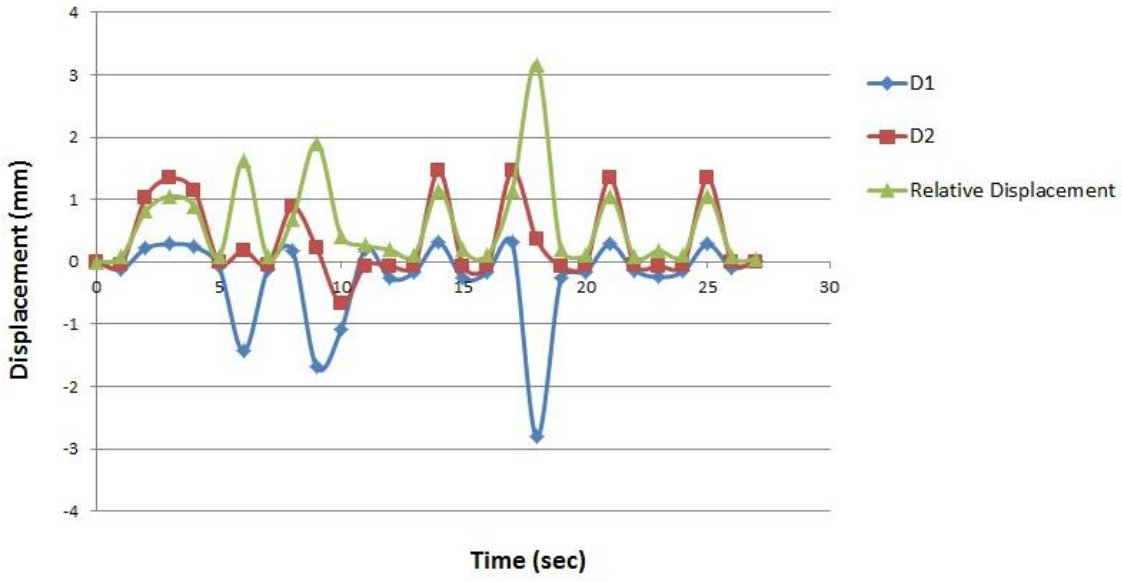

Figure (5.35): Relative Displacement for Node (8) - Y direction

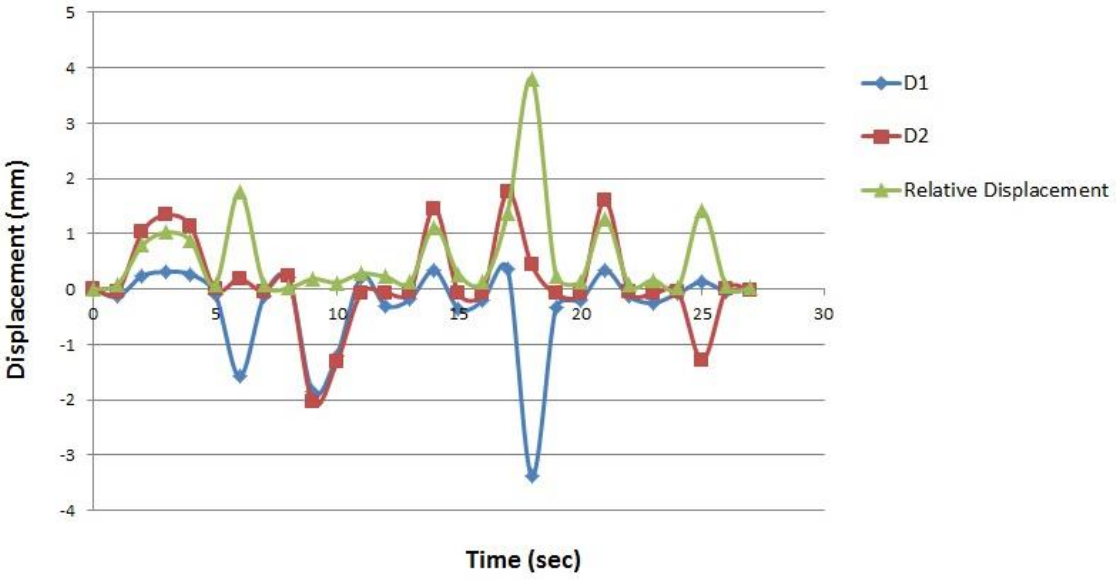

Figure (5.36): Relative Displacement for Node (9) - Y direction

The figures of these points emphasize the relative displacement at two critical locations; the first is located at the center of transverse wall, and the other on the connection between transverse and longitudinal wall (south wall). For the point located at their center which is designating as (8), the relative displacement is 3.12 mm, and for the point designating as (9) it's 3.81 mm. By continue with side apses and shoulder walls of the church, node (10) which is located on the vaults of side apse (south one), exposed to maximum absolute relative displacement of 3.11 mm, figures (5.37).

This value might be annoying, but for this curved walls exposed to in plane excitation, this value can be smoothly accepted, within the reason of walls thickness (this walls has a thickness of 1.8 m).

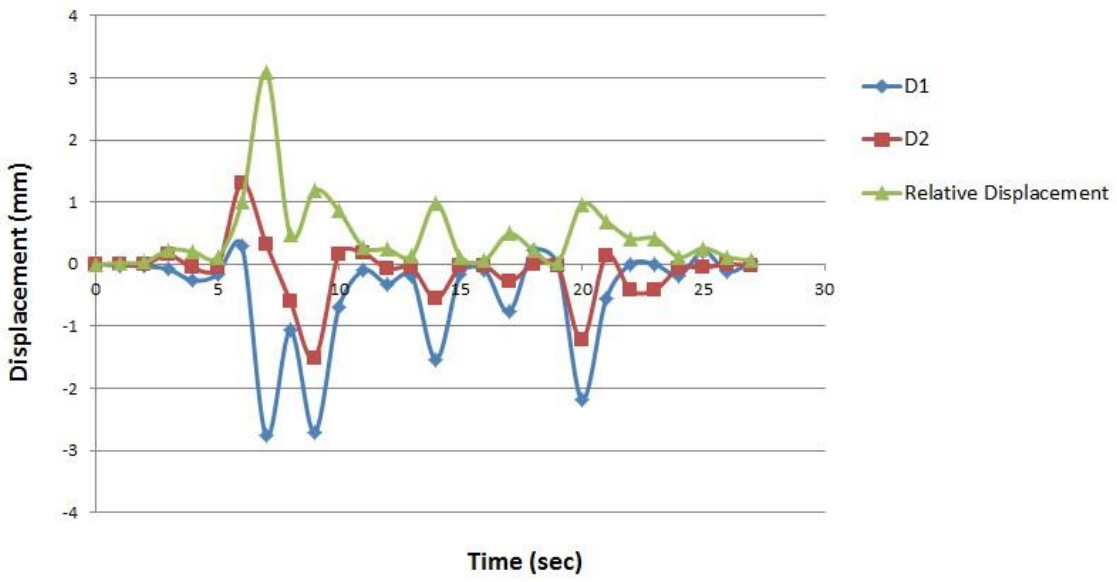

Figure (5.37): Relative Displacement for Node (10) - Y direction

For the point located of the outer side and denoted by node (11), the value roughly is 2.92 mm, figures (5.38).

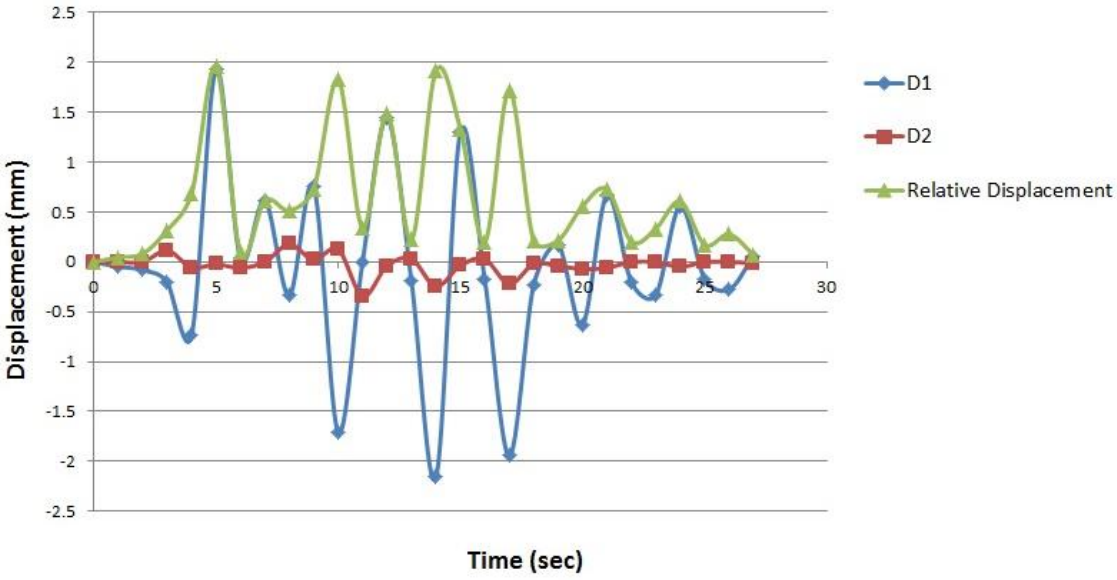

Figure (5.38): Relative Displacement for Node (11) - Y direction

The previous figure, show the two functions of displacement for the stone block, where the node was chosen, are quite different; D1 which is denoted by blue line has a sharp behavior against D2 with smooth behavior, which is denoted by red line, the absolute difference of these two functions gives the confused behavior for relative displacement, with green line.

Also for the shoulder walls, which are denoted by nodes (12), (13), (14), and (15), their maximum relative displacement have relatively constant and ranges about 2.00 mm – 2.50 mm, for example, node (12) has a value of 2.43 mm, figure (5.39), node (13) has a value of 2.09 mm, figure (5.40), node (14) has a value of 2.02 mm, figure (5.41), and the node (15) has a value of 2.77 mm, figure (5.42).

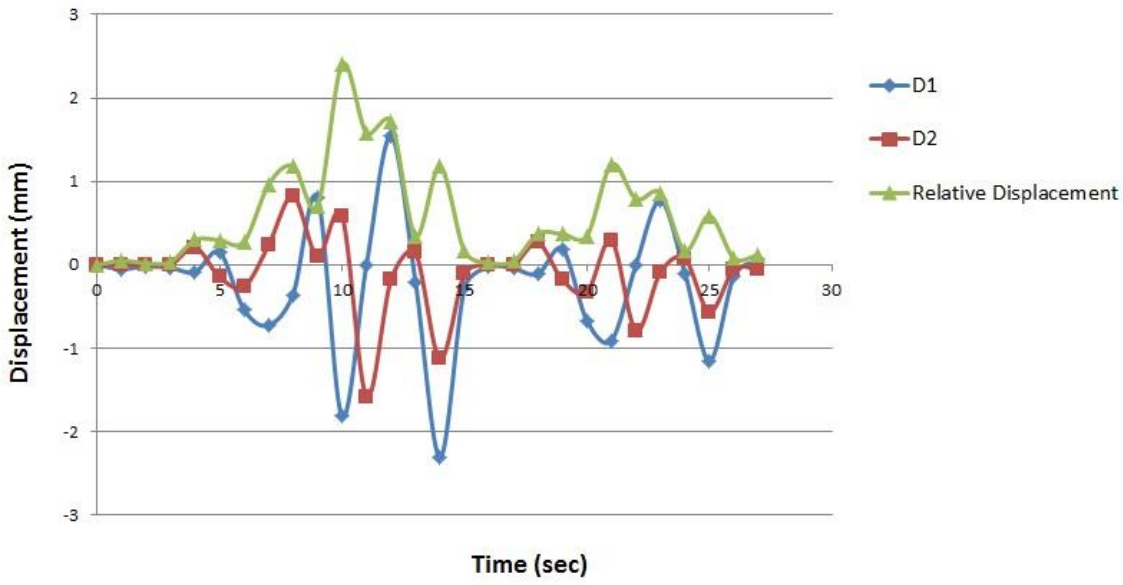

Figure (5.39): Relative Displacement for Node (12) - Y direction

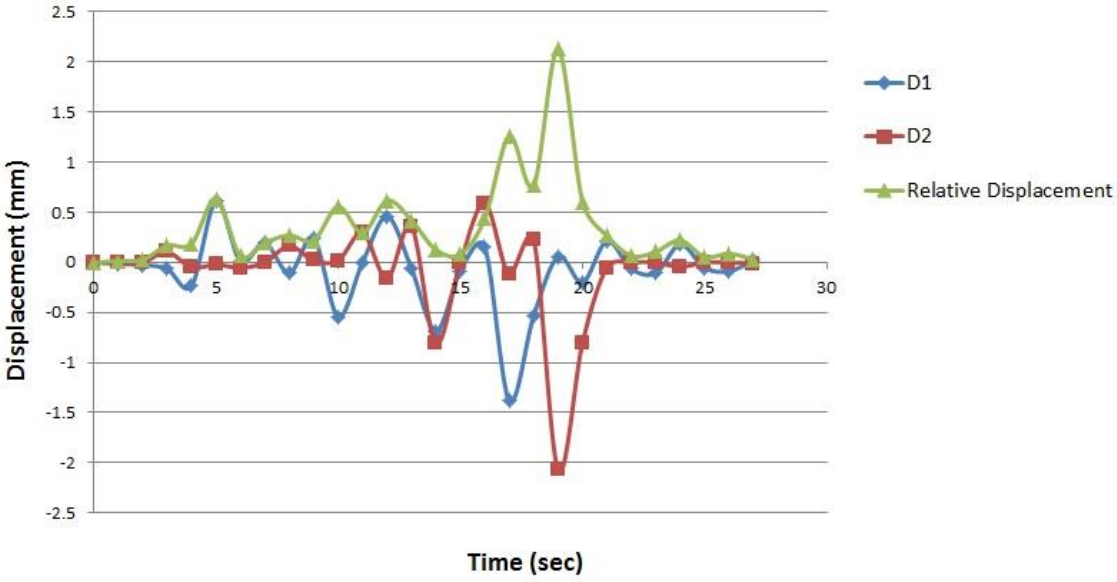

Figure (5.40): Relative Displacement for Node (13) - Y direction

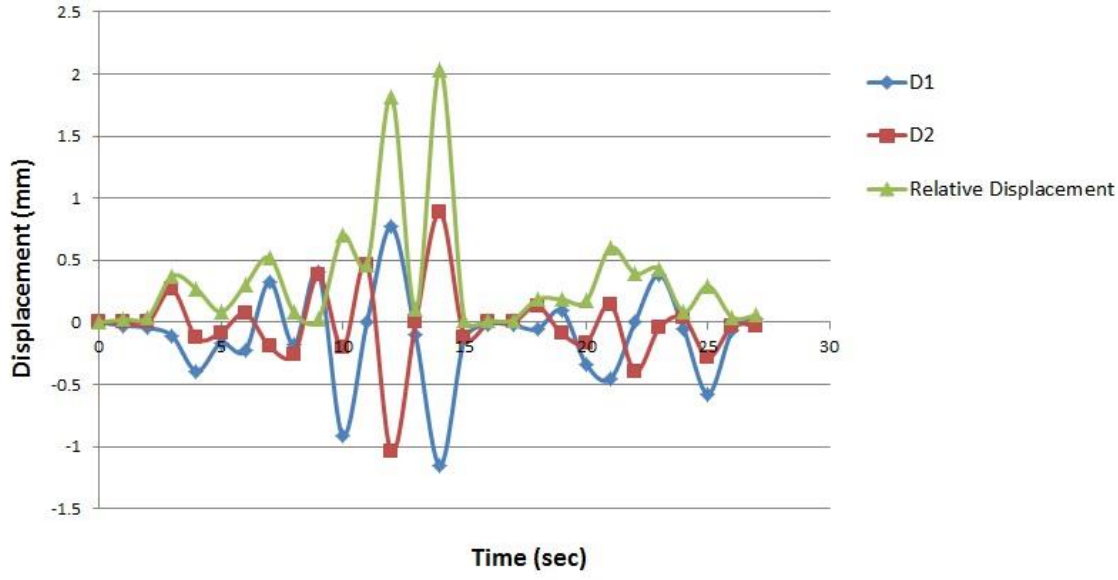

Figure (5.41): Relative Displacement for Node (14) - Y direction

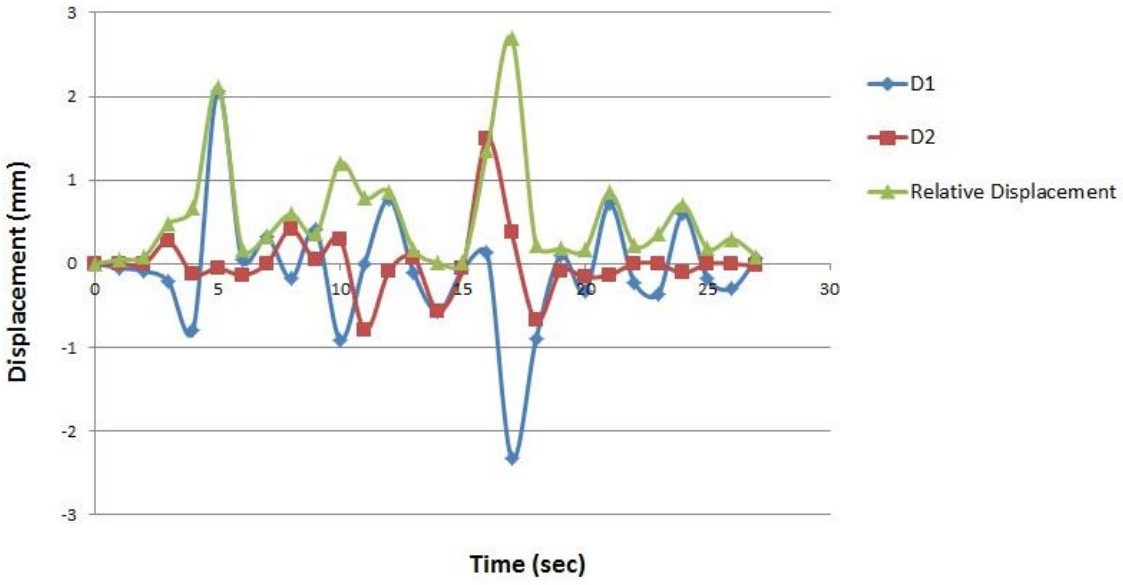

Figure (5.42): Relative Displacement for Node (15) - Y direction

In the same pattern, nodes (16) located on the opposite transverse wall has a value of relative displacement of 3.37 mm, figure (5.43), this valve is similar for the node (8), and this is predictable due to identical length, properties, and stiffness of two walls.

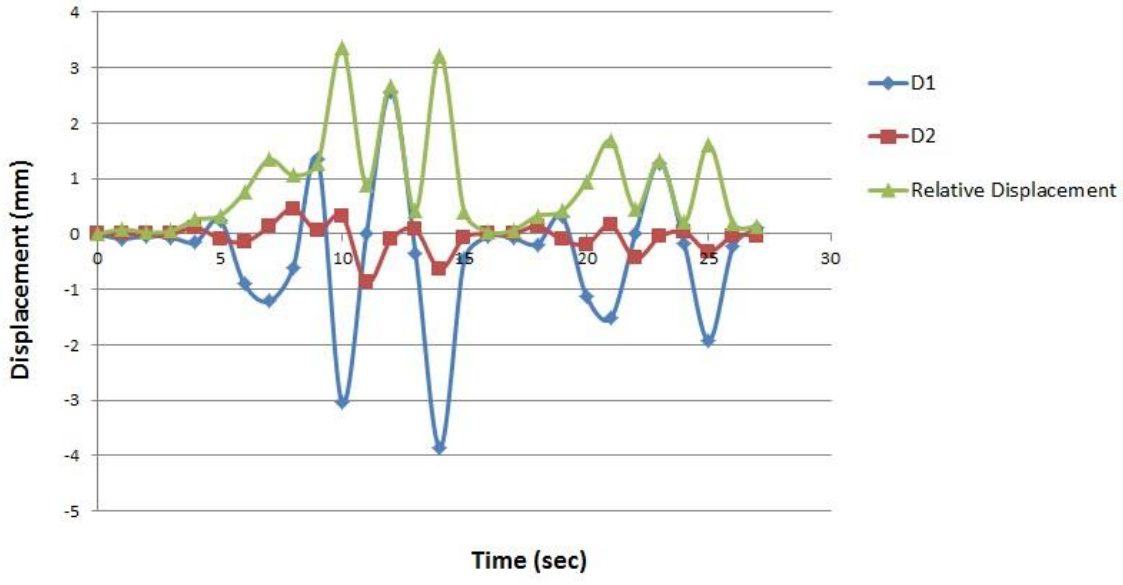

Figure (5.43): Relative Displacement for Node (16) - Y direction

Nodes (17), and (18), have maximum relative displacement of 10.03 mm, and 7.29 mm respectively, figures (5.44 and 5.45). In spite of existence the node (18) on the wall itself, node (17), have the maximum absolute relative displacement because it is located on the connection between walls, and play an important inspection for the connections, also emphasize that these concoctions exposed to discontinuity during horizontal movement in both directions, X and Y.

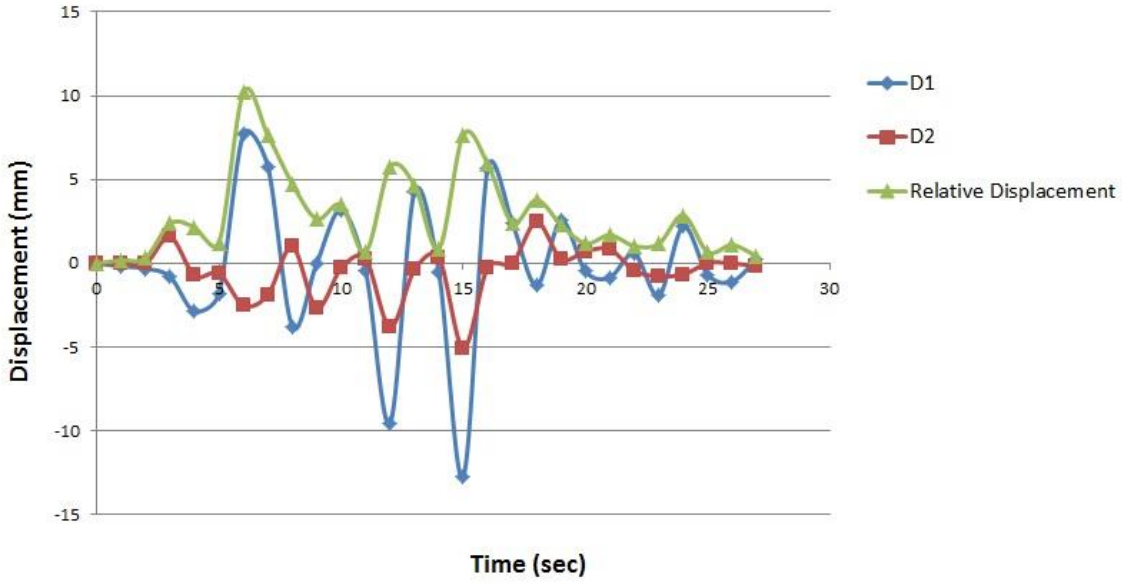

Figure (5.44): Relative Displacement for Node (17) - Y direction

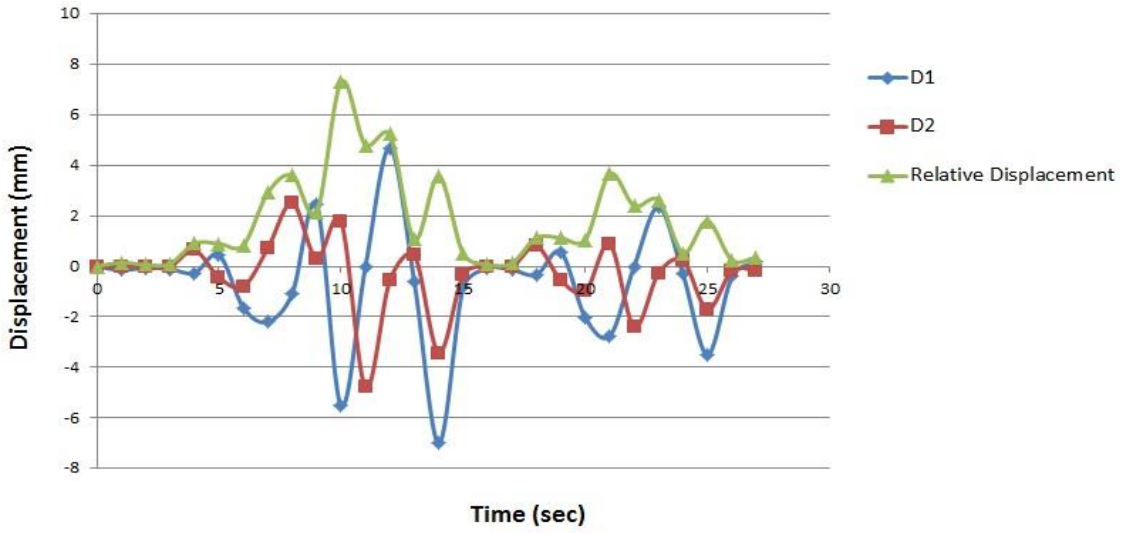

Figure (5.45): Relative Displacement for Node (18) - Y direction

For the final discussion of relative displacements, this section closes with nodes (19) and (20).

Node (19) which is located on the vaults of central apse, exposed to 6.92 mm deformation between two corner points, as figure (5.46) show, this point with its value of relative motion should be studied carefully.

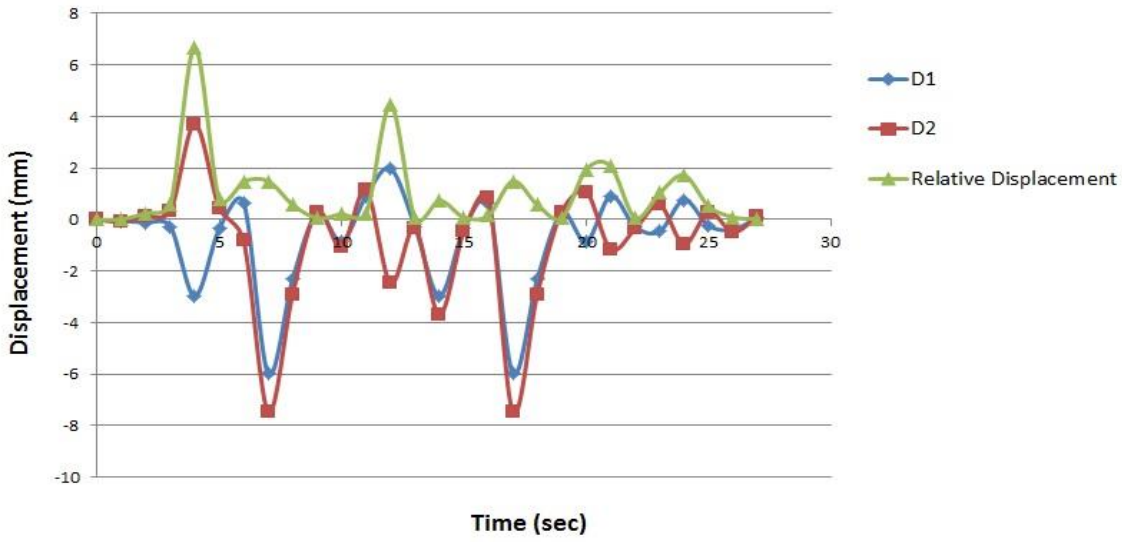

Figure (5.46): Relative Displacement for Node (19) - Y direction

For the point located of the outer side and designated by node (20), the maximum relative displacement reaches 2.13 mm, figure (5.47), and this vale is considered trivial with no meaning, because this wall has a thickness of 1.8 m , so a value of 2.13 mm is accepted

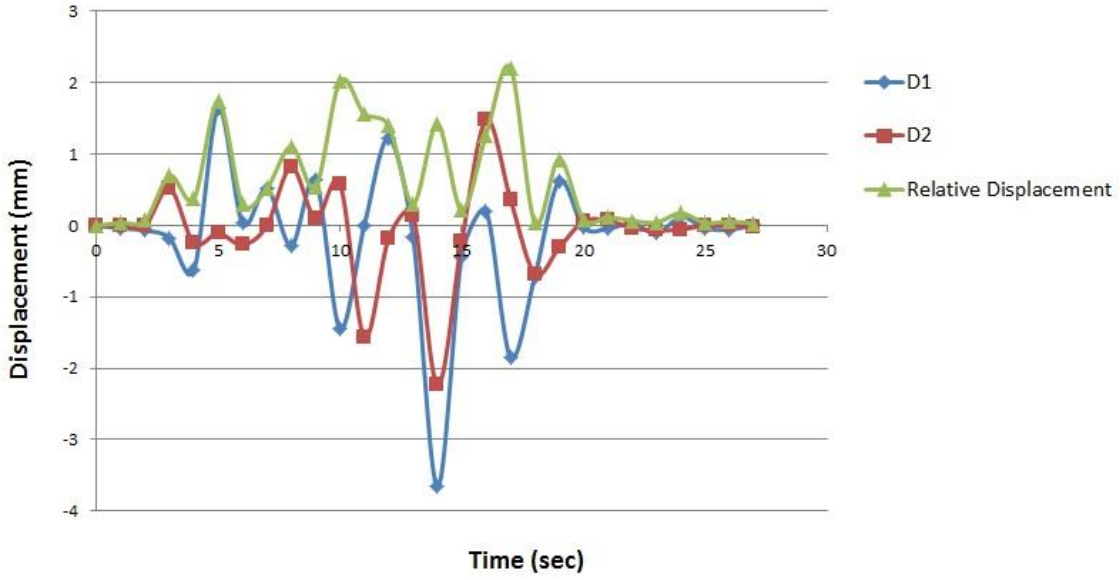

Figure (5.47): Relative Displacement for Node (20) - Y direction

Finally, the Appendix (D), show all the numerical results for the calculations of relative displacement in Y – direction, also the figure (5.48) below can show the maximum values of relative displacement according to each node.

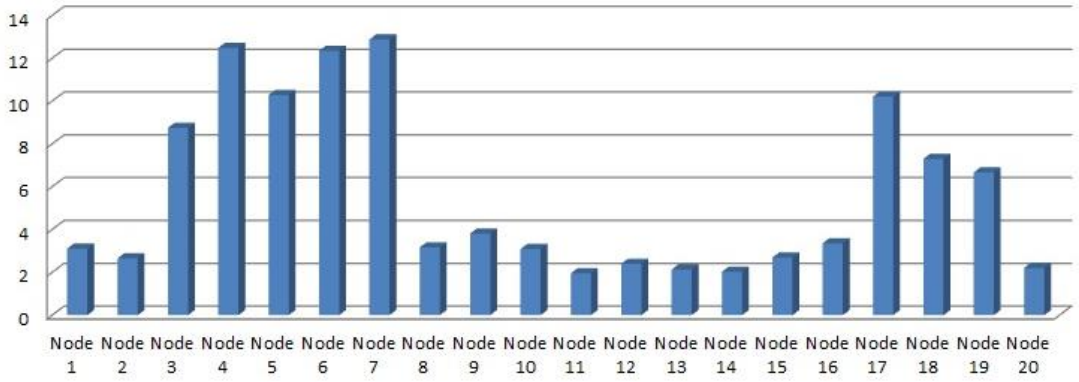

Figure (5.48): Maximum Relative Displacement for all Nodes - Y direction

CHAPTER SIX
PROGRESSIVE COLLAPSE

6. Progressive Collapse

6.1 Introduction

Progressive collapse of historical buildings occurs when a local failure of any structural component leads to failure and as a result collapses of adjoining members, with goes on promoting additional collapse. Therefore, it is necessary not only to evaluate the buildings' safety under traditional loads and earthquake actions, but also to evaluate the structural performance to resist the progressive collapse.

This chapter discusses the performance of The Church of Nativity, by modeling progressive collapse at each step when it is occur, and showing the mechanisms generated. The considerations make these types of building distinct from the modern buildings, summarized as; material properties which are usually decadent, and the structural system which may not meet the requirements of construction codes. The failure criteria for the structural elements as well as the damage limits for the structure follow the provisions addressed in American Unified Facilities Criteria "Design of Structure to Resist Progressive Collapse" (UFC 4-023-03 – Chapter 6).

6.2 Analysis Procedure

To prevent the collapse of valuable and historical buildings, it is necessary to fully understand their failure mechanisms and to improve safe earthquake excitations period by focusing on critical regions of the structure, so because the masonry structures present substantial vulnerability to rock falls, with scarce methodologies for the damage

quantification of structures subjected to rock falls, an analytical procedure for the damage assessment of masonry structures is presented in this section.

The procedure connects three stages of work, starts firstly from applying the dynamic analysis with real earthquake accelerogram to the model, secondly adapting failure criterion to masonries (Von Misses) to gain results from analysis which is applied, then compare it to the limit state values assumes as ultimate shear stress of each component, and finally, locate the critical and collapsed regions in the model, also when this collapse will happen during the earthquake duration.

The analysis is carried out with the finite element program SAP2000 on the model of Nativity Church. In details, The dynamic analysis is carried out using the accelerogram regards the 1940 El Centro earthquake which was occurred at 21:35 Pacific Standard Time on May 18 (05:35 UTC on May 19) in the Southern California near the international border of the United States and Mexico, figure (6.1). This earthquake had a magnitude of 6.9 on the Mercalli intensity scale and was the first major earthquake to be recorded by a strong-motion seismograph located next to a fault rupture, (Trifunac, M.D.; Brune, J.N.).

In this chapter the applied accelerogram lasts 39.00 seconds and all information is obtained from U.S. Geological Survey website (USGS.GOV). Subsequently, the principle stresses distributions over the model are shown, also the Von Misses stresses are calculated for each time

step. It's important also to mention the scale used to determine the seismicity of location with amplitude, and distance. The mathematical formula used is:

$$\text{Scaling Factor} = \frac{I * Z}{Z1 * R} \qquad (6.1)$$

- I; Importance factor,
- Z; Seismic Zone Factor of Bethlehem, (0.15g), according to Seismic Hazard Map
- Z1; Amplitude for chosen earthquake,
- R; inelastic factor.

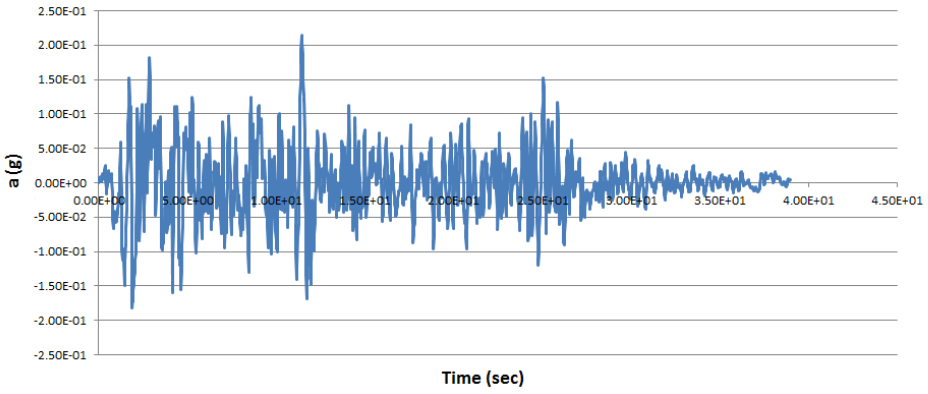

Accelerogram of El Centro Earthquake (1940) in the EW direction,

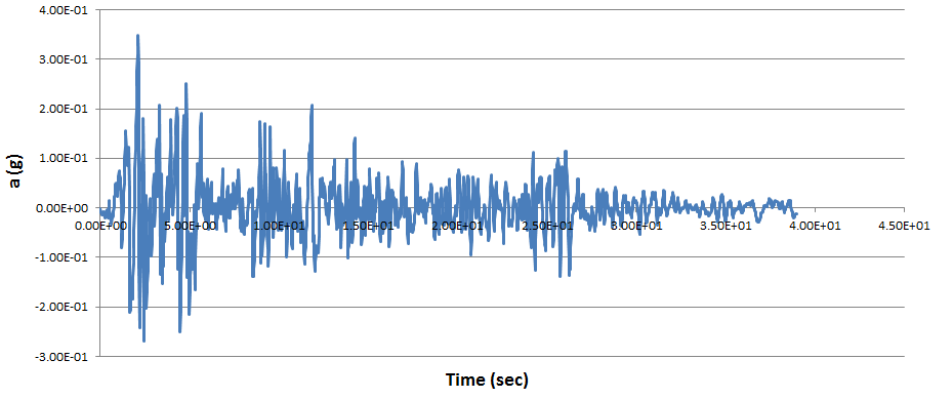

Accelerogram of El Centro Earthquake (1940) in the NS direction,

Figure (6.1): Accelerogram of El Centro Earthquake.

6.3 Failure Criterion

The selection of failure criterion concerning the damaged areas of a structure is crucial. When bi-dimensional assumptions are made, a modified Von Misses criterion, using the two produced principal stresses, can be employed.

Syrmakezis and Asteris, Modified the original criterion in order to be consistent with masonry structural properties. The modified failure criterion is a semi-empirical failure criterion, based on experimental results, figure (6.2), which present the failure curve that formed by the interaction of four surfaces S_1, S_2, S_3 and S_4, each one represents a certain biaxial stress state.

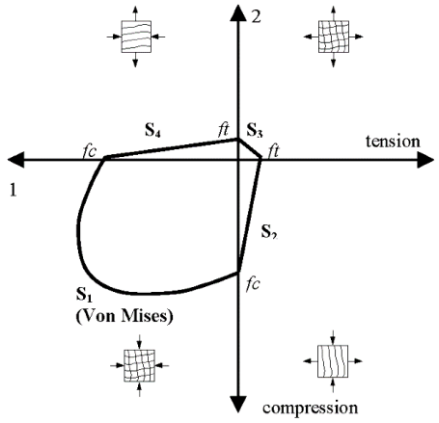

Figure (6.2): Modified Von-Mises Failure Criterion for Masonry Structures [Syrmakezis and Asteris]

Failure analysis is carried out by application of the modified Von Misses failure criterion, the stresses at reference nodes, figure (6.3) are calculated and compared with the permissible values of the stresses given

in table (3.1) mentioned in section 3.3.2 taken the shear stress must not exceed 0.089 MPa for Perimeter walls, 0.067 MPa for specific narthex components, and 0.02 MPa for vaults.

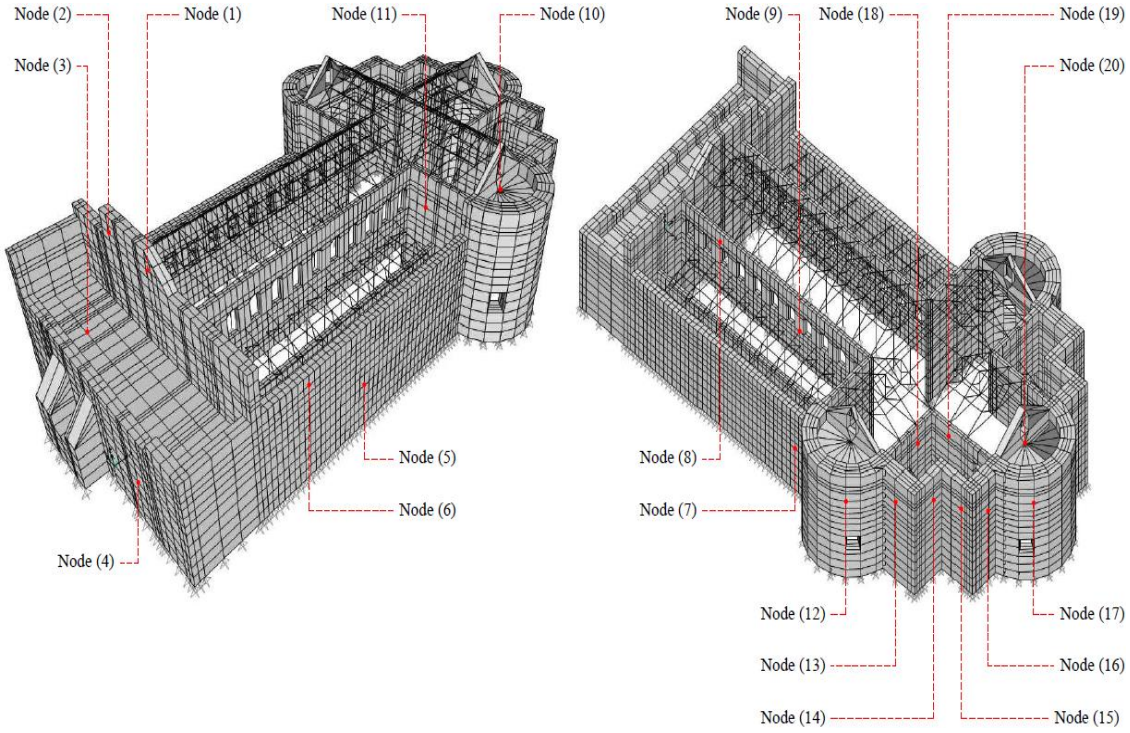

Figure (6.3) : Locations of the Reference Nodes for Progressive Analysis

In masonry structures such as the entire church and other historical building in Palestine, the masonry walls constitute the building's band, starts from resisting the gravity load, to end by a resisting system of lateral load. Therefore, any loss of integrity or partial collapse of the building components directly affects the integrity of the entire structural system i.e. the loss of load bearing members can cause catastrophic failures without much warning or time for evacuation of the building. As a result, studying codes and specifications that relate to progressive collapse analysis, such as the Unified Facilities Criteria (UFC) 04-023-03, which cover steel and

concrete structures in more depth and detail than masonry structures, making the analysis of existing masonry structures challenging.

6.4 Principle Stresses

The principal stresses resulted from dynamic analysis of El Centro are presented in figure (6.5) for X - direction, and figure (6.8), for Y – direction, the following sections discuss in details each direction.

6.4.1 X - Direction

Starting with X – direction, the scanning of contours give a glimpse for the mechanisms of collapse for the model, i.e. the loss of balance, collapse of triangular walls over apses, disconnections between transverse walls and main façade, figure (6.4). In details, the principal stresses σ_{11}, σ_{22}, σ_{33}, and out of plane shearing stresses σ_{12}, σ_{13}, σ_{23}, are found within permissible limits at the most part of the structure, except some locations over it, both principle and out of plane shearing stresses exceeds permissible limits, figure (6.5).

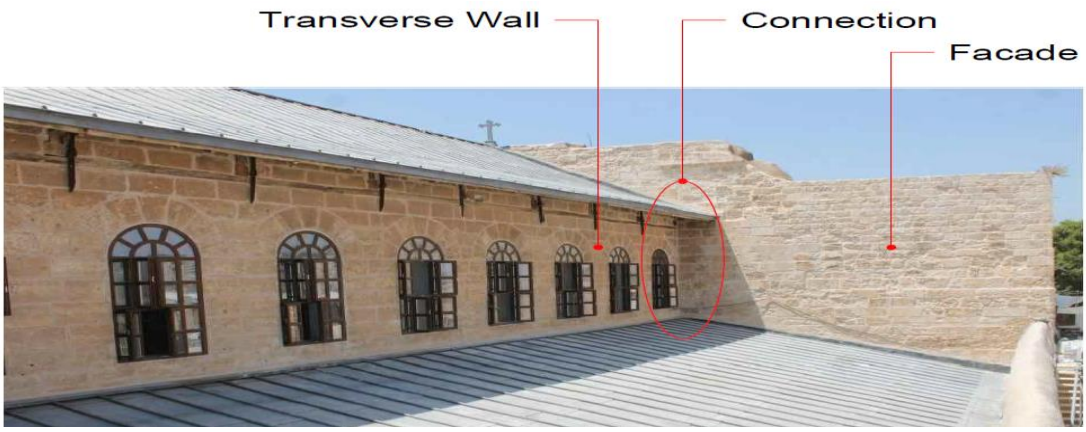

Figure (6.4): Connections Between Transverse walls and Façade

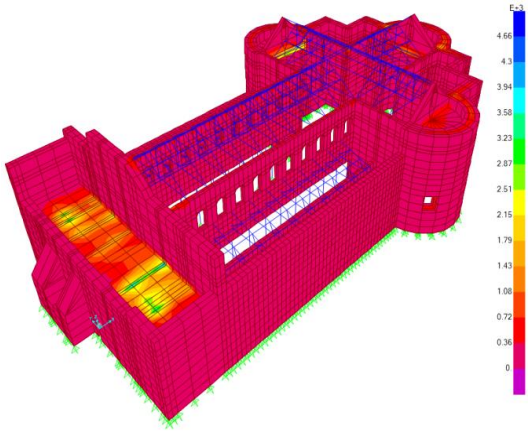

a. Maximum principal stress (σ_{11})

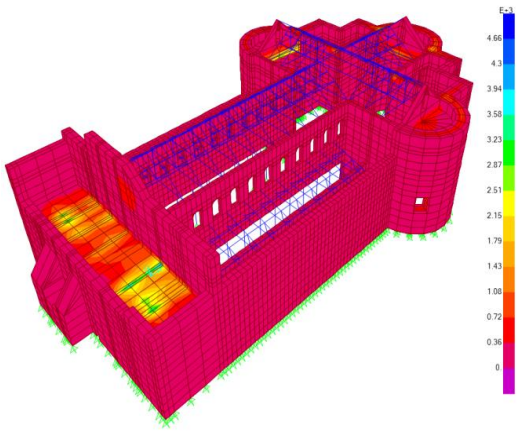

b. Maximum principal stress (σ_{22})

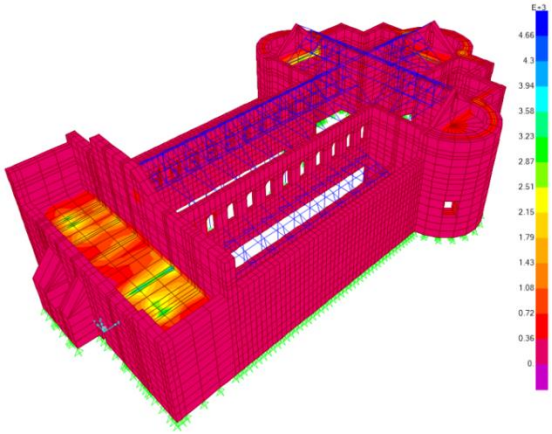

c. Maximum principal stress (σ_{33})

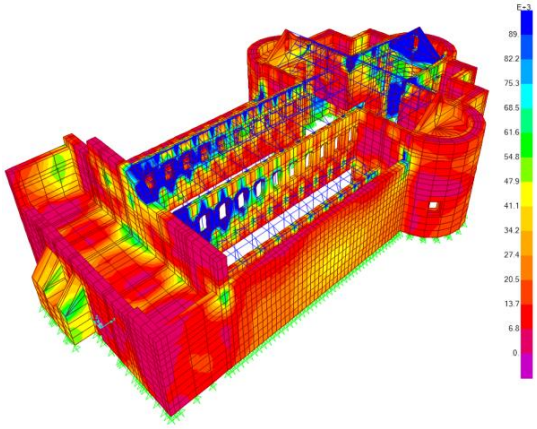

d. Out-of-plane shearing stresses (σ_{12})

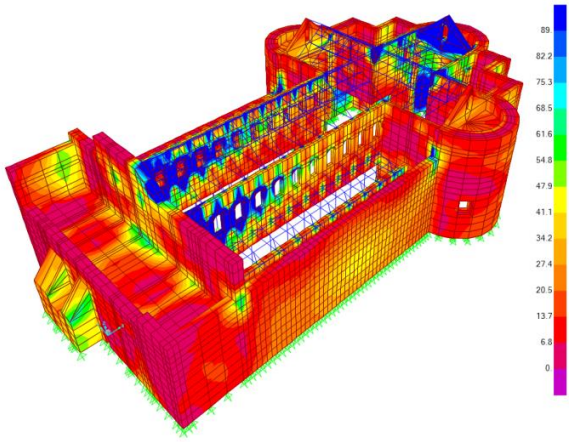

e. Out-of-plane shearing stresses (σ_{13})

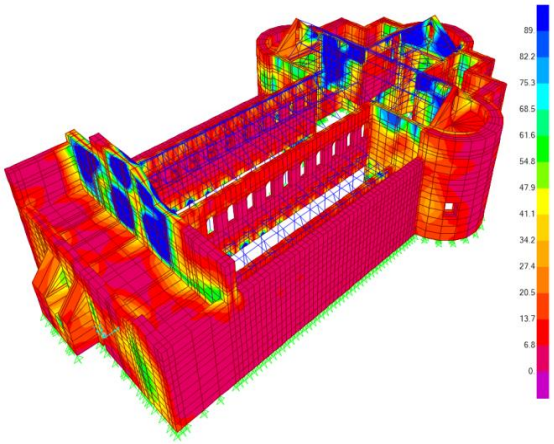

f. Out-of-plane shearing stresses (σ_{23})

Figure (6.5): Principle Stresses for X – Direction

6.4.2 Y - Direction

For the other direction Y, the collapse mechanisms descried as a shear failure at the connection of wooden trusses with masonry walls, and the out of plane failure in the south and north walls which are shown in the plan of figure (6.6).

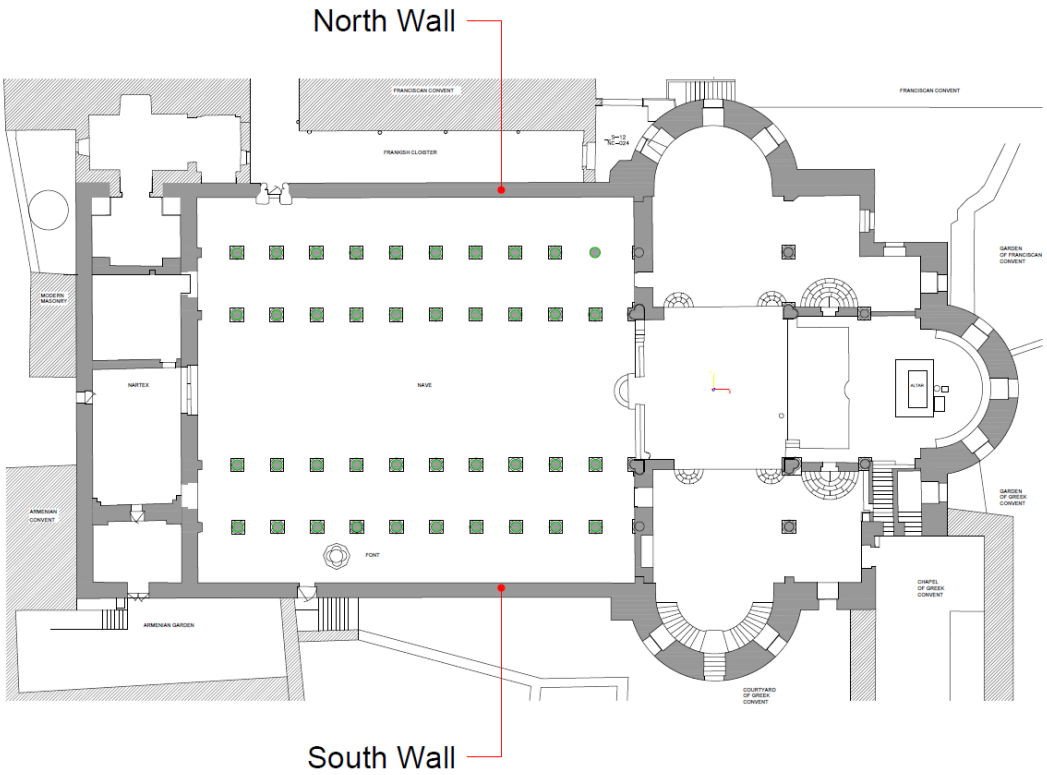

Figure (6.6): The Church's Plan, Showing Locations of South and North Walls.

The principal stresses σ_{11}, σ_{22}, σ_{33}, and out of plane shearing stresses σ_{12}, σ_{13}, σ_{23}, in Y - direction are found within permissible limits at the most part of the structure as done in X - direction. Figure (6.8), present the contours on the three dimensional model, these results of the distribution of out of plane shearing stresses (σ_{13}) in Y-direction, figure (6.8e), clearly and critically show the parts of the Church where collapse

mechanisms are more likely to occur, namely the tympanum and the Crusade-era wall on both the north and south sides. The biggest concern is for the south wall, which is 8.40 m high, 30.25 m long and ranges from 90 to 110 cm in thick, if this wall would collapse, it may endanger the existence of visitors, and cause considerable damage to the roof, figure (6.7).

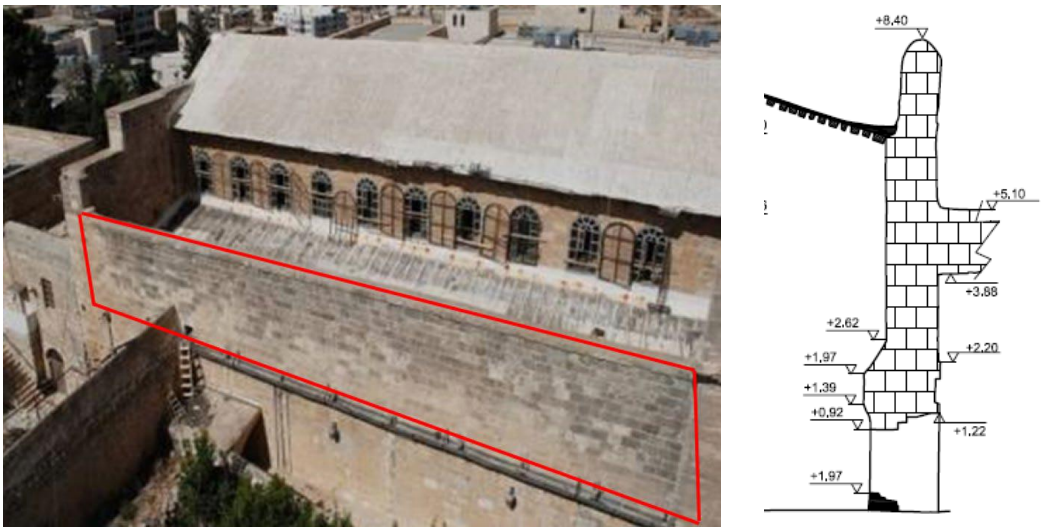

Figure (6.7): South Masonry Wall Location With Geometric Section Height.

In the second part, also the triangular pieces located over each apse, significantly exhibit overturning collapse mechanism, due to exceeding the permissible bounding limits, this may permit these parts to collapse according to lateral movements in Y – direction.

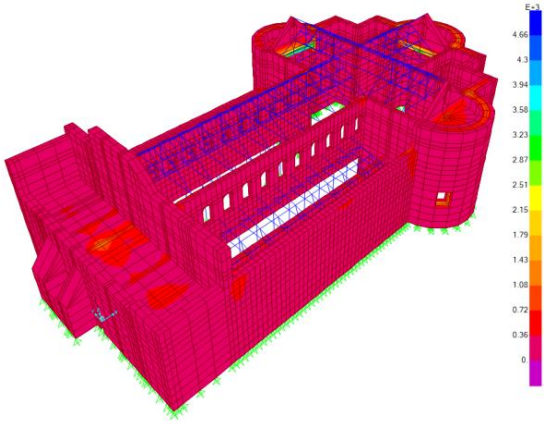

a. Maximum principal stress (σ_{11})

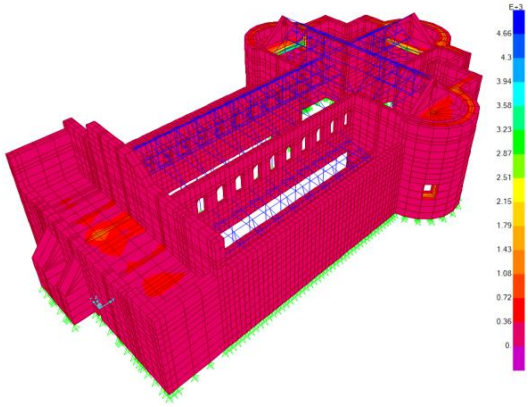

b. Maximum principal stress (σ_{22})

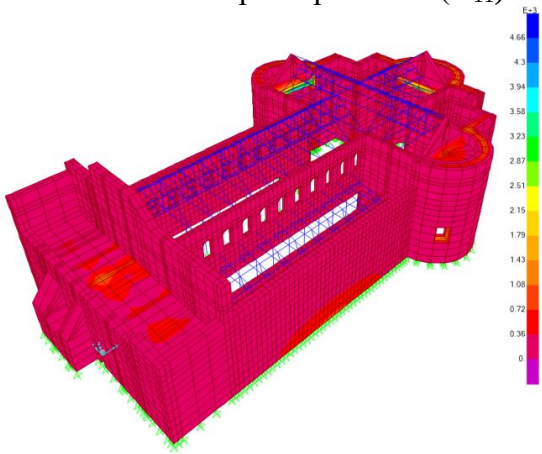

c. Maximum principal stress (σ_{33})

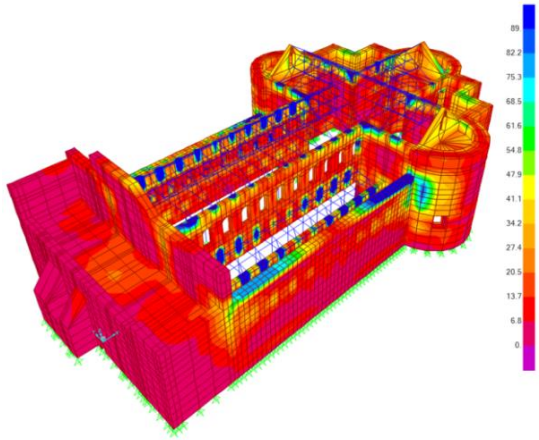

d. Out-of-plane shearing stresses (σ_{12})

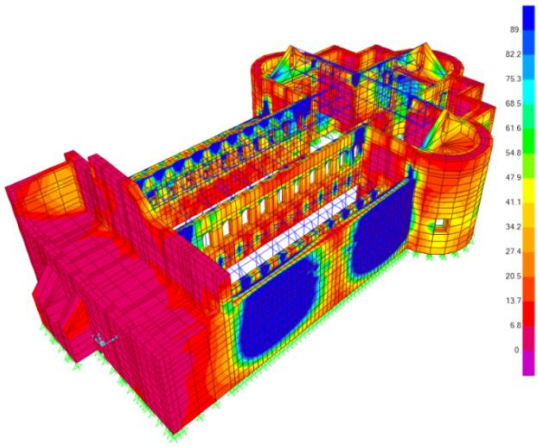

e. Out-of-plane shearing stresses (σ_{13})

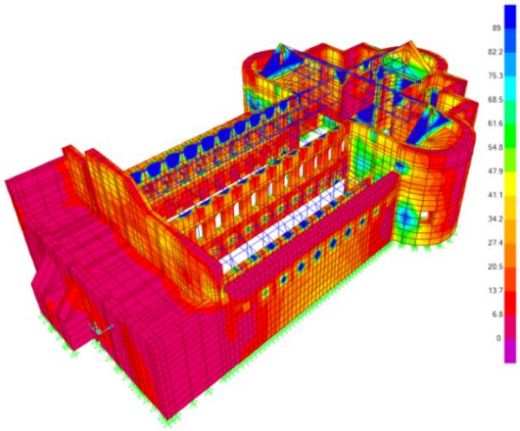

f. Out-of-plane shearing stresses (σ_{23})

Figure (6.8): Principle Stresses for Y – Direction

6.5 Critical Region Identification

The main objective of this section is to identify the critical and vulnerable regions of stone components considering the church, also indicates that collapses are often caused by defects or damage at the critical regions during the service stage. The church of Nativity or any other historical structure in Palestine consists of a series of components; each of them has a different degree of importance subjected to external loads. So to ensure global integrity and safety, the critical components and regions should be given greater safety margins.

The basic concept behind the determination of the critical components and regions is to strengthen these structural elements, so the building turn into the phase to be capable for resisting a specific level of threat, which may be in the form of blast, impact or any other abnormal event coming from this “key” elements. The limits of allowable progressive collapse as given in many design codes and guidelines are slightly different. For example, UK building regulations require the key elements to be designed for resisting an abnormal load of 34 KN/m2 applied in any direction. The work in this section describes simulating a complete progressive-collapse process using SAP2000, to find with according to Von Misses results the Critical Region Identification.

6.5.1 Evaluation Results : X-Direction

Figure (6.9) shows the Von Misses results with respect to time for each component of the case study. In details the collapse of the structure caused by excitation of earthquake explained before give arithmetic explanation of the critical region according to the ultimate shear strength.

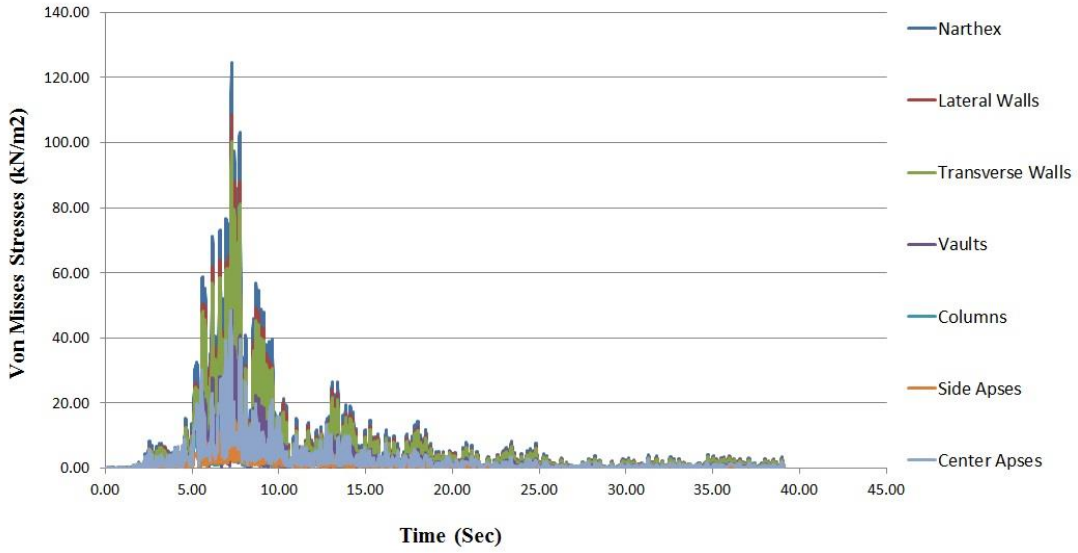

Figure (6.9): Von Misses Function for Church Components, X – Direction.

Based on the dynamic analysis, the following results can be discussed, based on the failure criteria. The von misses stress exceeds the limiting value of shear stress that the masonry walls resist, this leads to collapse of blocks at certain region after 7.53 seconds of analysis. The first failure, summarized in the mechanism regarding the narthex overturning, and the loss of connection in the lateral walls connected to façade, the maximum von misses results is 125.00 KN/m2 which exceeds the upper limit 89 KN/m2, so each element in the structure treated individually and the area collapse is shown in figure (6.10).

As a second stage, figure (6.9) also show the lateral walls reaches a maximum von misses stress 106.50 KN/m2 which is exceeds the upper limit 89.00 KN/m2, and the blocks that located their will fall ! Figure (6.11) show the detached areas. Surly the building is not fit enough to prevent the excitation as well as expected.

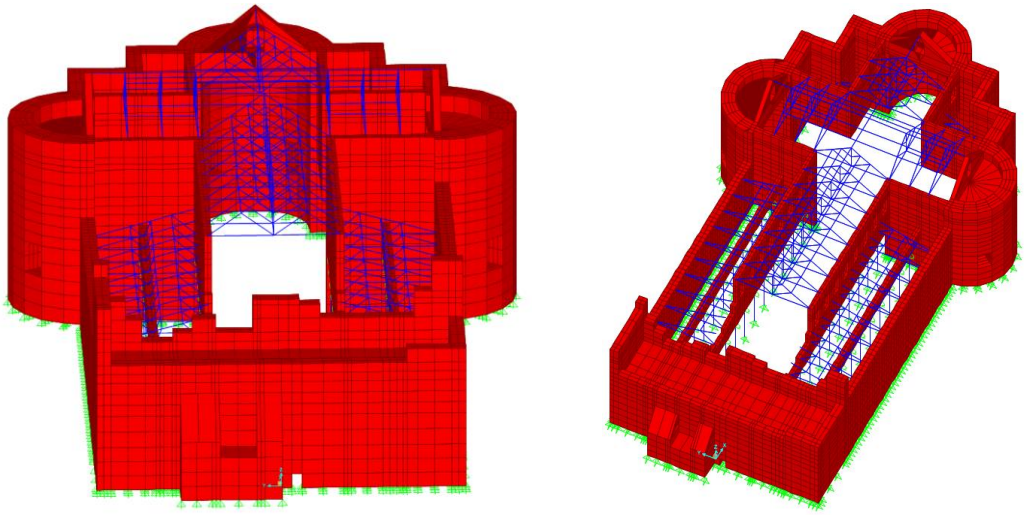

Figure (6.10): Facade Overturning Failure After 7.53 sec

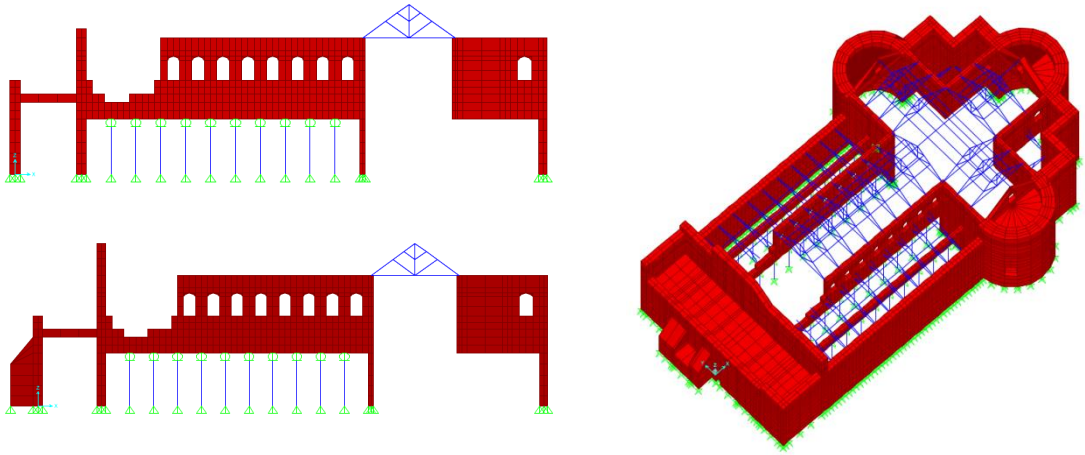

Figure (6.11): Lateral Walls Failure After 7.53 sec

Before going on to the Y direction, the results checked again for the rest duration (between 7.53 sec to 39.09 sec) to ensure that there are no other failed areas, figure (6.9) shows the results within permissible limit.

This means that in plane behavior of church suffering only from narthex disruptive motion and detachment between the connections between members of walls and façade.

6.5.2 Evaluation Results: Y-Direction

As done in the X direction, the evaluation in Y direction show the von misses' results is frightful in the out of plane direction. The collapse is the crash of the longitudinal walls connected façade and transverse walls, at the time of 7.53 sec, in similar manner as X - direction, this mechanism reaches a von misses stress of 167.22 KN/m2, (about 57.01% more than X-direction), and this value is expected due to butters absence in this direction for the external walls, also the large height, and columns support for the internal walls, figure (6.13), shows the collapse of these walls.

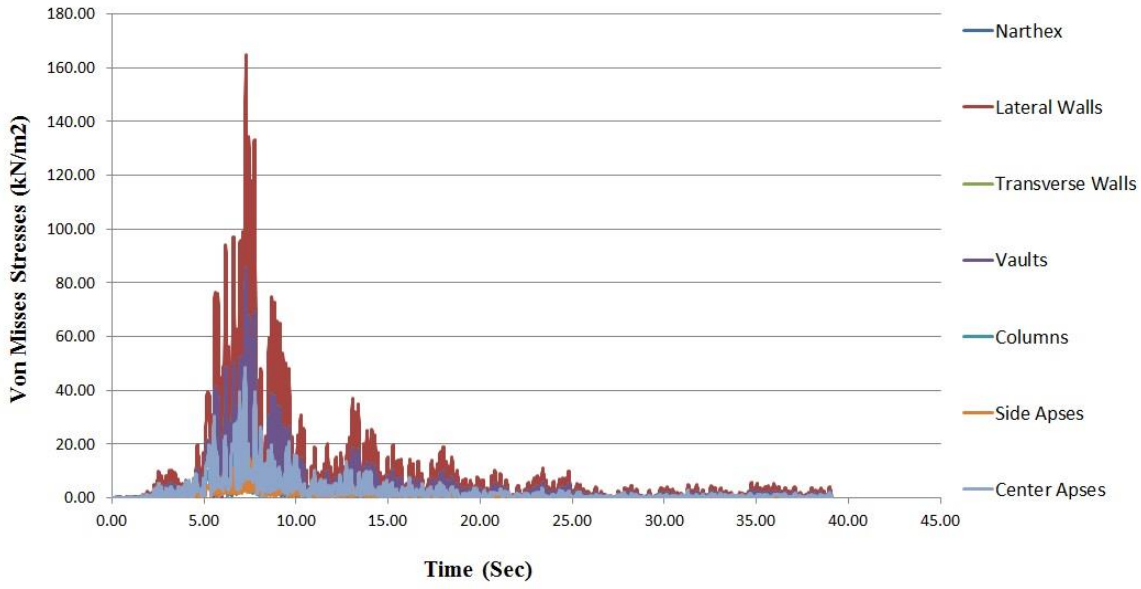

Figure (6.12): Von Misses Function for Church Components, Y – Direction.

Finally, the rest of earthquake excitation (between 7.53 sec to 39.09 sec) shows no more failed elements, the figure (6.12) also present the values of von misses stresses that lie on permissible limits. So we can summarize that in out of plane orientation of entire structure, the relatively long walls are the critical element. Add to that, the trusses that lies on these walls will collapse, with the upper roof of church carried on, which means almost complete collapse for the mosaic panels on walls

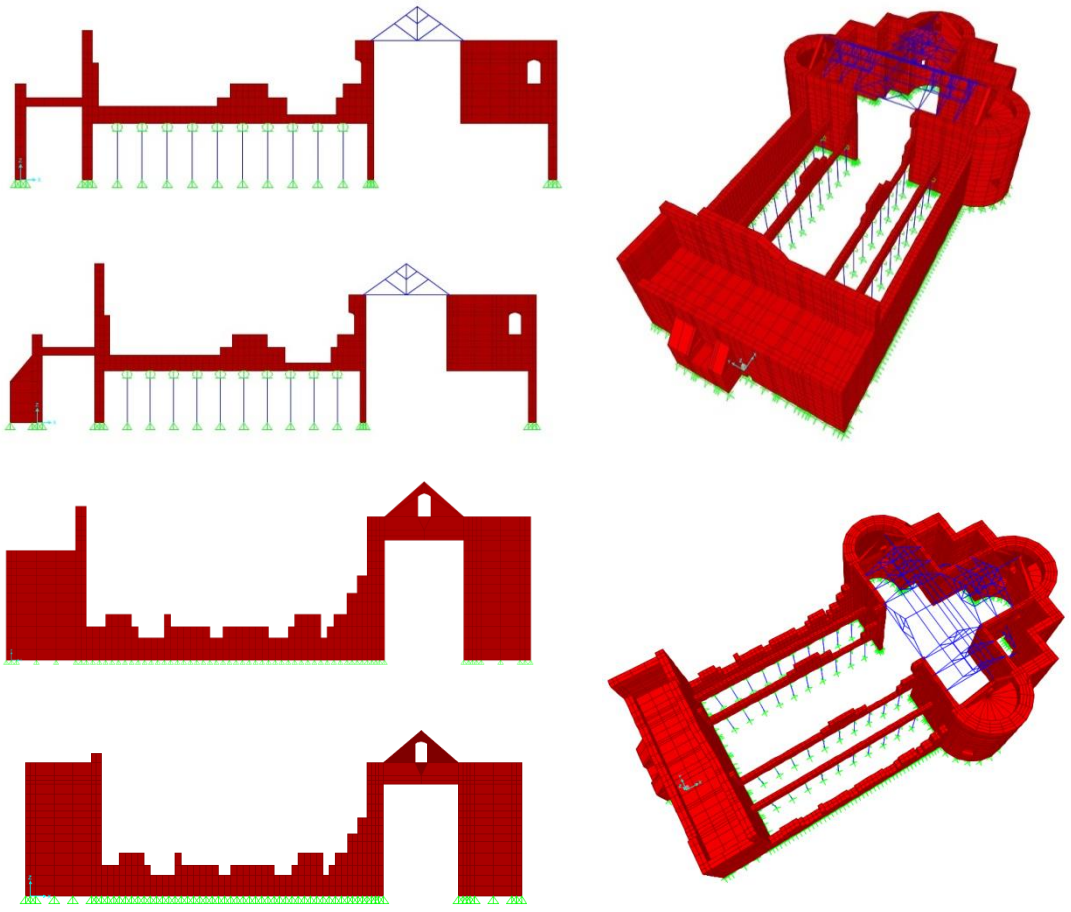

Figure (6.13): External and Internal Lateral Walls Failure

CHAPTER SEVEN

DISCUSSION AND CONCLUSION

7. Discussion and Conclusion

7.1 Discussion of Results

The Heritage constructions pose the largest challenges to the engineering researches, due to the limited knowledge of the existing structure and the difficulty to improve the knowledge without compromising the preservation of the assets.

Provisions of existing codes inadequate to capture the uncertainty of the analysis of historic churches, or any historical structure, also the lack of reference values of critical variables from literature, and the limitations of carrying out tests to measure these critical variables, results in levels of uncertainty larger than the typical uncertainty of the assessment of existing buildings made of modern materials. Moreover, existing codes and guidelines for assessment of existing constructions ignore the fact mentioned in this thesis that decisions made by the analyst during the analysis and definition of actions contribute to the overall uncertainty as much as other aspects, such as the geometry, materials and structural details of the heritage construction.

The most critical aspect of the modeling is simulation of the response of stone masonry by appropriate constitutive model. Under earthquake loading, thick walls and buttresses respond mainly in shear, with a low tensile strength and brittle response.

In the following sections, the discussion will start from the static analysis to the dynamic analysis, in order to show that there are vaguest points should be analyze in different levels.

7.1.1 Discussion of Pushover analysis

Starting from pushover results, there are two types of local mechanisms in the church of Nativity, parallel of the plane of the wall (in plane direction), or perpendicular to the plane of the wall (out of plane direction). The first type of mechanisms is more stiff than the other, from figure (7.1), which present the comparison between maximum crack propagation in each direction with respect to load step, the maximum crack width in X- direction approximately remain slightly small with modest difference, this is evident by examine the points before load step (10), which refer to gravity loads excitations, and after load step (10) which refer to the pushover excitations. For example, the load step (9), has a crack width of 2.40 mm, and for the load step (11), the crack width is 2.29 mm in X – direction (difference of 5%).

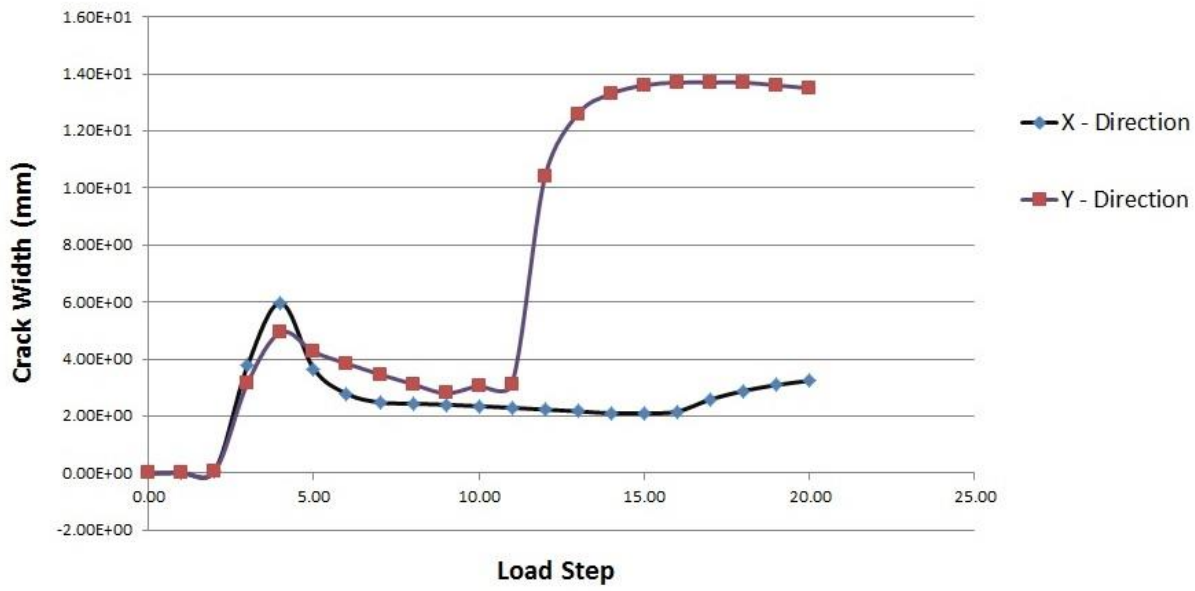

Figure (7.1): Maximum Crack Propagation in Each Direction With Respect to Load Step

On another hand, the out of plane stiffness for the church is lower than in plane stiffness, the Y – direction is more deformed and have a larger cracks width. By numerical show, the maximum crack width before load step (10), i.e. load step (9) has a maximum crack width of 2.80 mm, and after the load step (10), i.e. load step (12), has a maximum crack width of 1.04 cm. Figure (7.1) also present the jump between two directions.

According to the IBC 2015 – (2109.3.1.4) *"The Shrinkage cracks in adobe units shall not contain more than three shrinkage cracks and any single shrinkage crack shall not exceed 3 inches (76 mm) in length or 1/8 inch (3.2 mm) in width"* so if the shrinkage cracks used as a limit state (the values larger than shrinkage cracks are critical and must be given good treatment), the decision will be that; cracks propagation indicate there is a large problem in out of plane direction (Y – direction), but still at the upper limit in the in plane direction (X – direction), in more details, Y – direction, exceeds the limits in width and length with maximum width of 13.7 mm (approximately more than 400% of the values considered in the IBC 2015 as shrinkage crack !), also in length of cracks, they are continues with each other (no specified length). Otherwise, X – direction is failed in length but still utmost width, with no ignoring to the problem of a lot of cracks. Table (7.1) summarizes the results of cracks details for each structural element of the church.

Table (7.1): Max Crack Width In X Vs. Y Directions

Elements of Church	X – Direction (In plane)		Y – Direction (Out of Plane)	
	Width of Crack	Length of Crack	Width of Crack	Length of Crack
Façade	3.24 mm	Continuous	13.7 mm	Continuous
buttress	~ Zero	~ Zero	~ Zero	~ Zero
Columns	3.24 mm	Continuous	13.7 mm	Continuous
Exterior Lateral Walls	~ Zero	Zero	13.7 mm	Continuous
Interior Lateral Walls	3.24 mm	Continuous	13.7 mm	Continuous
Transverse Walls	3.24 mm	Continuous	13.7 mm	Continuous
Side Apses	~ Zero	~ Zero	13.7 mm	Continuous
Central Apse	~ Zero	~ Zero	~ Zero	~ Zero
Shoulders	~ Zero	~ Zero	~ Zero	~ Zero
Vaults	3.24 mm	Continuous	13.7 mm	Continuous

By studying the previous results, it's obvious that cracks propagation reliable in investigation the historical masonry structures, because not only the band width for cracks was checked, also the length of cracks can be checked and investigated, and give a good indication of what will happen for seismic loads, but the work still need a more precise indication for failure of the masonry walls, that's what will discussed in the next section of time history analysis.

7.1.2 Discussion of Time History Analysis

A new idea for model of masonry structure is presented after dynamic analysis, which employs relative displacement of adjacent masonry blocks (RDAMB). The accuracy of this proposed method was proved by a case study of Nativity Church, and the applicability of

RDAMB for calibration of other analysis methods is also investigated and compared to the results gained from pushover analysis and progressive collapse.

By studying the results of nonlinear time history analysis, it's obvious that reference nodes defined where the rocking falls may be occur, so by gathering the behavior of all nodes in figure (7.2) for X – direction, and figure (7.4) for Y – direction, two groups of results are specified, the one is critical group which show relatively large value of relative displacement (more than 1.50 mm) and the another is acceptable group with relatively small value of relative displacement (less than 1.50 mm). In this thesis the value of 1.50 mm is chosen because 1.00 ~ 1.50 mm is considered observable and indicate detachment of mortar, and less of that value is considered negligible.

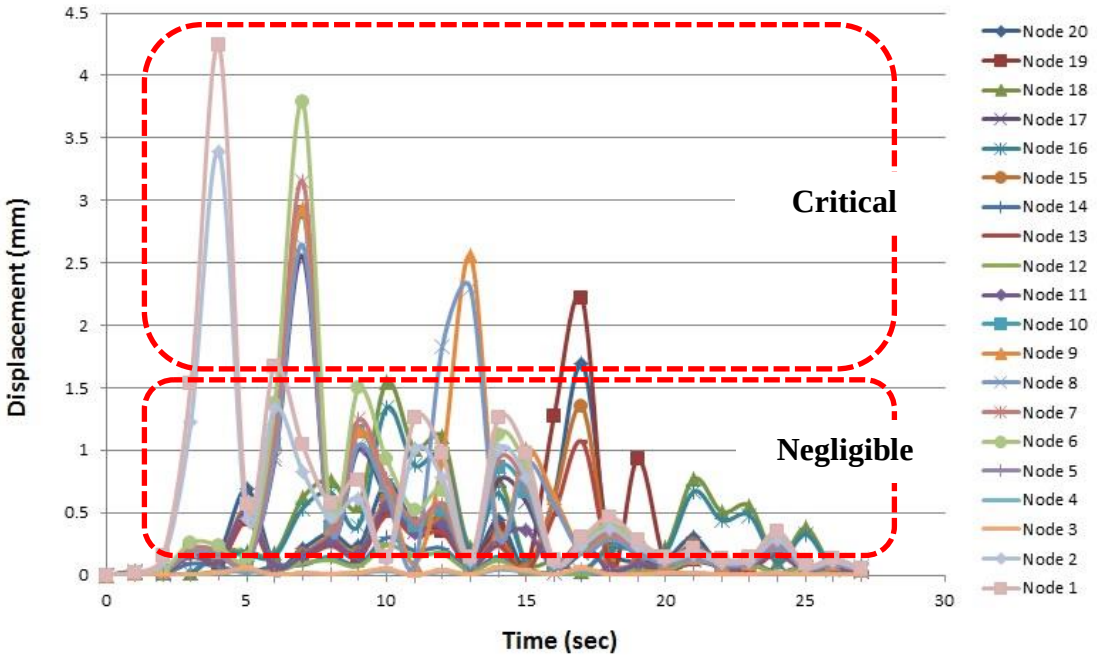

Figure (7.2): Maximum Crack Propagation, X- Direction.

By starting with X – direction, the figure (7.2), show that node (1) and node (2), locating in the façade suffering mainly from inadequate connection between wythes, the poor connection between the two outer stone wythes with the middle constructed of rubble has exhibited poor seismic performance, so the relative displacement and separation of the two wythes expected to occurred, that mean partial or total collapse of the this part of walls, figure (7.3)

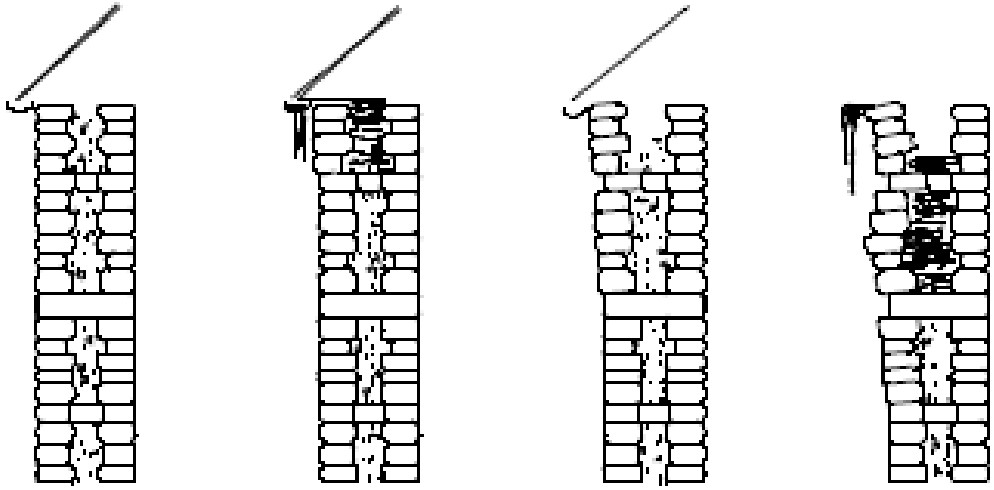

Figure (7.3): Inadequate Connection Between Wythes

But for the node (6) and node (7), which are in the interior lateral wall, the slender walls will exhibit little resistance to lateral loads; also mortar used in the construction of stone masonry often consists of sand and lime, with little or no Portland cement. This mortar mix is known to have little shear strength. Consequently, sliding along the mortar joint has been observed as one of the common failure mechanisms, resulting in either partial collapse of the transverse wall or total failure of the structure.

Finally, node (19) and node (20) are a good example of poorly engineered corner connection, in details, the separation of the walls, followed by collapse, was observed in non-engineered buildings with inadequate wall corner detailing.

In similar way, the Y – direction, figure (7.4) prove that there are problems in nodes (3), (4), (5), (6), (7), (8), (9), (17), (18), (19).

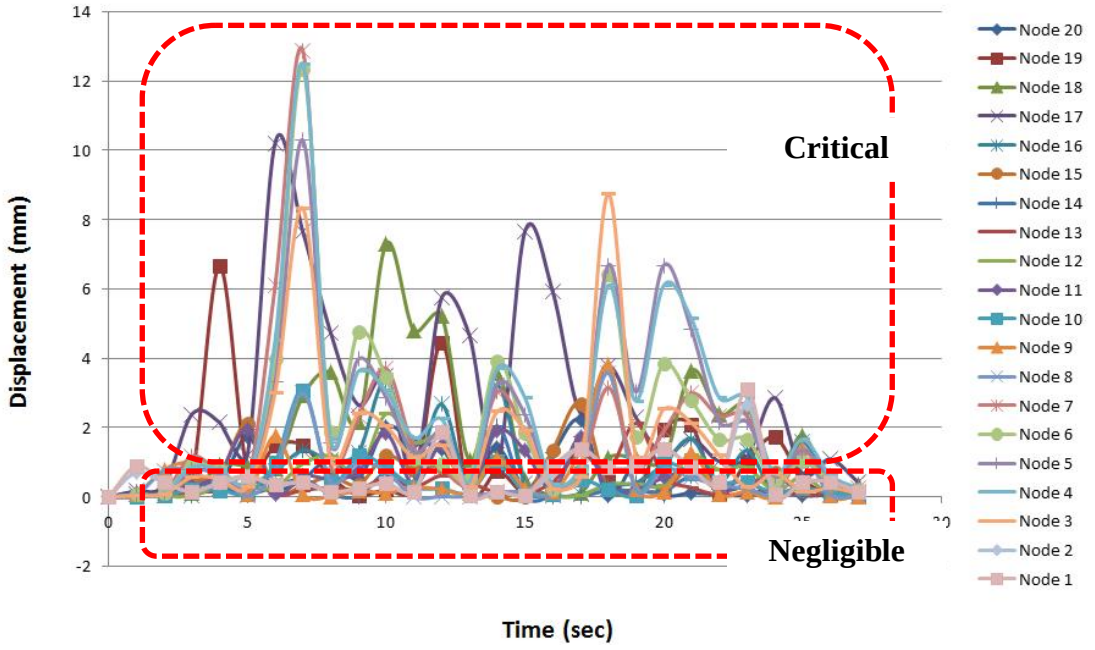

Figure (7.4): Maximum Crack Propagation, Y- Direction.

In details node (3), node (4), and node (5), emphasize that out of plane failure of walls not adequately connected at the top, or braced! These nodes are locating in the critical region and present the dangerous of lateral walls.

For the node (6) and node (7), which are location also in critical group, they show large window openings effect. In stone masonry walls,

large window openings cause reduction in lateral shear capacity, which means diagonal tension failure is observed under seismic load, and help to enlarge the relative displacement.

Also node (8), node (9), node (17), and node (18), prove there are poorly engineered corner connection as X – direction, and at the final node (19) which show the most common damage patterns observed in walls connected to heavy loads of vaults, which make horizontal cracks at the floor to wall joints, or out of plane collapse of walls. Finally, table (7.2) summarizes the failure in each element of Nativity Church, which show each group of classification with reference to the nodes used.

Table (7.2): Effect of Relative Displacement Analysis

Elements of Church	X - Direction	Y - Direction
Façade	Critical	Negligible
Buttress	Negligible	Negligible
Columns	Critical	Critical
Exterior Lateral Walls	Negligible	Critical
Interior Lateral Walls	Critical	Critical
Transverse Walls	Critical	Critical
Side Apses	Negligible	Negligible
Central Apse	Negligible	Negligible
Shoulders	Negligible	Negligible
Vaults	Critical	Critical

7.1.3 Discussion of Progressive Collapse

The comprehensive evaluation process of progressive collapse includes the aspects related to building layout, i.e. investigation of geometrical information, material properties, structural constructions etc... The development of all kinds of detection techniques will help to improve the objectivity and accuracy of the evaluation for structures to resist progressive collapse.

Based on the finite element simulation, the study replicated the collapse process and evaluated the importance indices of all the structural elements, the limit used was by application of the modified von misses failure criterion, the stresses at reference nodes are calculated and compared with the permissible values of the stresses given in table (4.1) taken the shear stress must not exceed 0.089 MPa for Perimeter walls, 0.067 MPa for specific narthex components, and 0.02 MPa for vaults.

Based on these results of progressive collapse, reliable and simple identification method of the critical regions was proposed. The identified critical regions can be used to facilitate a rational design, construction, inspection and maintenance practice, which would thereby lead to prevention strategies and minimize the likelihood of any failure. Table (7.3) show the elements of church which are failed in shear.

Table (7.3): Effect of Progressive Collapse Analysis

Elements of Church	X - Direction	Y - Direction
Façade	Collapse Progressively	Doesn't Collapse Progressively
Buttress	Doesn't Collapse Progressively	Doesn't Collapse Progressively
Columns	Doesn't Collapse Progressively	Doesn't Collapse Progressively
Exterior Lateral Walls	Doesn't Collapse Progressively	Collapse Progressively
Interior Lateral Walls	Collapse Progressively	Collapse Progressively
Transverse Walls	Doesn't Collapse Progressively	Doesn't Collapse Progressively
Side Apses	Doesn't Collapse Progressively	Doesn't Collapse Progressively
Central Apse	Doesn't Collapse Progressively	Doesn't Collapse Progressively
Shoulders	Doesn't Collapse Progressively	Doesn't Collapse Progressively
Vaults	Doesn't Collapse Progressively	Doesn't Collapse Progressively

7.2 Conclusion

Within this thesis, a detailed study of the historical buildings in Palestine, after concentration on The Church of Nativity as a case study, was done. The modal analysis was carried out and used to assess the quality of the model, also the structural stability and seismic performance of the building was studied by means of gravity loads and lateral loadings.

In general, three main various numerical analyses were performed, by two non-linear methods were used to assess the seismic behavior of the church: static pushover and time history dynamic analyses. Based on the accomplished work and results, the following conclusion can be summarized, with regarding to the historical damage survey and visual inspection:

1. From historical data, it is possible to observe that the Nativity Church suffered much damage in the past, probably due to a

combination of many factors such as earthquakes and material deterioration. At present, after the rehabilitation works done, it is difficult to distinguish the old damage. Based on this, today it is a complicated task to tell with absolute certainty, and by using the visual inspection, which damage was caused by seismic effects.

2. The modal analysis was done using the material properties that obtained from previous research, and adopted through literature recommendations. The modal analysis indicated frequencies ranging from 1.82 Hz to 5.56 Hz for the first eight modes of vibration of the structure. These modes possess a cumulative mass participation above 70% in both orthogonal directions (X and Y directions).
3. The comparison of the numerical frequencies and mode shapes, made for the first eight modes of vibration, resulted in a significant variation of the frequencies with max error of 11.23%, which indicate the need of calibration of some properties of the model.
4. The pushover analyses performed and showed that the seismic performance of the Nativity Church is dependent on its critical transversal Y - direction. From these analyses, and by using the provision of IBC 2015 for masonry walls, the cracks propagation was done and present the result of large problem in out of plane direction (Y – direction), but still at the upper limit in the in plane direction (X – direction), in details, Y – direction, exceeds the limits of width, length, and density of cracks. Also, X – direction is failed

in length of cracks but still utmost width, with no ignoring to heavy distribution cracks.

5. The time history method was able to effectively simulate some of the real behavior of the Nativity Church, by employing relative displacement of adjacent masonry blocks (RDAMB). These method present problems of inadequate connection between wythes, sliding along the mortar joints, poorly engineered corner connection, effect of windows openings, heavy loads of vaults. etc.
6. The (RDAMB) results should be treating in wide range, by studying the compression results and tension results, in separate manner; this can be slightly difficult in this thesis.
7. The progressive collapse method, with using of modified von misses failure criterion, show the stresses at reference nodes and compared with the permissible values of the shear stress (0.089 MPa for Perimeter walls, 0.067 MPa for specific narthex components, and 0.02 MPa for vaults).
8. Based on these results of progressive collapse, the critical regions can be defined, and this is used to facilitate a rational design, construction, inspection and maintenance practice, also results of progressive collapse prove that there was no adequate load path for masonry structure.
9. The results of both dynamic and static analyses confirmed again that the seismic behavior of the church is governed by its transversal

direction, which is predictable to be the cause of global failure of the structure.

10. The application of the progressive collapse, in opposition with the dynamic time history and static push over techniques, presented advantages regarding time. In addition, the applied progressive collapse configurations were able to validate important damage of the structure, principally in the transversal walls of the church.

7.3 Recommendations and Future Studies

Final of this dissertation and based on the previous remarks and tasks performed, there are some recommendations for future work shown below, aiming to think over this field of researchers especially in Palestine:

1- Some improvements can be carried out in future works, regarding the modeling and analysis of the case study.

2- A more accurate characterization of the geometrical features and material properties is imperative, including a fine calibration of the numerical model. Due to the limited time to carry out further works, the completion of these tasks would need to be performed in future works.

3- Investigating some valuable and other complex historical structures, with more nonlinearities and irregular geometrical configuration.

4- Taking into account more parameters in the sensitivity analysis, like focusing on the influence of vertical acceleration in time history analysis, the influence of compressive strength parameters, and the

use of more advanced pushover methods, such as adaptive or multimodal.

5- Evaluate the response for impulse earthquakes, which may cause more mechanism of out of plane failure.

6- Carry out more analyses with and without the vertical earthquake component, for different types of earthquakes and seismic amplitudes.

7- For future work, any researcher can study the relative displacement results by dividing it into two different categories (compression and tension).

8- validate the structural performance of the strengthening technique proposal with steel ties through the nonlinear dynamic analysis

9- Try to evaluate the seismic performance of the case study (Nativity Church) with other types of structural analysis, for example, limit analysis or models based on the discrete element method.

10- Furthermore, the preparation, maintenance and monitoring plan is recommended.

11- Development of empirical vulnerability methods for the assessment of seismic behavior for the case study.

References

- Mosalam, Glascoe, & Bernier. (2009). ***Mechanical Properties of Unreinforced Brick Masonry, Section1.***
- Lourenco, Paulo. (1996). ***Computational Strategy for Masonry Structures.***
- Milosevic, Jelena & Lopes, Mário & Gago, António & Bento, Rita. (2015). ***In-plane seismic response of rubble stone masonry specimens by means of static cyclic tests. Construction and Building Materials.***
- ElGawady, M. A., Lestuzzi, P., and Badoux, M. (2005). ***Performance of masonry walls under in-plane seismic loading.*** Masonary Soc. J., 23(1), 85–104.
- ElGawady, M. A., Lestuzzi, P., and Badoux, M. (2007). ***Static cyclic response of masonry walls retrofitted with fiber-reinforced polymers.***
- (Calvi, Pinho, Magenes, Bommer, Restrepo-Vélez, & Crowley. (2006). ***Development of Seismic Vulnerability Assessment Methodologies over the Past 30 Years***
- Doherty, K., Griffith, M.C., Lam, N. and Wilson, J. (2012) . ***Displacement-based Analysis for Out-of-Plane Bending of Unreinforced Masonry Walls***. Earthquake Engineering and Structural Dynamics, John Wiley and Sons, 31(4): pp. 833-850.

- FEMA 356. (2000). ***Prestandard and Commentary for the Seismic Rehabilitation of Buildings.*** American society of civil engineers.

- Facconi, Luca & Plizzari, Giovanni & Vecchio, Frank. (2013). ***Disturbed Stress Field Model for Unreinforced Masonry. Journal of Structural Engineering.***

- EN 1998-1 (2004). ***Design of structures for earthquake resistance – Part 1: General rules, seismic actions and rules for buildings.*** The European Union Per Regulation 305/2011, Directive 98/34/EC, Directive 2004/18/EC

- EN 1998-3 (2005). ***Design of structures for earthquake resistance – Part 3: Assessment and retrofitting of buildings***. The European Union Per Regulation 305/2011, Directive 98/34/EC, Directive 2004/18/EC

- Chen, Wai & Lui, Eric. (2005). ***Handbook of Structural Engineering.***

- Correia A.A., Almeida J.P. Pinho R. (2013). ***Seismic energy dissipation in inelastic frames: understanding state-of-the-practice damping models.*** Structural Engineering International, Issue 2013/2, pp. 148-158.

- Abou Karaki, Najib. (2000). ***About Seismic Hazard and mitigation measures in Jordan. Royal Defense Academy.***

- Offir, Yaron & Yankelevsky, David & Schwarz, Stephan. (2008). ***A New Approach for Earthquake Vulnerability and Damage Assessment of a Large Group of Existing Residential Buildings.***

- Zvi Ben-Avraham, Michael Lazar, Uri Schattner, Shmuel Marco. (2001). ***The Dead Sea Fault and its Effect on Civilization.***

- Abdul Razzaq Touqan, & Suhaib Salawdeh. (2016). ***Major Steps Needed Towards Earthquake Resistant Design.***

- Ana S. Araújo, Paulo B. Lourenço, Daniel V. Oliveira & João Leite. (2012). ***Seismic Assessment of St James Church by Means of Pushover Analysis – Before and After the New Zealand Earthquake.***

- Lourenço, Paulo, Roque, João, Oliveira, Daniel. (2012). ***SEISMIC SAFETY ASSESSMENT OF THE CHURCH OF MONASTERY OF JERÓNIMOS, PORTUGAL.***

- F. Bucchi, S. Arangio and F. Bontempi. (2013). ***Seismic Assessment of an Historical Masonry Building using Nonlinear Static Analysis.***

- G. Castellazzi, C. Gentilini, and L. Nobile. (2013). ***Seismic Vulnerability Assessment of a Historical Church: Limit Analysis and Nonlinear Finite Element Analysis 2013***

- P.G. Asteris a, , M.P. Chronopoulos b, C.Z. Chrysostomou c, H. Varum d, V. Plevris a, N. Kyriakides c, V. Silva. (2014). ***Seismic vulnerability assessment of historical masonry structural systems.***
- Andrés Alberto Burgos Braga, Paulo B. Lourenço. (2014). ***Study of the Armenian Church in Famagusta.***
- H. Animas, M. Navarro, J. Pacheco-Martínez, J. L. García, T. Cordero, C. J. Espar-za, and J. A. Ortiz-Lozano. (2014). ***Structural Analysis of the Temple of San Antonio in Aguascalientes Mexico.***
- Saloustros, Savvas & Pelà, Luca & Roca, Pere & Portal, Jorge. (2014). ***Assessment of structural damage in historical constructions using numerical models: the case of the church of the Poblet Monastery.***
- M. Shariqa, S. Haseebb and M. Arifc. (2016). ***Analysis of existing masonry heritage building subjected to earthquake loading.***
- L. Mangia, B. Ghisaasi, E. Sayın, O. Onat, P. B. Lourenço. (2016). ***Pushover Analysis of Historical Eltihatun Mosque.***
- K. Ip, J. Lester & A. Brown. (2016). ***Seismic Non-Linear Analysis of Damaged Historic Buildings : Cathedral of the Blessed Sacrament, Christchurch***
- Panagiotis G. Asteris 1,*, Maria G. Douvika 1, Maria Apostolopoulou 2 and Antonia Moropoulou. (2017). ***Seismic and Restoration Assessment of Monumental Masonry Structures.***

- Giulio Castori , Antonio Borri, Alessandro De Maria, Marco Corradi, Romina Sisti. (2017). ***Seismic vulnerability assessment of a monumental masonry building.***

- Gabriele Milani, Marco Valente, Claudio Alessandri. (2016). ***Full 3D non-linear FE approach for structural damage prediction.***

- Claudio Alessandri & Jessica Turrioni. (2017). ***The Church of the Nativity in Bethlehem: Analysis of a Local Structural Consolidation.***

- McGuire & Leyendesker. (1974). ***Analysis of Non-Reinforced Masonry Building Response to Abnormal Loading and Resistance to Progressive Collapse***.

- F. Palmisano, A. Vitone, & C. Vitone. (2005). ***Load path method in the interpretation of masonry vault behavior.***

- LIN Feng, WANG Ying, GU Xianglin and ZHAO Xinyuan, .(2010). ***Progressive Collapse Evaluation for Historic Building Structures***.

- Xu, Zhen, Lu, Xinzhrng, Guan, Hong, Lu, Xiao, Ren, and Aizhu. (2013). ***Progressive Collapse Simulation and Critical Region Identification of a Stone Arch Bridge***

- IBC 2012. ***International Building Code.*** International Code council, INC

- ASCE 2016. ***Minimum design loads for buildings and other structures***. Reston, Va., American Society of Civil Engineers: Structural Engineering Institute.

- UFC 04-023-03. (2016). **Design Buildings to Resist Progressive Collapse, U.S Army Corps of Engineers, Naval Facilities Engineering Command, and Air Civil Engineering Support Agency.**

Appendices

Appendix A: General Drawings for Nativity Church

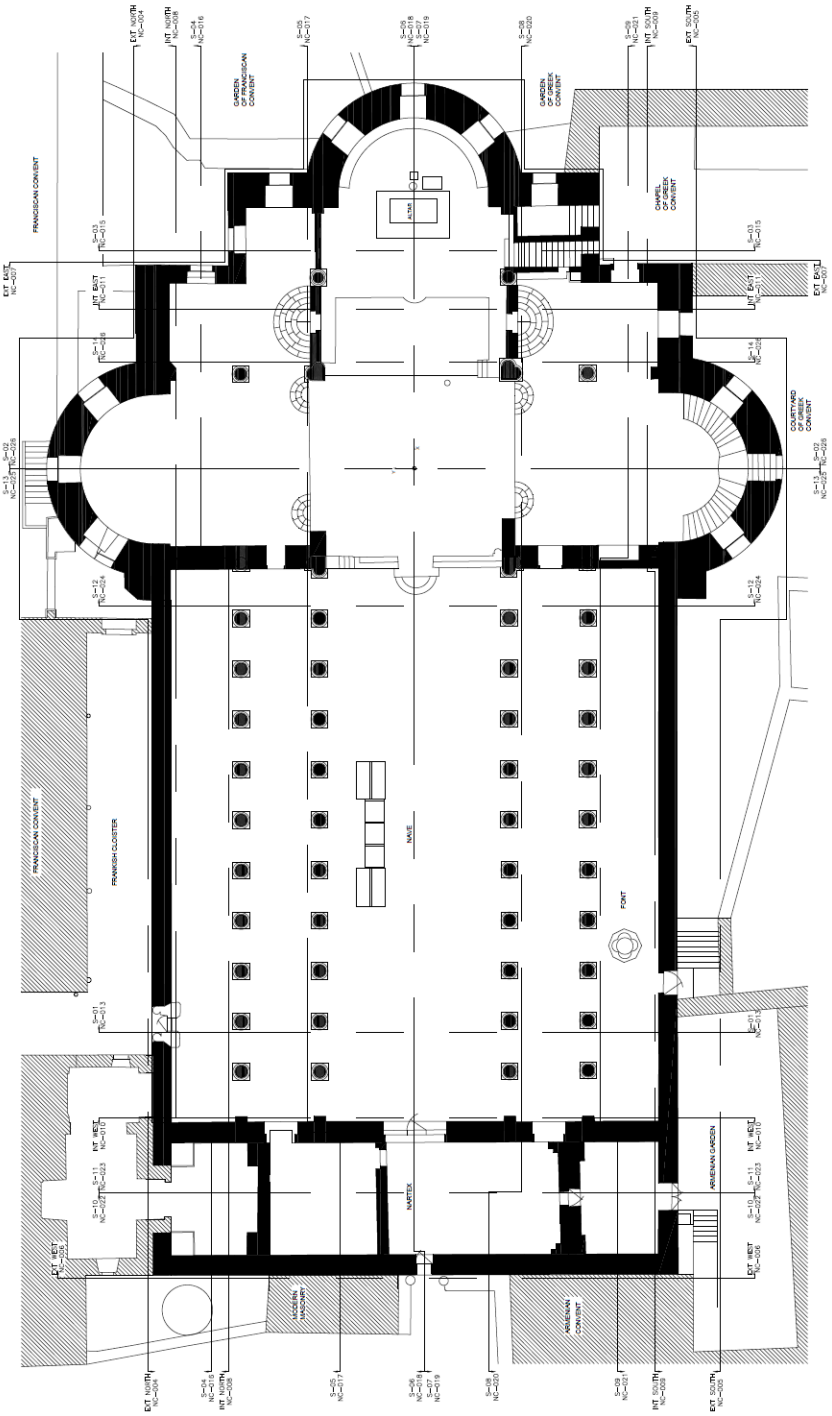

Figure (A.1) : General Plan

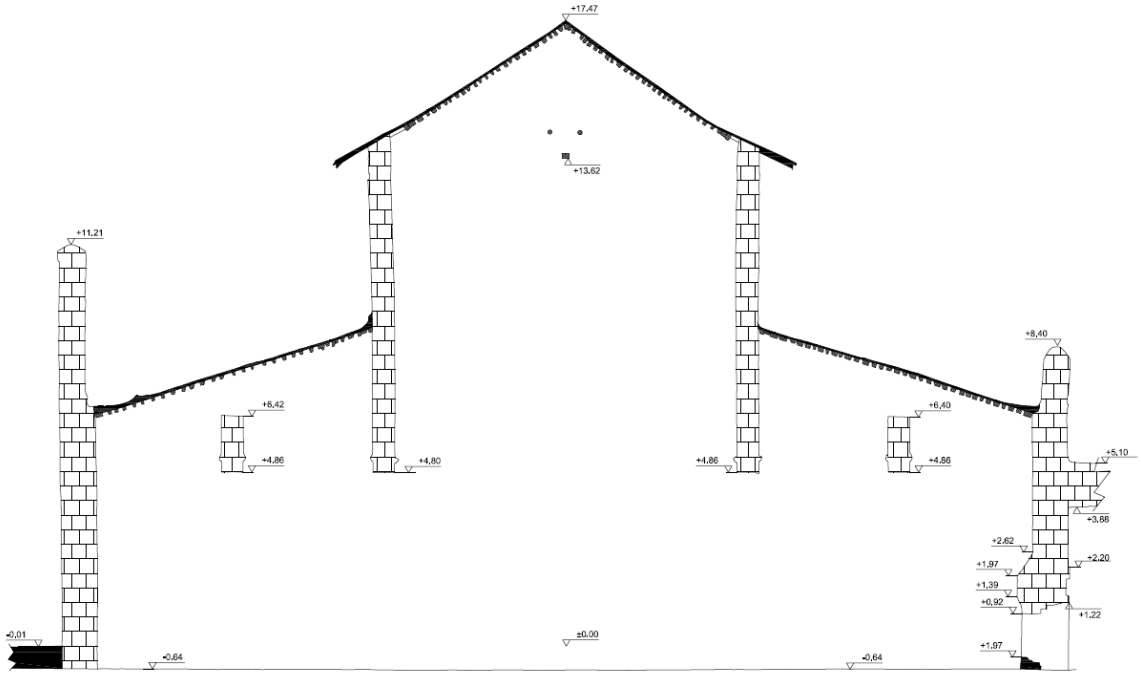

Figure (A.2) : Section 1-1

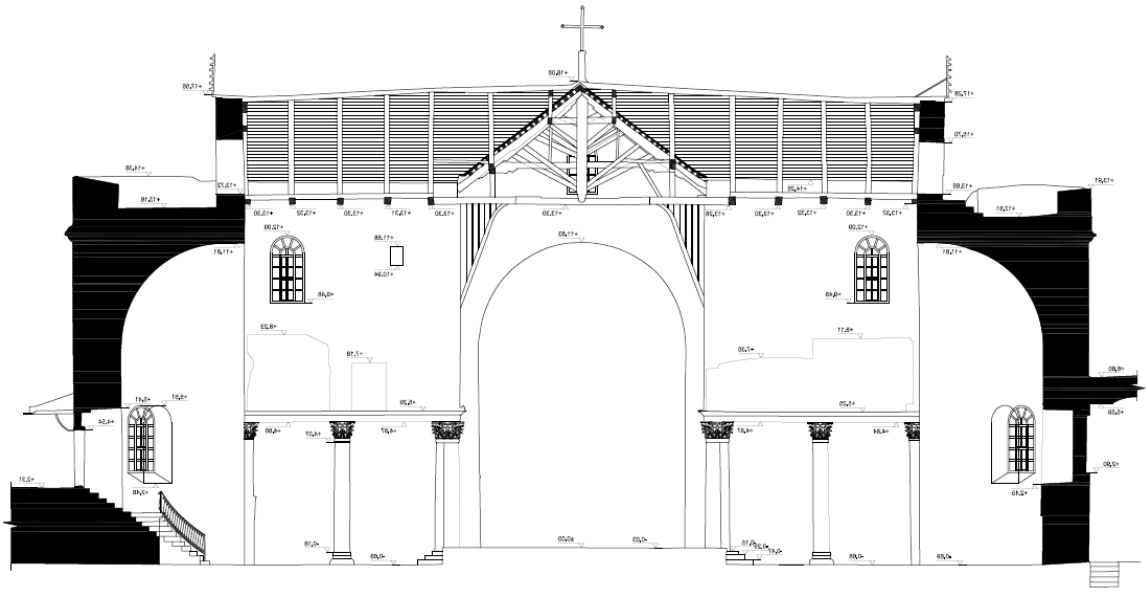

Figure (A.3) : Section 2-2

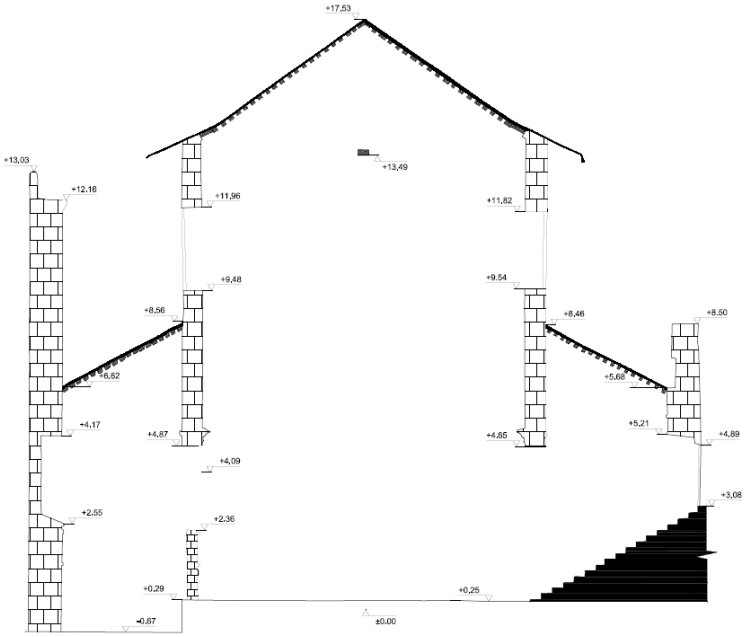

Figure (A.4) : Section 3-3

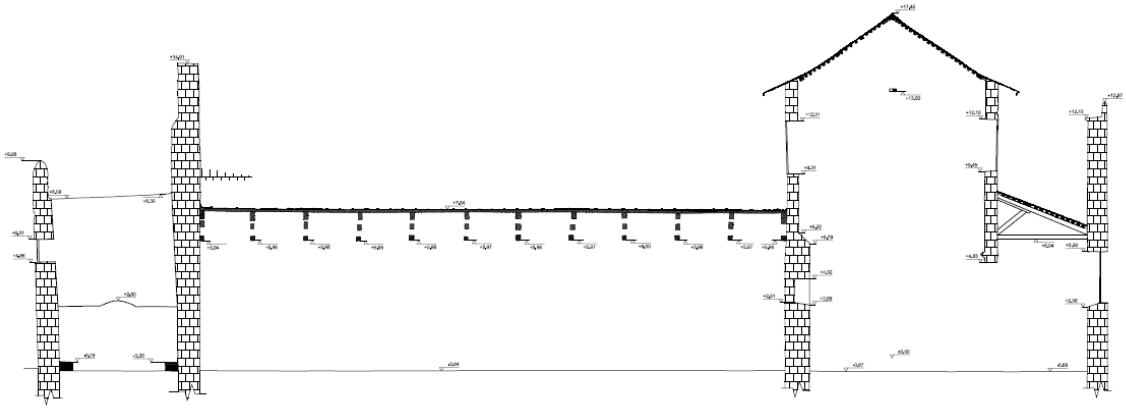

Figure (A.5) : Section 4-4

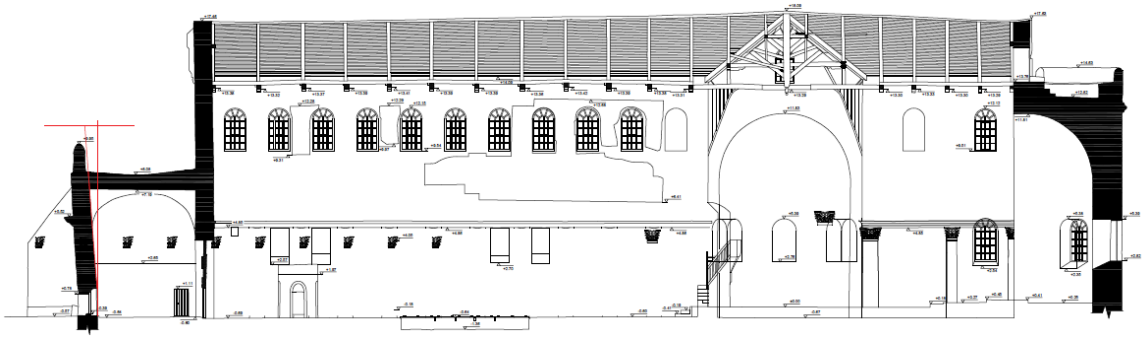

Figure (A.6) : Section 6-6

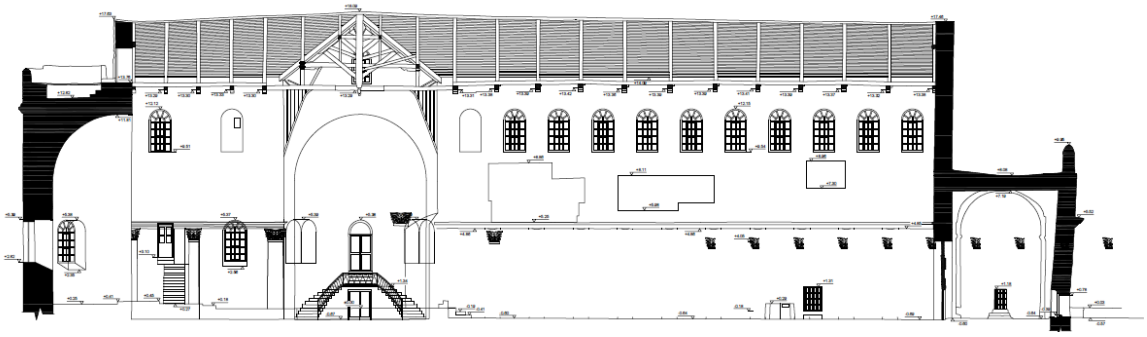

Figure (A.7) : Section 7-7

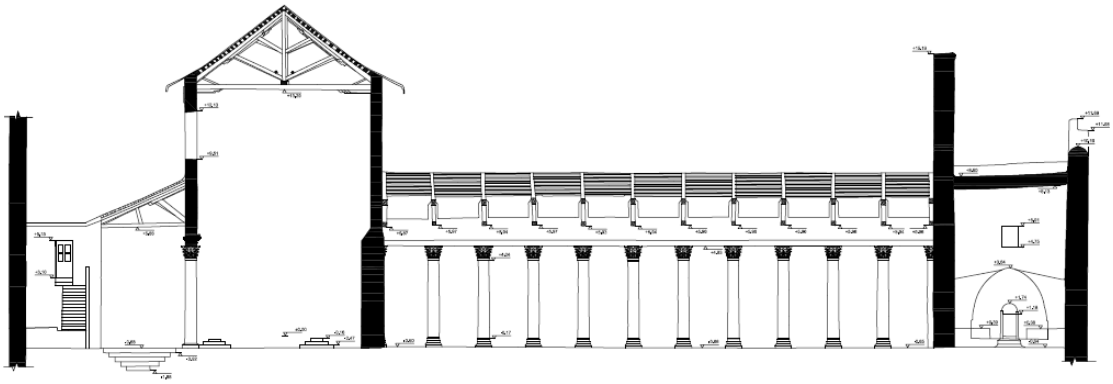

Figure (A.8) : Section 8-8

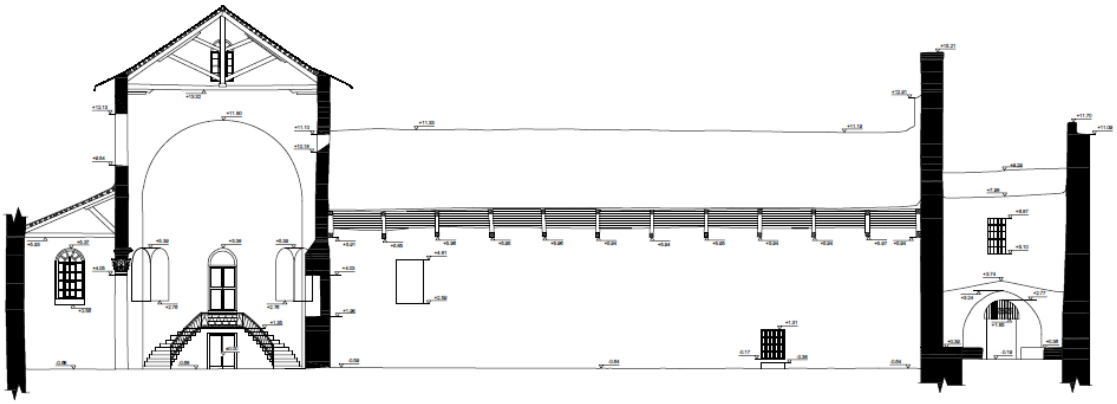

Figure (A.9) : Section 9-9

Appendix B: Procedure of Push over Analysis in DIANA FEA

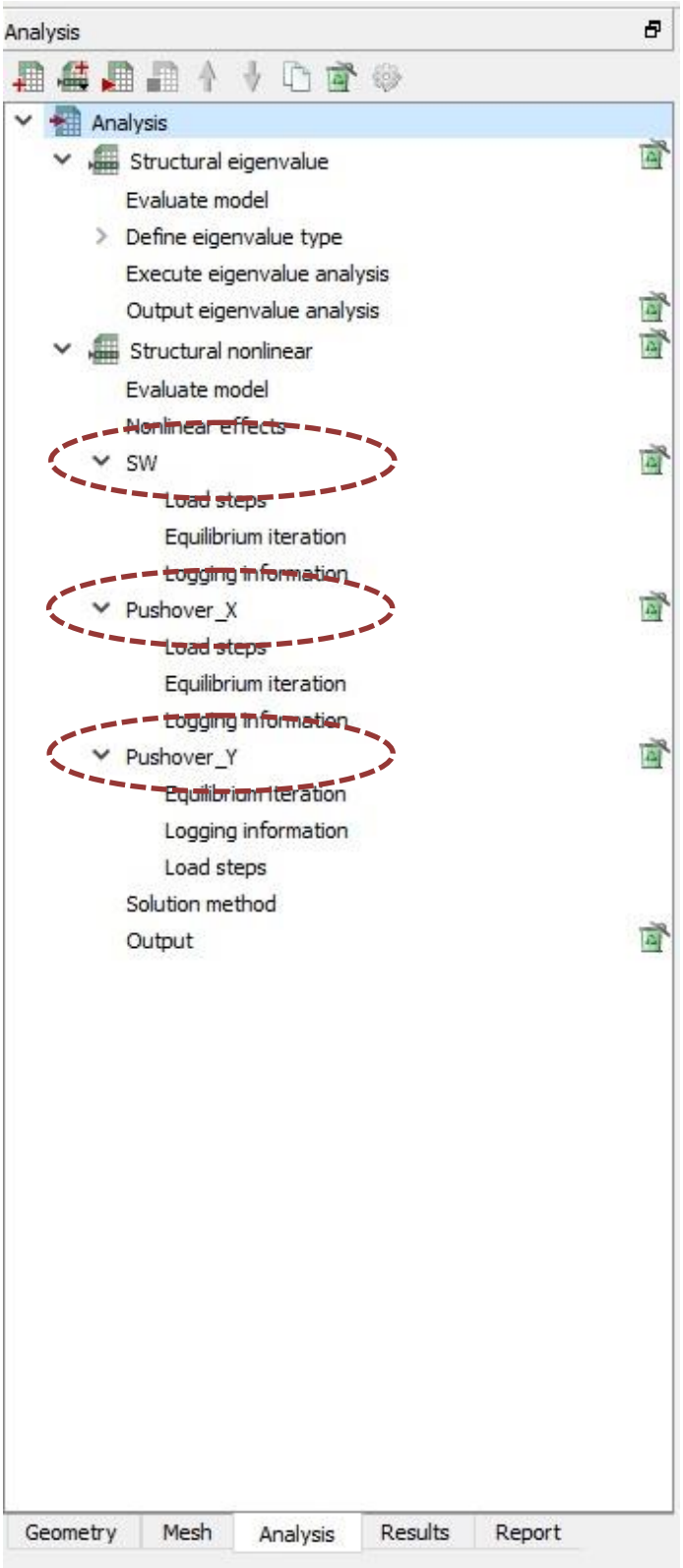

Figure (B.1) : Defining Analysis for the Model

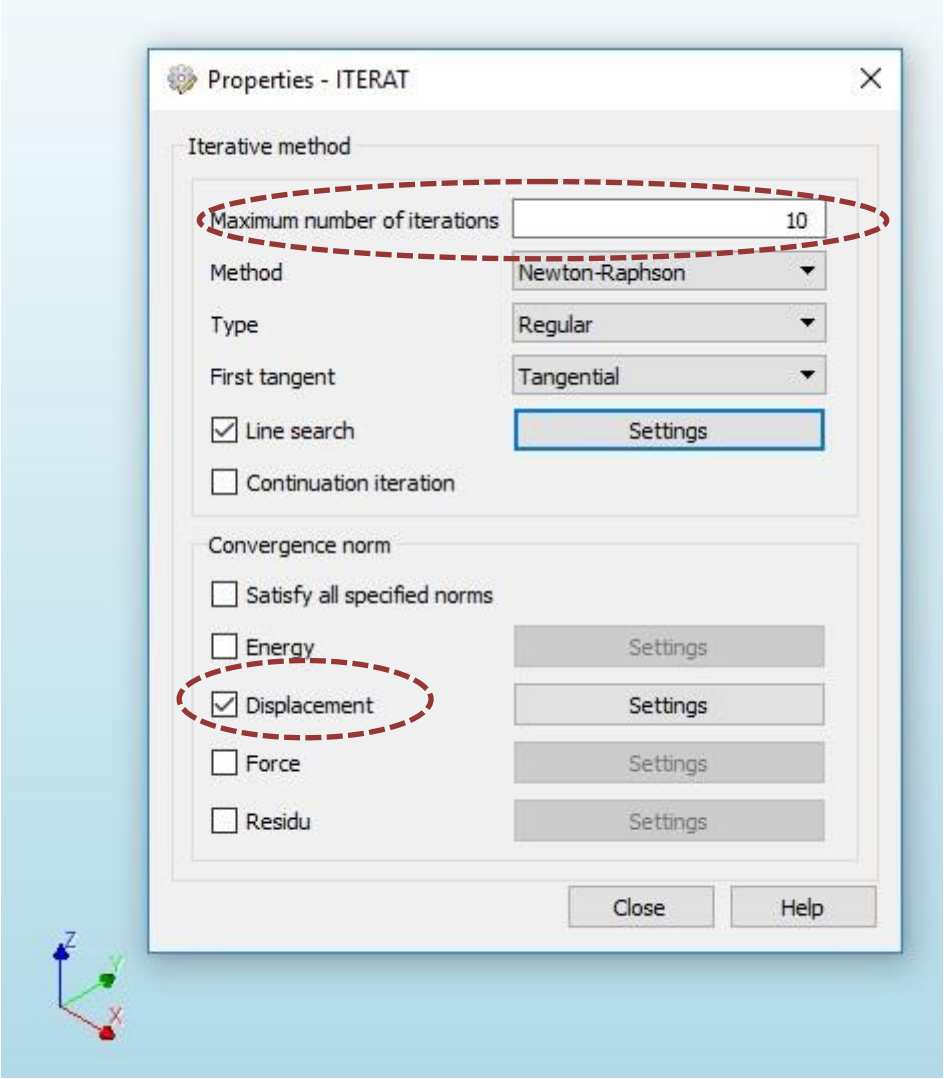

Figure (B.2) : The Iterations Based on Displacement Approach

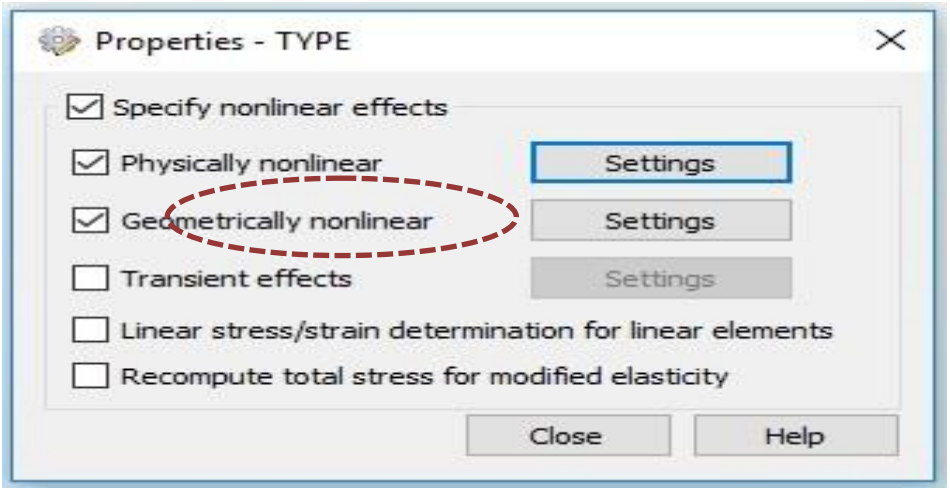

Figure (B.3) : Considering Geometrical Non-Linearity

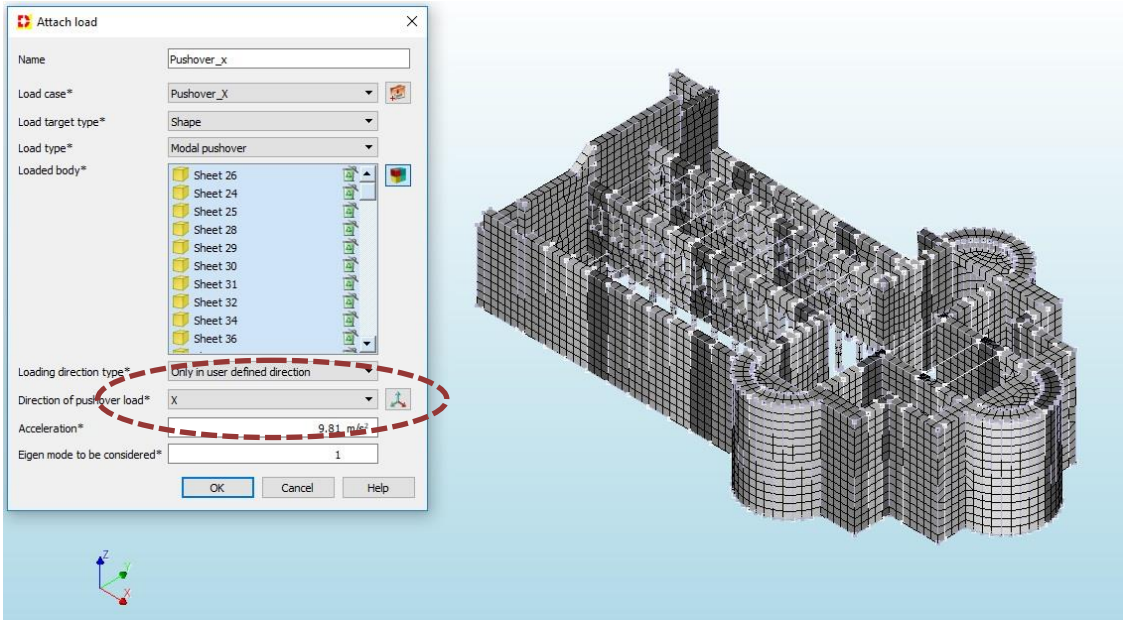

Figure (B.4) : Adapting Pushover Analysis for X - Direction

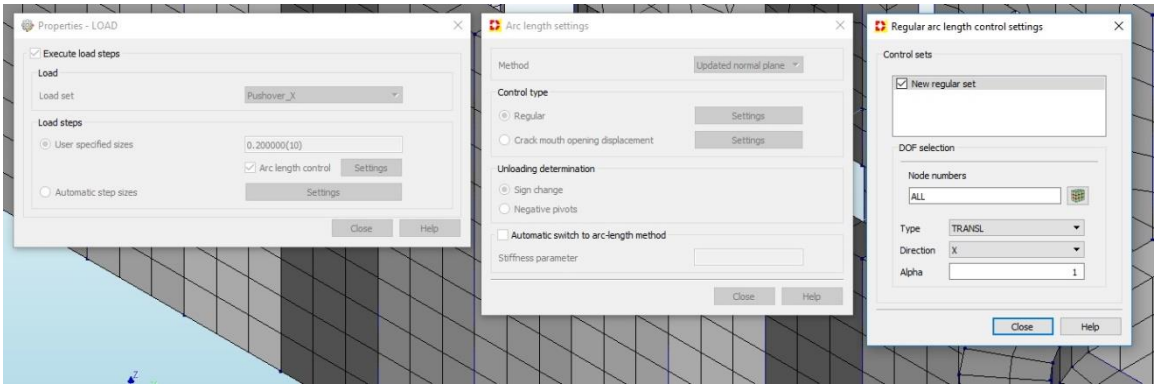

Figure (B.5) : Details of Load Steps, and Arc Length for X - Direction

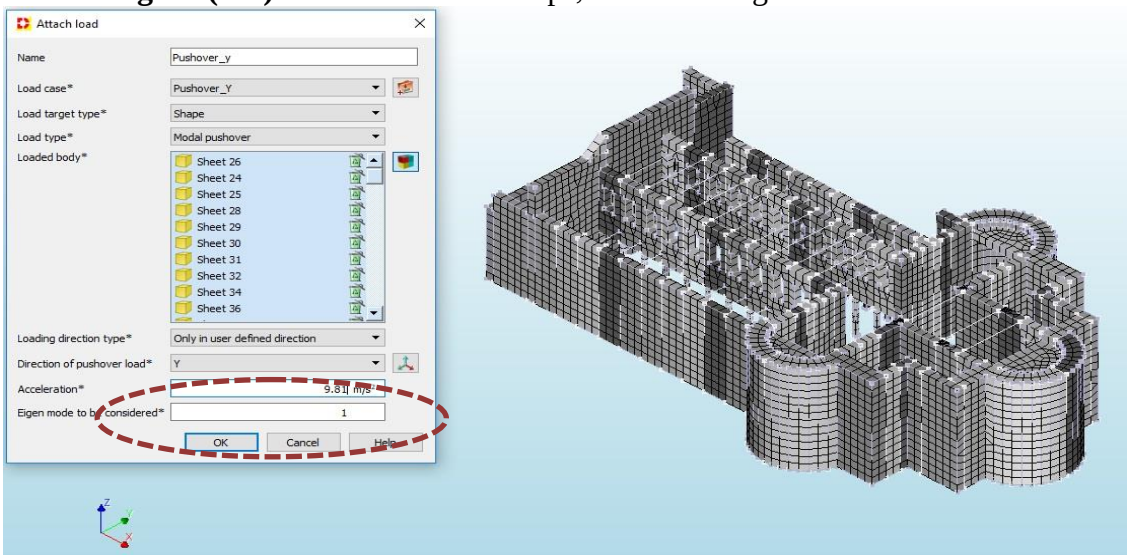

Figure (B.6) : Adapting Pushover Analysis for Y - Direction

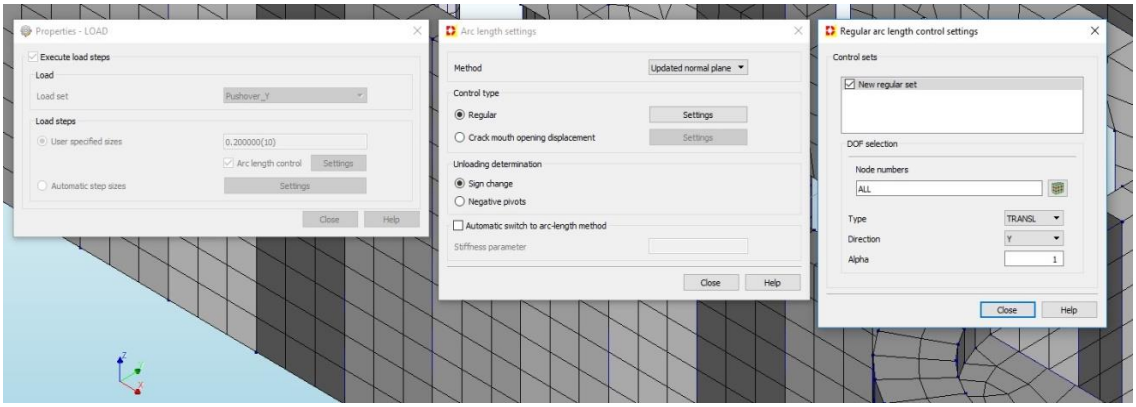

Figure (B.7) : Details of Load Steps, and Arc Length for Y - Direction

Appendix C: Details of Relative Displacement for X - Direction

Node (1)_X-Direction			
Time (Sec)	D1 (mm)	D2 (mm)	R-Disp. (mm)
0	0.0000	0.0000	0.0000
1	-0.0226	0.0000	0.0226
2	-0.2226	-0.0734	0.1492
3	0.4154	1.9526	1.5372
4	-3.7510	0.4894	4.2404
5	-1.4548	-0.8948	0.5600
6	1.2638	-0.4098	1.6736
7	-0.8221	0.2158	1.0378
8	0.0000	-0.5800	0.5800
9	0.6976	-0.0659	0.7635
10	-0.0927	0.0527	0.1454
11	-2.0858	-0.8300	1.2558
12	0.9325	-0.0397	0.9722
13	-0.0927	0.0527	0.1454
14	-2.0858	-0.8300	1.2558
15	0.9325	-0.0397	0.9722
16	0.0186	-0.1001	0.1187
17	0.2980	0.0000	0.2980
18	-0.1621	0.3041	0.4662
19	0.3138	0.0315	0.2822
20	-0.0580	0.0871	0.1451
21	-0.1032	0.1036	0.2069
22	0.0706	-0.0558	0.1265
23	-0.2366	-0.0937	0.1429
24	0.2699	-0.0820	0.3520
25	-0.0824	0.0000	0.0824
26	-0.1344	0.0000	0.1344
27	0.0323	-0.0213	0.0535

Node (2)_X-Direction			
Time (Sec)	D1 (mm)	D2 (mm)	R-Disp. (mm)
0	0.0000	0.0000	0.0000
1	-0.0181	0.0000	0.0181
2	-0.1781	-0.0587	0.1194
3	0.3323	1.5621	1.2298
4	-3.0008	0.3915	3.3923
5	-1.1639	-0.7158	0.4480
6	1.0110	-0.3278	1.3389
7	-0.6577	0.1726	0.8303
8	0.0000	-0.4640	0.4640
9	0.5581	-0.0527	0.6108
10	-0.0742	0.0422	0.1163
11	-1.6687	-0.6640	1.0046
12	0.7460	-0.0317	0.7777
13	-0.0742	0.0422	0.1163
14	-1.6687	-0.6640	1.0046
15	0.7460	-0.0317	0.7777
16	0.0149	-0.0801	0.0949
17	0.2384	0.0000	0.2384
18	-0.1297	0.2432	0.3730
19	0.2510	0.0252	0.2258
20	-0.0464	0.0697	0.1161
21	-0.0826	0.0829	0.1655
22	0.0565	-0.0447	0.1012
23	-0.1893	-0.0750	0.1143
24	0.2159	-0.0656	0.2816
25	-0.0659	0.0000	0.0659
26	-0.1076	0.0000	0.1076
27	0.0258	-0.0170	0.0428

Node (3)_X-Direction			
Time (Sec)	D1 (mm)	D2 (mm)	R-Disp. (mm)
0	0.0000	0.0000	0.0000
1	-0.0070	-0.0056	0.0014
2	-0.0122	-0.0098	0.0024
3	-0.0306	-0.0245	0.0061
4	-0.1107	-0.0885	0.0221
5	0.2898	0.2318	0.0580
6	0.0058	0.0046	0.0012
7	0.0926	0.0741	0.0185
8	-0.0504	-0.0403	0.0101
9	0.1132	0.0905	0.0226
10	-0.2554	-0.2044	0.0511
11	0.0000	0.0000	0.0000
12	0.2168	0.1734	0.0434
13	-0.0288	-0.0231	0.0058
14	-0.3241	-0.2593	0.0648
15	0.1951	0.1561	0.0390
16	-0.0259	-0.0207	0.0052
17	-0.2917	-0.2333	0.0583
18	-0.0349	-0.0279	0.0070
19	0.0263	0.0211	0.0053
20	-0.0945	-0.0756	0.0189
21	0.1007	0.0805	0.0201
22	-0.0307	-0.0246	0.0061
23	-0.0501	-0.0401	0.0100
24	0.0839	0.0671	0.0168
25	-0.0256	-0.0205	0.0051
26	-0.0418	-0.0334	0.0084
27	0.0091	0.0073	0.0018

Node (4)_X-Direction			
Time (Sec)	D1 (mm)	D2 (mm)	R-Disp. (mm)
0	0.0000	0.0000	0.0000
1	-0.0088	-0.0098	0.0011
2	-0.0153	-0.0171	0.0018
3	-0.0383	-0.0429	0.0046
4	-0.1383	-0.1549	0.0166
5	0.3622	0.4057	0.0435
6	0.0072	0.0081	0.0009
7	0.1157	0.1296	0.0139
8	-0.0630	-0.0705	0.0076
9	0.1415	0.1584	0.0170
10	-0.3193	-0.3576	0.0383
11	0.0000	0.0000	0.0000
12	0.2710	0.3035	0.0325
13	-0.0360	-0.0403	0.0043
14	-0.4051	-0.4537	0.0486
15	0.2439	0.2731	0.0293
16	-0.0324	-0.0363	0.0039
17	-0.3646	-0.4083	0.0438
18	-0.0436	-0.0488	0.0052
19	0.0329	0.0369	0.0040
20	-0.1182	-0.1324	0.0142
21	0.1258	0.1409	0.0151
22	-0.0384	-0.0430	0.0046
23	-0.0627	-0.0702	0.0075
24	0.1048	0.1174	0.0126
25	-0.0320	-0.0358	0.0038
26	-0.0522	-0.0585	0.0063
27	0.0114	0.0128	0.0014

Node (5)_X-Direction			
Time (Sec)	D1 (mm)	D2 (mm)	R-Disp. (mm)
0	0.0000	0.0000	0.0000
1	-0.0108	-0.0118	0.0010
2	-0.0188	-0.0205	0.0017
3	-0.0471	-0.0514	0.0043
4	-0.1705	-0.1859	0.0155
5	0.4463	0.4868	0.0405
6	0.0089	0.0097	0.0008
7	0.1426	0.1556	0.0130
8	-0.0776	-0.0846	0.0070
9	0.1743	0.1901	0.0158
10	-0.3934	-0.4292	0.0357
11	0.0000	0.0000	0.0000
12	0.3339	0.3642	0.0303
13	-0.0444	-0.0484	0.0040
14	-0.4991	-0.5444	0.0453
15	0.3005	0.3278	0.0273
16	-0.0399	-0.0436	0.0036
17	-0.4492	-0.4900	0.0408
18	-0.0537	-0.0586	0.0049
19	0.0406	0.0443	0.0037
20	-0.1456	-0.1588	0.0132
21	0.1550	0.1691	0.0141
22	-0.0473	-0.0516	0.0043
23	-0.0772	-0.0842	0.0070
24	0.1292	0.1409	0.0117
25	-0.0394	-0.0430	0.0036
26	-0.0643	-0.0702	0.0058
27	0.0141	0.0153	0.0013

Node (6)_X-Direction			
Time (Sec)	D1 (mm)	D2 (mm)	R-Disp. (mm)
0	0.0000	0.0000	0.0000
1	-0.0202	0.0000	0.0202
2	-0.0351	0.0000	0.0351
3	-0.0880	0.1740	0.2620
4	-0.3180	-0.0818	0.2362
5	-0.1988	-0.0655	0.1332
6	0.3709	1.7434	1.3725
7	-3.3491	0.4369	3.7861
8	-1.2990	-0.7989	0.5000
9	1.1284	-0.3659	1.4943
10	-0.7340	0.1927	0.9266
11	0.0000	-0.5179	0.5179
12	0.6229	-0.0588	0.6817
13	-0.0828	0.0470	0.1298
14	-1.8624	-0.7411	1.1212
15	0.8326	-0.0354	0.8680
16	0.0166	-0.0894	0.1060
17	0.2661	0.0000	0.2661
18	-0.1448	0.2715	0.4162
19	0.2801	0.0282	0.2520
20	-0.0518	0.0778	0.1296
21	-0.0922	0.0925	0.1847
22	0.0631	-0.0498	0.1129
23	-0.2113	-0.0837	0.1276
24	0.2410	-0.0733	0.3143
25	-0.0736	0.0000	0.0736
26	-0.1200	0.0000	0.1200
27	0.0288	-0.0190	0.0478

Node (7)_X-Direction			
Time (Sec)	D1 (mm)	D2 (mm)	R-Disp. (mm)
0	0.0000	0.0000	0.0000
1	-0.0168	0.0000	0.0168
2	-0.0292	0.0000	0.0292
3	-0.0733	0.1450	0.2183
4	-0.2650	-0.0681	0.1969
5	-0.1656	-0.0546	0.1110
6	0.3091	1.4528	1.1438
7	-2.7909	0.3641	3.1550
8	-1.0825	-0.6658	0.4167
9	0.9403	-0.3049	1.2452
10	-0.6117	0.1605	0.7722
11	0.0000	-0.4315	0.4315
12	0.5191	-0.0490	0.5681
13	-0.0690	0.0392	0.1082
14	-1.5520	-0.6176	0.9344
15	0.6938	-0.0295	0.7233
16	0.0138	-0.0745	0.0883
17	0.2217	0.0000	0.2217
18	-0.1206	0.2262	0.3469
19	0.2334	0.0235	0.2100
20	-0.0432	0.0648	0.1080
21	-0.0768	0.0771	0.1539
22	0.0526	-0.0415	0.0941
23	-0.1761	-0.0697	0.1063
24	0.2008	-0.0610	0.2619
25	-0.0613	0.0000	0.0613
26	-0.1000	0.0000	0.1000
27	0.0240	-0.0158	0.0398

Node (8)_X-Direction			
Time (Sec)	D1 (mm)	D2 (mm)	R-Disp. (mm)
0	0.0000	0.0000	0.0000
1	-0.0141	0.0000	0.0141
2	-0.0245	0.0000	0.0245
3	-0.0614	0.1215	0.1829
4	-0.2221	-0.0571	0.1650
5	-0.1388	-0.0457	0.0930
6	0.2590	1.2174	0.9584
7	-2.3386	0.3051	2.6437
8	-0.9070	-0.5579	0.3492
9	0.7879	-0.2555	1.0434
10	-0.5125	0.1345	0.6471
11	-0.1207	-0.0398	0.0809
12	0.2252	2.0586	1.8334
13	-2.0336	0.2653	2.2989
14	-0.7887	-0.4851	0.3036
15	0.6851	-0.2222	0.9073
16	-0.4457	0.1170	0.5627
17	0.1858	0.0000	0.1858
18	-0.1011	0.1896	0.2907
19	0.1956	0.0197	0.1760
20	-0.0362	0.0543	0.0905
21	-0.0644	0.0646	0.1290
22	0.0440	-0.0348	0.0788
23	-0.1475	-0.0584	0.0891
24	0.1683	-0.0512	0.2194
25	-0.0514	0.0000	0.0514
26	-0.0838	0.0000	0.0838
27	0.0201	-0.0133	0.0334

Node (9)_X-Direction			
Time (Sec)	D1 (mm)	D2 (mm)	R-Disp. (mm)
0	0.0000	0.0000	0.0000
1	-0.0157	0.0000	0.0157
2	-0.0272	0.0000	0.0272
3	-0.0682	0.1350	0.2033
4	-0.2467	-0.0634	0.1833
5	-0.1542	-0.0508	0.1034
6	0.2878	1.3527	1.0649
7	-2.5985	0.3390	2.9375
8	-1.0078	-0.6199	0.3879
9	0.8755	-0.2839	1.1593
10	-0.5695	0.1495	0.7189
11	-0.1341	-0.0442	0.0899
12	0.2502	1.1762	0.9260
13	-2.2595	0.2948	2.5543
14	-0.8764	-0.5390	0.3373
15	0.7613	-0.2469	1.0081
16	-0.4952	0.1300	0.6252
17	0.2064	0.0000	0.2064
18	-0.1123	0.2106	0.3229
19	0.2173	0.0218	0.1955
20	-0.0402	0.0603	0.1005
21	-0.0715	0.0718	0.1433
22	0.0489	-0.0387	0.0876
23	-0.1639	-0.0649	0.0990
24	0.1870	-0.0568	0.2438
25	-0.0571	0.0000	0.0571
26	-0.0931	0.0000	0.0931
27	0.0223	-0.0148	0.0371

Node (10)_X-Direction			
Time (Sec)	D1 (mm)	D2 (mm)	R-Disp. (mm)
0	0.0000	0.0000	0.0000
1	-0.0155	0.0000	0.0155
2	-0.0269	0.0000	0.0269
3	-0.0674	0.1334	0.2009
4	-0.2438	-0.0627	0.1811
5	-0.1524	-0.0502	0.1022
6	0.2844	1.3366	1.0523
7	-2.5676	0.3350	2.9026
8	-0.9959	-0.6125	0.3833
9	0.8651	-0.2805	1.1456
10	-0.5627	0.1477	0.7104
11	0.0000	-0.3970	0.3970
12	0.4775	-0.0451	0.5226
13	-0.0635	0.0361	0.0995
14	-1.4278	-0.5682	0.8596
15	0.6383	-0.0272	0.6655
16	0.0127	-0.0685	0.0812
17	0.2040	0.0000	0.2040
18	-0.1110	0.2081	0.3191
19	0.2148	0.0216	0.1932
20	-0.0397	0.0596	0.0993
21	-0.0707	0.0709	0.1416
22	0.0484	-0.0382	0.0866
23	-0.1620	-0.0642	0.0978
24	0.1848	-0.0562	0.2409
25	-0.0564	0.0000	0.0564
26	-0.0920	0.0000	0.0920
27	0.0221	-0.0146	0.0367

Node (11)_X-Direction			
Time (Sec)	D1 (mm)	D2 (mm)	R-Disp. (mm)
0	0.0000	0.0000	0.0000
1	-0.0117	0.0000	0.0117
2	-0.0203	0.0000	0.0203
3	-0.0510	0.1150	0.1661
4	-0.1845	-0.0541	0.1304
5	0.4829	-0.0234	0.5063
6	0.0096	-0.0591	0.0687
7	0.1543	0.0000	0.1543
8	-0.0840	0.1795	0.2634
9	0.1886	0.0216	0.1670
10	-0.4257	0.1273	0.5531
11	0.0000	-0.3423	0.3423
12	0.3613	-0.0389	0.4002
13	-0.0480	0.0311	0.0791
14	-0.5401	-0.2449	0.2952
15	0.3252	-0.0350	0.3602
16	-0.0432	0.0280	0.0712
17	-0.4861	-0.2205	0.2657
18	-0.0581	-0.0218	0.0363
19	0.0439	-0.0395	0.0834
20	-0.1576	-0.0711	0.0864
21	0.1678	-0.0581	0.2259
22	-0.0512	0.0000	0.0512
23	-0.0836	0.0000	0.0836
24	0.1398	-0.0484	0.1882
25	-0.0427	0.0000	0.0427
26	-0.0696	0.0000	0.0696
27	0.0152	-0.0114	0.0267

Node (12)_X-Direction			
Time (Sec)	D1 (mm)	D2 (mm)	R-Disp. (mm)
0	0.0000	0.0000	0.0000
1	-0.0050	0.0000	0.0050
2	-0.0020	0.0000	0.0020
3	-0.0035	0.0000	0.0035
4	-0.0087	0.0212	0.0299
5	0.0150	-0.0146	0.0296
6	-0.0538	-0.0262	0.0276
7	-0.0727	0.0235	0.0962
8	-0.0358	0.0827	0.1185
9	0.0805	0.0100	0.0705
10	-0.1817	0.0587	0.2404
11	0.0000	-0.1578	0.1578
12	0.1542	-0.0179	0.1721
13	-0.0205	0.0143	0.0348
14	-0.2305	-0.1129	0.1176
15	-0.0276	-0.0112	0.0164
16	-0.0025	0.0000	0.0025
17	-0.0043	0.0000	0.0043
18	-0.0109	0.0265	0.0374
19	0.0187	-0.0182	0.0370
20	-0.0672	-0.0328	0.0345
21	-0.0908	0.0293	0.1202
22	0.0000	-0.0789	0.0789
23	0.0771	-0.0090	0.0861
24	-0.0102	0.0072	0.0174
25	-0.1153	-0.0564	0.0588
26	-0.0138	-0.0056	0.0082
27	0.0065	-0.0053	0.0118

Node (13)_X-Direction			
Time (Sec)	D1 (mm)	D2 (mm)	R-Disp. (mm)
0	0.0000	0.0000	0.0000
1	-0.0099	0.0000	0.0099
2	-0.0172	0.0000	0.0172
3	-0.0432	0.1052	0.1484
4	-0.1562	-0.0494	0.1068
5	0.4089	-0.0214	0.4303
6	0.0081	-0.0540	0.0622
7	0.1307	0.0000	0.1307
8	-0.0711	0.1641	0.2352
9	0.1597	0.0198	0.1399
10	-0.3605	0.1165	0.4770
11	0.0000	-0.3130	0.3130
12	0.3059	-0.0356	0.3415
13	-0.0407	0.0284	0.0691
14	-0.4574	-0.2240	0.2334
15	-0.0547	-0.0222	0.0325
16	0.1020	0.5902	0.4882
17	-0.9212	0.1479	1.0691
18	-0.3573	-0.2705	0.0868
19	0.0372	-0.0362	0.0733
20	-0.1334	-0.0651	0.0684
21	0.1420	-0.0531	0.1952
22	-0.0434	0.0000	0.0434
23	-0.0707	0.0000	0.0707
24	0.1184	-0.0443	0.1627
25	-0.0361	0.0000	0.0361
26	-0.0590	0.0000	0.0590
27	0.0129	-0.0105	0.0233

Node (14)_X-Direction			
Time (Sec)	D1 (mm)	D2 (mm)	R-Disp. (mm)
0	0.0000	0.0000	0.0000
1	-0.0062	0.0000	0.0062
2	-0.0108	0.0000	0.0108
3	-0.0272	0.0663	0.0935
4	-0.0984	-0.0311	0.0673
5	-0.0420	-0.0205	0.0215
6	-0.0568	0.0183	0.0751
7	0.0823	0.0000	0.0823
8	-0.0448	0.1034	0.1482
9	0.1006	0.0124	0.0882
10	-0.2271	0.0734	0.3005
11	0.0000	-0.1972	0.1972
12	0.1927	-0.0224	0.2151
13	-0.0256	0.0179	0.0435
14	-0.2881	-0.1411	0.1470
15	-0.0344	-0.0140	0.0205
16	-0.0031	0.0000	0.0031
17	-0.0054	0.0000	0.0054
18	-0.0136	0.0331	0.0467
19	0.0234	-0.0228	0.0462
20	-0.0841	-0.0410	0.0431
21	-0.1136	0.0367	0.1502
22	0.0000	-0.0986	0.0986
23	0.0964	-0.0112	0.1076
24	-0.0128	0.0090	0.0218
25	-0.1441	-0.0706	0.0735
26	-0.0172	-0.0070	0.0102
27	0.0081	-0.0066	0.0147

Node (15)_X-Direction			
Time (Sec)	D1 (mm)	D2 (mm)	R-Disp. (mm)
0	0.0000	0.0000	0.0000
1	-0.0125	0.0000	0.0125
2	-0.0217	0.0000	0.0217
3	-0.0544	0.1326	0.1870
4	-0.1968	-0.0623	0.1345
5	0.5152	-0.0270	0.5422
6	0.0103	-0.0681	0.0783
7	0.1646	0.0000	0.1646
8	-0.0896	0.2068	0.2964
9	0.2012	0.0249	0.1763
10	-0.4542	0.1467	0.6010
11	0.0000	-0.3944	0.3944
12	0.3855	-0.0448	0.4303
13	-0.0512	0.0358	0.0871
14	-0.5763	-0.2822	0.2940
15	-0.0689	-0.0279	0.0409
16	0.1285	0.7436	0.6151
17	-1.1607	0.1864	1.3470
18	-0.4502	-0.3408	0.1094
19	0.0468	-0.0456	0.0924
20	-0.1681	-0.0820	0.0861
21	0.1790	-0.0670	0.2459
22	-0.0546	0.0000	0.0546
23	-0.0891	0.0000	0.0891
24	0.1492	-0.0558	0.2049
25	-0.0455	0.0000	0.0455
26	-0.0743	0.0000	0.0743
27	0.0162	-0.0132	0.0294

Node (16)_X-Direction			
Time (Sec)	D1 (mm)	D2 (mm)	R-Disp. (mm)
0	0.0000	0.0000	0.0000
1	-0.0278	0.0000	0.0278
2	-0.0111	0.0000	0.0111
3	-0.0193	0.0000	0.0193
4	-0.0485	0.1181	0.1666
5	0.0835	-0.0812	0.1646
6	-0.2996	-0.1461	0.1535
7	-0.4047	0.1307	0.5355
8	-0.1996	0.4606	0.6602
9	0.4482	0.0554	0.3928
10	-1.0118	0.3269	1.3387
11	0.0000	-0.8786	0.8786
12	0.8586	-0.0998	0.9585
13	-0.1141	0.0798	0.1939
14	-1.2836	-0.6287	0.6549
15	-0.1534	-0.0622	0.0912
16	-0.0139	0.0000	0.0139
17	-0.0242	0.0000	0.0242
18	-0.0606	0.1476	0.2083
19	0.1043	-0.1015	0.2058
20	-0.3745	-0.1826	0.1919
21	-0.5059	0.1634	0.6693
22	0.0000	-0.4393	0.4393
23	0.4293	-0.0499	0.4792
24	-0.0571	0.0399	0.0970
25	-0.6418	-0.3143	0.3275
26	-0.0767	-0.0311	0.0456
27	0.0362	-0.0294	0.0655

Node (17)_X-Direction			
Time (Sec)	D1 (mm)	D2 (mm)	R-Disp. (mm)
0	0.0000	0.0000	0.0000
1	-0.0136	0.0000	0.0136
2	-0.0237	0.0000	0.0237
3	-0.0593	0.1174	0.1767
4	-0.2145	-0.0552	0.1594
5	-0.1341	-0.0442	0.0899
6	0.2502	1.1762	0.9260
7	-2.2595	0.2948	2.5543
8	-0.8764	-0.5390	0.3373
9	0.7613	-0.2469	1.0081
10	-0.4952	0.1300	0.6252
11	0.0000	-0.3494	0.3494
12	0.4202	-0.0397	0.4599
13	-0.0559	0.0317	0.0876
14	-1.2565	-0.5000	0.7565
15	0.5617	-0.0239	0.5856
16	0.0112	-0.0603	0.0715
17	0.1795	0.0000	0.1795
18	-0.0977	0.1832	0.2808
19	0.1890	0.0190	0.1700
20	-0.0349	0.0525	0.0874
21	-0.0622	0.0624	0.1246
22	0.0426	-0.0336	0.0762
23	-0.1425	-0.0565	0.0861
24	0.1626	-0.0494	0.2120
25	-0.0496	0.0000	0.0496
26	-0.0810	0.0000	0.0810
27	0.0194	-0.0128	0.0323

Node (18)_X-Direction			
Time (Sec)	D1 (mm)	D2 (mm)	R-Disp. (mm)
0	0.0000	0.0000	0.0000
1	-0.2530	0.0000	0.2530
2	-0.1012	0.0000	0.1012
3	-0.1757	0.0000	0.1757
4	-0.4409	1.0737	1.5146
5	0.7588	-0.7379	1.4967
6	-2.7233	-1.3278	1.3955
7	-3.6793	1.1886	4.8679
8	-1.8141	4.1872	6.0014
9	4.0748	0.5041	3.5708
10	-9.1982	2.9714	12.1696
11	0.0000	-7.9874	7.9874
12	7.8057	-0.9076	8.7133
13	-1.0375	0.7256	1.7631
14	-11.6694	-5.7154	5.9540
15	-1.3948	-0.5658	0.8290
16	-0.1265	0.0000	0.1265
17	-0.2197	0.0000	0.2197
18	-0.5511	1.3421	1.8932
19	0.9485	-0.9224	1.8709
20	-3.4042	-1.6598	1.7444
21	-4.5991	1.4857	6.0848
22	0.0000	-3.9937	3.9937
23	3.9029	-0.4538	4.3567
24	-0.5187	0.3628	0.8816
25	-5.8347	-2.8577	2.9770
26	-0.6974	-0.2829	0.4145
27	0.3286	-0.2671	0.5957

Node (19)_X-Direction			
Time (Sec)	D1 (mm)	D2 (mm)	R-Disp. (mm)
0	0.0000	0.0000	0.0000
1	-0.0099	0.0000	0.0099
2	-0.0172	0.0000	0.0172
3	-0.0432	0.1315	0.1747
4	-0.1562	-0.0618	0.0944
5	0.4089	-0.0268	0.4357
6	0.0081	-0.0675	0.0757
7	0.1307	0.0000	0.1307
8	-0.0711	0.2051	0.2762
9	0.1597	0.0247	0.1350
10	-0.3605	0.1456	0.5061
11	0.0000	-0.3913	0.3913
12	0.3059	-0.0445	0.3504
13	-0.0407	0.0355	0.0762
14	-0.9147	-0.5600	0.3547
15	-0.1093	-0.0554	0.0539
16	0.2040	1.4755	1.2714
17	-1.8423	0.3698	2.2121
18	-0.7145	-0.6761	0.0384
19	0.6207	-0.3097	0.9304
20	-0.0254	0.0588	0.0842
21	-0.0453	0.0699	0.1152
22	0.0310	-0.0377	0.0686
23	-0.1112	-0.0678	0.0434
24	0.1184	-0.0554	0.1737
25	-0.0361	0.0000	0.0361
26	-0.0590	0.0000	0.0590
27	0.0129	-0.0131	0.0260

Node (20)_X-Direction			
Time (Sec)	D1 (mm)	D2 (mm)	R-Disp. (mm)
0	0.0000	0.0000	0.0000
1	-0.0161	0.0000	0.0161
2	-0.0279	0.0000	0.0279
3	-0.0700	0.1420	0.2120
4	-0.2530	-0.0667	0.1863
5	0.6625	-0.0289	0.6914
6	0.0132	-0.0729	0.0861
7	0.2117	0.0000	0.2117
8	-0.1152	0.2215	0.3367
9	0.2587	0.0267	0.2320
10	-0.5840	0.1572	0.7412
11	0.0000	-0.4226	0.4226
12	0.4956	-0.0480	0.5436
13	-0.0659	0.0384	0.1043
14	-0.7409	-0.3024	0.4385
15	-0.0886	-0.0299	0.0586
16	0.1653	0.7967	0.6315
17	-1.4923	0.1997	1.6920
18	-0.5788	-0.3651	0.2137
19	0.0602	-0.0488	0.1090
20	-0.2161	-0.0878	0.1283
21	0.2301	-0.0717	0.3019
22	-0.0702	0.0000	0.0702
23	-0.1146	0.0000	0.1146
24	0.1918	-0.0598	0.2515
25	-0.0585	0.0000	0.0585
26	-0.0955	0.0000	0.0955
27	0.0209	-0.0141	0.0350

Appendix D: Details of Relative Displacement for Y - Direction

Node (1)_Y-Direction			
Time (Sec)	D1 (mm)	D2 (mm)	R-Disp. (mm)
0	0.0000	0.0000	0.0000
1	0.8939	0.0000	0.8939
2	-0.2782	0.1581	0.4362
3	0.0968	-0.0639	0.1606
4	-0.1741	0.2613	0.4354
5	-0.3097	0.3109	0.6207
6	0.2119	-0.1675	0.3794
7	-0.2782	0.1581	0.4362
8	0.0968	-0.0639	0.1606
9	-0.2471	0.0000	0.2471
10	-0.4033	0.0000	0.4033
11	0.0968	-0.0639	0.1606
12	-1.4797	0.3884	1.8681
13	-0.0407	0.0000	0.0407
14	0.0968	-0.0639	0.1606
15	0.0968	0.1581	0.0613
16	0.8939	0.0000	0.8939
17	-0.4864	0.9122	1.3986
18	0.9413	0.0946	0.8467
19	0.8939	0.0000	0.8939
20	-0.4864	0.9122	1.3986
21	0.9413	0.0946	0.8467
22	-0.6678	-0.2201	0.4477
23	-2.4662	0.6473	3.1135
24	-0.0678	0.0000	0.0678
25	-0.6678	-0.2201	0.4477
26	-0.2782	0.1581	0.4362
27	0.0968	-0.0639	0.1606

Node (2)_Y-Direction			
Time (Sec)	D1 (mm)	D2 (mm)	R-Disp. (mm)
0	0.0000	0.0000	0.0000
1	0.8939	0.1888	0.7051
2	-0.2782	0.1344	0.4125
3	0.0968	-0.0543	0.1511
4	-0.1741	0.2221	0.3962
5	-0.3097	0.2643	0.5740
6	0.2119	-0.1423	0.3542
7	-0.2782	0.1344	0.4125
8	0.0968	-0.0543	0.1511
9	-0.2471	0.0000	0.2471
10	-0.4033	0.0000	0.4033
11	0.0968	-0.0639	0.1606
12	-1.4797	0.3884	1.8681
13	-0.0407	0.0000	0.0407
14	0.0968	-0.0639	0.1606
15	0.0968	0.1581	0.0613
16	0.8939	0.1888	0.7051
17	-0.4864	0.9122	1.3986
18	0.9413	0.0946	0.8467
19	0.8939	0.0000	0.8939
20	-0.4864	0.9122	1.3986
21	0.9413	0.0946	0.8467
22	-0.6678	-0.2201	0.4477
23	-2.4662	0.1888	2.6550
24	-0.0678	0.0000	0.0678
25	-0.6678	-0.2201	0.4477
26	-0.2782	0.1581	0.4362
27	0.0968	-0.0639	0.1606

Node (3)_Y-Direction			
Time (Sec)	D1 (mm)	D2 (mm)	R-Disp. (mm)
0	0.0000	0.0000	0.0000
1	-0.0444	0.0000	0.0444
2	-0.0771	0.0000	0.0771
3	-0.1935	0.3829	0.5764
4	-0.6996	-0.1799	0.5197
5	-0.4373	-0.1441	0.2931
6	0.8160	3.8355	3.0195
7	-7.3680	0.9613	8.3293
8	-2.8577	-1.7577	1.1000
9	-6.2869	-3.8668	2.4201
10	-1.6148	0.4238	2.0386
11	0.0000	-1.1393	1.1393
12	1.3703	-0.1295	1.4998
13	-0.1821	0.1035	0.2856
14	-4.0972	-1.6304	2.4667
15	1.8317	-0.0779	1.9096
16	0.0365	-0.1966	0.2331
17	0.5853	0.0000	0.5853
18	-7.7364	1.0094	8.7458
19	-3.0006	-1.8455	1.1550
20	-6.6013	-4.0602	2.5411
21	-1.6955	0.4450	2.1405
22	0.0000	-1.1963	1.1963
23	-0.4648	-0.1841	0.2807
24	0.5302	-0.1612	0.6914
25	-0.1618	0.0000	0.1618
26	-0.2641	0.0000	0.2641
27	0.0634	-0.0418	0.1052

Node (4)_Y-Direction			
Time (Sec)	D1 (mm)	D2 (mm)	R-Disp. (mm)
0	0.0000	0.0000	0.0000
1	-0.0666	0.0000	0.0666
2	-0.1157	0.0000	0.1157
3	-0.2902	0.5743	0.8645
4	-1.0494	-0.2698	0.7796
5	-0.6559	-0.2162	0.4397
6	1.2240	5.7533	4.5293
7	-11.0520	1.4419	12.4940
8	-4.2865	-2.6365	1.6501
9	-9.4304	-5.8003	3.6301
10	-2.4222	0.6358	3.0579
11	0.0000	-1.7089	1.7089
12	2.0555	-0.1942	2.2497
13	-0.2732	0.1553	0.4285
14	-6.1458	-2.4457	3.7001
15	2.7475	-0.1169	2.8644
16	0.0547	-0.2949	0.3497
17	0.8780	0.0000	0.8780
18	-15.8430	-9.7444	6.0986
19	-7.2014	-4.4293	2.7721
20	-15.8430	-9.7444	6.0986
21	-4.0692	1.0681	5.1373
22	0.0000	-2.8710	2.8710
23	0.0000	-2.8710	2.8710
24	-1.1155	-0.4419	0.6736
25	1.2725	-0.3868	1.6593
26	-0.6338	0.0000	0.6338
27	0.1520	-0.1004	0.2524

Node (5)_Y-Direction			
Time (Sec)	D1 (mm)	D2 (mm)	R-Disp. (mm)
0	0.0000	0.0000	0.0000
1	-0.0638	0.0000	0.0638
2	-0.1107	0.0000	0.1107
3	-0.2778	0.4996	0.7774
4	-0.8737	-0.2042	0.6695
5	-0.5461	-0.1636	0.3825
6	1.0191	4.3546	3.3356
7	-9.2018	1.0914	10.2932
8	-3.5689	-1.9956	1.5734
9	-9.0249	-5.0462	3.9787
10	-2.3180	0.5531	2.8711
11	0.0000	-1.2935	1.2935
12	1.7114	-0.1470	1.8583
13	-0.2275	0.1175	0.3450
14	-5.1169	-1.8511	3.2658
15	2.2876	-0.0885	2.3760
16	0.0524	-0.2566	0.3090
17	0.8402	0.0000	0.8402
18	-15.1618	-8.4777	6.6841
19	-6.8917	-3.8535	3.0382
20	-15.1618	-8.4777	6.6841
21	-3.8942	0.9292	4.8235
22	0.0000	-2.1731	2.1731
23	0.0000	-2.1731	2.1731
24	-0.9288	-0.3345	0.5943
25	1.0595	-0.2928	1.3523
26	-0.6065	0.0000	0.6065
27	0.1455	-0.0873	0.2329

Node (6)_Y-Direction			
Time (Sec)	D1 (mm)	D2 (mm)	R-Disp. (mm)
0	0.0000	0.0000	0.0000
1	-0.0765	0.0000	0.0765
2	-0.1329	0.0000	0.1329
3	-0.3333	0.5996	0.9329
4	-1.0485	-0.2451	0.8034
5	-0.6553	-0.1964	0.4589
6	1.2229	5.2256	4.0027
7	-11.0422	1.3097	12.3519
8	-4.2827	-2.3947	1.8881
9	-10.8299	-6.0555	4.7744
10	-2.7816	0.6637	3.4453
11	-0.4000	0.7195	1.1195
12	-1.2582	-0.2941	0.9641
13	-0.7864	-0.2356	0.5507
14	-6.1403	-2.2214	3.9189
15	1.7568	-0.0679	1.8248
16	0.0402	-0.1971	0.2373
17	0.8066	0.0000	0.8066
18	-14.5553	-8.1385	6.4168
19	-3.9696	-2.2196	1.7500
20	-8.7332	-4.8831	3.8501
21	-2.2431	0.5352	2.7783
22	0.0000	-1.6689	1.6689
23	0.0000	-1.6689	1.6689
24	-0.7133	-0.2569	0.4564
25	0.8137	-0.2248	1.0385
26	-0.4658	0.0000	0.4658
27	0.1397	-0.0839	0.2235

Node (7)_Y-Direction			
Time (Sec)	D1 (mm)	D2 (mm)	R-Disp. (mm)
0	0.0000	0.0000	0.0000
1	-0.0765	0.0000	0.0765
2	-0.1329	0.0000	0.1329
3	-0.3333	0.8394	1.1727
4	-1.0485	-0.3431	0.7054
5	-0.6553	-0.2749	0.3804
6	1.2229	7.3158	6.0929
7	-11.0422	1.8335	12.8757
8	-4.2827	-3.3525	0.9302
9	-10.8299	-8.4777	2.3522
10	-2.7816	0.9292	3.7108
11	-0.4000	1.0073	1.4072
12	-1.2582	-0.4118	0.8464
13	-0.7864	-0.3299	0.4565
14	-6.1403	-3.1099	3.0304
15	1.7568	-0.0951	1.8520
16	0.0402	-0.2759	0.3161
17	0.8066	0.0000	0.8066
18	-14.5553	-11.3940	3.1614
19	-3.9696	-3.1074	0.8622
20	-8.7332	-6.8364	1.8968
21	-2.2431	0.7493	2.9924
22	0.0000	-2.3365	2.3365
23	0.0000	-2.3365	2.3365
24	-0.7133	-0.3596	0.3537
25	0.8137	-0.3148	1.1285
26	-0.4658	0.0000	0.4658
27	0.1397	-0.1174	0.2571

Node (8)_Y-Direction			
Time (Sec)	D1 (mm)	D2 (mm)	R-Disp. (mm)
0	0.0000	0.0000	0.0000
1	-0.1180	-0.0389	0.0791
2	0.2201	1.0348	0.8146
3	0.2849	1.3391	1.0542
4	0.2422	1.1383	0.8961
5	-0.0784	0.0000	0.0784
6	-1.4362	0.1874	1.6236
7	-0.1180	-0.0389	0.0791
8	0.1871	0.8796	0.6924
9	-1.6896	0.2204	1.9101
10	-1.0884	-0.6695	0.4190
11	0.2020	-0.0614	0.2633
12	-0.2665	-0.0685	0.1980
13	-0.1665	-0.0549	0.1117
14	0.3108	1.4609	1.1501
15	-0.2665	-0.0685	0.1980
16	-0.1665	-0.0549	0.1117
17	0.3108	1.4609	1.1501
18	-2.8063	0.3661	3.1725
19	-0.2665	-0.0685	0.1980
20	-0.1665	-0.0549	0.1117
21	0.2849	1.3391	1.0542
22	-0.1328	-0.0438	0.0890
23	-0.2443	-0.0628	0.1815
24	-0.1527	-0.0503	0.1023
25	0.2849	1.3391	1.0542
26	-0.0922	0.0000	0.0922
27	0.0221	-0.0146	0.0367

Node (9)_Y-Direction			
Time (Sec)	D1 (mm)	D2 (mm)	R-Disp. (mm)
0	0.0000	0.0000	0.0000
1	-0.1298	-0.0389	0.0909
2	0.2422	1.0348	0.7926
3	0.3134	1.3391	1.0257
4	0.2664	1.1383	0.8719
5	-0.0862	0.0000	0.0862
6	-1.5798	0.1874	1.7672
7	-0.1298	-0.0389	0.0909
8	0.2058	0.2264	0.0206
9	-1.8586	-2.0445	0.1859
10	-1.1973	-1.3170	0.1197
11	0.2221	-0.0614	0.2835
12	-0.2931	-0.0685	0.2246
13	-0.1832	-0.0549	0.1283
14	0.3419	1.4609	1.1190
15	-0.3517	-0.0822	0.2695
16	-0.1999	-0.0659	0.1340
17	0.3730	1.7530	1.3801
18	-3.3676	0.4394	3.8070
19	-0.3198	-0.0822	0.2375
20	-0.1999	-0.0659	0.1340
21	0.3419	1.6070	1.2651
22	-0.1328	-0.0525	0.0802
23	-0.2443	-0.0754	0.1689
24	-0.0733	-0.0483	0.0250
25	0.1367	-1.2856	1.4223
26	-0.0443	0.0000	0.0443
27	0.0106	-0.0140	0.0246

Node (10)_Y-Direction			
Time (Sec)	D1 (mm)	D2 (mm)	R-Disp. (mm)
0	0.0000	0.0000	0.0000
1	-0.0191	0.0000	0.0191
2	-0.0332	0.0000	0.0332
3	-0.0833	0.1499	0.2332
4	-0.2621	-0.0613	0.2008
5	-0.1638	-0.0491	0.1147
6	0.3057	1.3064	1.0007
7	-2.7605	0.3274	3.0880
8	-1.0707	-0.5987	0.4720
9	-2.7075	-1.5139	1.1936
10	-0.6954	0.1659	0.8613
11	-0.1000	0.1799	0.2799
12	-0.3145	-0.0735	0.2410
13	-0.1966	-0.0589	0.1377
14	-1.5351	-0.5553	0.9797
15	-0.1573	-0.0368	0.1205
16	-0.0983	-0.0295	0.0688
17	-0.7675	-0.2777	0.4899
18	0.2196	-0.0085	0.2281
19	0.0050	-0.0246	0.0297
20	-2.1833	-1.2208	0.9625
21	-0.5608	0.1338	0.6946
22	0.0000	-0.4172	0.4172
23	0.0000	-0.4172	0.4172
24	-0.1783	-0.0642	0.1141
25	0.2034	-0.0562	0.2596
26	-0.1165	0.0000	0.1165
27	0.0349	-0.0210	0.0559

Node (11)_Y-Direction			
Time (Sec)	D1 (mm)	D2 (mm)	R-Disp. (mm)
0	0.0000	0.0000	0.0000
1	-0.0468	0.0000	0.0468
2	-0.0813	0.0000	0.0813
3	-0.2041	0.1150	0.3191
4	-0.7378	-0.0541	0.6838
5	1.9317	-0.0234	1.9552
6	0.0385	-0.0591	0.0976
7	0.6173	0.0000	0.6173
8	-0.3359	0.1795	0.5153
9	0.7544	0.0216	0.7328
10	-1.7030	0.1273	1.8303
11	0.0000	-0.3423	0.3423
12	1.4452	-0.0389	1.4841
13	-0.1921	0.0311	0.2232
14	-2.1605	-0.2449	1.9156
15	1.3007	-0.0350	1.3357
16	-0.1729	0.0280	0.2009
17	-1.9445	-0.2205	1.7240
18	-0.2324	-0.0218	0.2106
19	0.1756	-0.0395	0.2151
20	-0.6303	-0.0711	0.5591
21	0.6710	-0.0581	0.7291
22	-0.2048	0.0000	0.2048
23	-0.3342	0.0000	0.3342
24	0.5592	-0.0484	0.6076
25	-0.1707	0.0000	0.1707
26	-0.2785	0.0000	0.2785
27	0.0608	-0.0114	0.0723

Node (12)_Y-Direction			
Time (Sec)	D1 (mm)	D2 (mm)	R-Disp. (mm)
0	0.0000	0.0000	0.0000
1	-0.0500	0.0000	0.0500
2	-0.0200	0.0000	0.0200
3	-0.0347	0.0000	0.0347
4	-0.0871	0.2121	0.2992
5	0.1499	-0.1458	0.2956
6	-0.5379	-0.2623	0.2757
7	-0.7268	0.2348	0.9616
8	-0.3584	0.8271	1.1855
9	0.8049	0.0996	0.7053
10	-1.8169	0.5869	2.4039
11	0.0000	-1.5778	1.5778
12	1.5419	-0.1793	1.7212
13	-0.2049	0.1433	0.3483
14	-2.3051	-1.1290	1.1761
15	-0.2755	-0.1118	0.1638
16	-0.0250	0.0000	0.0250
17	-0.0434	0.0000	0.0434
18	-0.1089	0.2651	0.3740
19	0.1873	-0.1822	0.3696
20	-0.6724	-0.3279	0.3446
21	-0.9085	0.2935	1.2019
22	0.0000	-0.7889	0.7889
23	0.7709	-0.0896	0.8606
24	-0.1025	0.0717	0.1741
25	-1.1525	-0.5645	0.5880
26	-0.1378	-0.0559	0.0819
27	0.0649	-0.0528	0.1177

Node (13)_Y-Direction			
Time (Sec)	D1 (mm)	D2 (mm)	R-Disp. (mm)
0	0.0000	0.0000	0.0000
1	-0.0149	0.0000	0.0149
2	-0.0258	0.0000	0.0258
3	-0.0648	0.1052	0.1700
4	-0.2343	-0.0494	0.1849
5	0.6134	-0.0214	0.6348
6	0.0122	-0.0540	0.0662
7	0.1960	0.0000	0.1960
8	-0.1067	0.1641	0.2708
9	0.2396	0.0198	0.2198
10	-0.5408	0.0183	0.5591
11	0.0000	0.2940	0.2940
12	0.4589	-0.1600	0.6189
13	-0.0610	0.3593	0.4203
14	-0.6860	-0.8111	0.1251
15	-0.0820	0.0000	0.0820
16	0.1530	0.5902	0.4372
17	-1.3817	-0.1230	1.2587
18	-0.5359	0.2295	0.7654
19	0.0558	-2.0726	2.1284
20	-0.2001	-0.8039	0.6037
21	0.2131	-0.0531	0.2662
22	-0.0650	0.0000	0.0650
23	-0.1061	0.0000	0.1061
24	0.1776	-0.0443	0.2218
25	-0.0542	0.0000	0.0542
26	-0.0884	0.0000	0.0884
27	0.0193	-0.0105	0.0298

Node (14)_Y-Direction			
Time (Sec)	D1 (mm)	D2 (mm)	R-Disp. (mm)
0	0.0000	0.0000	0.0000
1	-0.0250	0.0000	0.0250
2	-0.0434	0.0000	0.0434
3	-0.1089	0.2651	0.3740
4	-0.3936	-0.1246	0.2690
5	-0.1681	-0.0820	0.0861
6	-0.2271	0.0734	0.3005
7	0.3293	-0.1933	0.5226
8	-0.1792	-0.2612	0.0820
9	0.4025	0.3787	0.0238
10	-0.9085	-0.2061	0.7024
11	0.0000	0.4628	0.4628
12	0.7709	-1.0447	1.8157
13	-0.1025	0.0000	0.1025
14	-1.1525	0.8866	2.0391
15	-0.1378	-0.1178	0.0199
16	-0.0125	0.0000	0.0125
17	-0.0217	0.0000	0.0217
18	-0.0544	0.1326	0.1870
19	0.0937	-0.0911	0.1848
20	-0.3362	-0.1639	0.1723
21	-0.4542	0.1467	0.6010
22	0.0000	-0.3944	0.3944
23	0.3855	-0.0448	0.4303
24	-0.0512	0.0358	0.0871
25	-0.5763	-0.2822	0.2940
26	-0.0689	-0.0279	0.0409
27	0.0325	-0.0264	0.0588

Node (15)_Y-Direction			
Time (Sec)	D1 (mm)	D2 (mm)	R-Disp. (mm)
0	0.0000	0.0000	0.0000
1	-0.0500	0.0000	0.0500
2	-0.0868	0.0000	0.0868
3	-0.2177	0.2651	0.4828
4	-0.7872	-0.1246	0.6626
5	2.0610	-0.0540	2.1150
6	0.0411	-0.1361	0.1772
7	0.3293	0.0000	0.3293
8	-0.1792	0.4136	0.5927
9	0.4025	0.0498	0.3527
10	-0.9085	0.2935	1.2019
11	0.0000	-0.7889	0.7889
12	0.7709	-0.0896	0.8606
13	-0.1025	0.0717	0.1741
14	-0.5763	-0.5645	0.0118
15	-0.0689	-0.0559	0.0130
16	0.1285	1.4873	1.3587
17	-2.3213	0.3727	2.6941
18	-0.9003	-0.6815	0.2188
19	0.0937	-0.0911	0.1848
20	-0.3362	-0.1639	0.1723
21	0.7159	-0.1339	0.8498
22	-0.2185	0.0000	0.2185
23	-0.3566	0.0000	0.3566
24	0.5966	-0.1116	0.7082
25	-0.1821	0.0000	0.1821
26	-0.2971	0.0000	0.2971
27	0.0649	-0.0264	0.0913

Node (16)_Y-Direction			
Time (Sec)	D1 (mm)	D2 (mm)	R-Disp. (mm)
0	0.0000	0.0000	0.0000
1	-0.0835	0.0000	0.0835
2	-0.0334	0.0000	0.0334
3	-0.0580	0.0000	0.0580
4	-0.1455	0.1181	0.2636
5	0.2504	-0.0812	0.3316
6	-0.8987	-0.1461	0.7526
7	-1.2142	0.1307	1.3449
8	-0.5987	0.4606	1.0593
9	1.3447	0.0554	1.2892
10	-3.0354	0.3269	3.3623
11	0.0000	-0.8786	0.8786
12	2.5759	-0.0998	2.6757
13	-0.3424	0.0798	0.4222
14	-3.8509	-0.6287	3.2222
15	-0.4603	-0.0622	0.3981
16	-0.0417	0.0000	0.0417
17	-0.0725	0.0000	0.0725
18	-0.1819	0.1476	0.3295
19	0.3130	-0.1015	0.4145
20	-1.1234	-0.1826	0.9408
21	-1.5177	0.1634	1.6811
22	0.0000	-0.4393	0.4393
23	1.2879	-0.0499	1.3379
24	-0.1712	0.0399	0.2111
25	-1.9254	-0.3143	1.6111
26	-0.2301	-0.0311	0.1990
27	0.1085	-0.0294	0.1378

Node (17)_Y-Direction			
Time (Sec)	D1 (mm)	D2 (mm)	R-Disp. (mm)
0	0.0000	0.0000	0.0000
1	-0.1839	0.0000	0.1839
2	-0.3193	0.0000	0.3193
3	-0.8011	1.5850	2.3861
4	-2.8964	-0.7448	2.1516
5	-1.8103	-0.5967	1.2136
6	7.7079	-2.4994	10.2073
7	5.7809	-1.8746	7.6555
8	-3.7604	0.9870	4.7474
9	0.0000	-2.6531	2.6531
10	3.1911	-0.3015	3.4926
11	-0.4241	0.2410	0.6652
12	-9.5413	-3.7969	5.7444
13	4.2548	-0.4020	4.6568
14	-0.5655	0.3214	0.8869
15	-12.7217	-5.0625	7.6592
16	5.6874	-0.2420	5.9293
17	2.4232	0.0000	2.4232
18	-1.3185	2.4726	3.7911
19	2.5515	0.2564	2.2950
20	-0.4718	0.7084	1.1802
21	-0.8396	0.8429	1.6824
22	0.5744	-0.4539	1.0284
23	-1.9243	-0.7623	1.1620
24	2.1951	-0.6672	2.8624
25	-0.6699	0.0000	0.6699
26	-1.0933	0.0000	1.0933
27	0.2623	-0.1732	0.4355

Node (18)_Y-Direction			
Time (Sec)	D1 (mm)	D2 (mm)	R-Disp. (mm)
0	0.0000	0.0000	0.0000
1	-0.1518	0.0000	0.1518
2	-0.0607	0.0000	0.0607
3	-0.1054	0.0000	0.1054
4	-0.2645	0.6442	0.9087
5	0.4553	-0.4428	0.8980
6	-1.6340	-0.7967	0.8373
7	-2.2076	0.7131	2.9207
8	-1.0885	2.5123	3.6008
9	2.4449	0.3024	2.1425
10	-5.5189	1.7829	7.3018
11	0.0000	-4.7924	4.7924
12	4.6834	-0.5446	5.2280
13	-0.6225	0.4354	1.0579
14	-7.0016	-3.4292	3.5724
15	-0.8369	-0.3395	0.4974
16	-0.0759	0.0000	0.0759
17	-0.1318	0.0000	0.1318
18	-0.3307	0.8053	1.1359
19	0.5691	-0.5534	1.1225
20	-2.0425	-0.9959	1.0466
21	-2.7595	0.8914	3.6509
22	0.0000	-2.3962	2.3962
23	2.3417	-0.2723	2.6140
24	-0.3112	0.2177	0.5289
25	-3.5008	-1.7146	1.7862
26	-0.4185	-0.1698	0.2487
27	0.1972	-0.1603	0.3574

Node (19)_Y-Direction			
Time (Sec)	D1 (mm)	D2 (mm)	R-Disp. (mm)
0	0.0000	0.0000	0.0000
1	-0.0643	-0.0803	0.0161
2	-0.1116	0.1395	0.2510
3	-0.2635	0.3294	0.5929
4	-2.9637	3.7046	6.6682
5	-0.3542	0.4428	0.7970
6	0.6611	-0.8263	1.4874
7	-5.9691	-7.4614	1.4923
8	-2.3151	-2.8939	0.5788
9	0.2409	0.3011	0.0602
10	-0.8645	-1.0807	0.2161
11	0.9205	1.1506	0.2301
12	1.9824	-2.4780	4.4604
13	-0.2635	-0.3294	0.0659
14	-2.9637	-3.7046	0.7409
15	-0.3542	-0.4428	0.0886
16	0.6611	0.8263	0.1653
17	-5.9691	-7.4614	1.4923
18	-2.3151	-2.8939	0.5788
19	0.2409	0.3011	0.0602
20	-0.8645	1.0807	1.9452
21	0.9205	-1.1506	2.0711
22	-0.2809	-0.3512	0.0702
23	-0.4584	0.5731	1.0315
24	0.7671	-0.9588	1.7259
25	-0.2341	0.2926	0.5267
26	-0.3820	-0.4775	0.0955
27	0.0835	0.1043	0.0209

Node (20)_Y-Direction			
Time (Sec)	D1 (mm)	D2 (mm)	R-Disp. (mm)
0	0.0000	0.0000	0.0000
1	-0.0397	0.0000	0.0397
2	-0.0689	0.0000	0.0689
3	-0.1728	0.5260	0.6988
4	-0.6248	-0.2472	0.3776
5	1.6357	-0.1071	1.7428
6	0.0326	-0.2701	0.3027
7	0.5227	0.0000	0.5227
8	-0.2844	0.8205	1.1049
9	0.6388	0.0988	0.5400
10	-1.4420	0.5823	2.0243
11	0.0000	-1.5652	1.5652
12	1.2237	-0.1779	1.4016
13	-0.1626	0.1422	0.3048
14	-3.6588	-2.2400	1.4188
15	-0.4373	-0.2218	0.2156
16	0.2040	1.4755	1.2714
17	-1.8423	0.3698	2.2121
18	-0.7145	-0.6761	0.0384
19	0.6207	-0.3097	0.9304
20	-0.0254	0.0588	0.0842
21	-0.0453	0.0699	0.1152
22	0.0310	-0.0377	0.0686
23	-0.1112	-0.0678	0.0434
24	0.1184	-0.0554	0.1737
25	-0.0361	0.0000	0.0361
26	-0.0590	0.0000	0.0590
27	0.0129	-0.0131	0.0260

جامعة النجاح الوطنية
كلية الدراسات العليا

التقييم الانشائي الزلزالي للمباني التاريخية في فلسطين
كنيسة المهد كحالة دراسية

إعداد
علي عبد اللطيف علي ابو صفية

إشراف
د. منذر ابراهيم

قُدمت هذه الأطروحة إستكمالاً لمتطلبات الحصول على درجة الماجستير في هندسة الانشاءات بكلية الدراسات العليا في جامعة النجاح الوطنية في نابلس ، فلسطين

2019

التقييم الانشائي الزلزالي للمباني التاريخية في فلسطين
كنيسة المهد كحالة دراسية

إعداد

علي عبد اللطيف علي ابو صفية

إشراف

د. منذر إبراهيم

الملخص

ركزت هذه الدراسة على دراسة التقييم الانشائي الزلزالي للمباني التاريخية في فلسطين، لما لها من قيمة معمارية ودينية وثقافية، وقد ركزت الدراسة على الحالة الدراسية: كنيسة المهد، الواقعة في محافظة بيت لحم – فلسطين. تعتبر هذه الكنيسة من اهم الكنائس للمسيحين بشكل عام وللفلسطينيين بشكل خاص، فقد كانت مكان مولد السيد المسيح – عليه السلام – وقد اضيفت في عدة تصنيفات للتراث العالمي.

انطلقت هذه الدراسة في عدة مراحل من خلال عمل بحث وتمحيص للمخططات الخاصة بهذه الكنيسة وخصائصها وموادها، ومن ثم مراجعة للأبحاث والدراسات السابقة المشابهة لهذا الموضوع. بعد ذلك تم الانتقال الى مرحلة عمل النماذج ثلاثية الابعاد على برامج العناصر المحددة لدراسة سلوكها وخصائصها، وتم عمل نموذجين احدهم للدراسة الاستاتيكية والاخر للدراسة الديناميكية. كمرحلة اخرى لاحقة تم استخدام طريقتي الدفع المكافئ الاستاتيكي وطريقة التاريخ الزمني الديناميكية من خلال استخدام زلازل معدة مسبقا، تم من خلالهما معرفة تكون الشقوق في الجدران الحجرية للكنيسة، وقياس الازاحة النسبية بين العناصر الحجرية ذاتها ومن ثم معرفة الامكان المتوقع حصول انهيار فيها، وقد تم اثبات كفاءة هذه النتائج وتأكيد عدم وجود مسار اخر بديل للأحمال اثناء الانهيار.

تعتبر هذه الدراسة معقدة قليلا لأنها تعتمد بشكل اساسي توفر المعلومات الدقيقة للمواد وخصائصها، لذلك تم عمل فرضيات في بعض الاحيان ودراسة نتائجها وتأثيراتها.